Staggarenes - A New Family of Extended Aromatic Systems Based on Fused Anthracenes

Faisal Alkahtani

This thesis is submitted in fulfilment of the requirements of the degree of Doctor of Philosophy at the University of East Anglia

School of Chemistry

University of East Anglia, Norwich, United Kingdom

January 2024

Declaration

The research described in this thesis is, to the best of my knowledge, original except where due reference is made.

Faisal Alkahtani

2024

Abstract

The overall objective of this project is to synthesise and design unique new extended aromatic structures assembling fundamental three-ring aromatic units (anthracenes) iteratively into more complex arrangements. In particular, we aim to annulate more than two functionalized anthracene cores together in a stepwise manner by extending the conjugation of the π-system *via* a Suzuki coupling reaction and Scholl reaction. The targeted materials may be recognized as a structural fragment of graphene and we term them "staggarenes". Indeed, the annulation of anthracene units in a lateral position is an appealing target; the stepwise staggared extension of the π-conjugated systems laterally suggests a structure that is likely to be a stable candidate for optoelectronics. However, the target molecule can be synthetically challenging due to the need for stepwise procedures including the preparation of functionalized anthracene components. Unsubstituted/ substituted bianthracenes have been constructed by the palladium-catalyzed Suzuki cross-coupling reaction using unsubstituted/ substituted 9-anthracenyl (pinacol) boronate ester and iodoanthracene partners. Extension of the π-conjugated system of several anthracene fused anthracene (AFA) derivatives has been designed to investigate their reactivity under Scholl oxidative cyclodehydrogenation reaction conditions. These novel precursors have been successfully characterized using NMR spectroscopy, MALDI-TOF MS, single-crystal X-ray diffraction, UV–vis, and emission spectroscopy.

Acknowledgements

First of all, I wish to express my deep gratitude to Prof. Andrew Cammidge for the opportunity to work on such a great project, and the freedom to explore new areas, particularly in extending macrocyclic cores. Many thanks to Andy also for his generous assistance and advice in the evolution of this project over the last four years. His leadership, support, and friendship have been crucial to the completion of this thesis. His help and encouragement were always present when I knocked on his door and when things weren't working so well, and his patience was considerable for answering my endless questions.

Many thanks must go to Dr. Isabelle Fernandes for her assistance, advice, time, and understanding. Indeed, I am grateful to her for giving me this opportunity to work under her guidance and for providing the best suggestions regarding the lab work. I wouldn't be the researcher I am now without Andy and Isabelle. I am so lucky that I have experienced this invaluable opportunity to work under their lovely supervision.

I would like also to thank the past and current colleagues of the Cammidge group for a wonderful work environment, especially for Muteb, Ala, and Reem who gave me a constant support when I got frustrated or lost confidence. Extending thanks to all people in chemistry school, especially those who work on the second and third floors.

Special thanks to King Faisal University for funding my PhD research and giving me this opportunity to achieve my goal and to UEA in all aspects during my stay at the university. Many thanks to the staff on the 01 floor for providing the solvents always on time whenever needed, to David for analysing the X-ray data and providing comments, and to Matthew for making/fixing any glassware I gave him.

Finally, I am very thankful to my parents for their enduring support throughout my education and rearing as well as to my wife, Saja, for her love and continuing support through the difficult periods of this work.

Contents

List of Figures

List of Schemes

List of Tables

Abbreviations

AFA	Anthracene fused anthracene
Bpin	Bis (pinacolato) diboron
°C	Celsius temperature
DBU	1,8-Diazabicyclo[5.4.0]undec-7-ene
DCM	Dichloromethane
DDQ	2,3-Dichloro-5,6-dicyano-*p*-benzoquinone
DME	1,2-Dimethoxyethane
DMF	Dimethylformamide
dppf	(Diphenylphosphino) ferrocene
E	Energy gap (as defined in text)
eV	Electronvolt
g	Gram
h	Hour
HOMO	Highest occupied molecular orbital
λ	Wavelength
LUMO	Lowest unoccupied molecular orbital
m	Meta
M	Molarity
MALDI	Matrix-assisted-laser-desorption-ionisation
Me	Methyl
mg	Milligram
MHz	Megahertz
min	Minutes
mL	Millilitre
mmol	Millimole
MP	Melting point
6-MRs	Six-membered rings
MS	Mass spectrometry
MsOH	methanesulfonic acid
NBS	*N*-bromosuccinimide
NIR	Near-infrared
nm	Nanometre

NMR	Nuclear magnetic resonance
OFETs	Organic field-effect transistors
OLEDs	Organic light-emitting diodes
PAH	Polycyclic aromatic hydrocarbon
Pet	Petroleum
ppm	Parts per million
rb	Round-bottomed
rt	Room temperature
SMC	Suzuki-Miyaura cross-coupling
TfOH	Trifluoromethanesulfonic acid
TOF	Time of flight
TLC	Thin-layer chromatography
UV	Ultraviolet
Vis	Visible
wt	Weight

Introduction

1.1 Polycyclic Aromatic Hydrocarbons

Polycyclic aromatic hydrocarbons (PAHs) are a class of organic compounds comprised of multiple fused aromatic rings in which the electrons are delocalized. They can be naturally formed by combustion processes such as coal, diesel, tobacco, wood, incense, or fat.[1] PAHs are key components in several biological and physical fields including optoelectronic and electronic materials, agrochemicals, and pharmaceuticals. Because of their expanded π-conjugation, they are capable of showing long-wavelength absorptions and emissions, small HOMO–LUMO bandgaps, strong π-π interactions, high mechanical strengths, and low redox potentials. As a result of these outstanding advantages, they are usually utilized in a variety of materials such as organic photovoltaics, organic light-emitting diodes (OLEDs), organic field-effect transistors (OFETs), functional fluorescent dyes, pharmaceuticals, and liquid crystals.[2–8] PAHs are divided into multiple groups as represented in Figure 1.1. In the present chapter, I will shed more light on cata-fused and peri-fused classes which can be considered as the most essential groups.

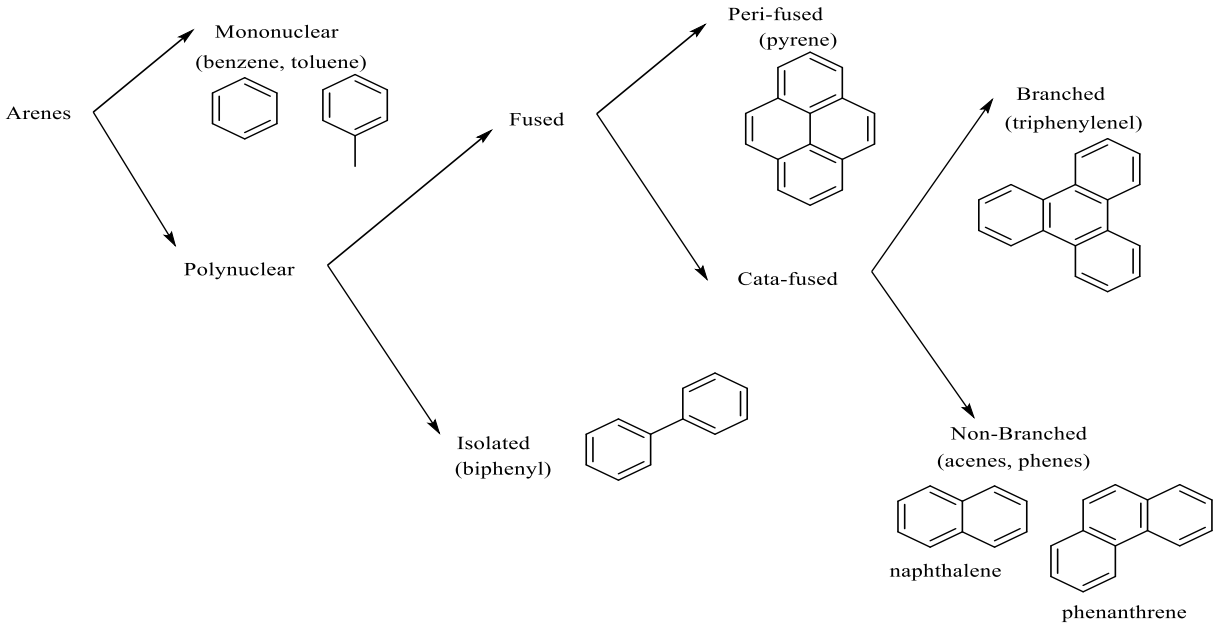

Figure 1.1: General categorization of arenes (examples are presented in brackets).

1.1.1 Linear Polycyclic Aromatic Hydrocarbons

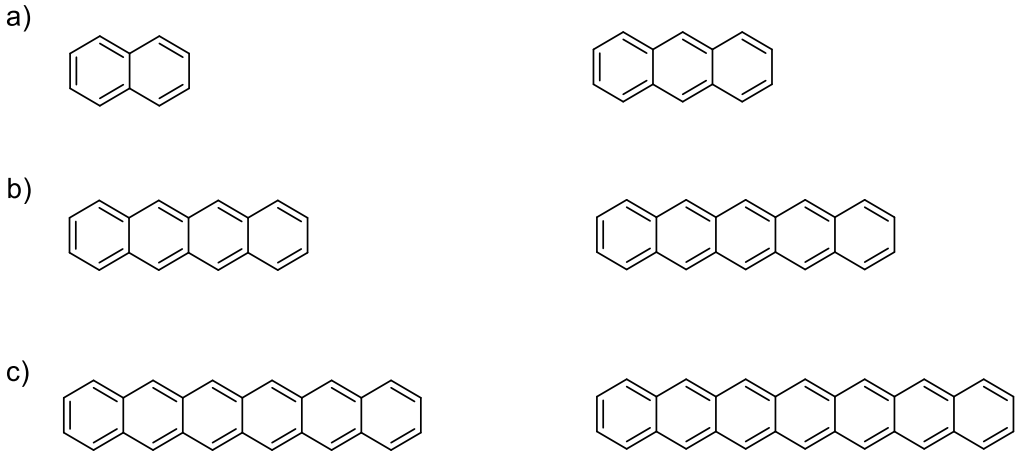

Figure 1.2: Common structures of acenes.

Linear PAHs involve all acenes that possess linearly fused aromatic rings such as anthracene ($C_{14}H_{10}$), tetracene ($C_{18}H_{12}$), and pentacene ($C_{22}H_{14}$). The smallest of such acenes is naphthalene, holding two aromatic rings, and anthracene, having three aromatic rings (Figure 1.2-a). They are commercially available since most of them are derived from coal tar products. They also can be synthesized from small arenes in multiple steps using different types of reactions. For example, anthracene could be obtained simply via the stepwise π-extension of benzene treated with phthalic anhydride using Friedel–Crafts acylation reaction, followed by reducing anthraquinone (Scheme 1.1).[9]

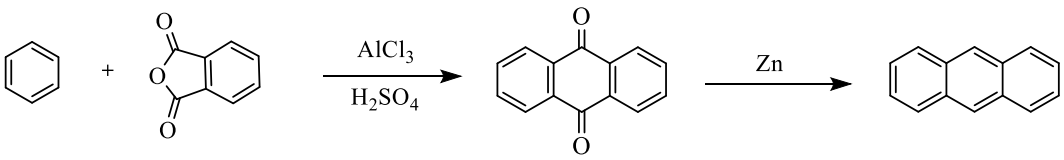

Scheme 1.1: Stepwise π-extension method for the preparation of anthracene.

Tetracene, consisting of four linearly-fused aromatic rings, and pentacene, having the five-ringed member of the series of benzene rings (Figure 1.2-b), can be isolated from diesel exhaust and charred food, respectively.[10] They also could be prepared from smaller arenes using several syntheses. For example, pentacene can be synthesised in multiple steps from *m*-xylene and benzoyl chloride by a sequence of Friedel–Crafts acylation reactions, followed by pyrolysis and oxidation (Scheme 1.2).[11]

These two particular compounds have been widely studied because they are determined to be excellent molecular organic semiconductors, and used most commonly in OFETs and OLEDs. Unlike anthracene, tetracene, or pentacene, larger acenes like hexacene and heptacene (Figure 1.1-c) cannot be found in petroleum resources or charred food; thus, they need to be synthesized.

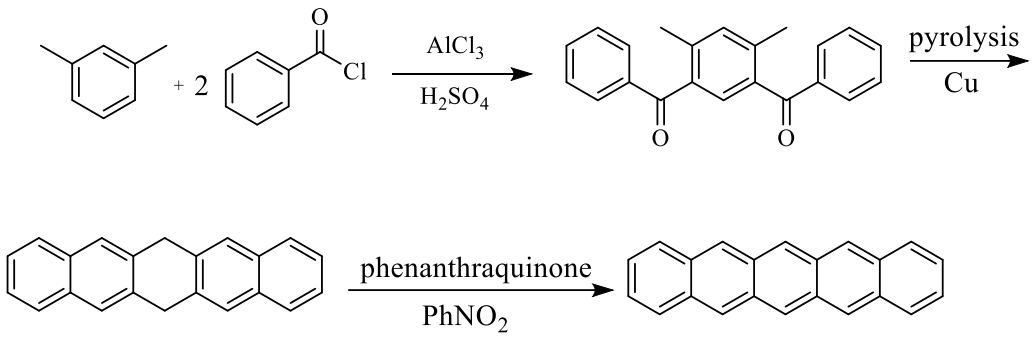

Scheme 1.2: Pathway for synthesis of pentacene.

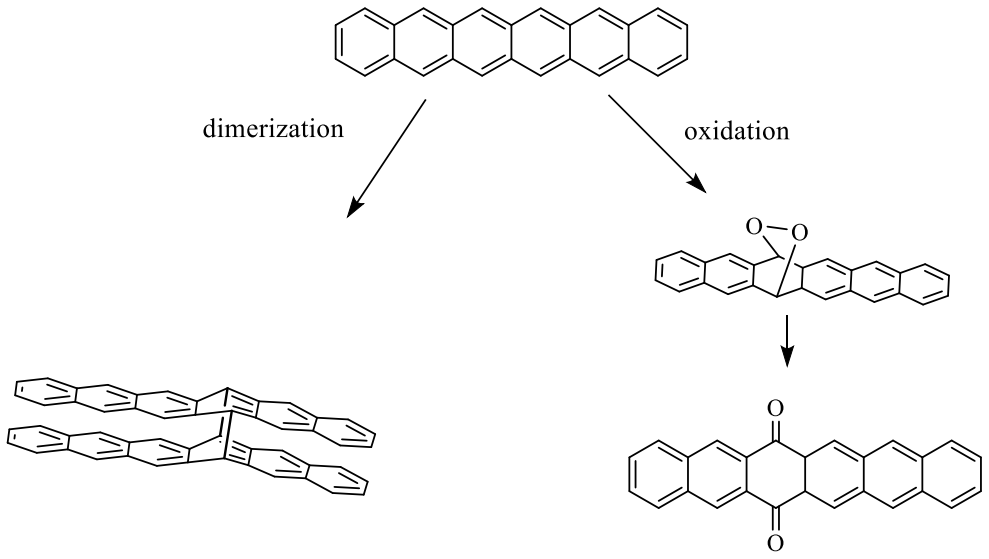

Figure 1.3: Decomposition of hexacene.

Although PAHs larger than pentacene have likely promising uses in electronic devices and can be highly useful in materials science, as the HOMO-LUMO band-gap decreases with increasing the length of acene, they are excessively sensitive upon exposure to air and light as a result of the lack of stability (very reactive in solution). For instance, decomposition can easily occur in hexacene due to photochemical dimerization or oxidation, indicating that hexacene is extremely unstable in solution due to air/light

exposure, leading to decomposition into the quinone and butterfly dimers (Figure 1.3).[12] Insolubility is an additional issue of larger acenes, so they tend to not dissolve in most organic solvents. These properties are undesirable when synthesizing acenes for applications in organic materials and devices, especially where the photophysical properties are of relevance, as the product properties differ from the parent acene, and could cause device degradation.

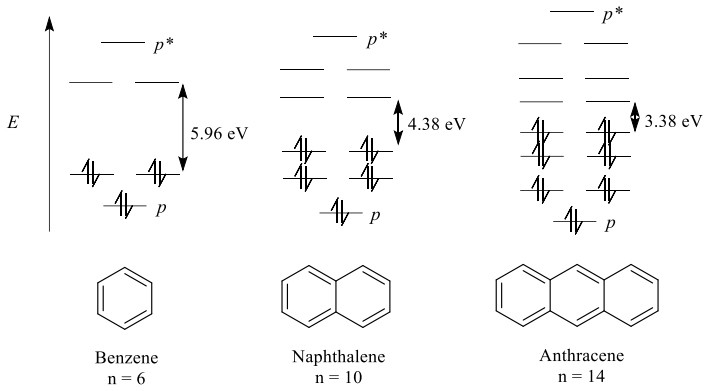

Figure 1.4: Molecular orbitals diagrams for the first three arenes, benzene, naphthalene and anthracene, and their HOMO-LUMO gap magnitude.

In general, as the number of linearly-fused aromatic rings increases, the energy gap between molecular orbitals (HOMO-LUMO gap) decreases, as illustrated in Figure 1.4. It can be clearly seen that as the number of the conjugated π-bonds increases, the energy of the HOMO-LUMO gap decreases. Since naphthalene has ten electrons in the π-system, only the five lowest energy (bonding) molecular orbitals must be filled. Moreover, it can be observed that the HOMO of naphthalene is higher than that for benzene, while the LUMO of naphthalene is lower than for benzene. Similarly, anthracene has higher HOMO and lower LUMO than naphthalene. This demonstrates that increasing the number of annulated benzene rings increases the number of molecular orbitals and decreases the HOMO-LUMO gap of the linear π-conjugated system. The next linear PAHs in this sequence, tetracene which holds a HOMO-LUMO gap of 2.71 eV, and pentacene which holds a HOMO-LUMO gap of 2.23 eV.[13] However, as already mentioned, increasing the number of linearly-fused aromatic rings may also reduce the stability and solubility of the π-conjugated systems.

1.1.2 Non-linear Polycyclic Aromatic Hydrocarbons

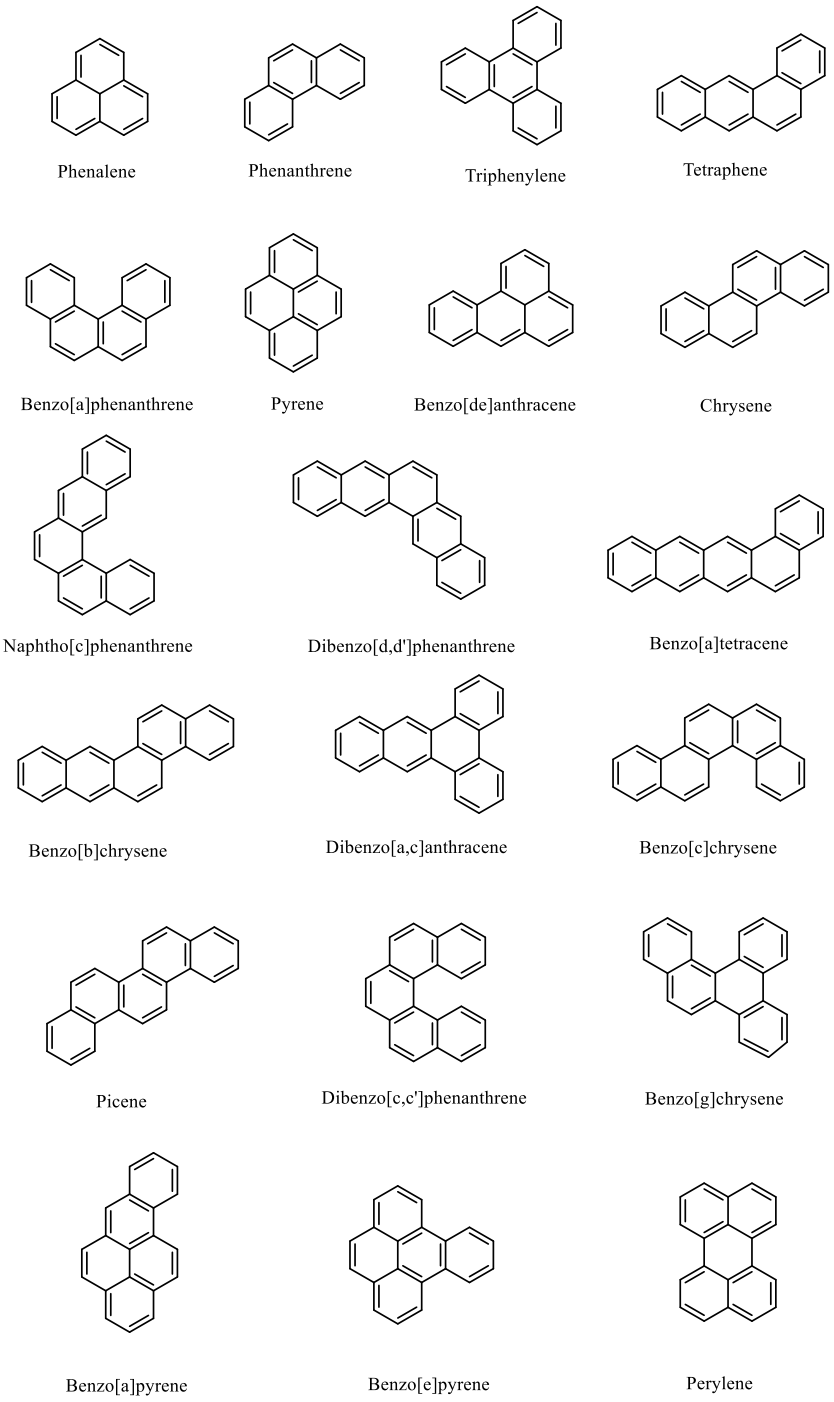

Figure 1.5: Several possible configurations of non-linear PAHs of ring count 3-5.

Non-linear PAHs can roughly be grouped into two main classes: cata-fused (branched, phenes) PAHs where no more than two rings share common carbon atoms and peri-fused (compact) PAHs where three rings share common carbon atoms (Figure 1.1). Examples of cata-fused PAHs are triphenylene, phenanthrene, tetraphene, benzo[a]phenanthrene, chrysene, naphtho[c]phenanthrene, dibenzo[d,d']-

phenanthrene, benzo[a]tetracene, benzo[b]chrysene, dibenzo[a,c]anthracene, benzo[c]chrysene, picene, dibenzo[c,c']phenanthrene, and benzo[g]chrysene (Figure 1.5). Examples of peri-fused PAHs include phenalene, pyrene, benzo[de]anthracene, benzo[a]pyrene, benzo[e]pyrene, and perylene (Figure 1.5). In general, non-linear PAHs are more stable than linear PAHs and consequently phenes, branched, or compact species would not undergo dimerization and oxidation unlike acenes. Compact PAHs are typically expected to have higher stability than non-compact PAHs with the same number of rings.[14] This refers to the absolute effect of electron delocalization throughout the entire system besides the strong aromatic bond between all adjacent carbon atoms.[15]

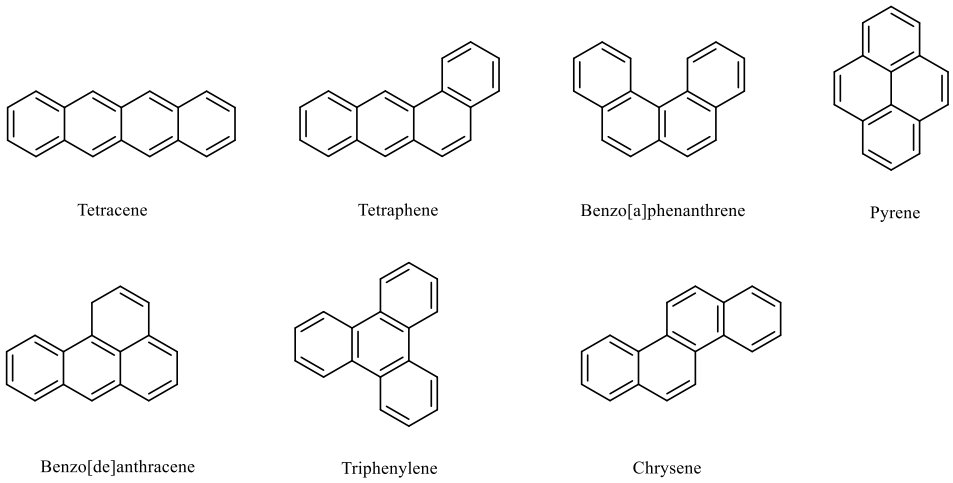

Figure 1.6: The diversity of PAH structures as displayed by the fusion of four benzene rings.

Based on the molecular structures, one class of PAHs may reveal much higher stability than other structures having the same number of rings. There are several thousands of PAH structures (approximately 20,600 possible alternating PAHs) as for systems having four to ten annulated benzene rings. The variety of enormous structures becomes clear if four benzene rings are directly condensed giving seven possible configurations namely tetracene, tetraphene, benzo[a]phenanthrene, pyrene, benzo-[de]anthracene, triphenylene, and crysene (Figure 1.6). However, they may not be isomeric despite them having the same number of cycles. To clarify, all cata-fused systems having the same number of cycles are isomeric as they have the same molecular formula $C_{4n+2}H_{2n+4}$ (where n = number of cycles). This is not in line with peri-fused systems which may hold different molecular formula. Therefore, the peri-fused

system pyrene ($C_{16}H_{10}$) is not an isomer of the cata-fused system tetracene ($C_{18}H_{12}$), neither is pentacene ($C_{22}H_{14}$) an isomer of perylene ($C_{20}H_{14}$). In order to gain a relatively clear picture about non-linear PAHs, we need to understand Clar aromatic π-sextet rule in many aspects.

1.1.3 Clar's Aromatic π-Sextet Rule

Hückel rule (4n+2), which states whether a monocyclic π-conjugated system is aromatic and hence stable or not, can only be applied to mononuclear aromatic structures like benzene. Clar π-sextet rule provides a qualitatively better understanding of stability for multi-ringed aromatic species. Clar's rule suggests that the Kekulé structural resonance with the highest number of isolated aromatic π-sextets will be the most substantial and thus most likely for the representation of properties of PAHs.[16] Aromatic π-sextet can be described as the localization of six π-electrons in one benzene ring separated from adjacent rings by carbon-carbon single bonds.[16,17]

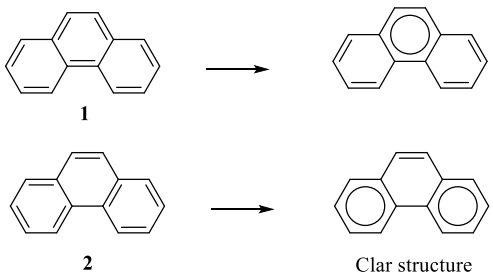

Figure 1.7: Two Kekulé resonance structures of phenanthrene and their analogical Clar structures marked with a circle.

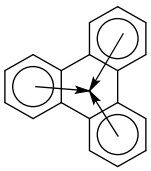

Figure 1.8: The Clar structure for triphenylene.

According to Clar's theory, the resonance structure of phenanthrene (**2**) in Figure 1.7 is more important than the resonance structure of phenanthrene (**1**). As a result, terminal rings in phenanthrene tend to have more local aromaticity than the centre ring. The structure with closed-shell configuration

and the maximum number of aromatic π-sextets is called Clar structure. Furthermore, Figure 1.8 displays the Clar structure of triphenylene, which is considered to be the most stable among its corresponding representations due to the fact that it possesses fully benzenoid species comparing to others that have less aromatic π-sextets.[16–18] The central ring, having a single double bond, can be named as "empty ring", whereas the outer rings can be called as "fully benzenoid".

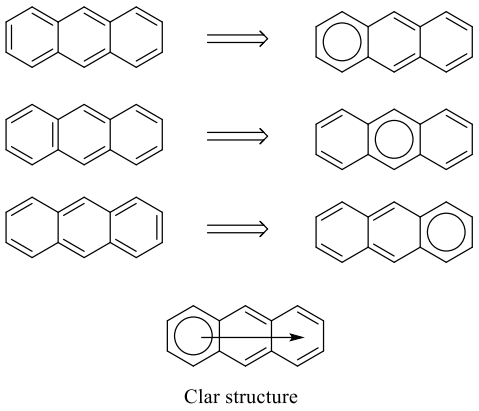

Figure 1.9: Several Kekulé resonance structures of anthracene and their corresponding Clar structures marked with a circle.

On the other hand, the chemical structures of acenes are mostly pictured with only one π-sextet as stated in Clar's rule. As for anthracene, there are three structures that share π-sextet "aromaticity" between the three rings as can be seen in Figure 1.9. All the three structures hold a unique Clar's sextet localized in a single benzene-like ring of the six-membered rings (6-MRs) that have two double bonds. This type of 6-MRs is called "migrating sextet".

Generally, as the level of rings extends in acenes, the number of π-sextet gradually decreases, explaining the decrease in stability. It has also been demonstrated that the central ring has the highest reactivity among the rest of 6-MRs of an acene. In this respect, cutting the conjugation of the central ring breaks the acene into two smaller acenes, each with more migrating sextet character than the parent acene, as has been previously confirmed in Figure 1.3.

The investigation of non-linear PAHs by Clar's rule has also shown that the kinked phenes are more stable than their linear PAHs isomers acenes.[19] For example, pentacene (**3**) and its isomer picene

(**4**) (Figure 1.10) both contain five aromatic rings. Picene (bandgap = 3.3 eV) exhibited a much higher stability and lower reactivity than pentacene (bandgap = 1.8 eV) since the resonance structure for picene allows for three aromatic sextets to be drawn, compared to a single migrating sextet for pentacene.[20,21] Moreover, the model proves that fully benzenoid non-linear PAHs (as in the case of triphenylene) present largest resonance energy, largest HOMO-LUMO gap, maximum first ionization potential, and least chemical reactivity.[19]

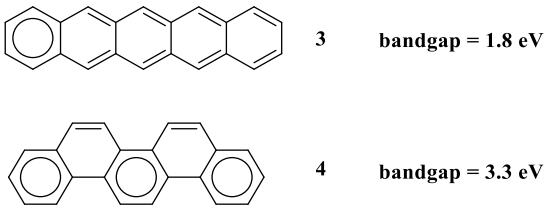

Figure 1.10: Clar structures for pentacene (**3**) and picene (**4**).

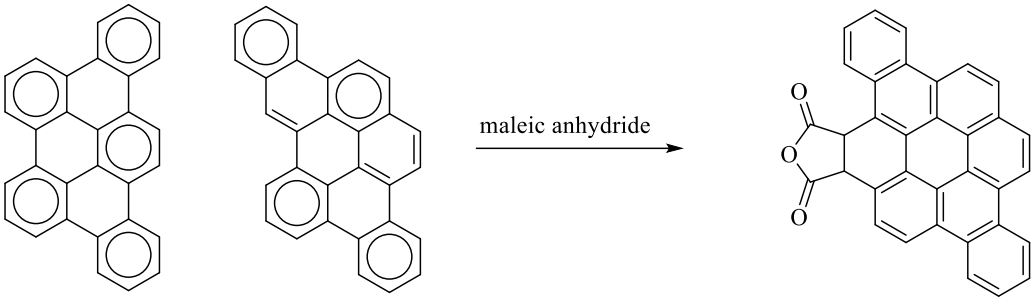

5 **6** **7**

Scheme 1.3: benzo[*qr*]naphtho[2,1,8,7-*fghi*]pentacene (**5**) and its corresponding isomer benzo[*qr*]naphtho[2,1,8,7-*fghi*]pentacene (**6**), illustrating that **6** is more reactive than **5**.

Interestingly, Clar and Zander found out that tribenzo[*b*,*n*,*pqr*]perylene (**5**) is more chemically inert than benzo[*qr*]naphtho[2,1,8,7-*fghi*]pentacene (**6**) which reacts with maleic anhydride to give the desired product (**7**), while **5** does not (Scheme 1.3).[22] The chemical inertness of **5** relates to the fact that **5** is completely benzenoid, and hence extremely stable unlike its isomer **6** that can behave as a diene in Diels-Alder reaction. For this reason, fully benzenoid compounds have large HOMO-LUMO bandgaps and thereby very stable.

Ultimately, Clar's rule, essentially developed for benzenoid species, has been successfully expanded in a further interesting class of complex components to characterize aromaticity as those found in aromatic cycles larger than 6-MRs and graphene derivatives.[23,24] Finally, various analysis methods of aromaticity have been investigated and their values measured in benzenoid species are quite proportional to Clar's rule. These local measures include the harmonic oscillator model of aromaticity, the *para*-delocalization index, and Nucleus independent chemical shift.[25–27]

1.1.4 Extension of π-Conjugation of Polycyclic Aromatics

Chemistry of PAHs involving their functionalization to improve solubility and stability is currently gaining growing interest.[28,29] Compared to traditional polyene and cyanine, PAHs can be regarded as promising materials in many areas because of their exceptional advantages such as low toxicity and ease of functional and tunable structure.[30–32] PAHs with larger π-conjugated systems exhibit remarkable physicochemical properties compared to small aromatics.[33–35] For instance, they show rigid π-π interactions, longer-wavelength absorptions and emissions, narrower HOMO–LUMO gaps, higher mechanical strengths, and lower oxidation and/or reduction potentials.[36,37] In addition, they can be considered as model components to understand the substantial property of the structure relationship of diverse macrocycles (e.g., graphene and its derivates[38], and porphyrin and its derivates[39]).

PAHs and heteroaromatics are the most common classes of polyaromatics compounds and they gain significant attention due to their tremendous applications in electronics, pharmaceuticals, and optoelectronic materials, considering their shape, size, and edge structure.[10,40,41]Accordingly, polycyclic aromatics are expected to be excellent candidates for near-infrared (NIR) dyes. Extension of π-conjugation of acenes plays an essential role in enhancing the absorptions into NIR region, indicating definite smaller HOMO−LUMO bandgaps.[42]

1.1.5 Large *π*-Systems with Near-Infrared (NIR) Absorption

Organic near-infrared (NIR) extended π-conjugated chromophores are compounds absorbing and emitting light in the NIR spectral region (beyond visible region) and typically ranging from 780 nm to 2500 nm

(120 to 400 THz).[43] Study on NIR materials (e.g. dyes and pigments) have received great attention due to their potential applications in different fields such as sensing, OLEDs, thermal writing displays, laser printers, bioimaging, and advanced optoelectronics.[44–47] NIR materials are also ideal candidates in the field of photovoltaics. Nearly 50% of sunlight radiation energy falls into the NIR spectral region, explaining that the development of photovoltaic materials can result in magnificent improvements in solar energy conversion.[48]

As has been mentioned before in section 1.1.1, the energy of the HOMO-LUMO gap decreases with increasing the extent of conjugation in acenes. Consequently, light of longer wavelength (and thus lower energy) is suitable to promote one electron from the HOMO to LUMO. The colour of organic compounds is highly influenced by the size of the conjugation in molecules.[49] Molecules with large π-conjugated systems absorb light at more red-shifted wavelengths (around visible region) and for this reason, they are often coloured.

1.1.6 Annulative PAHs π-Extension Reactions Promoted by Suzuki Cross-Coupling

In recent decades, palladium-catalyzed reactions are the most efficient processes to achieve aryl–aryl conjugated systems in different transformations in organic synthesis such as Negishi coupling, Stille coupling, Sonogashira coupling, Mizoroki-Heck coupling, and Suzuki-Miyaura coupling reaction.[50–54] C-C bond formation reactions are important key steps in constructing complex molecules in the field of organic chemistry. More recently, palladium-catalyzed Suzuki- Miyaura reaction, commonly known as "Suzuki coupling reaction", has become the most attractive cross-coupling methodology.[55]

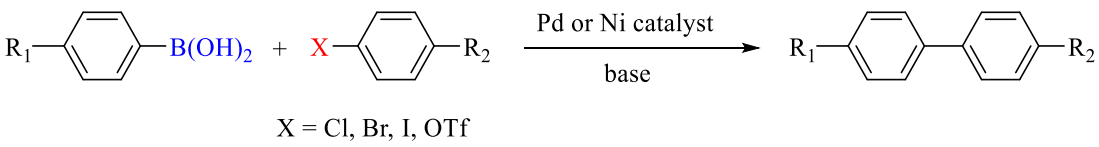

Scheme 1.4: Common Suzuki coupling reaction.

The Suzuki-Miyaura cross-coupling (SMC) reaction was first established by Akira Suzuki and Norio Miyaura in 1979.[56] The SMC reaction involves the cross coupling of organoboron reagents (e.g. boronic

acid) with aryl halides in the presence of a base using a palladium or nickel catalyst (Scheme 1.4). The SMC reaction provides several advantages compared to other related methods as its organoboron reagents are widely available, relatively stable when exposed to oxygen or heat, very selective, and environmentally friendly.[57,58] Additional features include mild reaction conditions, the boron-derived by-products are non-toxic and readily removed, high tolerance toward a variety of functional groups, the use of small quantities of catalysts, the reaction is unaffected in the presence of water, and the desired products can be gained in satisfying yields.[59–61]

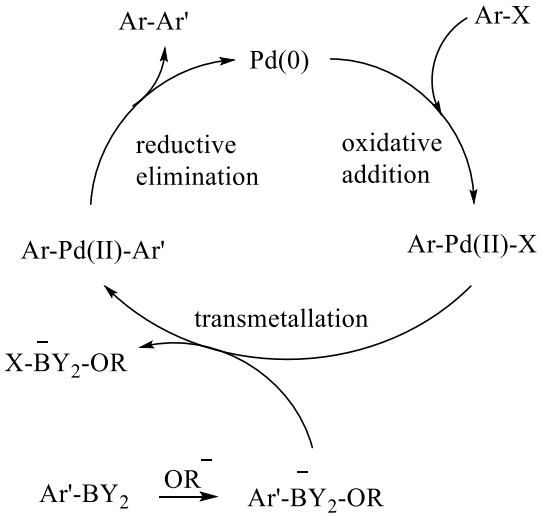

Figure 1.11: General Suzuki coupling catalytic cycle.

The known mechanism of palladium-catalyzed SMC reaction occurs sequentially through oxidative addition, transmetallation, and reductive elimination as depicted in Figure 1.11.[62–64] In the oxidative addition step, the aryl halide (Ar-X) is oxidatively added to the palladium(0) catalyst to form an intermediate of the arylpalladium(II) halide complex (Ar-Pd(II)-X). This step is often regarded as the rate-determining process in the catalytic cycle, therefore the reaction behaviour is more likely affected by the properties of Ar-X. The relative reactivity then decreases in the order X = I > OTf > Br » Cl. Aryl halides containing electron-withdrawing groups are more reactive to the oxidative addition than aryl halides containing electron-donating groups.[62] Transmetallation then follows between the organopalladium halide (Ar-Pd(II)-X) and the boronate anion $(Ar'\text{-}BY_2\text{-}OR)^-$ in the presence of a base giving the diarylpalladium(II) complex (Ar-Pd(II)-Ar'). Because organoboron reagents are highly

covalent in nature, transmetallation may not occur readily in the absence of a base. Hence, the chemical reaction of the organoboron compound (Ar'-BY_2) with the base (OR^-) to form (Ar'-BY_2-OR)$^-$ is of utmost importance. The last step is the reductive elimination step that leads to the formation of the carbon-carbon bond yielding the coupled product (Ar-Ar') and recovers the original Pd(0) catalyst.

1.1.7 Intramolecular Oxidative Cyclization (Scholl Reaction) of π-Conjugated PAHs

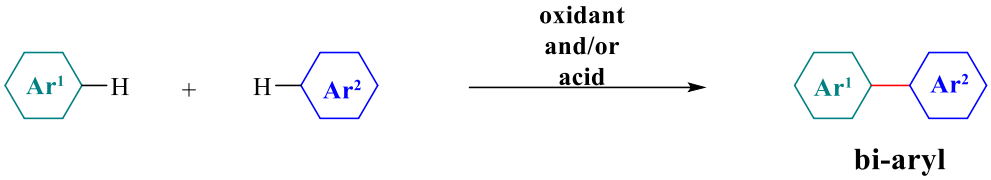

Scheme 1.5: General example of the intramolecular oxidative coupling (Scholl reaction), where an oxidant and an acid (Lewis or Brønsted) result in the formation of an aryl-aryl bond.

Over the years, a number of effective synthetic techniques for PAHs have been developed, including photochemical cyclodehydrohalogenation,[65] alkyne cyclization,[66] flash vacuum pyrolysis,[67] and Scholl reaction.[68] One of them, the Scholl reaction, or oxidative cyclodehydrogenation has been well-known for more than a century since the initial report by Scholl and Mansfeld in 1910.[69] It has been one of the most popular approaches to generate fused PAHs using an oxidant and an acid (Lewis or Brønsted) and involves the formal deprotonation and two-electron oxidation, leading to an intramolecular aryl-aryl bond, as shown in scheme 1.5 above. For instance, the Scholl reaction was used to produce structurally unique graphene nanoribbons with the formation of up to hundreds of C–C bonds in a single synthetic process.[70]

Mechanistically, two pathways have been proposed for the intramolecular oxidative cyclode-hydrogenation reaction: the arenium cation mechanism and the radical cation mechanism as demonstrated in Scheme 1.6 with the Scholl reaction of *o*-terphenyl as an example.[68,71,72] In both cases, the catalyst and oxidant drive cyclodehydrogenation, which results in the elimination of H_2 and the formation of a new C-C bond that leads to new aryl rings. In the arenium cation mechanism, the acid plays a significant role when a proton is added to an aryl moiety to generate a positive charge at the neighbouring position

(Scheme 1.6-a). This charge causes an interaction with the adjacent aromatic ring, resulting in the formation of a fused ring (dihydro intermediate) through two-electron oxidation and subsequently dehydrogenation. The majority of methods relating to this mechanism use strong Lewis acids such as $AlCl_3$ in chlorobenzene. Meanwhile, in the radical cationic mechanism, the oxidant first undergoes a one-electron oxidation of the phenyl group to form a new C–C bond with the neighbouring phenyl group, then undergoes an additional one-electron oxidation and dehydrogenation for the ring-closing (Scheme 1.6-b). Methodologies carried out for this mechanism involve the use of either strong oxidants like DDQ[72] or Lewis acids such as $FeCl_3$.[73]

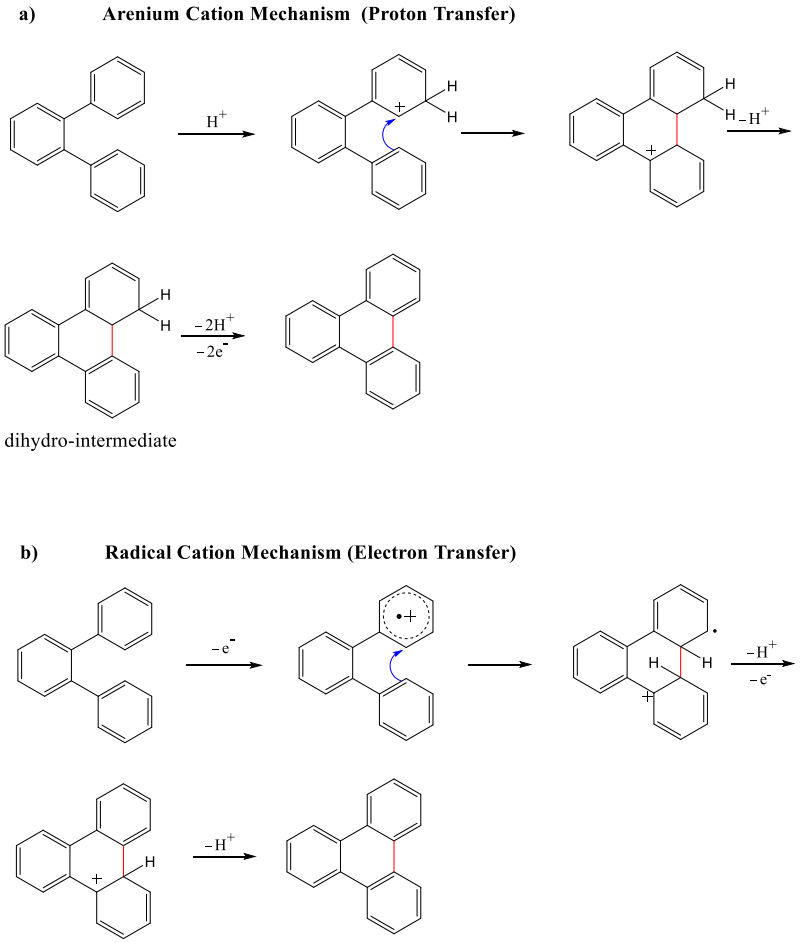

Scheme 1.6: Arenium cation (or proton transfer) (a) and radical cation (or electron transfer) (b) mechanisms for the Scholl reaction of *o*-terphenyl.

However, the exact mechanism outcome of the Scholl reaction is still unclear and poorly predictable. The selected mechanistic pathway can be affected by several variables, including the reagent

employed, the substitution positions, as well as electronic and steric effects, among others.[74,75] These reactions are thought to occur through the Scholl mechanism without any discrimination, which contributes to their ambiguity because there is insufficient proof of the operating mechanism. Moreover, most of the Lewis acids used in the Scholl reaction are also utilized as milder or stronger oxidants in oxidative aromatic coupling reactions, and that is one of the factors that contribute to this controversy. Therefore, it is still difficult to differentiate between these two possible mechanisms.

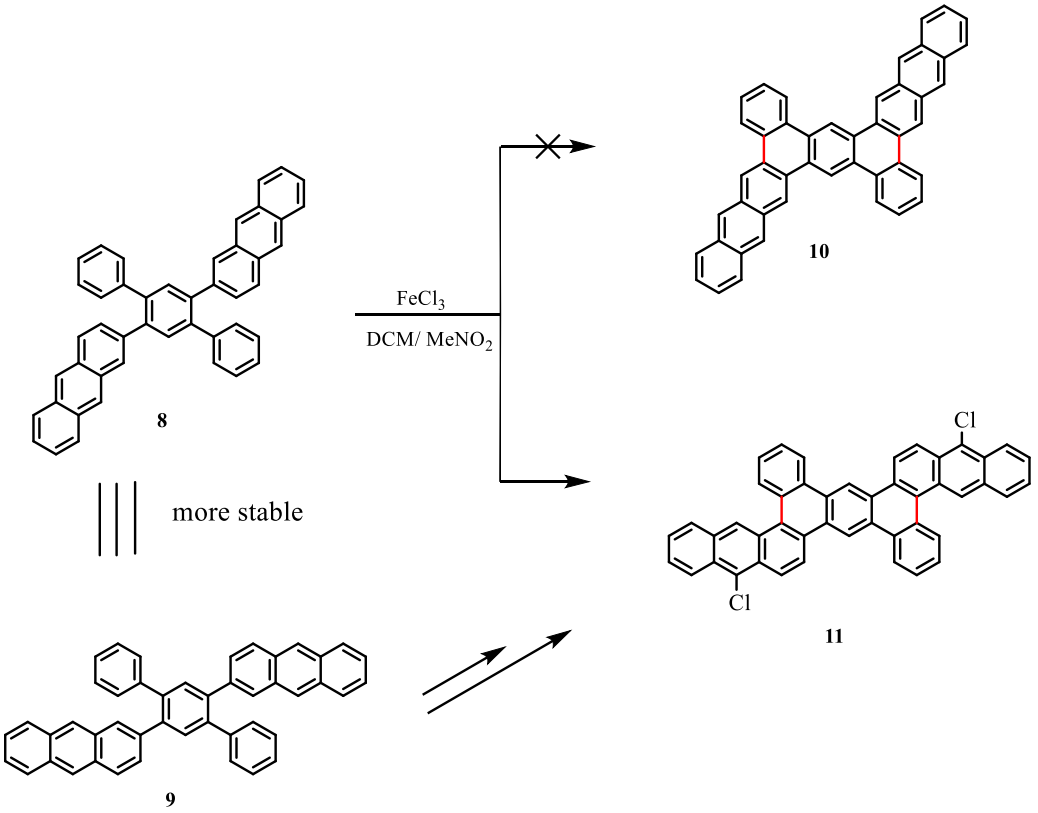

Scheme 1.7: An illustration of regioselective intramolecular oxidative cyclodehydrogenation. Component **8** reacts at the 1-position of the anthracene and chlorination takes place on the 10-position of the anthracene to produce **11** rather than **10.**

There have been some drawbacks and unintended consequences of using the Scholl reaction. Metal chlorides are among the Lewis acids/oxidants that are most commonly utilized for intramolecular Scholl reactions. One illustration of this is seen in Scheme 1.7, where the annulation of **8** occurs regioselectively in the 1-position of the anthracene unit and chlorination takes place on the 10-position of

the anthracene, resulting in **11** rather than **10**.[76] The authors rationalized the observed regioselectivities by the relative stability of the intermediates involved.

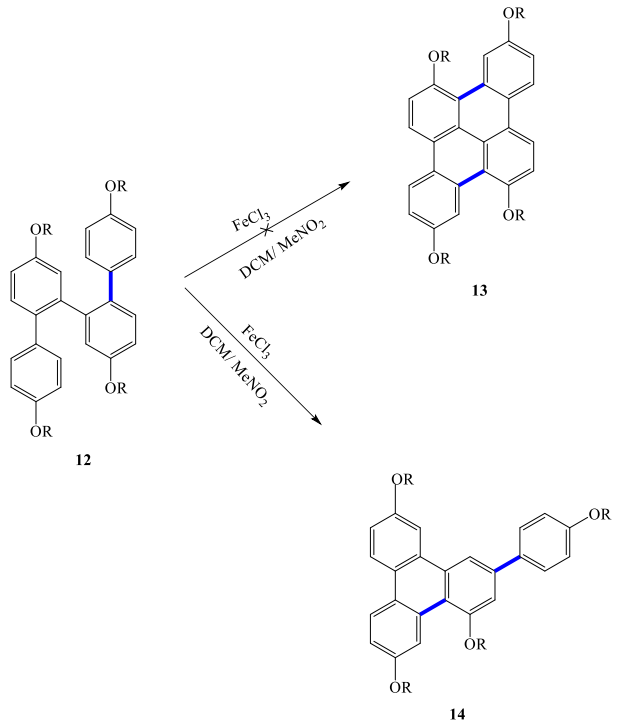

Scheme 1.8: Rearrangements of the *o*-phenylene tetramer. Direct oxidative cyclodehydrogenation toward **13** failed due to the backbone rearrangement producing **14**.

Rearrangements are also observed under Scholl reaction conditions, and they usually lead to the formation of five and/or seven-membered rings thereby discovering unexpected novel PAHs.[77–79] In fact, it has been found in various cases that oxidative cyclization is not as fast to occur as rearrangements.[80] For example, Hartley and coworkers have shown rearrangements in *o*-phenylene tetramer (**12**) in the presence of $FeCl_3$ in their investigation of oxidative planarization (Scheme 1.8). They observed that **12** underwent a single oxidative coupling affording **14** instead of the expected product hexacycle (**13**).[81]

Larger extended PAHs are of high interest for optical and electronic molecular materials since they are recognized as fragments of graphenes that possess a high degree of π-conjugated systems. There are tremendous applications for the expansion of PAHs ring systems using the SMC method in a diversity of fields such as synthetic chemistry, green chemistry, biological science, natural products,

pharmaceutical science, and material science.[9,63,82–85] The development of this approach enables the synthesis of several novel organic π-systems.

1.1.7.1 π-Extension of Pyrene

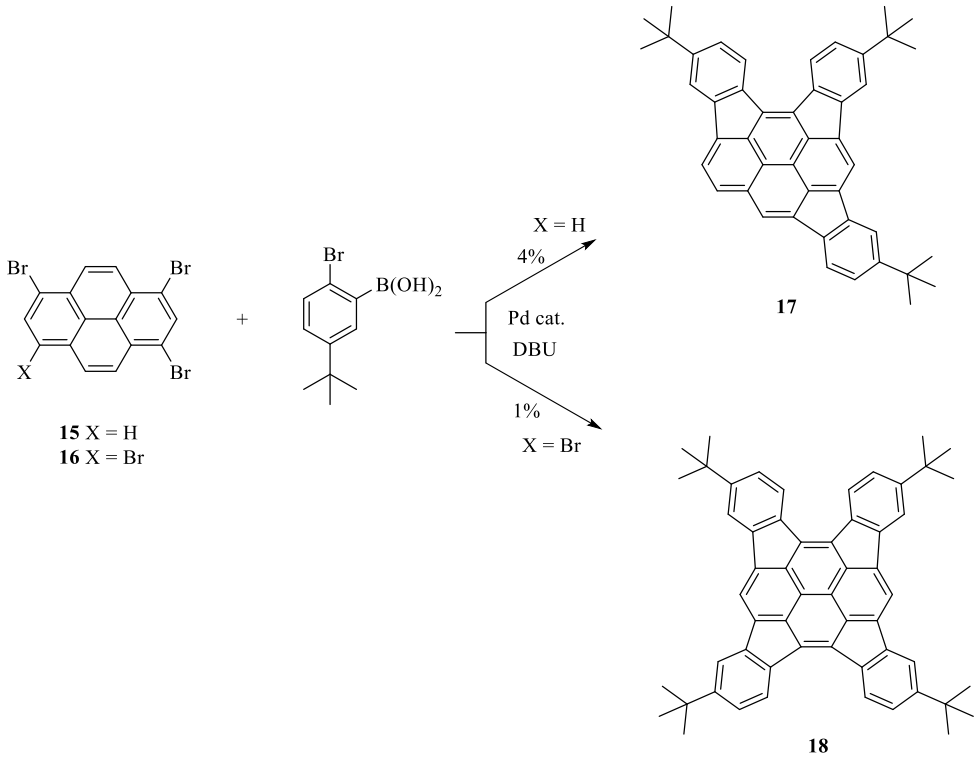

Scheme 1.9: The synthesis of triindenopyrene (**17**) and tetraindenopyrene (**18**) by SMC using a one-pot reaction.

In 2006, Scott and co-workers succeeded in the preparation of a new class of PAHs, oligoindenopyrenes, by the intramolecular palladium-catalyzed SMC arylation in one-pot method.[86] The reaction of the isomeric substituted pyrenes (**15** and **16**) in the presence of DBU as a base and $[PdCl_2(PPh_3)_2]$ as a catalyst gave triindenopyrene (**17**) and tetraindenopyrene (**18**) in low yields (Scheme 1.9). The incorporation of *tert*-butyl groups was to promote the solubility of the desired products. In spite of the low yields obtained, these oligoindenopyrenes displayed intense red colours and high thermal stability. The intense red colours, resulting from the high degree of π-conjugated systems, give these large non-linear indenopyrenes long-wavelength absorptions and make them attractive as perfect candidates for new dyes and photoelectronic devices.

1.1.7.2 π-Extension of Corannulene

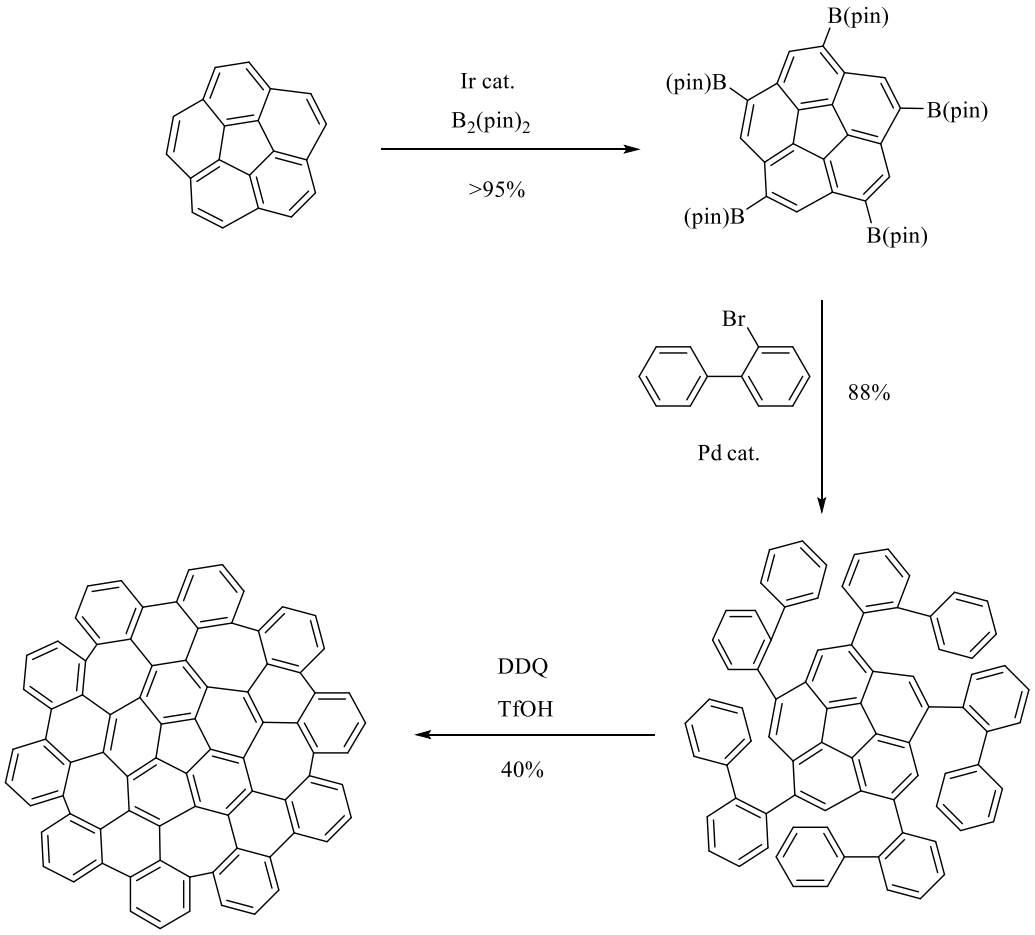

Scheme 1.10: The synthesis of distorted nanographene by the π-extension of corannulene.

The π-extension of the bowl-shaped PAH corannulene to form the carbon-rich distorted nanographene ($C_{80}H_{30}$) increases the number of atoms in the carbon lattice as well as the number of benzene rings from 6 to 26 in only two steps as illustrated in Scheme 1.10.[87] Corannulene was successfully functionalized as 1,3,5,7,9-pentakis(Bpin)corannulene by a five-fold C-H borylation. The resulting pentaboronate was then coupled with 2-bromobiphenyl using SMC reaction to afford the key intermediate 1,3,5,7,9-pentakis(2-biphenylyl)corannulene. An intramolecular oxidative cyclodehydrogenation of this intermediate with DDQ resulted in the formation of the warped nanographenes in moderate yield. Despite the stability and chirality of this distorted nanographene in the solid state, it exhibited some unusual properties such as solubility in common organic solvents, relatively large HOMO-LUMO bandgap (3.06 eV), relatively short wavelength absorption (λ_{max} = 418 nm), and green fluorescence (λ_{max} = 504, 535 nm).

1.1.7.3 π-Extension of Perylene

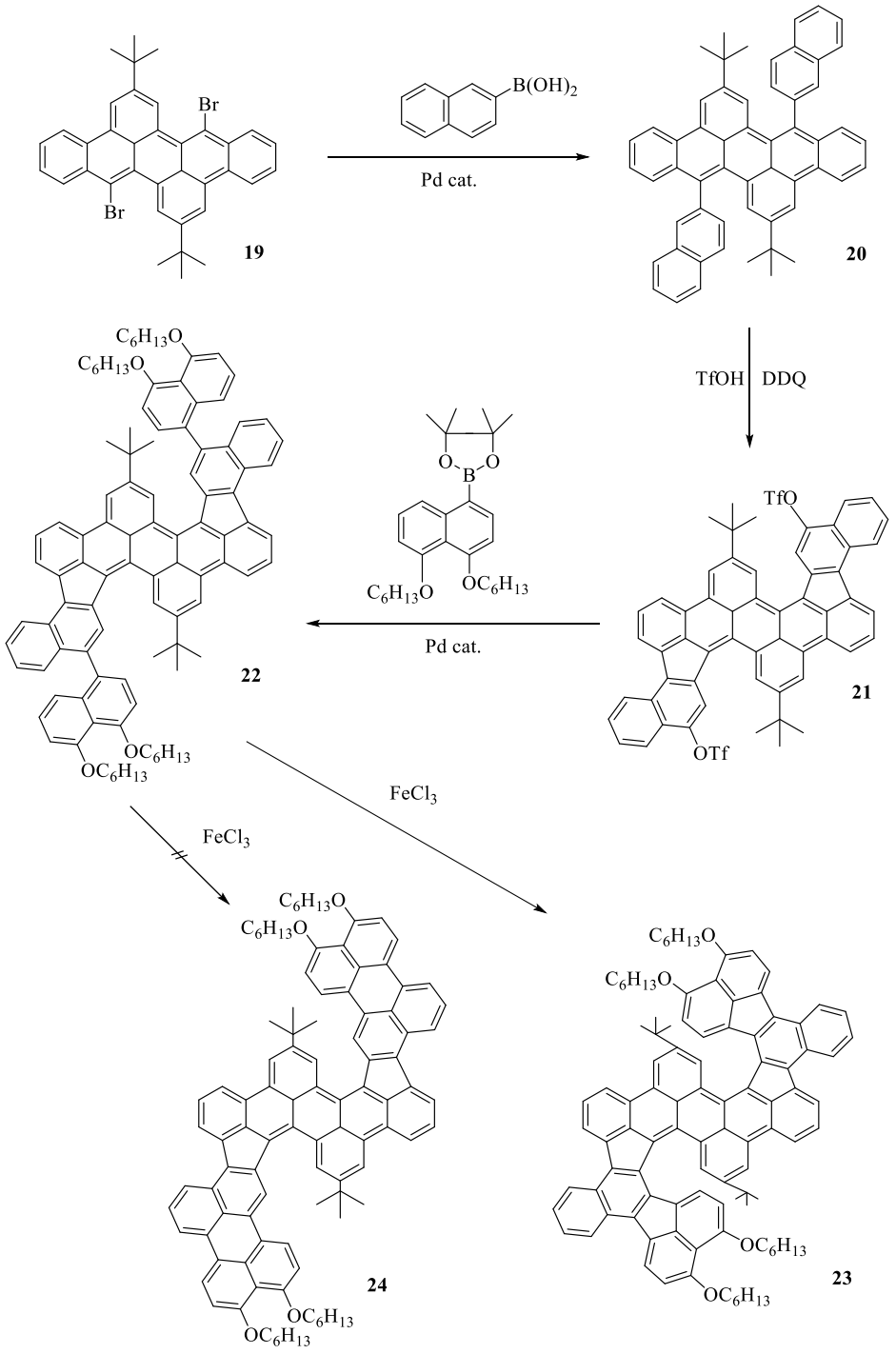

Scheme 1.11: Stepwise π-extension of substituted dibenzoperylene by the SMC approach.

Recently, a unique large extended PAH compound was generated by Mastalerz and coworkers, who performed the reaction from dibenzoperylene.[88] Their synthetic route was mainly controlled by two fundamental strategies; the SMC reaction and Scholl oxidation (oxidative cyclodehydrogenation) as depicted in Scheme 1.11. The substituted dibenzoperylene (**19**) was treated with 2-naphthylboronic acid

in a palladium-catalyzed SMC to give naphthyl-substituted dibenzoperylene (**20**). The resulting PAH **20** was then selectively oxidized with DDQ and triflic acid in one step cyclization-triflyloxylation-reaction affording the bistriflate (**21**), which underwent to another Pd-catalyzed SMC with dialkoxynaphthyl boronic ester, giving binaphthyl compound (**22**). Oxidizing compound **22** using $FeCl_3$ produced the contorted PAH (**23**) as a dark-red colour compound. Surprisingly, the proposed product of five-membered rings product **23** was formed instead of six-membered cyclized product (**24**). The PAH **23** showed remarkable red-shift absorption and emission spectra, compared to its parent PAHs (**20** and **21**), at 539 nm and 608 nm, respectively.

1.1.7.4 π-Extension of Benzene

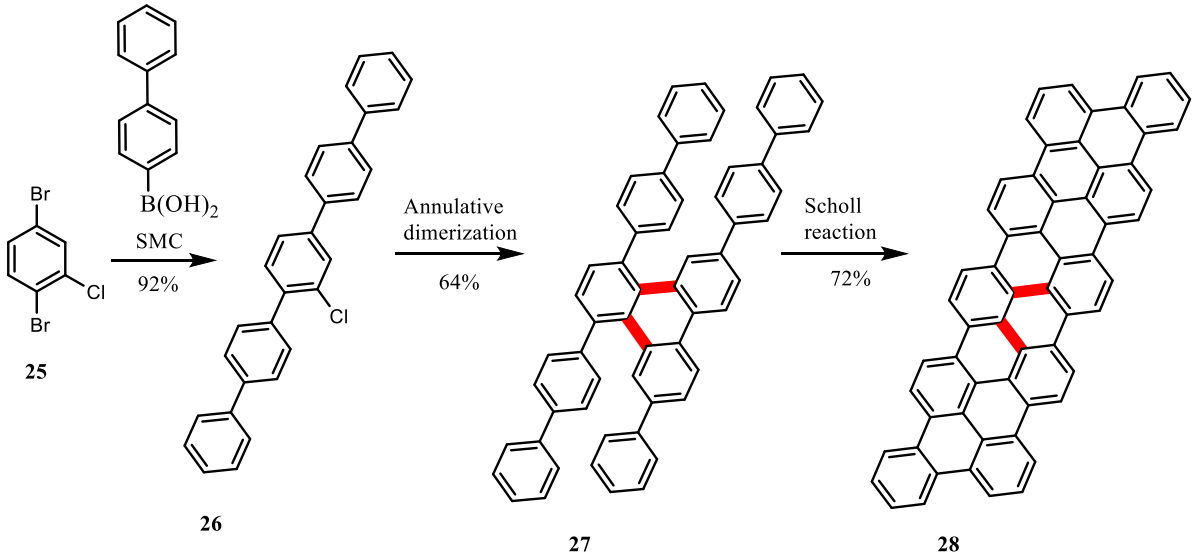

Scheme 1.12: Synthesis of graphene nanoribbon substructure using SMC, annulative dimerization, and Scholl reaction.

Another new approach that has allowed newfound access to structurally uniform nanographene is annulative dimerization. The Itami group developed a palladium-catalyzed double C–H bond activation method for the synthesis of triphenylene-cored fused aromatic π-systems (**28**), which are known as privileged structures for materials in OLEDs.[89] The synthesis of 60-carbon nanoribbon was obtained from 1,4-dibromo-2-chlorobenzene (**25**) in three steps (Scheme 1.12). The treatment of **25** with *p*-biphenylylboronic acid in the presence of a palladium catalyst using SMC afforded chloropentaphenyl

(**26**) in 92% yield. The palladium-catalyzed annulative dimerization of **26** furnished partially fused product **27** in 64% yield. Finally, the intermediate **27** underwent oxidative cyclization on treatment with $FeCl_3$ in dichloromethane to give the small graphene nanoribbon segment ($C_{60}H_{26}$) **28** with good yields (72%).

1.1.7.5 π-Extension of Anthracene

Very recently, both monomer and dimer syntheses were investigated by Tsurumaki and coworkers.[90] In these systems, the anthracene and benzene units were connected in a coplanar fashion to maximize the π-conjugation using the SMC and Scholl reaction. For the preparation of monomer, the Suzuki coupling of dibromoanthracene (**29**) and boronate **30** afforded the intermediate **31**, which was then reacted with 3 equiv. of DDQ in the presence of TfOH in DCM at 0 °C for 10 min to give the monomer **32** in 82% yield (Scheme 1.13). The absence of isomer **33** is due to the steric hindrance between the *t*-butyl groups.

For the synthesis of the dimer, the Suzuki coupling of **29** and **30** in 1:1 ratio gave compound **34**, which was then coupled with diboronate **35** to generate **36**. This precursor underwent the Scholl reaction and reacted with 6 equiv. of DDQ at 0 °C for 10 min giving the single product **38** (78% yield), in which the central phenylene unit remained unreacted. When the reaction was carried out at 20°C for 10 min, the structure was fully cyclized to obtain the dimer **37** in 71% yield. The absorption spectrum of **32** showed a broad band from 400 to 500 nm, while the absorption band of **37** (623 nm) was significantly red shifted as the rubicene structure was extended. The emission maxima of **32** and **37** exhibited broad bands at 572 and 650 nm, respectively. Subsequently, the π-conjugation was substantially extended in a trimer system displaying characteristic blue absorption and dark-red fluorescence that extended into the near-IR region.

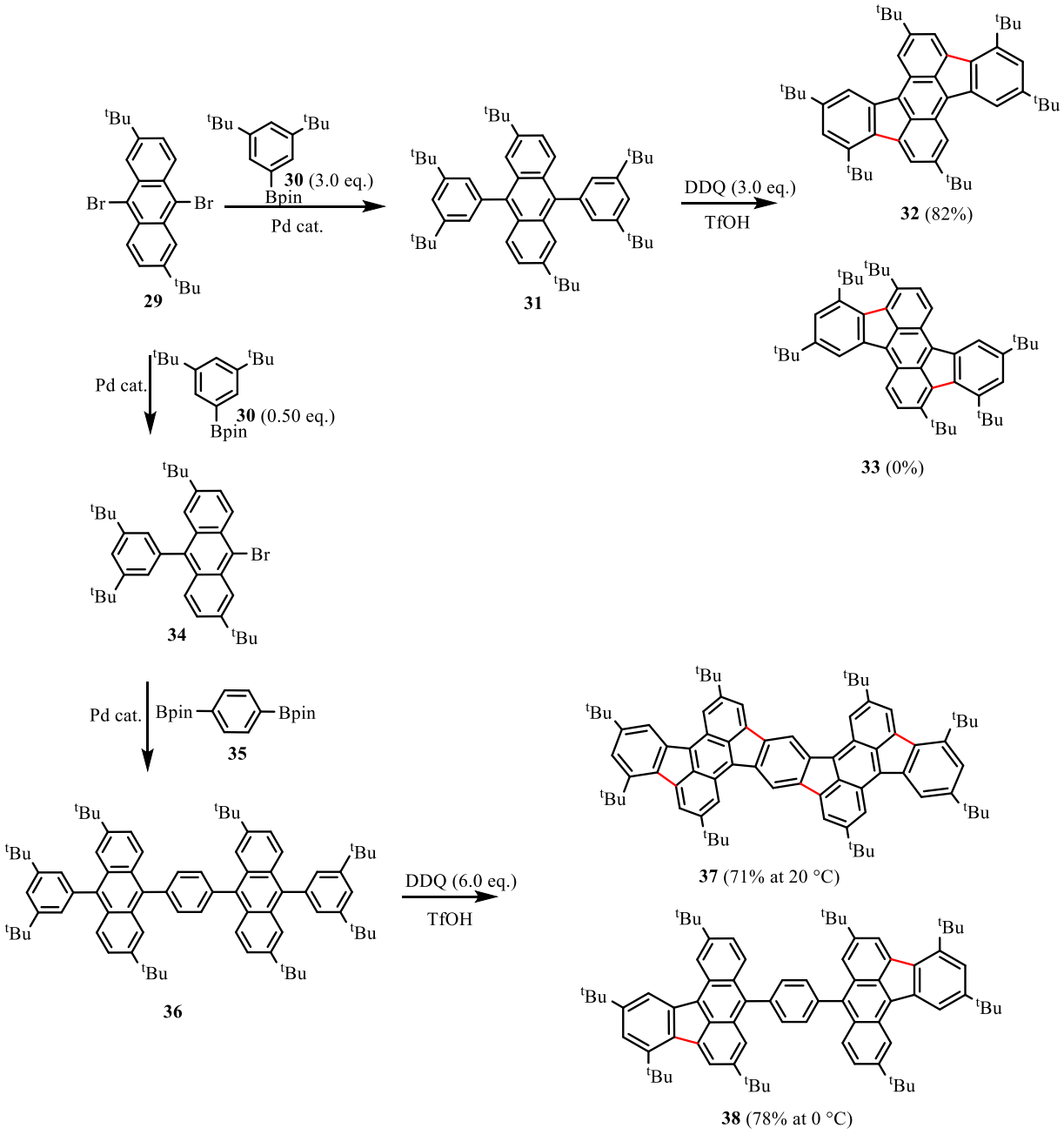

Scheme 1.13: Synthesis of monomer **32** and dimer **37** from dibromoanthracene **29** using SMC and Scholl reaction.

Results and Discussion

2.1 Aim

The overall objective of this project is to synthesise and design a unique lateral structure by assembling fundamental three-ring aromatic units – anthracenes - into more complex arrangements. In particular, we aim to annulate more than two functionalized anthracene cores together in a stepwise manner by extending the conjugation of the π-systems *via* a Suzuki coupling reaction and Scholl reaction.

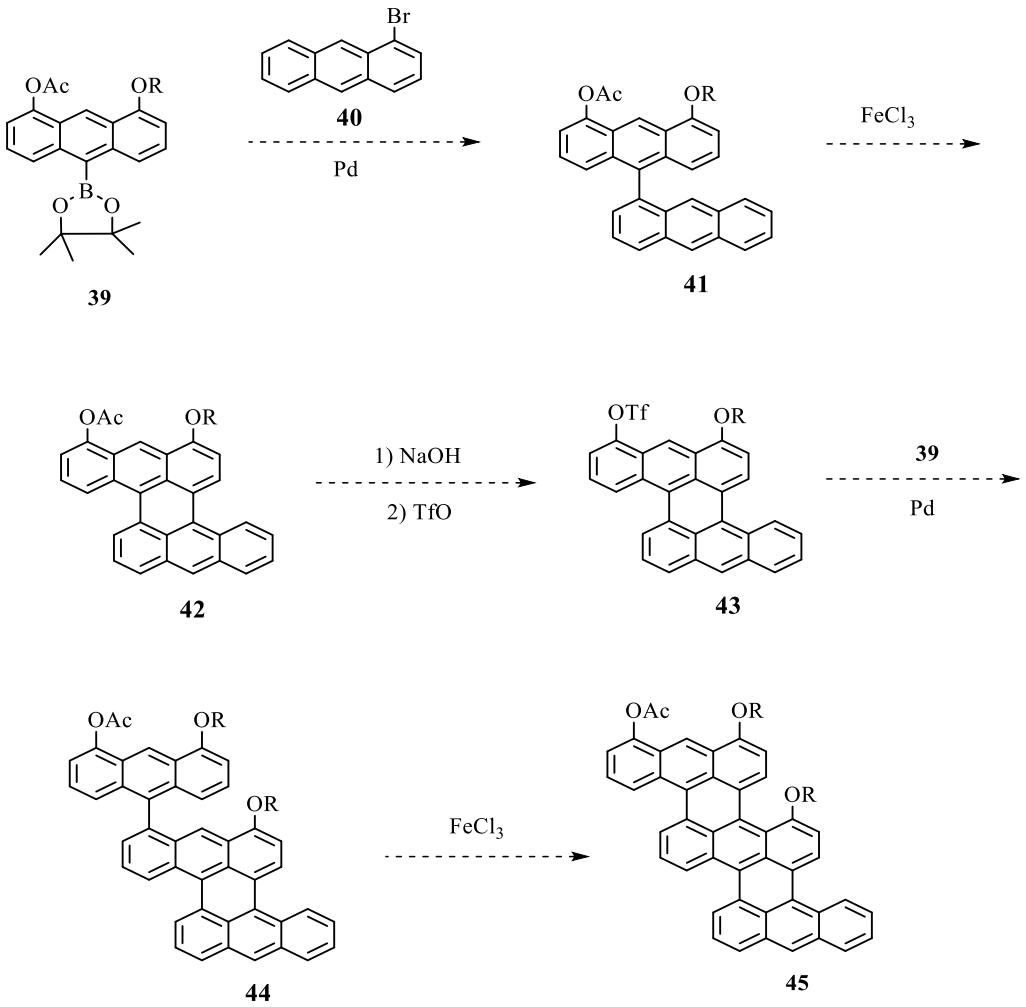

Scheme 2.1: Proposed synthesis for the formation of staggarene using SMC and Scholl reactions. R represents solubilising alkyl side-chains.

The proposed pathway for the synthesis of three fused anthracene units is illustrated in Scheme 2.1. Treating the anthracene boronic ester (**39**) with bromoanthracene (**40**) using Suzuki coupling would result in anthracene linked to anthracene (**41**). Dehydrogenation of the coupled unfused anthracene units

by iron(III) chloride would give the first target anthracene fused anthracene (**42**) in a stepwise lateral pattern. The resulting compound **42** would undergo hydrolysis of the acetoxy group, followed by regioselective triflation to produce PAH compound (**43**). An analogous coupling approach will be carried out between the resulting product **43** and the anthracene boronic ester **39** to give dibenzoperylene linked to anthracene (**44**), which can undergo oxidative ring-closure reaction by iron(III) chloride to afford the second target triply fused anthracene (**45**) in a stepwise lateral manner.

The targeted PAH compact compound **45** may be recognized as a structure cut out of graphene and can be called "a staggarene". Indeed, the annulation of anthracene units in a lateral position is an appealing target; the stepwise extension of the π-conjugated systems laterally suggests the structure is likely to adopt a staggering geometry that can be an ideal candidate for optoelectronic materials. However, the target molecule can be synthetically challenging due to the need for stepwise procedures including the preparation of functionalized anthracene components.

It is hoped that synthetic routes likely to be successful in the synthesis of a framework composed of two fused anthracene units would enable a pathway to be found to a framework composed of multiple fused anthracene units. Generally, compact PAHs tend to have higher stability than linear and non-compact PAHs with the same number of rings. Thus, the aim of this study is to design a family of multiple fused anthracene units and investigate their electronic and optical properties.

2.2 Strategy 1

2.2.1 Synthesis of 1-Acetyloxy-8-hexyloxy-10-Anthracenyl(Pinacol)Boronate Ester

Scheme 2.2 outlines the present synthetic approach to the anthracene boronic ester **39**. In order to avoid regioselectivity issues in activating 4- and 5- positions of an anthracene during bromination, the presence of electron donating alkoxy groups at the 1- and 8- positions of the anthracene should be avoided (Figure 2.1). The existence of alkoxy groups at the 1- and 8- positions was found to increase the reactivity of the *para* positions for these substituents, which may activate 4- and 5- positions towards bromination, thereby leading to other undesired multiply brominated products.[91] As a result, the attachment of poorly electron

donating substituents (acetoxy groups) at the 1- and 8- positions was necessary to achieve regioselective mono-bromination at the 10-position of the anthracene.

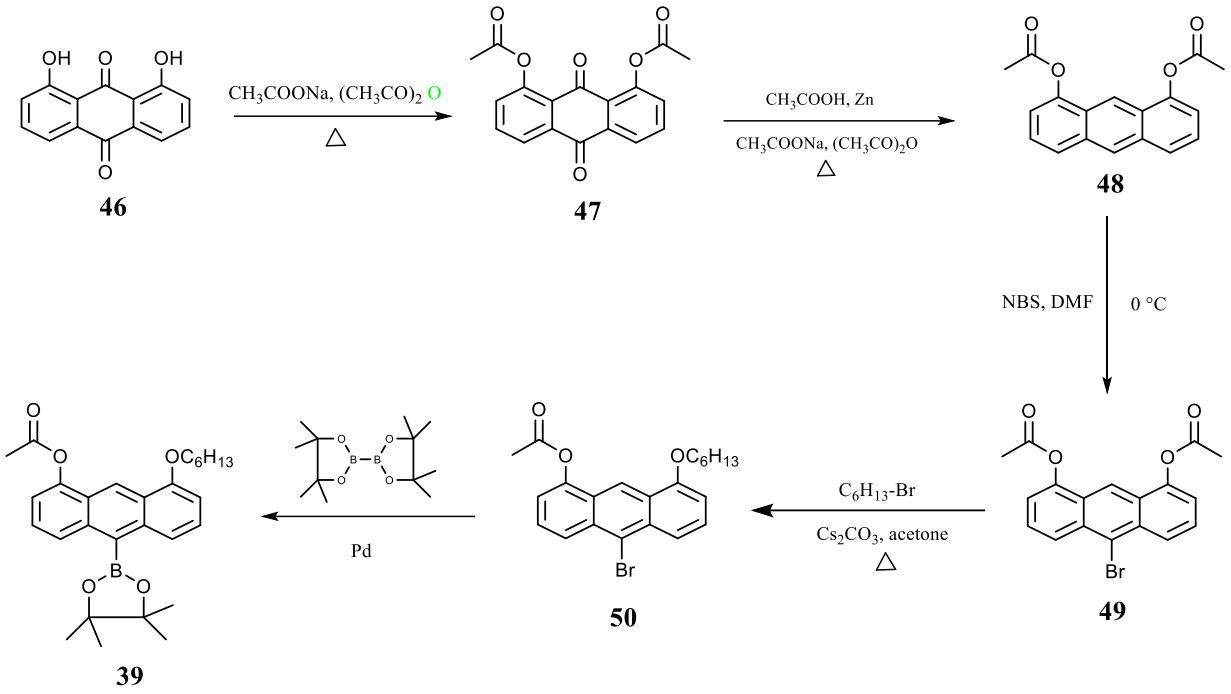

Scheme 2.2: Proposed synthetic route to the substituted anthracene boronic ester. R represents solubilising alkyl groups.

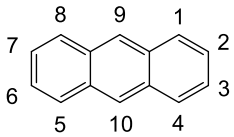

Figure 2.1: Numbering in anthracene.

1,8-diacetoxyanthraquinone (**47**) was prepared according to the procedure developed by Sundermeyer and coworkers,[92] which includes acetylation of commercially available 1,8-dihydroxyanthraquinone (**46**) with a small amount of sodium acetate in acetic anhydride at elevated temperature. Quenching the resulting solution with water furnished the product **47**. The acetoxy groups were introduced with high yields up to 98%. Besides the high yields, there were additional advantages of this procedure including that neither inert gas was needed, nor chromatographic purification was required, and nor recrystallization was necessary.

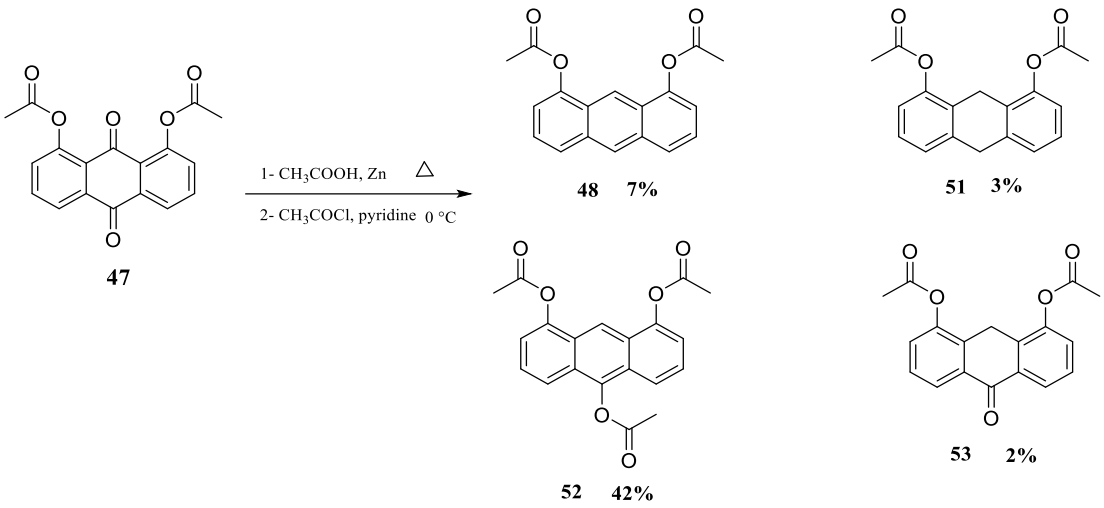

Scheme 2.3: The formation of several products from 1,8-diacetoxyanthraquinone.

The next step performed was the reduction of anthraquinone **47** to 1,8-diacetoxy-anthracene (**48**). This required large amounts of zinc dust according to a modified literature procedure.[93] Initially, **47** was heated at reflux in glacial acetic acid until the mixture became a clear solution. To this solution, 3 eq. of zinc was carefully added and the mixture was kept refluxing for 3 h, followed by adding a gradually increasing amount of zinc. The reaction was continuously monitored by thin-layer chromatography (TLC) which displayed several spots at the end of the reaction after 8 hours. The reaction mixture was then cooled to rt. and passed through a short silica plug with EtOAc to remove the remaining zinc powder and zinc salts. The solvent was removed by evaporation. Because of the full deacetylation occurring concomitantly with the reduction of quinone, the resulting mixture was directly subjected to acetylation again using acetyl chloride in the presence of pyridine. The products were analysed by NMR spectroscopy after chromatographic separation. Notably, 1,8,10-triacetoxyanthracene (**52**) was found as the major product, while 1,8-diacetoxy-10(9H)-anthrone (**53**) was obtained in trace amounts (Scheme 2.3). The desired product **48** was obtained as a mixture with 1,8-diacetoxy-9,10-dihydroanthracene (**51**) in a ratio of 1:0.5 according to ^{1}H NMR spectroscopy (Figure 2.2). Recrystallization from *i*-PrOH was not enough to remove of the side product **51**. In an attempt for optimization, this reaction was carried out using acetic anhydride and sodium acetate in the acetylation step, but there was no significant change in

the outcome. This indicates that the amount of zinc used for this procedure was insufficient to reduce the anthrone moieties apart from the over-reduced side product **51**.

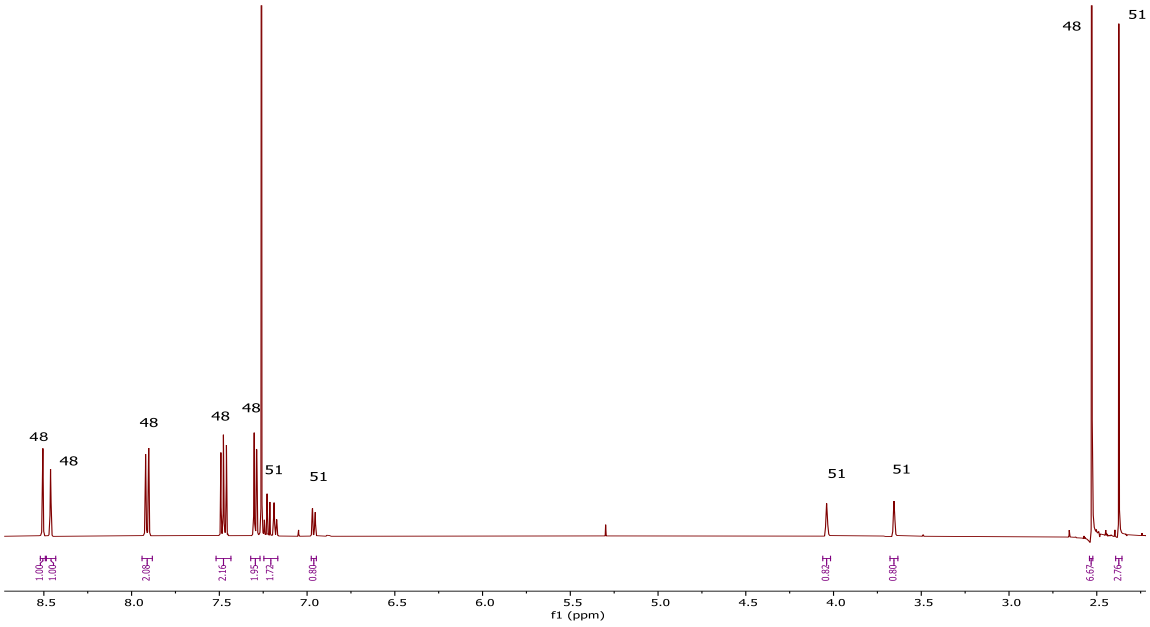

Figure 2.2: ^{1}H NMR spectrum (400 MHz, $CDCl_3$) of the inseparable mixture of compound **48** and compound **51**. Peaks are labelled with the corresponding compound numbers.

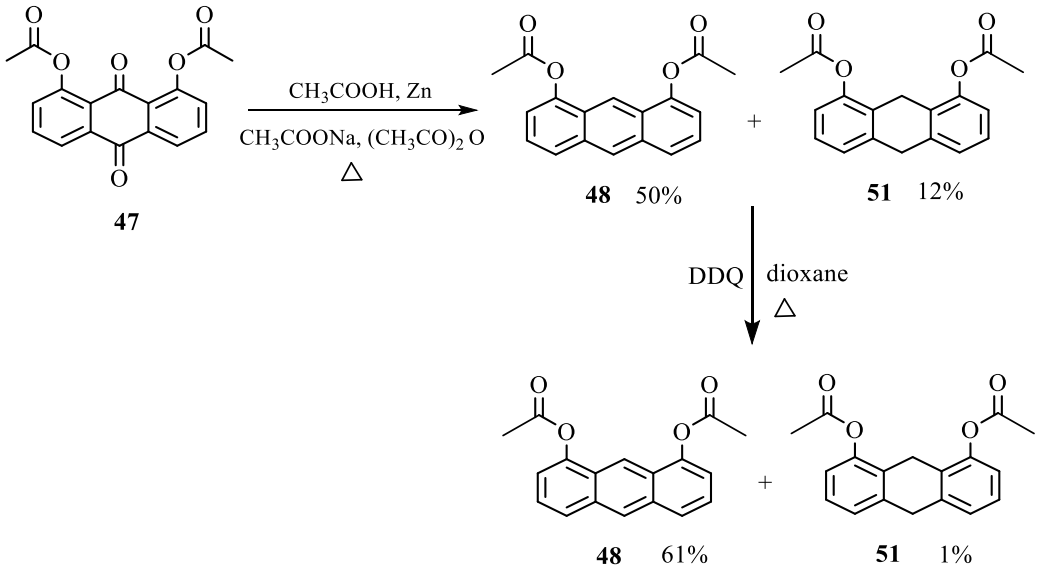

Scheme 2.4: An alternative route for the purification of 1,8-diacetoxy-anthracene **48**.

We therefore had to find another method in order to optimize the reaction conditions. The other method, involving the substrate **47** combined simultaneously with acetic acid, acetic anhydride, sodium

acetate, and zinc powder (9.5 eq) leading to **48** (Scheme 2.4), had already been reported.[94,95] According to ^{1}H NMR analysis, the products observed after chromatographic purification include triacetate **52** as a minor product and a mixture of **48** and **51** in a ratio of 1:0.4 with ~29% isolated yield. Although the product was still an inseparable mixture, this approach proved to be more effective and was therefore investigated further. Attempts to further optimise the reaction were performed using excess of zinc to reduce as much of the undesired product **52** as possible. Increasing the equivalents of zinc up to 18 led successfully to the desired product **48** mixed with the over-reduced side product **51** in a higher isolated yield up to 62% and molar ratio 1:0.2 determined by ^{1}H NMR spectroscopic analysis.

Unfortunately, when the reaction was performed on a larger scale, the overall yield of the mixture of **48** and **51** dropped from 62% to 41% and the amount of **52** was again increased. As a result, it was necessary to activate the zinc dust to improve the reaction by stirring 200 g of Zn dust vigorously in HCl solution (500 mL, 2%) for 5 minutes and then decanting it off. This process was repeated a second time, then 3 times with water and twice with absolute ethanol. Finally, the zinc was washed with diethyl ether, filtered, and dried under vacuum for 24 h. The resulting dust was stored under vacuum. Consequently, carrying out the reaction on a larger scale using freshly activated zinc dust improved the overall yield of the mixture of **48** and **51** up to 60%. Additionally, the isolated triacetate **52** was further reduced to **48** after 24 hours when the activated zinc was used.

Purification using column chromatography along with recrystallization from different solvents such as *i*-PrOH and DCM/MeOH was inefficient to remove the undesired side product **51**. For this purpose, a suggestion was made that a powerful dehydrogenating agent (e.g. DDQ) was necessary.[96,97] Fortunately, treatment with DDQ in dry dioxane transformed the mixtures of **48** and **51** (1:0.2 ratio) into a nearly complete conversion to **48**, increasing the ratio up to 1:0.01 according to the NMR spectroscopic analysis (Scheme 2.4). The yield of **48** was calculated as 61%.

By applying standard bromination conditions using a modified literature procedure,[98] diacetoxyanthracene **48** was reacted with NBS in DMF under inert gas at low temperature, and the

reaction was monitored by TLC until all starting material disappeared. After 5 h it showed a new single spot of 1,8-diacetoxy-10-bromoanthracene (**49**) (Scheme 2.5) However, the ^{1}H NMR spectroscopic analysis showed an undesired minor side product that cannot be observed in the TLC analysis and could not be identified by ^{1}H NMR and mass spectrometry. MALDI-TOF MS analysis showed the correct molecular mass but another isomer could have been formed. The isolation of pure bromide **49** proved to be exceedingly challenging since the recrystallization from *i*-PrOH and DCM/MeOH was inefficient. An effort was made to find the proper solvent system to separate the desired product **49** using column chromatography but unfortunately all systems used led to an unsuccessful separation. This reaction was carried out several times using different conditions and different amounts of **48**. The inseparable mixture (green product) was typically obtained in only 21-31% yield. However, when the reaction was scaled up, the yield was improved to 62% but careful monitoring of TLC was required. This was used for the next step as a mixture of **49** and the unknown compound.

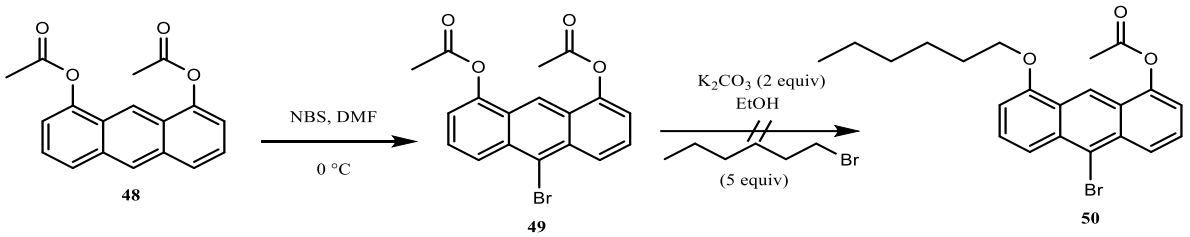

Scheme 2.5: An unsuccessful attempt to produce the mono-hexyloxy anthracene **50** from 1,8-diacetoxy-10-bromoanthracene **49**.

In an initial attempt to obtain 1-hexyloxy-8-acetoxy-10-bromoanthracene (**50**), **49** was reacted in ethanol under reflux with an excess of 1-bromohexane and potassium carbonate in air (Scheme 2.5). Several attempted reactions have been made in various conditions by testing compound **48** instead of compound **49** to obtain the required mono-acetoxy group. Even though **49** was practically easier to handle than **48**, we preferred to test the proper conditions using compound **48** since it has a similar chemical structure and more importantly was more readily available.

Alkylation to form the corresponding 1-hexyloxy-8-acetoxyanthracene (**54**) was one of the most challenging parts of the synthesis (Scheme 2.6) and an effort was made to improve the yield under inert gases as shown in Table 2.1. It can be noticed from the table that the optimization was performed by varying the solvent and testing the effect of two bases. Treating **48** with 1-bromohexane using different bases under reflux and room temperature in ethanol led to decomposition in a short time (Table 2.1, entries 1-3).

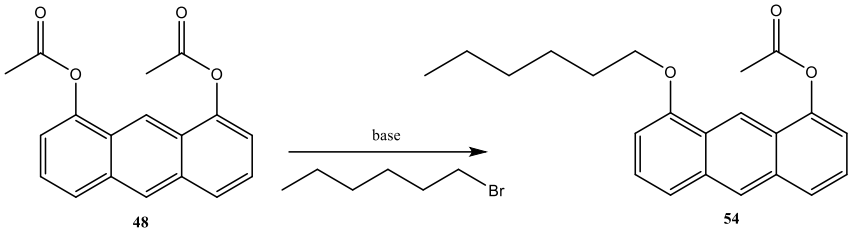

Scheme 2.6: An attempt to produce the mono-hexyloxy anthracene **54** from 1,8-diacetoxyanthracene **48**.

Entry	Base (equiv)	1-Bromohexane (equiv)	Solvent	Time	Temp (°C)	Yield
1	K_2CO_3 (2)	5	Ethanol	1 h	80	0
2	K_2CO_3 (4)	3	Ethanol	30 min	25	0
3	Cs_2CO_3 (2)	3	Ethanol	3 min	25	0
4	K_2CO_3 (4)	3	DMF	3 h	160	0
5	K_2CO_3 (4)	3	Acetone	24 h	60	0
6	Cs_2CO_3 (2)	3	Acetone	24 h	25	0
7	Cs_2CO_3 (2)	3	Acetone	21 h	68	10%
8	Cs_2CO_3 (2)	5	Acetone	27 h	68	15%
9	Cs_2CO_3 (2)	8	Acetone	24 h	68	35%

Table 2. 1: Several reaction conditions during the alkylation of **48** to produce 1-hexyloxy-8-acetoxyanthracene (**54**).

Analogously, the use of high boiling solvents such as DMF did not result in the desired product **54** (Table 2.1, entry 4). The reaction of **48** with 3 equiv. of 1-bromohexane in the presence of 4 equiv. of K_2CO_3 in acetone under reflux did not lead to **54** (Table 2.1, entry 5). An alternative base was chosen, caesium carbonate (Cs_2CO_3), that is stronger and has a higher solubility in most organic solvents, to accelerate the reaction at room temperature but no result was detected (Table 2.1, entry 6). Pleasingly, we

found out that higher temperatures (reflux) favoured the formation of **54** in acetone and the yield increased gradually when we increased the amount of 1-bromohexane (Table 2.1, entries 7-9).

By applying the same procedure on **49** with an excess of 1-bromohexane (10 equiv.) and caesium carbonate (5 equiv.) at room temperature, the formation of the desired product **50** took place in a moderate yield (34%). However, it was found that it was important to carry out this reaction with 7 equiv. of Cs_2CO_3 in higher temperatures and longer time (8 h) to improve the yield as can be observed in Table 2.2 and Scheme 2.7.

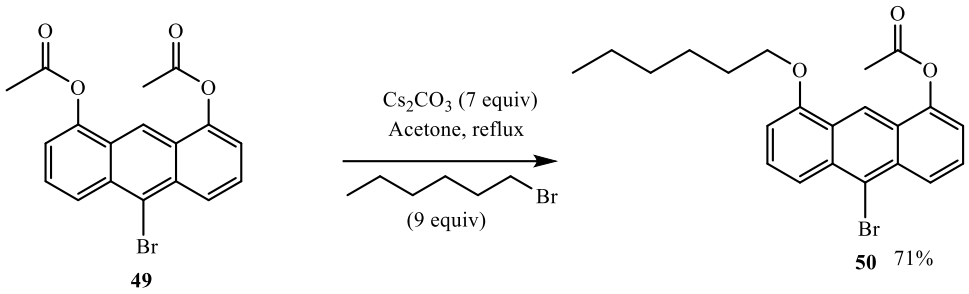

Scheme 2.7: The formation of 1-hexyloxy-8-acetoxy-10-bromoanthracene **50** from 1,8-diacetoxy-10-bromoanthracene **49**.

Entry	Cs_2CO_3 **(equiv)**	**1-Bromohexane (equiv)**	**Time**	**Temp (°C)**	**Yield**
1	5	10	6 d	25	34%
2	5	10	5 h	reflux	42%
3	7	9	7 h	reflux	57%
4	7	9	8 h	reflux	71%

Table 2. 2: Optimization of the reaction conditions for the preparation of 1-hexyloxy-8-acetoxy-10-bromoanthracene **50**.

The targeted aryl boronate (**39**) needed for cross-coupling was prepared by the borylation of **50** with bis(pinacolato) diboron (B_2pin_2) in dioxane.[88] This reaction was carried out in the presence of 3.5 equiv of potassium acetate (KOAc) and 0.05 equiv of $Pd(dppf)Cl_2$ at 90 °C (Scheme 2.8). The reaction showed an incomplete consumption of the starting material and several spots on TLC indicated the

formation of trace amounts of unbrominated compound (**54**) as a side-product arising from debromination of the starting bromide, the desired boronated compound (**39**), and unconverted starting bromide according to mass spectrosometry. An easy separation of these compounds by column chromatography was achieved due to their different polarity to afford **39** in 55% yield. The yield was slightly increased to 64% when DME was used instead of dioxane.

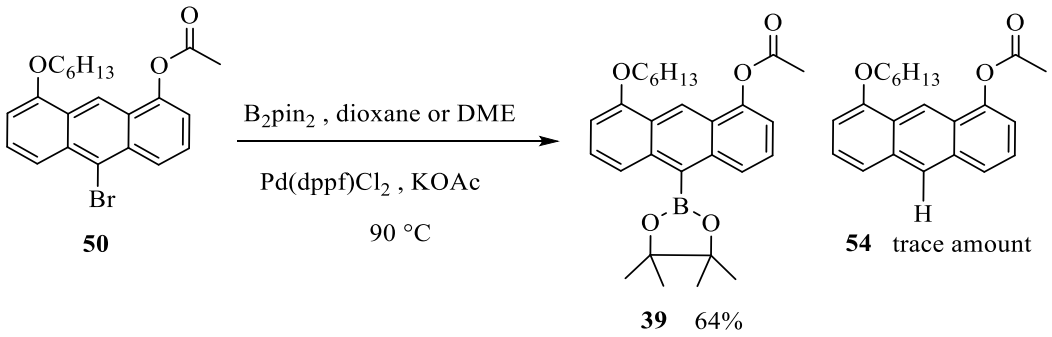

Scheme 2.8: The borylation of 1-hexyloxy-8-acetoxy-10-bromoanthracene **39**.

2.2.2 Synthesis of 1-Bromoanthracene

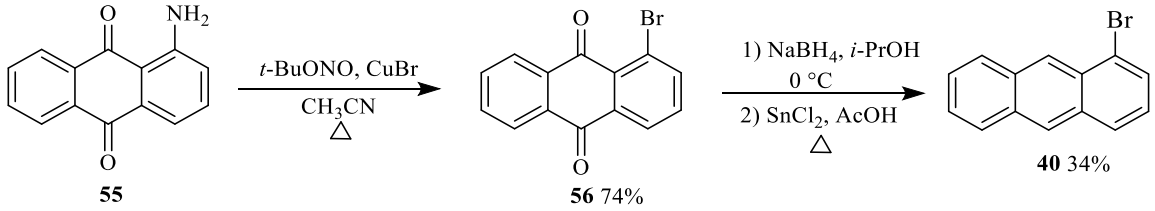

Scheme 2.9: Synthetic pathway for the preparation of 1-bromoanthracene **40**.

The aryl bromide necessary for cross-coupling was synthesised in two steps from commercially available 1-aminoanthracene-9,10-dione (**55**) by modifying a literature procedure.[88] The optimized procedure involves the reaction of the aryl amine **55** with copper(I) bromide and *tert*-butyl nitrite in acetonitrile at 90 °C to give 1-bromoanthracene-9,10-dione (**56**) in moderate yields (Scheme 2.9). The NMR spectrum showed the expected aryl bromide **56**, which underwent two sequential reduction reactions using sodium borohydride, and then tin(II) chloride to remove the ketones. After workup, as an alternative to the column chromatography utilized in the literature, a short silica plug was employed using DCM/pet ether mixture (1:5) giving the desired product 1-bromoanthracene **40** in 34% isolated yield.

2.2.3 Suzuki Coupling Reaction Between Anthracenyl Boronate 39 and 1-Bromoanthracene 40

The first attempt of SMC reaction was carried out by heating at 70 °C in dioxane with 1.2 equiv. of the substituted anthracene boronate ester **39** and bromoanthracene **40** in the presence of sodium carbonate and a catalytic amount of $Pd(dppf)Cl_2$ (10 mol%) (Scheme 10). However, no cross-coupling was observed. Anthracene (**57**) was found as the main product according to the ^1H NMR spectroscopic analysis, while the self-coupled product (**58**) and protodeboronated 1-hexyloxy-8-acetoxy-anthracene (**54**) were obtained in trace amounts. The possible cause of the failure of cross-coupling to form **41** is speculated to be due to a wide range of undesired chemical processes including protodeboronation (giving **54**), oxidation (giving homocoupling products), each dominating because of steric hindrance effects slowing the desired cross-coupling.[69–72] Protodeboronation, often caused by moisture from atmospheric air, was found as the major problematic issue in this procedure.

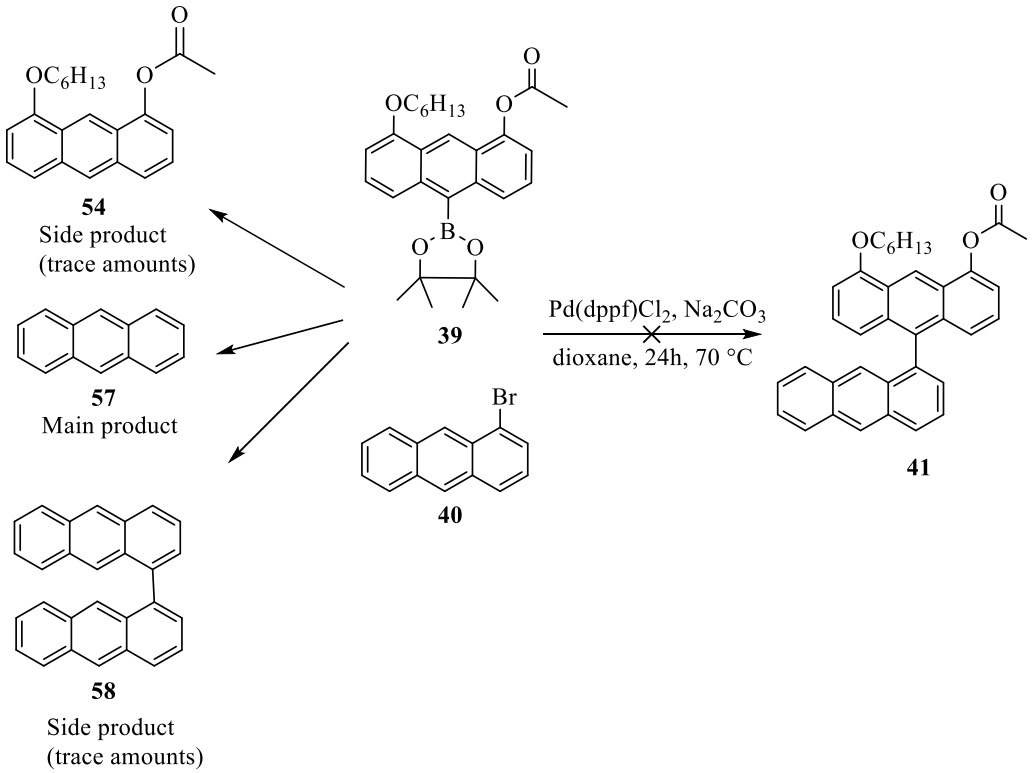

Scheme 2.10: Unsuccessful attempted SMC reaction for the preparation of substituted anthracene linked to anthracene **41**.

2.3 Strategy 2

The unsuccessful attempts of SMC reaction for the synthesis of mono-hexyloxy bianthracene **41** led to performing extensive model reactions using commercially available, simple pinacol boronate esters as starting materials. We hoped to be able to determine the proper conditions based on the results of a suitable model reaction.

2.3.1 Test Suzuki Coupling Reaction Using Unsubstituted 9-Anthracenyl (Pinacol) Boronate Ester with 1-Bromoanthracene

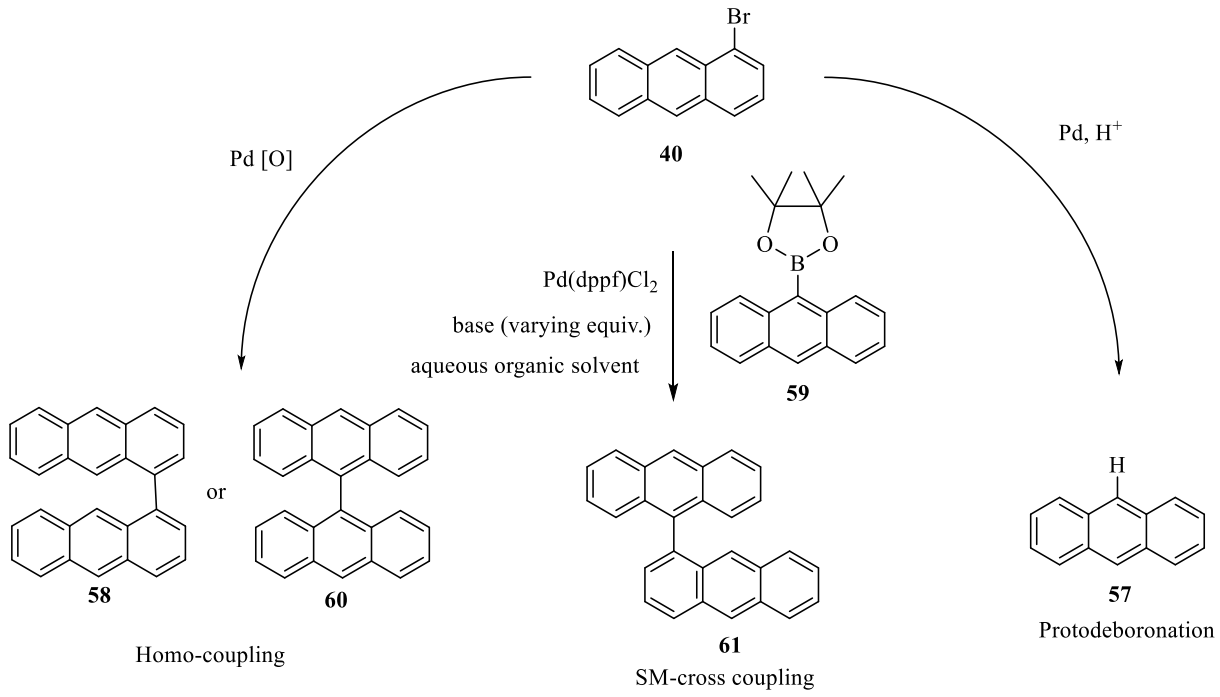

Scheme 2.11: The main competing reaction pathways in SMC for the preparation of unsubstituted anthracene linked to anthracene using 1-bromoanthracene **40** as a substrate.

Scheme 2.11 outlines the three competing reaction routes in SMC for the preparation of unsubstituted anthracene linked to anthracene, which would give some insights about the reaction pathway. The cross-coupling product 1,9`-bianthracene **61** was synthesised directly from unsubstituted 9-anthracenyl (pinacol) boronate ester **59** which was commercially available. A homo-coupled product **58** or **60** and, more frequently, deboronated product **57** were formed along with the desired compound **61** during this chemical reaction. The three pathways were investigated using **59** in place of the substituted 9-

anthracenyl(pinacol)boronate ester **39** because the preparation of compound **39** takes a long time and more importantly compound **59** is commercially available. Generally, pinacol esters are used as they are less prone to protodeboronation, nevertheless this does not completely solve this problem.

Entry	Aryl boronate 59 (equiv)	Base (equiv)	Pd(dppf)Cl_2 (equiv)	Solvent	Time	Temp (°C)	Product 61 (%)
1	1.2	Na_2CO_3[a]	0.05	dioxane	48h	75	0
2	0.95[b]	Na_2CO_3 (2M)	0.05	ethanol/ toluene/water	21	25	6[c]
3	0.95	Na_2CO_3 (2M)	0.05	ethanol/ toluene/water	30 min	80	8[c]
4	1.2	CsF (2)	0.05	DME	24h	70	0
5	2	CsF (3)	0.03	DME	24h	80	0
6	1.2	CsF (2.2)	0.03	DME	48h	90	10[c, d]

[a] Saturated aqueous solution. [b] Slow addition of boronate. [c]Inseparable mixture with the homo-coupled product **58** or **60**. [d]A Schlenk technique was used.

Table 2. 3: Screening of different reaction conditions for the Pd(dppf)Cl_2-catalyzed SMC of unsubstituted 9-anthracenyl(pinacol)boronate ester **59** and bromoanthracene **40**.

We initially examined the SMC reactions of **59** with **40** in different conditions (Table 2.3). The catalyst Pd(dppf)Cl_2 was used in every reaction, using different bases and solvents. The first attempt at the SMC was performed in dioxane at 75 °C, in the presence of sodium carbonate for 2 days (entry 1, Table 2.3) and led to the deboronated product **57**, unreacted halide **40**, homo-coupled product **58** or **60** and no cross-coupling was observed. These undesired products were observed in most of the reactions. Replacing dioxane with ethanol/toluene/water in this particular reaction, at room temperature after 21 hours (entry 2, Table 2.3), and at 80 °C after 30 minutes (entry 3, Table 2.3) resulted in a very low conversion yield to the cross-coupled product **61** (6% and 8% respectively) as ethanol/toluene/H_2O has been reported to be a good solvent mixture for SMC reactions.[88] The residue was purified by column chromatography to give an inseparable mixture of the cross-coupled product **61** (50% by ^{1}H NMR spectroscopic analysis) and the undesired homo-coupled product **58** or **60** (50% by ^{1}H NMR

spectroscopic analysis). Recrystallization from methanol/DCM (5:1) many times afforded pure **61**. All the reactions were monitored by TLC, and it appeared that the reaction carried out in DME, with a variety of the boronate, base, and Pd(dppf)Cl_2 equivalents, at 70 °C (entry 4, Table 2.3), and at 80 °C (entry 5, Table 2.3), went to completion giving the deboronated product **57** in the same period of time (24 hours) even with excess of **59** (2 equiv.). However, the cross-coupling was observed when a Schlenk line was used with a slow addition of boronate (1.2 equiv.) in the presence caesium fluoride (2.2 equiv.) and Pd(dppf)Cl_2 (3 mol %) at 90 °C for 48 hours in dry DME with 10% yield (entry 6, Table 2.3). This indicates that this reaction is very sensitive to air and moisture.

2.3.2 Test Suzuki Coupling Reaction Using Unsubstituted 9-Anthracenyl (Pinacol) Boronate Ester with 1-Bromonaphthalene

Entry	Aryl bromide 62 (equiv)	Aryl boronate 59 (equiv)	Base (equiv)	Pd(dppf)Cl_2 (equiv)	Solvent	Time	Temp (°C)	Product 63 (%)
1	1	1.5	Na_2CO_3[a]	0.05	dioxane	48h	75	0[d]
2	1	1	CsF (2)	0.05	DME	24h	100[b]	0[d]
3	1	1	CsF (2)	0.05	DME	24h	90[c]	0[d]
4	1	0.86	Cs_2CO_3 (3)	0.025	dioxane	5h	65	0[d]
5	1.2	1	NaOH (2)	0.02	THF	18h	55	0[d]
6	1	1	CsF (2)	0.02	DME	48h	25	0[d]
7	1.2	1	Na_2CO_3 (2M)	0.05	ethanol/ toluene/water	30 min	80	35

[a] Saturated aqueous solution. [b] Reflux under nitrogen. [c] Reaction was carried out using a sealed tube. [d] The yield of the side product **57** was not quantified.

Table 2. 4: Screening of different reaction conditions for the Pd(dppf)Cl_2-catalyzed SMC of unsubstituted 9-anthracenyl(pinacol)boronate ester **59** and bromonaphthalene **62**.

In view of the failure to achieve a good cross-coupling reaction between aryl halide **40** and aryl boronate **59** we decided to use 1-bromonaphthalene **62** as a commercially available substrate instead of **40** to produce an optimum set of conditions for this reaction (Table 2.4). Another reason for using **62** as a substrate in place of **40** is to prove whether the homo-coupling and/or deboronation issue arises from the aryl halide or aryl boronate. The treatment of **59** and **62** was performed several times with modification of

conditions (equiv. of $Pd(dppf)Cl_2$ and boronate, base (such as Na_2CO_3, CsF, Cs_2CO_3, and NaOH), solvent (such as dioxane, DME, THF, ethanol/ toluene/water), time, and temperature), but repeatedly generated similar disappointing outcomes (entries 1-6, Table 2.4), namely the recovery of the unconverted starting material **62** and dominating protodeboronation. No homocoupling was observed indicating that the homocoupling only occurs when bromoanthracene **40** applied as a substrate. These conditions failed to produce any of the targeted biaryl and unreacted **62** was reisolated along with **57** (resulting from protodeboronation), and complete consumption of the starting material **59** (Scheme 2.12).

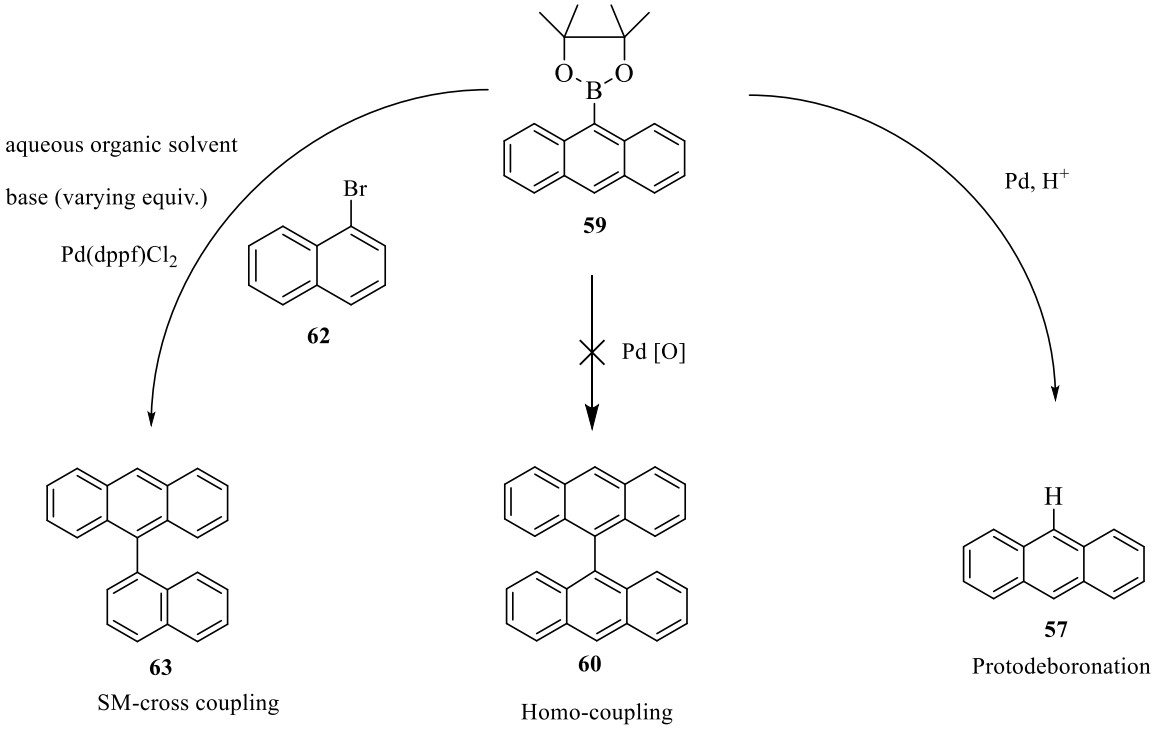

Scheme 2.12: The main competing reaction pathways in SMC for the preparation of unsubstituted anthracene linked to naphthalene using 1-bromonaphthalene **62** as a substrate.

An optimised set of conditions was achieved to promote cross coupling by treating **62** with **59** (0.95 equiv.) in the presence of sodium carbonate (2M) and $Pd(dppf)Cl_2$ (5 mol %) at 80 °C in ethanol and toluene in a very short time (30 minutes) with 35% conversion (entry 7, Table 2.4). The formation of anthracene **57** (by-product) was reduced in this reaction to 45%. Additionally, trace amounts of unchanged starting halide **62** was reisolated, and TLC analysis revealed complete consumption of the starting boronate **59** in less than one hour.

2.4 Strategy 3

Since the starting aryl bromide was not fully consumed in the previous cross-coupling reaction, we decided to replace bromide with iodide because iodide is regarded as a better leaving group than bromide and because the relative reactivity increases in this order X = Cl < Br < I.

2.4.1 Synthesis of 1-Iodoanthracene

2.4.1.1 Preparation of Iodoanthracene from Bromoanthracene

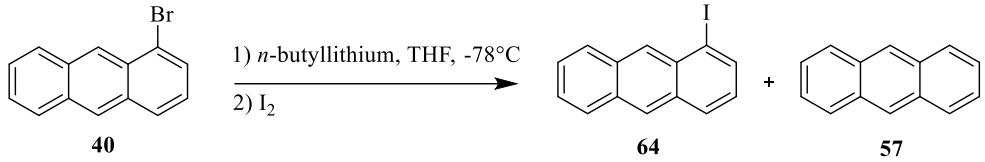

Scheme 2.13: The preparation of 1-iodoanthracene **64** from 1-bromoanthracene **40**.

The first planned synthesis of 1-iodoantharacene (**64**) was to follow the scheme depicted above (Scheme 2.13). It was found that the lithiation of **40** with *n*-BuLi 2.5 M in THF at -78 °C, followed by iodine (in THF) quench[99] led to an undesired result due to dehalogenation. After workup and purification by column chromatography, the product obtained was an inseparable mixture of 1-iodoantharacene **64** and anthracene **57** as identified by ^{1}H NMR spectroscopy in a ratio of 1:0.15 with a ~73% isolated yield. Therefore, we had to find another method to prepare a pure **64**.

2.4.1.2 Preparation of Iodoanthracene from 1-Amino-9,10-anthraquinone

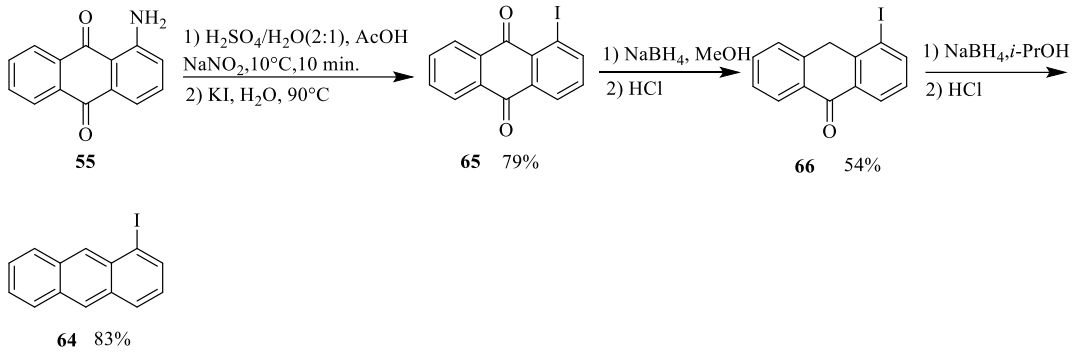

Scheme 2.14: The route for the formation of 1-iodoanthracene **64** from 1-Amino-9,10-anthraquinone **55**.

An alternative approach involved the diazotization of the amino group in 1-amino-9,10-anthraquinone **55** in aqueous AcOH and sulfuric acid solution at 10 °C. The solution of the diazonium salt was stirred rapidly with aqueous potassium iodide at 90 °C to replace the diazo-group by iodine (**65**) with a yield of 79% (Scheme 2.14).[100] The anthraquinone **65** was reduced with $NaBH_4$ in MeOH followed by hydrochloric acid workup to give the anthrone (**66**), presumed to be the isomer shown.[101,102] After many attempts, we found that the slow addition of $NaBH_4$ to the anthraquinone **65** solution at room temperature afforded a satisfying conversion to **66**. When sodium borohydride was added in small portions to a solution of **65** in methanol over four hours, **66** was obtained in 54% yield (R_f = 0.43) after purification by column chromatography along with small amounts of **64** in 1% yield (R_f = 0.80) and its derivative 10-methoxyanthracene (**67**) with a yield between 10-14% (R_f = 0.73) as illustrated in Scheme 2.15. It should be noted that the anthrone component **66** had an R_f value similar to the starting anthraquinone component **65** according to the TLC analysis. Compound **65** was insoluble in methanol when the reaction started, but it became soluble as the reaction proceeded over time. When sodium borohydride was added rapidly, the insoluble starting material was significantly recovered and by-products were formed.

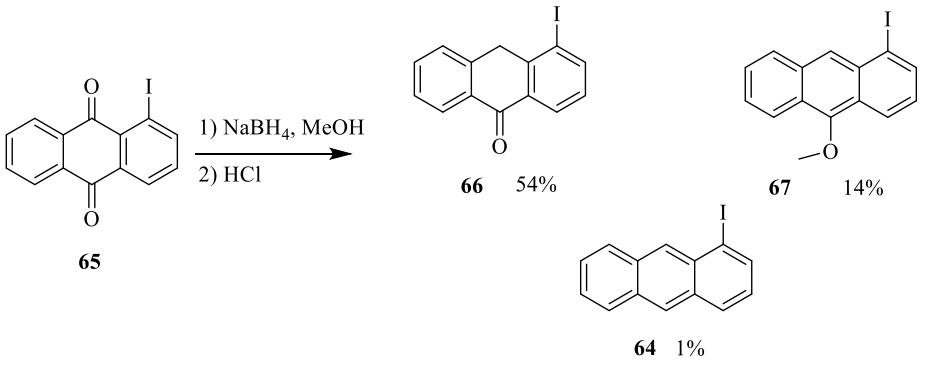

Scheme 2.15: The formation of iodoanthrone **66** and its derivatives.

The treatment of anthrone **66** with $NaBH_4$ in *i*-PrOH, followed by concentrated HCl afforded the anthracene **64** in 83% yield. Compound **66** was poorly soluble in methanol even with the slow addition of $NaBH_4$, but when the reaction was carried out in *i*-PrOH instead of MeOH, the reduction occurred smoothly at room temperature with the slow addition of $NaBH_4$.[102]

2.4.2 Test Suzuki Coupling Reaction Using Unsubstituted 9-Anthracenyl (Pinacol) Boronate Ester with 1-Iodonaphthalene/ 1-Iodoanthracene

Previously, the Cammidge group performed a series of experiments in homogeneous conditions to determine optimised conditions of base and solvent to minimise protodeboronation of the boronic acid derivative in challenging cross couplings.[99] They found that pinacol boronate ester components coupled smoothly with iodonaphthalene to give high conversions to binaphthalene. They proved that the use of caesium fluoride in DME and barium hydroxide in DME/water or in toluene/ethanol/water to be effective in the coupling of sterically congested substrates. However, as with several couplings involving sterically hindered partners, competing protonolysis (protodeboronation) was problematic in the reactions.

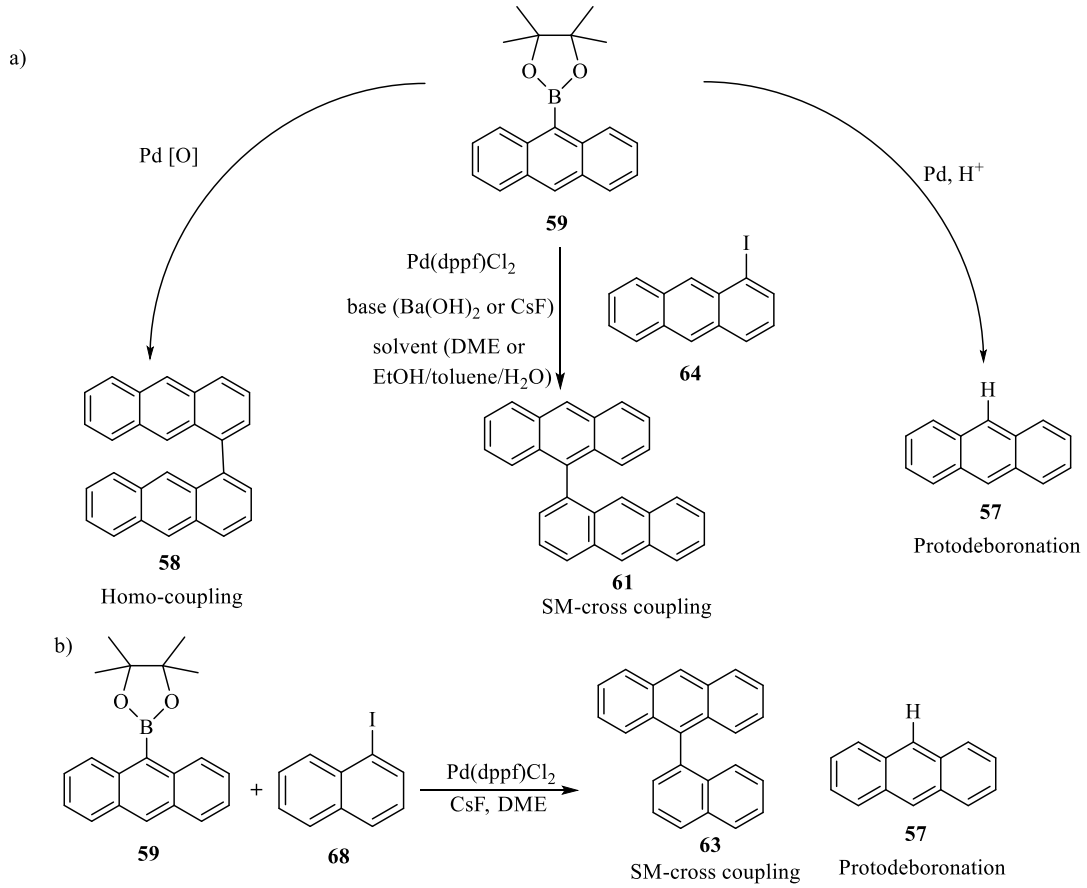

Scheme 2.16: The main competing reaction pathways in SMC for the preparation of unsubstituted biaryls using 1-iodoanthracene **64** and 1-iodonaphthalene **68** as substrates.

Suzuki coupling towards 1,9`-bianthracene **61** and 9-(1-naphthalenyl)anthracene **63** was performed in parallel to the above study (Scheme 2.16, Table 2.5). $Pd(dppf)Cl_2$ was used as the catalyst for cross coupling in all the reactions at 3-5 mol %. It was found that no cross-coupling occurred (entry 1, Table 2.5) when 1.1 equiv. of the parent boronate ester **59** was employed as the deboronation by-product **57** became more prominent and adversely consumed all the starting boronate reagent. This may be because the reaction was carried out under a poor inert atmosphere compared with the other reactions. Successful coupling was only achieved when all reagents were dried under vacuum and degassed by bubbling nitrogen for 1 hour. The reaction proved to be poorly reproducible but afforded the target bianthracene **61** after 30 minutes in improved conversion yield ranging from 28 to 44% when $Ba(OH)_2$ was used as a base in the mixture of solvent (ethanol/ toluene/water) at 75 °C and 80 °C (entries 2-3, Table 2.5). The desired biaryl **61** was isolated by chromatographic purification and obtained as an

inseparable mixture with the homo-coupled product **58** according to ^{1}H NMR spectroscopic analysis. Recrystallization from different alcohols (MeOH, EtOH, and *i*-PrOH) was performed several times and led to pure **61**.

Entry	Aryl iodide	Aryl boronate 59 (equiv)	Base (equiv)	Pd(dppf)Cl_2 (equiv)	Solvent	Time	Temp (°C)	Product/ Yield (%)
1	**64**	1.1	$Ba(OH)_2$ (1.5)	0.03	ethanol/ toluene/water	30 min	80	**61**(0)
2	**64**	1.5	$Ba(OH)_2$ (1.5)	0.05	ethanol/ toluene/water	30 min	75	**61**[a](44)
3	**64**	1.7	$Ba(OH)_2$ (1.7)	0.05	ethanol/ toluene/water	30 min	80	**61**[a](28)
4	**64**	1.2	CsF (3)	0.03	DME	48h	90	**61**[a,b](8)
5	**64**	2	CsF (4)	0.05	DME	48h	90	**61**[a,b](10)
6	**64**[c]	1.5[c]	CsF[c] (3.5)	0.05 [c]	DME[c]	72h	90	**61**[a](28)
7	**68**	1.5	CsF (3)	0.03	DME	24h	90	**63**[b](30)

[a] Inseparable mixture with the homo-coupled product **58** or **60**. [b] A Schlenk technique was used. [c] Reagents were added inside a glovebox.

Table 2. 5: Screening of different reaction conditions for the Pd(dppf)Cl_2-catalyzed SMC of unsubstituted 9-anthracenyl(pinacol)boronate ester **59** and iodoanthracene **64**/iodonaphthalene **68**.

It is possible that oxygen and moisture could contribute to the formation of the side products **57** and **58** or **60**. Likewise, cross coupling reactions under aqueous conditions can result in competitive protodeboronation. Therefore, the reactions were carried out under anhydrous conditions using CsF and dry DME at 90 °C using a Schlenk line technique. The reactants were oven dried and extensively degassed by N_2 before the reaction was started. Disappointingly, the yield for this reaction was slightly decreased to 8-10% (entries 4-5, Table 2.5). Even when the reagents were added inside a highly inert atmosphere glovebox (entry 6, Table 2.5), the overall yield was disappointing (28%). This indicated that the presence of water or oxygen plays an important role in the process but was not the only problem with this reaction.

The commercially available 1-iodonaphthalene **68** was also tested in place of **64** using the above optimised conditions (Scheme 2.16-b) (entry 7, Table 2.5). The cross-coupling proceeded in the presence

of **59** (1.5 equiv.), $Pd(dppf)Cl_2$ (3 mol %), CsF (3 equiv.), and dry DME at 90 °C in 30% isolated yield. Apparently, the poor yield observed was due to the formation of by-products resulting from competing protodeboronation that consumed most of the starting boronate.

2.5 Strategy 4

After low-yielding Suzuki cross-coupling reactions and difficulties encountered with selective halide reagents, an alternative strategy to **61** was considered in order to reduce protodeboronation. This strategy involves the synthesis of bianthracene by manipulating the organoboron species.

2.5.1 Preparation of 9-Anthracenyl(Ethylene Glycol)Boronate Ester

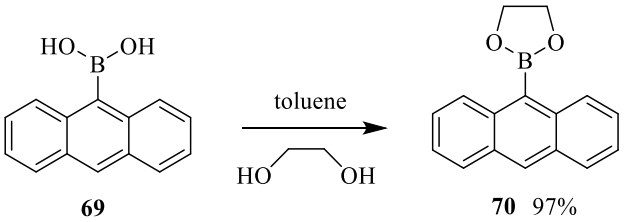

69 **70** 97%

Scheme 2.17: Formation of ethylene glycol boronate ester *via* esterification of the boronic acid.

Work by the Cammidge group has shown that the best result of cross-coupling challenging aryls was obtained when the ethylene glycol boronate ester was employed.[99] Consequently, it was decided that anthracene ethylene glycol boronate ester (**70**) should be employed. Due to the unavailability of compound **70**, necessary for the synthesis of **61**, the preparation of this component was the starting point for this strategy. A straightforward method for the synthesis of the boronate ester involves the esterification of the commercially available boronic acid (**69**) with ethylene glycol in refluxing toluene (Scheme 2.17).[99] The use of a Dean-Stark trap with azeotropic removal of water drives the formation of **70** in excellent yields (97%).

2.5.2 Test Suzuki Coupling Reaction Using Unsubstituted Anthracene Boronate Ester/ Boronic Acid with Iodoanthracene/ Bromoanthracene

Further optimisation of palladium-catalyzed SMC reaction conditions through several alterations were investigated using different halide reagents (iodoanthracene **64** and bromoanthracene **40**), boron species

(anthracene pinacol boronic ester **59**, anthracene boronic acid **69**, and anthracene ethylene glycol boronic ester **70**) and palladium catalysts ([1,1′-bis(diphenylphosphino)ferrocene]dichloropalladium(II) and tetrakis(triphenylphosphine) palladium(0)) (Table 2.6). Caesium fluoride as a base and dry DME as a solvent were used in all experiments and all reactions proceeded in 72 hours at 90 °C. All reactants were oven dried for 2 days, the solvent was freshly distilled, and added inside a glovebox in a sealed tube before the reactions were started. The equivalents of palladium chloride and ligands were calculated with reference to the aryl halide, while the equivalent of the base was calculated with reference to the aryl boronate. Total consumption of the organoboron derivatives and halide species was generally identified yielding a product mixture including target 1,9`-biantharacene, 1,1'-bianthracene (from homocoupling of aryl halides), and anthracene (from deboronation of aryl boron reagents) as summarised in Scheme 2.18.

2.5.3 Test Suzuki Coupling Reaction Employing $Pd(dppf)Cl_2$ As A Catalyst

When the experiments were conducted using the aryl iodide and boron derivatives (1.5 equiv) in the presence of $Pd(dppf)Cl_2$ (5 mol %) and 4 equivalent of CsF, bianthracene **61** was isolated in 35-41% yields as an inseparable mixture with the self-coupled product **58** (entries 1-3, Table 2.6). Protodeboronation was significantly increased when the bromide coupling partner was employed with a slight change in CsF loading (3.5 equiv) (entries 4-6, Table 2.6). In this manner, the yield increased from 17 to 42% when bromoanthracene was replaced with iodoanthracene, which proved to be a better starting halide (entry 7, Table 2.6). The aryl boronates and catalyst loadings could be lowered to 1.3 equiv and 3 mol%, respectively, but no change was observed (entry 8, Table 2.6).

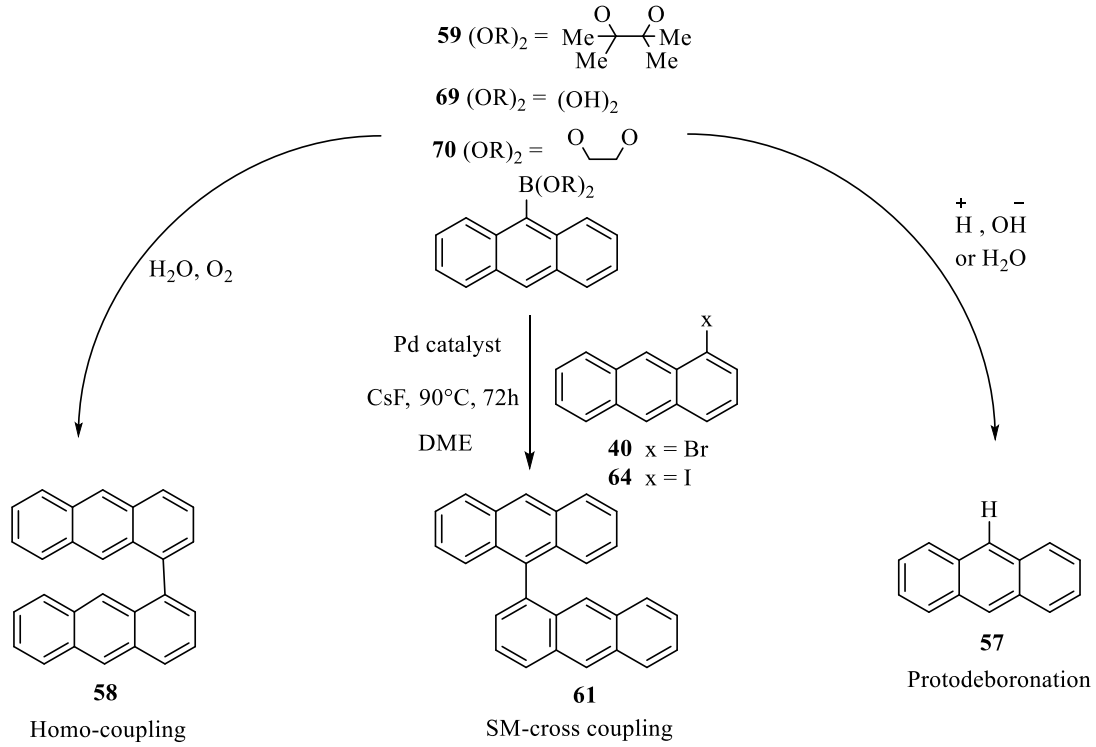

Scheme 2.18: The main competing reaction pathways in SMC using different halide and boron reagents.

According to the above results, the cross-coupling occurred more slowly when the starting bromide **40** was employed and protodeboronation occurred extremely rapidly. Unfortunately, the change in organoboron species was not sufficient to enhance the reactivity of cross-coupling and reduce the competitive protodeboronation. The reason for the low yield was not clear to us. The reaction may be affected by steric hindrance in the bulky aryl substrates, or the catalyst could be unsuitable for this reaction.

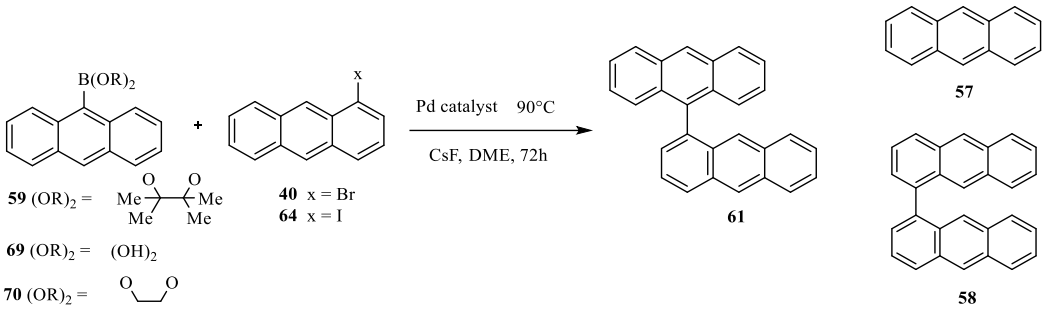

Entry	Aryl halide	Aryl boronate (equiv)	CsF (equiv)	Pd cat. (equiv)	Product (61) (Yield %)	By-product (57) (Yield %)
1	**64**	**59** (1.5)	4	$Pd(dppf)Cl_2$ (0.05)	41[a]	12
2	**64**	**69** (1.5)	4	$Pd(dppf)Cl_2$ (0.05)	37[a]	24
3	**64**	**70** (1.5)	4	$Pd(dppf)Cl_2$ (0.05)	35[a]	48
4	**40**	**59** (1.5)	3.5	$Pd(dppf)Cl_2$ (0.05)	15[a]	43
5	**40**	**69** (1.5)	3.5	$Pd(dppf)Cl_2$ (0.05)	17[a]	77
6	**40**	**70** (1.5)	3.5	$Pd(dppf)Cl_2$ (0.05)	13[a]	82
7	**64**	**59** (1.5)	3.5	$Pd(dppf)Cl_2$ (0.05)	42[a]	32
8	**64**	**59** (1.3)	3.5	$Pd(dppf)Cl_2$ (0.03)	37[a]	32
9	**64**	**59** (1.5)	3.5	$Pd(PPh_3)_4$ (0.03)	75	-
10	**64**	**59** (1.5)	3.5	$Pd(PPh_3)_4$ (0.03)	81	-
11	**64**	**70** (1.5)	3.5	$Pd(PPh_3)_4$ (0.03)	84	-
12	**64**	**59** (1.1)	3	$Pd(PPh_3)_4$ (0.03)	45	-
13	**64**	**69** (1.2)	3	$Pd(PPh_3)_4$ (0.03)	81	-
14	**64**	**70** (1.2)	3	$Pd(PPh_3)_4$ (0.03)	84	-

[a] Inseparable mixture with the homo-coupled product **58**

Table 2. 6: Optimization of reaction conditions for the Pd-catalyzed SMC.

2.5.4 Test Suzuki Coupling Reaction Employing $Pd(PPh_3)_4$ As A Catalyst

To circumvent this issue, an alternative palladium catalyst was examined in an effort to reduce protodeboronation side reactions. Interestingly, it was observed that the addition of $Pd(PPh_3)_4$ (3 mol %) was quite effective in improving the yield without the formation of the homo-coupled product **58** (entries 9-14, Table 2.6). The low yield of anthracene was not quantified as it was isolated with impurities that cannot be separated. The cross coupling proceeded smoothly in the presence of aryl iodide, boron derivatives (1.5 equiv), $Pd(PPh_3)_4$ (3 mol %), and CsF (3.5 equiv) in good to very good yields (75-84%) (entries 9-11, Table 2.6). It was noticed that the aryl boronic acid **69** and the aryl ethylene glycol boronate ester **70** provided higher yields than that from the aryl pinacol boronate ester **59.** A lowering in the yield was seen when the amounts CsF and aryl boronate **59** were reduced from 3.5 equivalents to 3 and from 1.5 equivalents to 1.1, respectively, and recovery of some starting material **64** was observed (entry 12, Table 2.6). It was noteworthy that the yield of bianthracene **61** did not decrease when we lowered the amounts of CsF and boron derivatives **69** and **70** from 3.5 equivalents to 3 and from 1.5 equivalents to 1.2, respectively, (entries 13–14, Table 2.6). The identity of the **61** was confirmed by NMR spectroscopy and MALDI-TOF MS analysis and its structure was identified by X-ray crystallographic analysis (Figure 2.3). The novel bianthracene **61** structure has been recently published in collaboration with photophysics groups to explore its excited state properties and assess its potential in optoelectronics.[103]

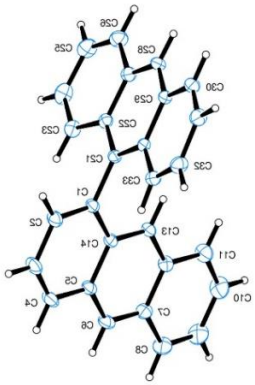

Figure 2.3: X-ray crystallographic structure of bianthracene **61**.

2.5.5 Test Suzuki Coupling Reaction Using Di/Mono-Hexyloxy-10-Anthracenyl (Pinacol) Boronate Ester with Iodoanthracene

2.5.5.1 Synthesis of Di-Hexyloxy-10-Anthracenyl(Pinacol)Boronate Ester

The synthetic protocol toward dihexyloxyanthracene pinacol boronate ester **72** involved functionalization in two steps from the prepared compound **49**. The alkylation of the ester **49** with bromohexane (9 equiv) in the presence of caesium carbonate (7 equiv) in acetone at refluxing temperature gave **71** in 51% yield. This reaction was very slow and reached completion after roughly 17 days. Analogously to the preparation of **39** in strategy 1, **71** was borylated by bis (pinacolato) diboron (B_2pin_2) in the presence of KOAc (3.5 equiv) and Pd(dppf)Cl_2 (0.05 equiv) in dioxane overnight at 90 °C to produce **72** in a poor yield (23%). When dried reagents were placed into a sealed tube in a glovebox and the reaction was carried out at 90 °C for 48 hours, the yield was significantly improved to 64% (Scheme 2.19).

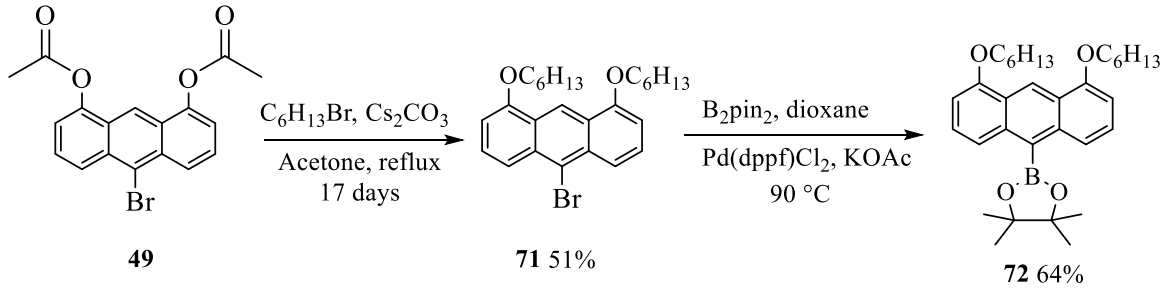

Scheme 2.19: Synthetic pathway towards di-substituted pinacol boronate ester **72**.

2.5.5.2 Suzuki Cross-Coupling Reactions Di/Mono-Hexyloxy-1,9'-Bianthracene

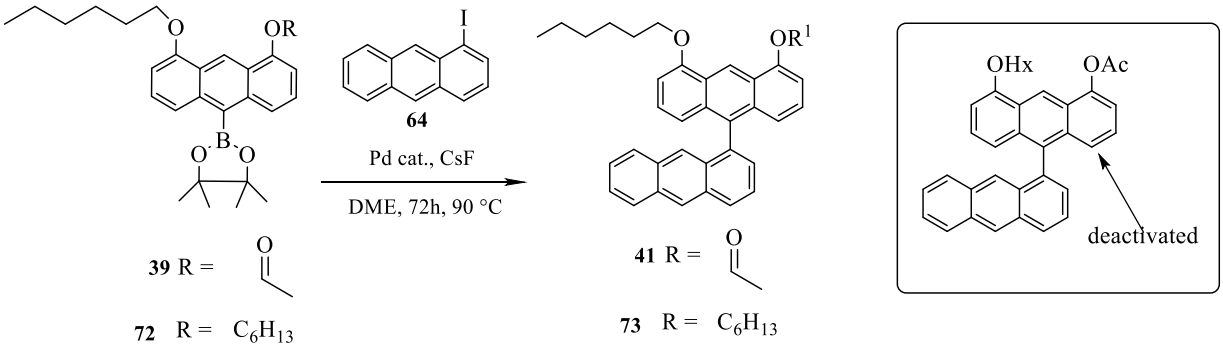

Scheme 2.20: Synthesis of substituted 1,9'-bianthracene by SMC reaction.

The mono-hexyloxy bianthracene **41,** required for the formation of the target staggarene **45,** and dihexyloxy bianthracene **73** were synthesised in the same manner *via* a SMC reaction in dry DME (Scheme 2.20). Two sources of palladium catalysts were examined ($Pd(dppf)Cl_2$ and $Pd(PPh_3)_4$) for the cross-coupling for **41** as depicted in Table 2.7. All reactants were added inside a glovebox in freshly distilled DME in a sealed tube and the resulting solution was stirred at 90 °C for 3 days.

The use of CsF (4 equiv) as the base and $Pd(dppf)Cl_2$ as the palladium catalyst source revealed the full consumption of the starting materials and multiple spots on TLC indicating the formation of many side-products including the formation of anthracene that was unexpectedly arising from protodeiodination of the starting iodide. These conditions were shown to be unsuitable for cross-coupling reactions and the desired **41** was obtained after chromatographic purification in low yields (<10%) (entry 1, Table 2.7). Formation of **41** was characterized and confirmed by NMR spectroscopy and mass spectrometry. It was noteworthy that the homo-coupled product **58** (resulting from the aryl iodide) was isolated in this process and identified by ^1H NMR spectroscopy.

Having identified $Pd(PPh_3)_4$ as the effective catalyst, the use of **39** (1 equiv), CsF (3 equiv), and $Pd(PPh_3)_4$ (3 mol %) enabled a higher reaction yield (45%) of **41** and afforded less side-product formation compared to the use of $Pd(dppf)Cl_2$ (entry 2, Table 2.7). Increasing the amounts of starting boronate and CsF to 1.2 and 3.5, respectively, did not indeed affect the yield of the coupling (entry 3, Table 2.7). Under these conditions, the di-hexyloxy bianthracene **73** was prepared in moderate yields (65%) (entry 4, Table 2.7). It can be clearly seen that the cross-coupled product **73** gave a higher yield than **41** although the two substituted bianthracene components were synthesised *via* the same approach. The presence of electron-withdrawing group in compound **41** appeared to have detrimental effects. Additionally, recrystallization of **73** was much easier than **41**, which was recrystallized several times from DCM-methanol and was barely collected.

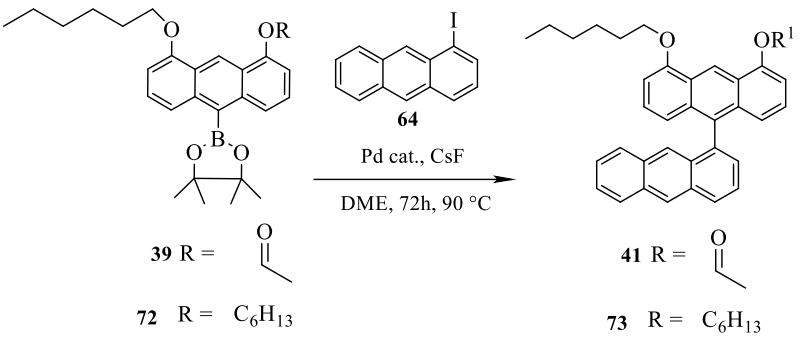

Entry	Aryl boronate	Pd cat.	Product (Yield %)
1	**39**	$Pd(dppf)Cl_2$	**41** (9%)
2	**39**	$Pd(PPh_3)_4$	**41** (45%)
3	**39**	$Pd(PPh_3)_4$	**41** (45%)
4	**72**	$Pd(PPh_3)_4$	**73** (65%)

Table 2. 7: Preparation of substituted 1,9'-bianthracene by SMC reaction.

Anthracene may require activation by electron donating substituents to undergo oxidative cyclization. As a result, the introduction of electron donating substituent at the 8-position of **41** was necessary to form anthracene fused anthracene **42** in a stepwise lateral pattern. The incorporation of acetyl group at the 1-position deactivates the 4-position and prevents cyclization (Scheme 2.20). The incorporation of greater electron donating alkyl substituents at the 1,8-positions of the anthracene ring **73** could promote the oxidative ring closure at the 4,5-positions in the next step and thus obstruct formation of the desired pattern. However, **73** was synthesised to study whether another electron-donating group could be used instead.

2.6 Strategy 5

The boronic acid components proved to be remarkable starting materials and afforded greater yields compared to pinacol boronate ester components as clarified in strategy 4 (Table 2.6). In addition, the pinacol boronate ester compounds require a lot of grams to start with due to their high molecular weight

compared to the boronic acid compounds. For this reason, we decided to replace the aryl pinacol boronate ester with the aryl boronic acid, which can be used as an appropriate partner for the SMC reaction.

2.6.1 Synthesis of Unsubstituted 1-Anthracenyl Boronic Acid and Mono-Hexyloxybianthracene

2.6.1.1 Preparation of 1-Anthracenyl Boronic Acid

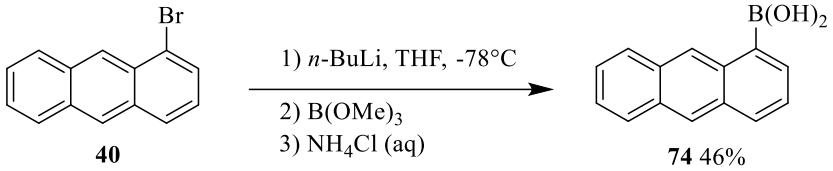

Scheme 2.21: Synthesis of 1-anthracenyl boronic acid **74** by lithiation of 1-bromoanthracene **40**.

The unsubstituted 1-anthracenyl boronic acid (**74**) was also examined by the same approach as the previous attempt following a reported procedure (Scheme 2.21).[105] Treatment of the previously synthesized bromoanthracene **40** with *n*-butyllithium at -78 °C in the presence of trimethyl borate in THF afforded the anthracene intermediate **74** (isolated yield = 46%) that is required for cross-coupling. This method allows for better control over regioselectivity than the synthesis of the substituted 10-anthracenyl boronic acid **32** involving the reduction of acetyl group.

2.6.1.2 Preparation of Mono-Hexyloxybianthracene by Suzuki Cross-Coupling

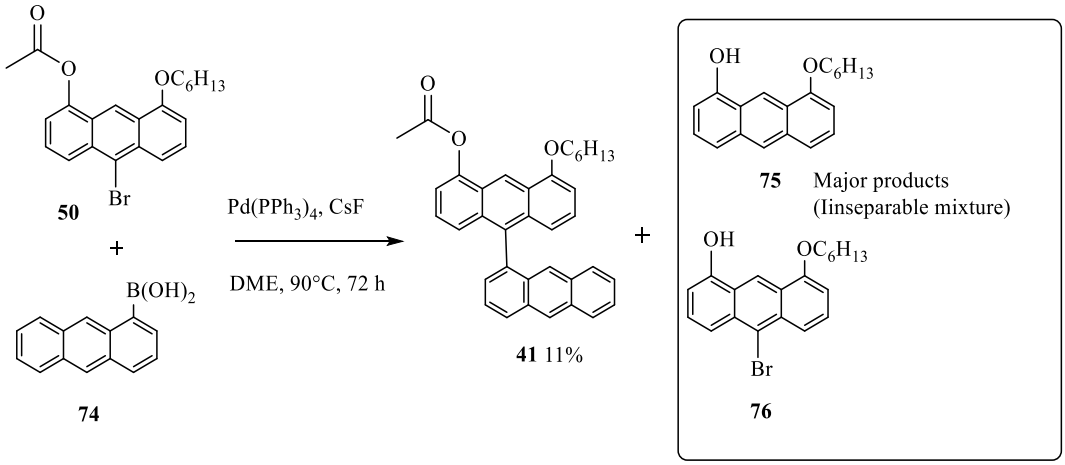

Scheme 2.22: Synthesis of mono-hexyloxybianthracene **41** by Suzuki cross-coupling reaction from 1-anthracenyl boronic acid **74**.

Finally, and to test the cross-coupling reaction with other functionalised organohalide species, the

reaction of intermediates **74** and **50** in DME in the presence of $Pd(PPh_3)_4$ and caesium fluoride did not appear to involve a better cross-coupling. TLC analysis of the crude mixture showed two additional fractions along with the unreacted starting material. One of the isolated products was confirmed by ^1H NMR spectroscopy as the desired product **41** in low yields 11%. The second isolated product, which is the major product, could not be identified by ^1H NMR spectroscopy but it displayed two possible components for the dihexyloxy anthracene moiety, however, they were difficult to distinguish due to the overlapping peaks. MALDI-TOF MS analysis of the unseparated products indicated the formation of hydrolysed precursors with and without bromine **75** and **76** as shown in Scheme 2.22. This unsuccessful result led us to remain focused on the previous strategy for the cross-coupling reaction.

2.7 Oxidative Cyclodehydrogenation of Substituted and Unsubstituted Bianthracene Moieties

Ultimately, after the construction of the two linked anthracene units, we aimed at the oxidative cyclodehydrogenation of the functionalized precursor **41** as the main objective of this project was the synthesis of the π-extended staggarene **45** (Scheme 2.1). To do this, the non-functionalized bianthracene model system **61** was first investigated in order to provide the knowledge required for the predicted reaction of its functionalized analogue **41** that would lead to **45**. As a result, the focus was set on the oxidative cyclodehydrogenation of **61**. Several Scholl cyclization reaction conditions, such as $FeCl_3$-$MeNO_2$/ DCM,[88,106–110] , $FeBr_3$/DCM, UV irradiation/ DDQ,[111,112] $AlCl_3$/NaCl,[113] $K_3Fe(CN)_6$ /DCM, DDQ/MsOH,[71] and DDQ/TfOH[71,114,115] were tested.

2.7.1 Test Scholl Cyclization Reaction Using Unsubstituted 1, 9'- Bianthracene with $FeCl_3$/$MeNO_2$

Initially, we tested the annulation using iron chloride as the oxidant as it was already tested in previous work of our group.[116,117] Generally, a considerable excess of $FeCl_3$ is required for the completion of intramolecular oxidative cyclization and in many cases, including our case, the resulting products are contaminated with chlorinated components.[76,118,119] Scheme 2.23 displayed that the use of $FeCl_3$ at 0 °C within 1 hour in the presence of $MeNO_2$ did not proceed to the desired product **77** and gave a mixture of non-cyclized **78** and cyclized **79** chlorinated products with 4-10% and trace amount respectively of

isolated yields (entries 1 and 2, Table 2.8), where the chlorination of **61** occurred regioselectively in the 9 and 10`-positions (Figure 2.4) as confirmed by X-ray crystallographic analysis (Figure 2.5). The yield of **78** increased slightly up to 14-15% when fewer equivalents of $FeCl_3$ (8 equiv.) were employed in the absence of $MeNO_2$ and full cyclodehydrogenation of **79** or **77** was not observed (entries 3 and 4, Table 2.8). Reducing the $FeCl_3$ loading (4 equiv.) for longer reaction time did not improve the result (entry 5, Table 2.8). Performing this reaction at lower temperatures (-78 °C) revealed that the starting material was still not completely consumed preventing the isolation of the chlorinated product **78**, which is an inseparable mixture with the starting material (entry 6, Table 2.8). The formation of the **78** can be relatively controlled when adding the substrate **61**/ DCM mixture into $FeCl_3$/ DCM solution at 0 °C allowing the temperature to rise to rt for 5 hours, delivering a better reaction yield of 20% (entry 7, Table 2.8).

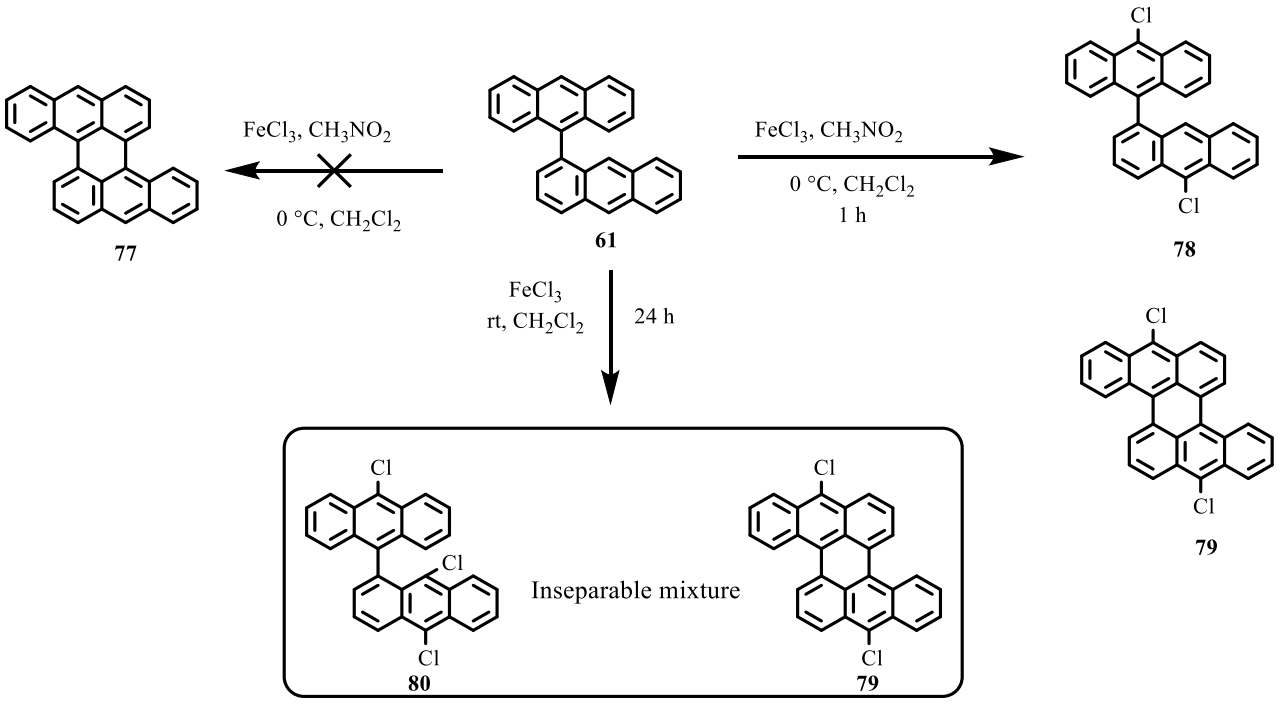

Scheme 2.23: An unsuccessful attempt to form anthracene fused anthracene (AFA) **77** using $FeCl_3$ as an oxidant. Note the formation of chlorinated products **78**, **79**, and **80**.

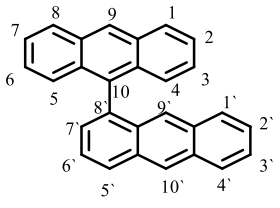

Figure 2.4: Numbering in bianthracene.

The resulting ^{1}H and ^{13}C NMR spectra proved the formation of non-cyclized chlorinated compound **78**. For the cyclized chlorinated compound **79**, the ^{1}H NMR spectrum displayed the absence of a singlet peak in the aromatic region, demonstrating the formation of **79**. However, attempts failed to record a ^{13}C NMR spectrum of **79** due to the insufficient sample that resulted in a very poor signal to noise ratio. MALDI-TOF MS spectrum also showed evidence of non-cyclized product attached to a single chlorine with a very complex mixture of products that could not be isolated by column chromatography or recrystallisation.

Entry	**Substrate (61) (µmol)**	**$FeCl_3$ (equiv)**	**$MeNO_2$**	**CH_2Cl_2**	**Temp/Time**	**78**	**79**	**80**	**77**
1	42.30	16	2.1 mL	40 mL	0 °C/ 1 h	(10%)	trace	(0%)	(0%)
2	140	16	7 mL	210 mL	0 °C/ 40 min	(4%)	trace	(0%)	(0%)
3	42.30	8	-	45 mL	0 °C/ 50 min	(15%)	trace	(0%)	(0%)
4	100	8	-	120 mL	-5 °C/ 40 min	(14%)	trace	(0%)	(0%)
5	56.42	4	0.42 mL	60 mL	0 °C, 10 °C/ 2 h	(6%)	(0%)	(0%)	(0%)
6	140	5	-	80 mL	-78 °C, rt/ 3 h	(18%)[a]	(0%)	(0%)	(0%)
7	280	5	-	250 mL	0 °C, rt/ 5 h	(20%)	(0%)	(0%)	(0%)
8	280	8	-	130 mL	-10 °C, rt/ 24 h	(0%)	32 mg of **79** and **80**[b]		(0%)

[a] Intractable mixture with the starting material **61**.
[b] From the reaction of 0.1 g (0.28 mmol) of the starting material **61**.

Table 2. 8: Different reaction conditions were used in attempts to synthesize **77** from **61** by Scholl reaction. The oxidant in each case was $FeCl_3$.

The oxidative cyclodehydrogenation using $FeCl_3$ was further investigated, as represented in Table 2.8 (entry 8), at room temperature in 24 hours and no $MeNO_2$ was added to the protocol. In this case, the chlorination also took place instead of cyclization, adding three chlorine atoms on the central rings (**80**) as an inseparable mixture with cyclized chlorinated product **79** (Scheme 2.23) and their structures were confirmed by X-ray crystallography and MALDI-TOF-MS. The integration by ^1H NMR spectroscopy showed a 1:0.75 mixture of **80** and **79**. The structures of the chlorinated derivatives were elucidated by X-ray crystallographic analysis as outlined in Figure 2.5. The experiments were performed under different reaction conditions such as changing the Lewis acid equivalency, diluting the solution, and longer reaction times. However, under any of the selected conditions, the intramolecular oxidative cyclodehydrogenation reaction of **61** was unsuccessful in the presence of $FeCl_3$. For this reason, the use of other oxidants rather than $FeCl_3$ was required as the chlorination by $FeCl_3$ strongly competes with the oxidative cyclodehydrogenation.

The crystallography results, performed and analysed by UEA collaborator Dr David Hughes, are very similar for the three structures **78**, **79** and **80**. Dr Hughes notes compound **78** is formed by the fusion of two planar anthracene rings through the C(1)–C(21) bond. The structure of molecule **78** can be seen in the appendix section. The angle between the normals to the meanplanes of the six-membered rings involving C(1) and C(21) is 89.99(4)°. The C(1)–C(21) bond thus forms the junction between the two anthracene planes; C(4), C(28) and Cl(28) lie close to this line. There is partial overlap of parallel anthracene rings of neighbouring molecules, e.g. the C(5)-C(6)-C(7)-C(8)-C(9) section overlaps the section related by the centre of symmetry at 1½-x,1½-y,1-z; also C(26)-C(27)-C(28) overlaps the related group by the centre at 1-x,1-y,1-z. Other short intermolecular contacts involve C-H bonds directed towards aromatic rings, e.g. H(9)...C(31') at 2.98 Å; also C(6)-Cl(6) points towards C(14") at 3.443 Å.

The molecule of **79** appears to have an extensive planar structure. It is wrapped around a twofold symmetry axis which is parallel to the crystallographic *c* axis. The three-ring anthracene unit is only slightly curved, folding away from the central C(3)…C(10) vector. Compound **80** consists of two approximately planar anthracene groups linked through the C(10)-C(15) bond. The angle between the

normals to the two bonded six-membered rings, viz the rings of C(10) and C(15), is 80.59(5)°. None of the rings is strictly planar and within each three-ring anthracene group, there is either bending (about the C(3)-C(10) vector) or twisting (rotation about the C(16)-C(24) vector; the torsion angle for C(17)-C(16)-C(24)-C(23) is 10.55°). The anthracene rings of C(15) to C(28) overlap with centrosymmetrically related rings on each side with interplanar distances of *ca* 3.50 Å and form columns of overlaid rings parallel to the *a* axis. The rings of C(1) to C(14) are barely overlapping, with only the C(7) and C(14') atoms, at the extremities of the rings, with an overlap distance at 3.368 Å. Structural data and tables are given in the Appendix.

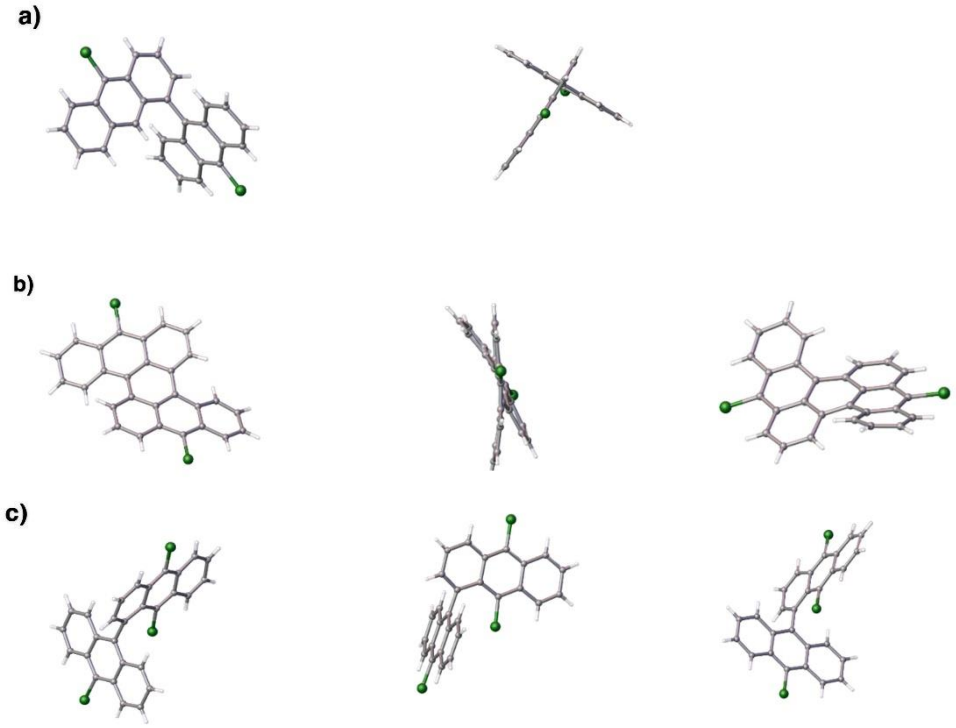

Figure 2.5: a) X-ray crystallographic structure of 9,10′-dichloro-10,8′-bianthracene **78**. b) X-ray crystallographic structure of 9,10′-dichloro-anthracene-fused-anthracene **79**. c) X-ray crystallographic structure of 9,9`,10′-trichloro-10,8′-bianthracene **80**.

2.7.2 Test Scholl Photocyclization Reaction Using Unsubstituted 1, 9'- Bianthracene with DDQ

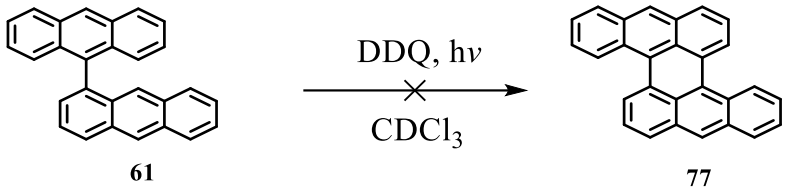

Scheme 2.24: Unsuccessful attempted oxidative photocyclization for the preparation of unsubstituted fused anthracenes **77** using DDQ/UV light in deuterated chloroform.

Oxidative photocyclization of π-conjugated PAHs under ultraviolet irradiation has been extensively studied.[111,112] Under UV irradiation, bianthracene **61** was dissolved in $CDCl_3$ in the presence of air and even DDQ in an NMR tube (Scheme 2. 24). However, the ^1H NMR spectroscopic analysis did not display evidence of any oxidative cyclodehydrogenation products.

2.7.3 Test Scholl Cyclization Reaction Using Unsubstituted 1, 9'- Bianthracene with DDQ/MsOH, $AlCl_3$/NaCl, and $K_3Fe(CN)_6$

Entry	Substrate (61) (mmol)	DDQ (equiv)	Catalist	CH_2Cl_2	Temp/Time	Yield 77 (%)
1	0.1	1.75	$MeSO_3H$/ 0.5 mL	9.5 mL	0 °C/ 15 min	0
2	0.1	2	$MeSO_3H$/ 1 mL	60 mL	0 °C, rt, then reflux overnight	0
3	0.1	1.1	$MeSO_3H$/ 1 mL	50 mL	0 °C/ 16 h at rt	0
4	0.03	1.5	$MeSO_3H$/ 0.1 mL	5 mL	-10 °C/ 50 min	0
5	0.03	-	$AlCl_3$/NaCl (5:1)	5 mL	rt/ 1h	0
6	0.03	-	$K_3Fe(CN)_6$/ 2 equiv.	5 mL	rt/ 1h	0

Table 2. 9: Scholl reaction conditions for the attempted anthracene fused anthracene **77** using various oxidants.

As can be seen in Table 2.9, further Scholl reaction experiments towards anthracene fused anthracene **77** were also carried out using alternative oxidants such as DDQ/MsOH mixture, $K_3Fe(CN)_6$, and $AlCl_3$/NaCl mixture. It has been reported that DDQ easily oxidizes a number of aromatic donors in the presence of an acid.[71,120] In addition, using DDQ as an oxidant in Scholl reactions is preferable compared to the commonly utilized $FeCl_3$ because contamination by chlorinated products can be avoided as well as the use of large excess of $FeCl_3$ can be avoided by using only 1 equiv. of DDQ per C-C bond formation for the completion of Scholl reactions. Generally, the reactions were performed as it is reported in the literature.[71,88,114,115] The starting material and DDQ were dissolved in anhydrous DCM in a Schlenk flask under nitrogen. After adding methanesulfonic acid (MsOH) dropwise under ice bath cooling, the solution colour immediately changed to dark green. The reaction was monitored by TLC. The reaction mixture was then quenched by the addition of a saturated aq. $NaHCO_3$. The organic layer was separated and washed with aq. $NaHCO_3$. The crude products obtained were investigated *via* MALDI-TOF MS, which revealed the presence of the starting material and unknown species and no oxidative cyclodehydrogenation was observed (entries 1-4, Table 2.9). ^{1}H NMR spectroscopic analysis of the mixture of products revealed a featureless spectrum in the aromatic region, indicating strong molecular aggregation. Further Scholl and oxidative aromatic coupling attempts were evaluated using $AlCl_3$/NaCl and $K_3Fe(CN)_6$ /DCM mixtures (entries 5 and 6, Table 2.9).[113,121] No reactions occurred when those systems were applied as the colour of the solution did not change.

2.7.4 Test Scholl Cyclization Reaction Using Unsubstituted 1, 9'- Bianthracene with DDQ/TfOH

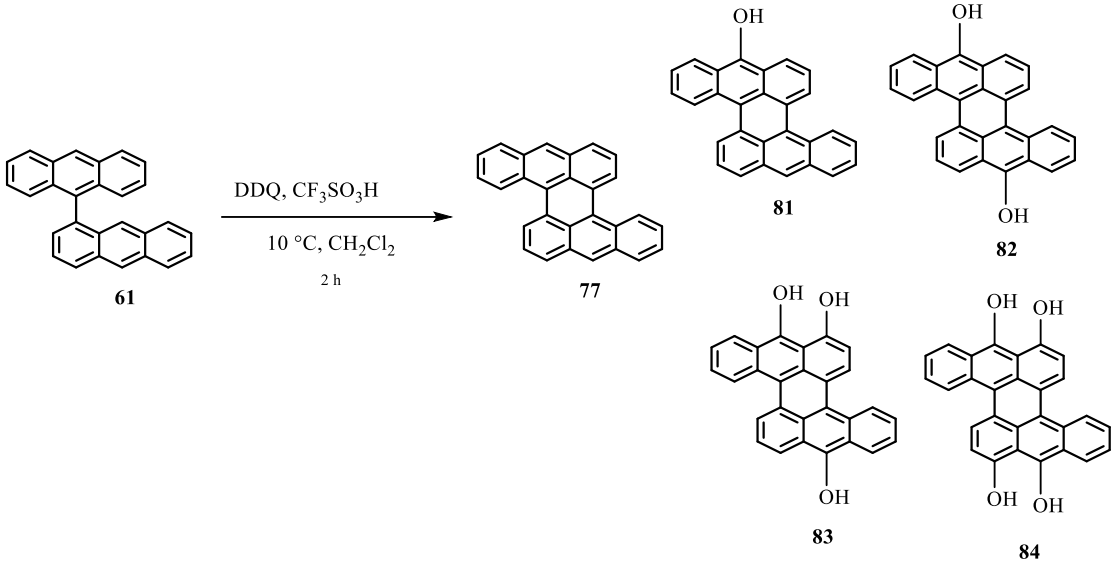

Scheme 2.25: Synthesis of anthracene fused anthracene and possible subsequent hydroxyl derivatives formed. Compound **61** readily undergoes overoxidation upon exposure to light/air in a solution at room temperature to produce **81**, **82**, **83**, and **84** according to MALDI-TOF-MS.

It was concluded that changing the equivalence of DDQ has no effect on the cyclization step and the reaction was completely ineffective when MsOH was used as the acid. Therefore, we decided to explore the oxidative cyclization reaction using stronger acid named trifluoromethanesulfonic acid (TfOH).[71,72,114,115,122,123] It can be seen from Table 2.10 that several annulation attempts using DDQ/TfOH mixture have been used under different reaction conditions, such as different temperatures and duration. In the first approach, precursor **61** was oxidized with DDQ (1.5 - 1.8 equiv.) at -10 °C in dry DCM (entries 1-3, Table 2.10). Subsequently, triflic acid (0.1 - 1 mL) was added as a catalyst in one portion. The reaction mixture was allowed to warm up to 10 °C and was tracked with TLC, which showed the formation of the desired product after 2 hours. However, after workup and column chromatography, TLC analysis revealed the presence of the product **77** along with the unseparable fluorescent spot of the starting material **61** as well as the formation of a new species. In addition to the product **77** and starting material **61** signals at m/z 352 and m/z 354, respectively, MALDI-TOF MS analysis exhibited signals at

m/z 368, 384, 400, and 416 which could be assigned to the molecular ion peaks of the corresponding hydroxyl species **81**, **82**, **83**, and **84**, respectively (Scheme 2. 25**)**.

Entry	Substrate (61) (mmol)	DDQ (equiv)	TfOH (equiv)	CH_2Cl_2	Temp/Time	Yield 77 (%)
1	0.10	1.5	57	80 mL	-10 °C, 10 °C/ 2 h	Trace[a]
2	0.28	1.8	40.5	80 mL	-10 °C, 10 °C/ 2 h	Trace[a]
3	0.02	1.5	57	10 mL	-10 °C, 10 °C/ 2 h	Trace[a]
4	0.01	1.25	22.5	2 mL	-10 °C, rt / 3 days	Trace[a]
5	0.03	2	38	10 mL	-78 °C, rt/ 24 h	0
6	0.03	1	38	15 mL	0 °C, rt/ 8 h	Trace[a]
7[b]	0.70	1	32.4	250 mL	rt/ 4 h	6
8[b]	0.70	1	40.5	150 mL	rt/ 1:30 h	12
9[b]	0.70	1.5	13.5	150 mL	rt/ 4 h	10
10[b]	0.42	1	7	30 mL	rt, reflux / 3 h	4
11[b]	0.42	1	4	30 mL	0 °C, rt/ 6 h	16

[a] Inseparable mixture with the starting material **61.**

[b] All reactions were carried out under a steady stream of N_2 in a Schlenk flask in the dark.

Table 2. 10: Optimization of anthracene fused anthracene **77** cyclization using a combination of DDQ and triflic acid in DCM.

The next reaction tests were carried out at rt for longer times (entries 4-6, Table 2.10). Nevertheless, similar outcomes were observed in these reactions and the hydroxyl species were identified during the reaction by TLC. In an attempt to get a ^{1}H NMR spectrum of either of these isolated products, crystals were carefully collected, and washed with hexane or methanol, then dissolved up for NMR spectroscopic analysis. Unfortunately, none of these samples showed a clear NMR spectrum due to the small reaction scale.

Generally, it turned out to be quite difficult to fuse the unfunctionalized-bianthracene structure **61**. Additionally, it has been observed that the characteristic colour of all cyclized products changes from purple to yellow in a solution when exposed to light in a short time (less than 1 hour) resulting in decomposition. The following experimental attempts therefore were carried out under harsher reaction conditions involving the even more rigorous exclusion of oxygen by degassing the reaction mixture continuously by bubbling N_2 through a needle and exclusion of light by carrying out the reaction in the dark.

The objective was therefore to optimize the reaction conditions to avoid the formation of the hydroxyl side products. As can be seen in Table 2.10, further Scholl reaction attempts were carried out with TfOH/DDQ mixture in the dark (entries 7-11, Table 2.10). The reaction proceeded at room temperature in the absence of light and the starting bianthracene was totally consumed within 4 hours. However, MALDI-TOF MS and TLC analyses revealed the formation of the oxidized side products along with the starting material **61** after aq. workup, suggesting that the oxidative cyclized product **77** is highly unstable upon exposure to light during the extraction process. As a result, the desired compound was isolated in a low yield of 6% (entry 7, Table 2.10). Because the cyclized product **77** decomposes in light, all the subsequent workups including extraction, purification in column chromatography, and removing solvent under reduced pressure were performed in the absence of light. Diluting the reaction to 150 mL of DCM and reducing the acid loading along with time gave the cyclodehydrogenated compound **77** in an improved yield of 12% (entry 8, Table 2.10). The equivalency of the oxidant was slightly increased to 1.5 and the equivalency of the acid was decreased to 13.5 at longer reaction time, but no significant change in the yield was observed (entry 9, Table 2.10). It should be pointed out that the choice of reaction temperature plays a crucial role in the intramolecular cyclodehydrogenation. In order to accelerate the reaction, the temperature was increased to reflux and the reaction was running in diluted concentration, but without improvement of the yield (entry 10, Table 2.10). Carrying out the reaction with only 4 equiv. of TfOH at room temperature for 6 hours in diluted concentration and complete isolation from light improved the yield slightly to 16% (entry 11, Table 2.10) (Scheme 2. 26**)**.

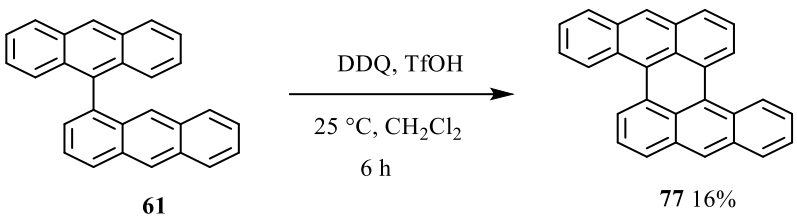

Scheme 2.26: Successful attempted Scholl reaction for the preparation of unsubstituted fused anthracenes **77**.

It was hypothesized that most of the desired product **77** decomposed during chromatographic purification on silica gel. The identity of anthracene fused anthracene was successfully confirmed by NMR spectroscopic and X-ray crystallographic analyses. The ^{1}H NMR spectrum of AFA elucidated its symmetrical structure, exhibiting the distinct singlet peak resonated at δ 8.34 in the aromatic region (Figure 2.6). This is also consistent with the ^{13}C NMR spectrum that only 14 peaks were observed.

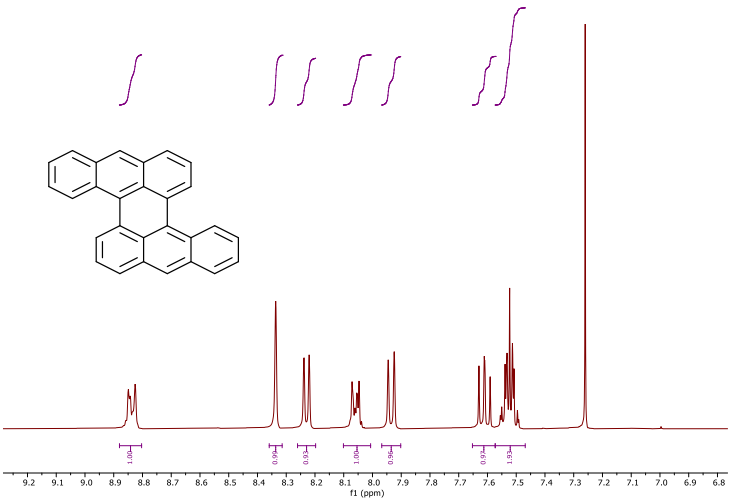

Figure 2.6: The aromatic region of the ^{1}H NMR spectrum of the fully fused anthracene **77** in $CDCl_3$.

2.7.5 Test Scholl Cyclization Reaction Using Unsubstituted 1, 9'- Bianthracene with $FeBr_3$

The oxidative cyclodehydrogenation was further investigated using $FeBr_3$ as represented in Table 2.11. The reaction was very slow with 3 equiv. of $FeBr_3$ in DCM at rt, and no full conversion was obtained in 3 days (entry 1, Table 2.11).

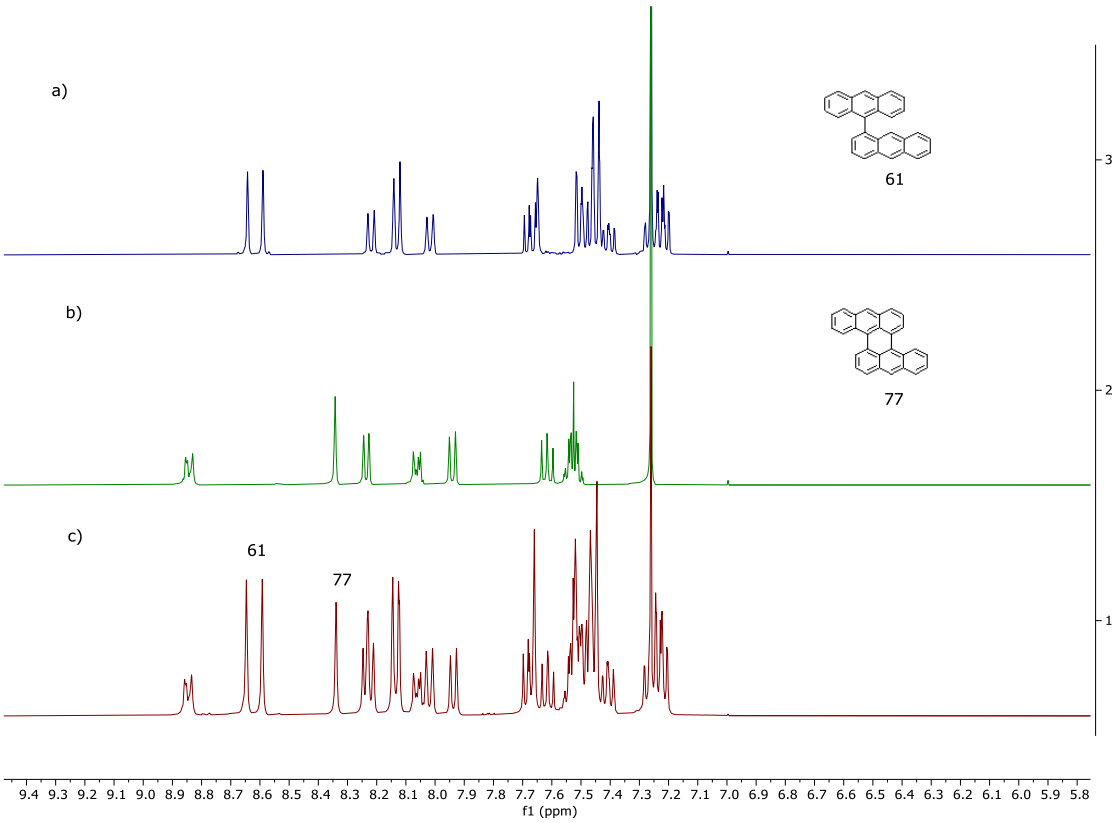

d)

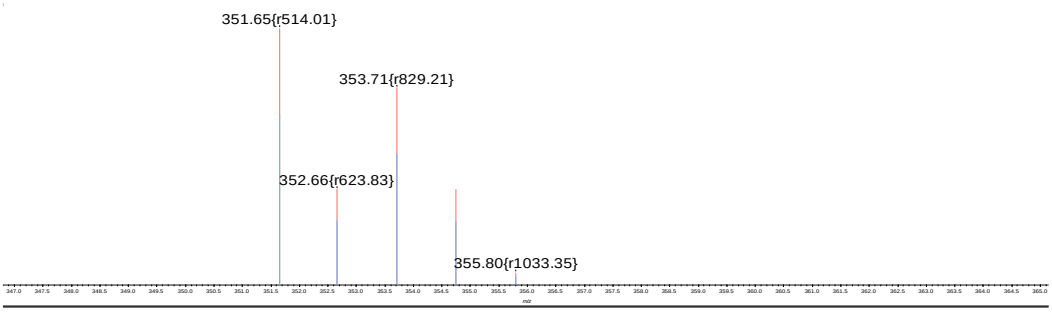

Figure 2.7: a) ^{1}H NMR spectrum of bianthracene **61** in $CDCl_3$ after SMC reaction. b) ^{1}H NMR spectrum of the fully fused anthracene **77** in $CDCl_3$ after Scholl reaction using TfOH/DDQ mixture. c) ^{1}H NMR spectrum of the inseparable mixture of compound **61** and compound **77** in $CDCl_3$ after Scholl reaction using $FeBr_3$. Singlet peaks are labelled with the corresponding compound numbers. d) MALDI-TOF MS chart confirms the formation of mixture product **77** and **61**.

The ^{1}H NMR spectroscopic analysis corroborated the MALDI-TOF MS analysis exhibiting a 1:1 mixture of the product **77** and the remaining starting material **61** which prevented isolation of the desired product (Figure 2.7 -c and d). Due to the slow process of cyclodehydrogenation, the reaction was run with

a higher amount of $FeBr_3$ (7 equiv.) for a longer reaction time (7 days), but this led to decomposition of the residual starting material (entry 2, Table 2.11). FeI_3 could not be applied as a catalyst because of its instability that results from a self-redox reaction, unlike the regularly used catalysts $FeCl_3$ and $FeBr_3$.[124]

Entry	Reaction Conditions[a]	Outcome
1	$FeBr_3$ (3 equiv.), dry CH_2Cl_2 rt, 3 days	mixture of AFA **77** and starting material **61**
2	$FeBr_3$ (7 equiv.), dry CH_2Cl_2 rt, 7 days	Decomposition

[a] All reactions were carried out under a steady stream of N_2 in a Schlenk flask in the dark.

Table 2. 11: Oxidative cyclodehydrogenation reactions towards AFA **77** using $FeBr_3$ as an oxidant.

2.7.6 Test Scholl Cyclization Reaction Using Unsubstituted 1, 9'- Bianthracene with DDQ/TfOH and Toluene

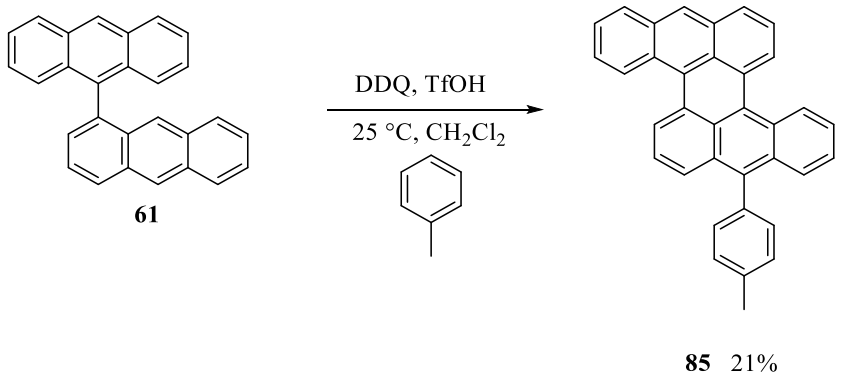

Scheme 2.27: The attempted oxidative cyclodehydrogenation of **61** towards **85** in the presence of toluene.

Tolyl-anthracenyl-anthracene (**85**) was obtained by accident while attempting to form anthracene fused anthracene using DDQ/TfOH mixture in dry DCM at room temperature. The isolated compound was pure but it did not correspond to the desired product **77**. According to NMR spectroscopic analysis, the symmetry was broken and the alkyl region showed a distinct singlet peak. MALDI-TOF MS of the isolated product exhibited a signal at m/z 442 indicating the presence of toluene. It was assumed that the dry DCM was contaminated with toluene. The X-ray crystallography proved that toluene was incorporated onto the central bottom ring of fused anthracene. The source of toluene was not certainly known but it could be contaminant in dry DCM obtained from a different lab. Once contamination of toluene was verified, the same procedure was repeated with a known quantity of dry toluene (0.05 mL)

using DDQ/TfOH mixture in dry DCM (100 mL) at room temperature to generate **85** in 21% yield (Scheme 2.27). The single X-ray crystal structure of **85** (again solved by our collaborator Dr David Hughes) displayed a slightly twisted structure at the two anthracene units along with the twisted conformation of benzene ring (Figure 2.8). Despite having so many (approximately) planar, aromatic rings there is little π…π stacking of molecules; part of the C_6 ring of C(23-28) plus C(22) lies parallel to and *ca* 3.6 Å from an inverted unit. Most of the shorter intermolecular contacts involve perpendicular C-H…π interactions. The excess of toluene can cause the formation of two toluene groups at the 9-10` positions (according to MALDI-TOF MS) as a side-product, which was impossible to isolate.

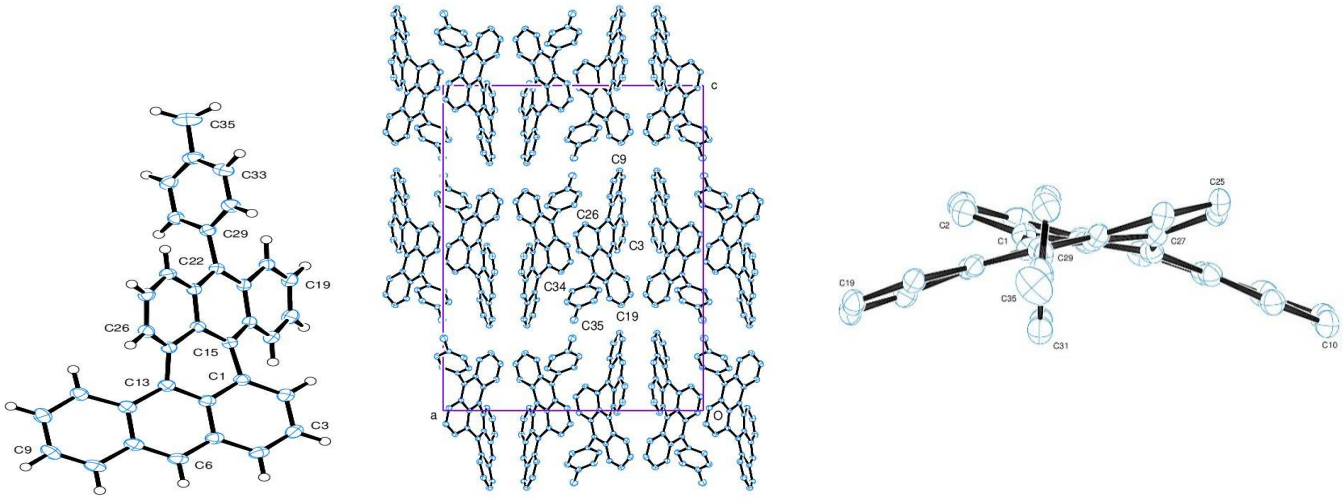

Figure 2.8: X-ray crystallographic structure of tolyl-anthracenyl-anthracene **85**.

2.7.7 Test Scholl Cyclization Reaction Using Unsubstituted 1, 9'- Bianthracene with DDQ/TfOH and Anisole

The aforementioned method also proved to be more effective when a highly reactive aryl group (anisole) was attached to **61** using the DDQ/TfOH mixture to produce AFA-anisole (**86**) with a 25% yield. The presence of methoxy group on the anisole enhanced the rate of reaction. It is worth mentioning that TLC analysis of the crude reaction mixture revealed complete consumption of the starting material after 1 hour. However, the ^{1}H NMR and mass spectra of the purified (column chromatography) product indicated the presence of the corresponding anisole-bianthracene (**87**) in 40% yield (Scheme 2.28). This

intermediate was further oxidatively cyclized overnight to give the fused product **86**. MALDI-TOF MS analysis exhibited a signal at m/z 457 and NMR spectroscopy further supported the identity of the desired product **86**.

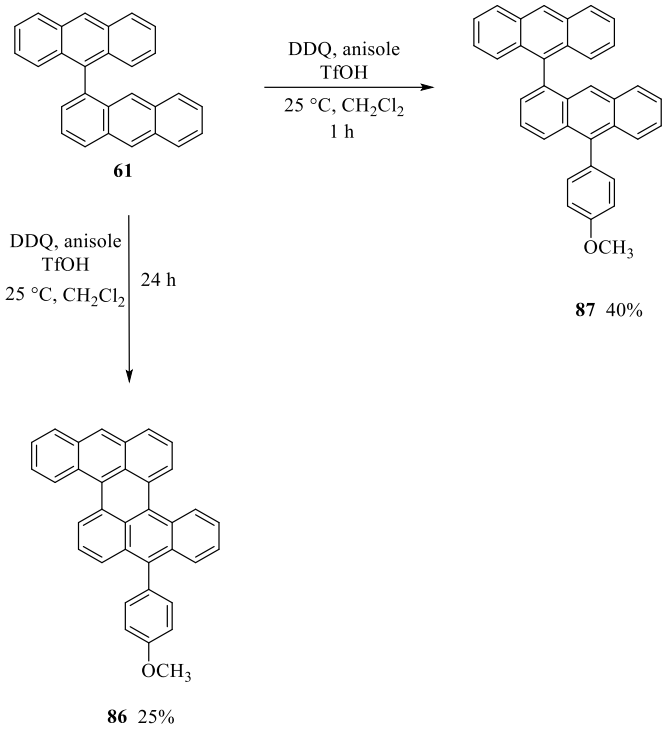

Scheme 2.28: The attempted oxidative cyclodehydrogenation of **61** towards species **86** and **87** in the presence of anisole.

2.7.8 Test Scholl Cyclization Reaction Using Di/Mono-Hexyloxy-1, 9' Bianthracene with DDQ/TfOH

2.7.8.1 Test Scholl Cyclization Reaction Using Substituted Bianthracene with DDQ/TfOH

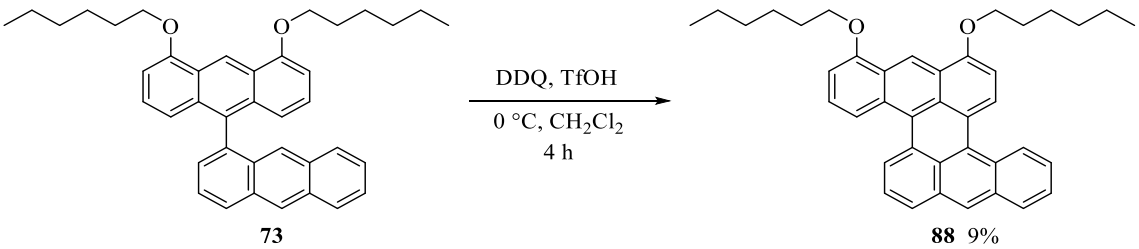

Scheme 2.29: Successful attempted Scholl reaction for the preparation of dihexyloxy fused anthracenes.

In an attempt to promote the Scholl cyclization reaction, bianthracene should bear electron donating substituent in the 8-position activating the formation of a new bond to the adjacent anthracene ring. However, Scholl reactions do not always require electron-donating groups on the aromatic ring as demonstrated previously in unsubstituted bianthracene **61**. The dihexyloxy bianthracene **73** was chosen over the monohexyloxy bianthracen **82** as starting material for this reaction. Dihexyloxy fused anthracene (**88**) was obtained under similar conditions after attempting several purification procedures as shown in Scheme 2.29. At shorter reaction times and lower temperature in the presence of DDQ/TfOH, **73** was converted into the desired product **88** in only 9% yield. The identity of the synthesized **88** was confirmed by NMR spectroscopy and MALDI-TOF MS analysis but its structure could not be identified by X-ray crystallographic analysis.

2.7.8.2 Test Scholl Cyclization Reaction Using Di-Hexyloxy-1, 9' Bianthracene with DDQ/TfOH and Phenyl Rings (Anisole and Toluene)

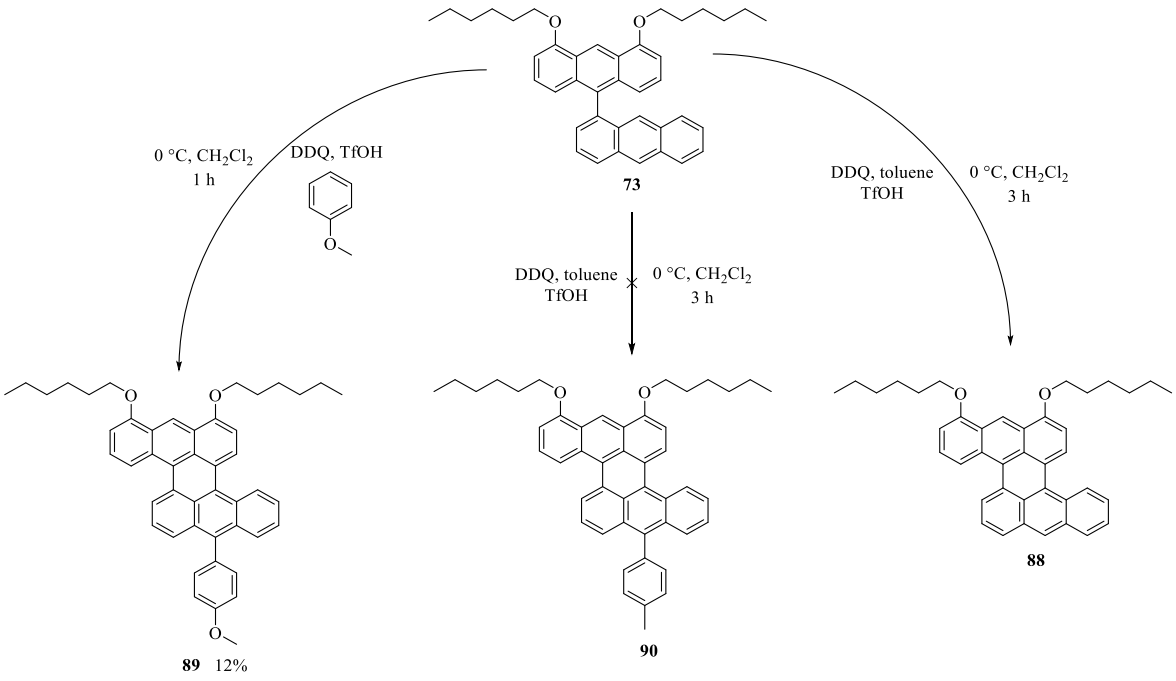

Scheme 2.30: The attempted oxidative cyclodehydrogenation of **73** towards species **89** and **90** in the presence of anisole and toluene, respectively. Compound **88** was produced instead of **90** in the presence of toluene.

As in the unsubstituted bianthracene compounds, the introduction of anisole onto the central ring of the substituted bianthracen **73** afforded anisole-dihexyloxy-anthracene fused anthracene (**89**) with a slight increase of the yield to 12% compared to the corresponding species **88** (Scheme 2.30). MALDI-TOF MS analysis displayed a signal at m/z 657 and NMR spectroscopic analysis along with X-ray crystallography further corroborated the identity of the desired product **89** (Figure 2.9). Our collaborator Dr David Hughes solve the crystal structure and commented that the two anthracene units are each close to planar but are twisted *ca* 25 ° apart through the central connecting six-membered ring. There is a rotation of 64.26(5) ° in the C(5)-C(51) bond between the six-membered ring of C(6) and the phenyl group. The *n*-hexyl group chain on O(31) has an all-*trans* conformation, whereas the chain of the O(41) hexyl group shows a rearrangement about O(41) before alignment of the outermost $(CH_2)_3Me$ atoms to the all-*trans* conformation. The solvent molecule, CH_2Cl_2, lies disordered about a centre of symmetry; at least four distinct sites for the chlorine atom were identified. The carbon atom, C(91), and the major Cl atom, Cl(92), were refined with anisotropic thermal parameters, but the minor Cl atoms, having low site occupancies, were refined isotropically. Despite the extensive, planar, aromatic anthracene units, we cannot identify any π…π contacts between molecules; the principal intermolecular interactions are of C-H groups directed side-on towards the aromatic planes.

Under analogous reaction conditions, at longer reaction time, the introduction of toluene was attempted but no conversion towards the anticipated product **90** was observed. TLC results showed complete consumption of the starting material after 3 hours and only a new single spot was observed. However, the ^{1}H NMR and mass spectra of the purified (column chromatography) product showed the formation of the corresponding dihexyloxy-AFA **88** instead. This result demonstrated that the use of toluene in the substituted bianthracen **73** did not impact the reaction.

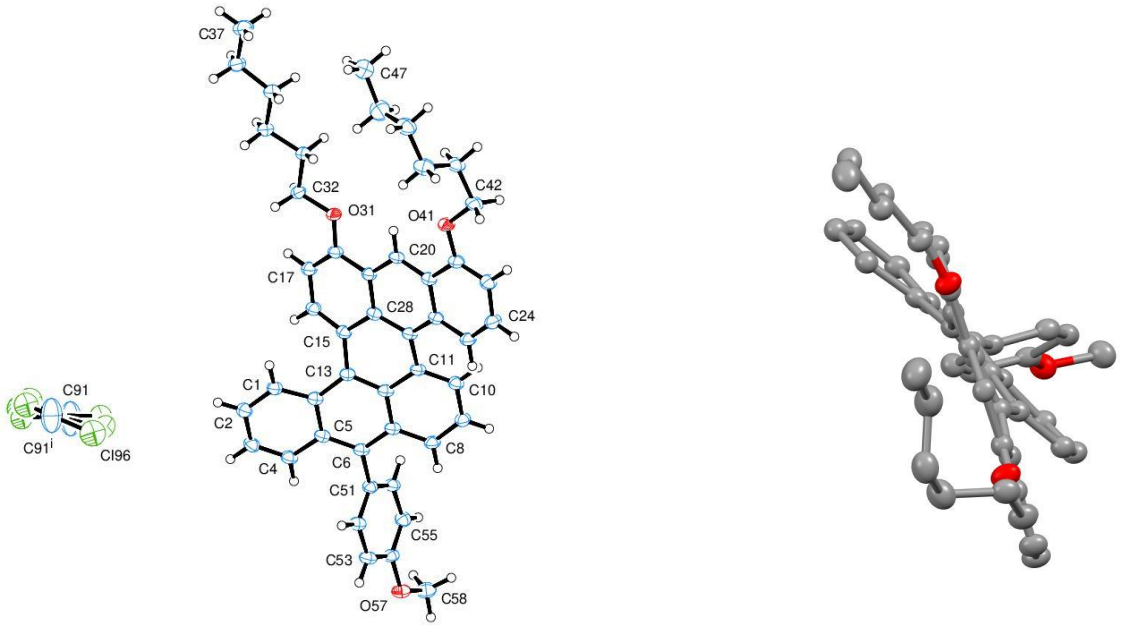

Figure 2.9: X-ray crystal structure of anisole-dihexyloxy-anthracene fused anthracene **89**.

2.7.8.3 Test Scholl Cyclization Reaction Using Mono-Hexyloxy-1, 9' Bianthracene with DDQ/TfOH

The formation of unsubstituted and di-substituted fused anthracene frameworks **77** and **88** from bianthracene derivatives was successfully accomplished using the Scholl cyclization reaction. From these results, it was postulated that the mono-substituted bianthracene **41** would undergo oxidative cyclodehydrogenation to form the framework of the targeted mono-hexyloxy fused anthracenes **42**. Similarly, fusion of the mono-substituted **41** was attempted with DDQ in dry DCM at room temperature followed by the addition of TfOH. Analysis of the reaction mixture by TLC showed the full consumption of the starting material in 50 minutes. ^{1}H NMR spectroscopic analysis of the isolated sample in deuterated chloroform, however, gave a featureless spectrum, indicating possible aggregation between molecules was occurring.

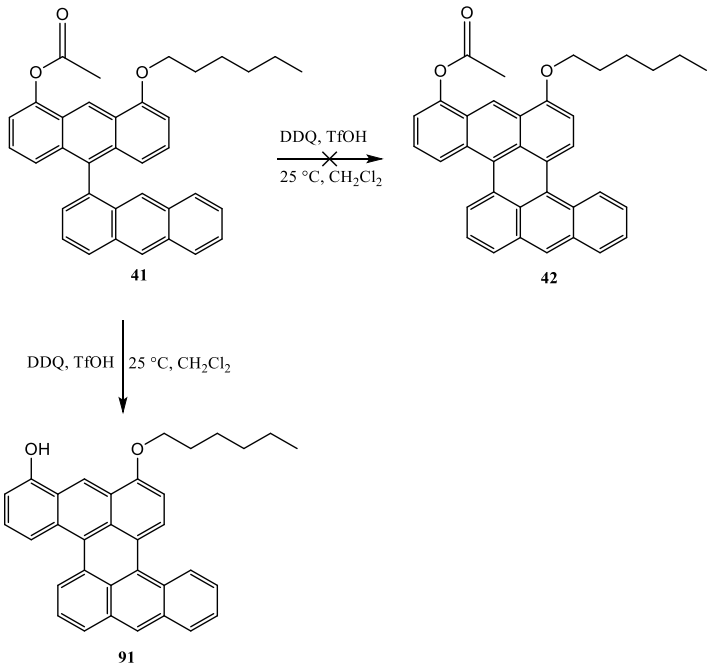

Scheme 2.31: Unsuccessful attempted Scholl reaction for the preparation of mono-hexyloxy fused anthracene and the proposed structure of the product **91** that was assumed from signals in the MALDI-TOF MS.

Unfortunately, MALDI-TOF MS analysis of the isolated purple product did not support the formation of the assumed product **42**. It exhibited a signal at m/z 467, indicating that the ester group could be selectively hydrolysed to hydroxyl by TfOH, whereas the oxidative cyclization occurred and hexyloxy group was still present generating compound **91** (Scheme 2.31).

2.7.8.4 Test Scholl Cyclization Reaction Using Mono-Hexyloxy-1, 9' Bianthracene with DDQ/TfOH and Anisole

As already described before, TfOH/DDQ mixture represents a powerful oxidant for the intramolecular Scholl reactions starting from bianthracene precursors. Fusion of mono-hexyloxy bianthracene linked anisole (**93**) was attempted following the typical reaction conditions at 0 °C. However, TLC analysis displayed the full consumption of starting material **41** after 5 minutes and revealed several new fluorescent and purple spots. MALDI-TOF MS analysis of the crude reaction mixture showed signals at m/z 469, 510, 573, and 615 which could be fully cyclodehydrogenated species and those corresponding to the molecular ion peaks of hydrolysed precursor **91**, **42**, hydrolysed precursor linked anisole (**92**), and

target product **93**, respectively (Scheme 2.32) (Figure 2.10-a). After 50 minutes and after workup of the reaction mixtures, additional MALDI-TOF MS of the crude reaction mixture showed a higher abundance peak of **92** at m/z 573 and lower abundance peak of **93** at m/z 615 (Figure 2.10-b). This can be attributed to the hydrolysis of ester group to alcohol over time.

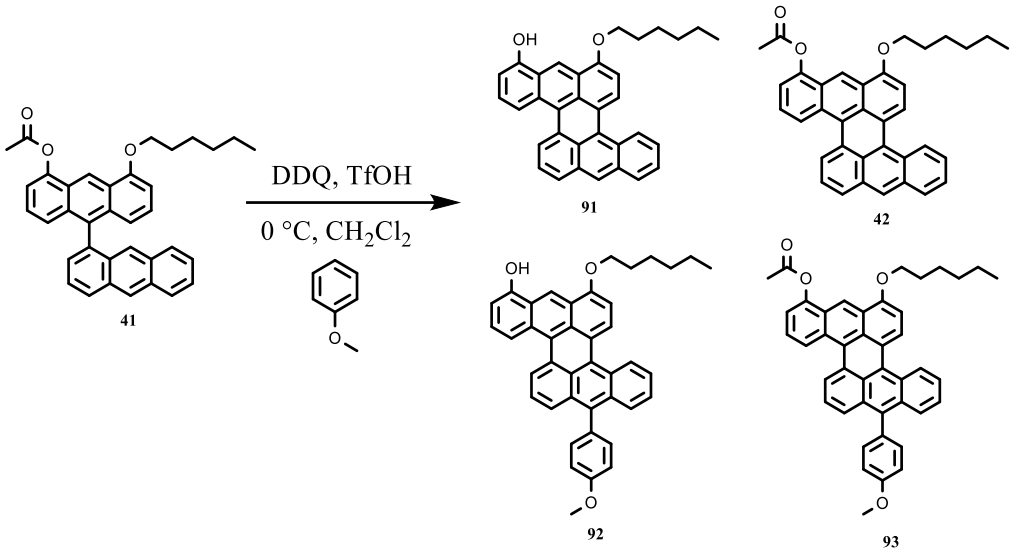

Scheme 2.32: The attempted Scholl reaction for the preparation of mono-hexyloxy fused anthracene linked anisole **93** and the proposed side products **91**, **42**, and **92** assumed from signals in the MALDI-TOF MS.

Once again, the oxidative cyclodehydrogenation reaction when the substrate bears the ester group turned out to be very challenging, even when anisole was attached. Unfortunately, the attempted separation of the four compounds *via* column chromatography could not be achieved, probably due to very close R_f values of the products formed and decomposition that might occur during chromatographic purification on silica gel. As a result, compounds **42**, **91**, **92**, and **93** could not be further characterized and their formation was analysed from signals in the MALDI-TOF MS associated to the loss of hydrogen atoms in the starting material.

a)

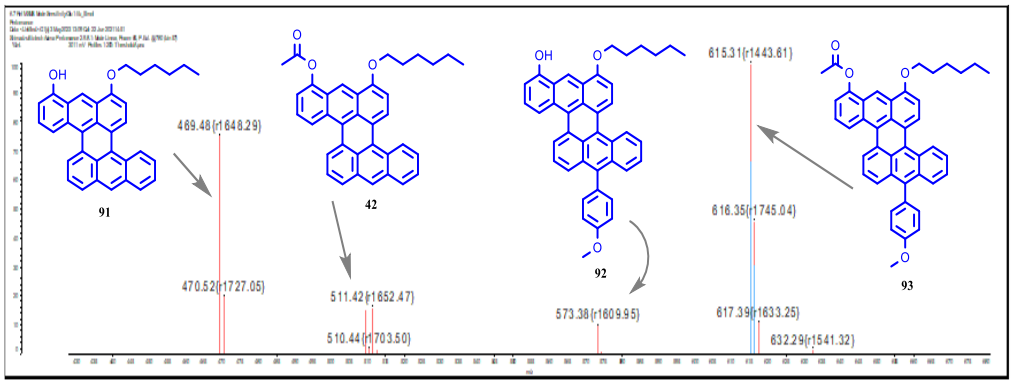

b)

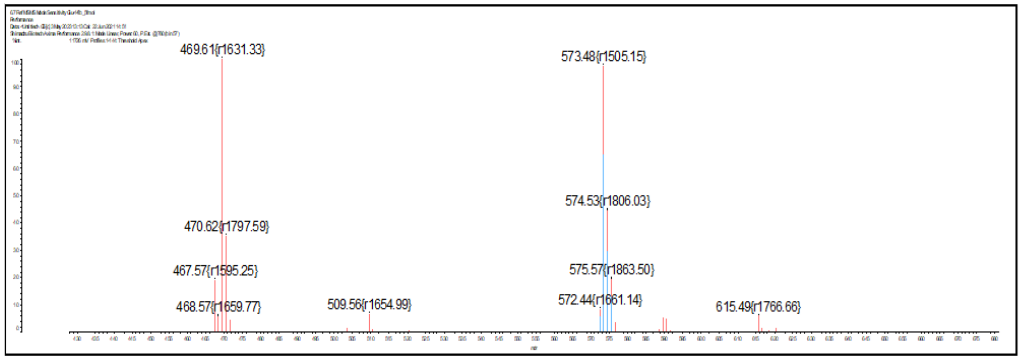

Figure 2.10: a) The MALDI-TOF MS spectrum for the oxidative cyclodehydrogenation products of **41** after 5 minutes. b) The MALDI-TOF MS spectrum for the oxidative cyclodehydrogenation products of **41** after 50 minutes.

2.8 Optical Properties

The photophysical properties (including absorption and emission) of the unfused and fused products were investigated. The unsubstituted bianthracene **61** exhibits a long wavelength absorption band at λ_{abs} 388 nm measured in DCM (Figure 2.11-a). Chlorination and incorporation of anisole cause 13 nm and 9 nm bathochromic shifts (λ_{abs} = 401and 397 nm, respectively) when compared to the unsubstituted molecule (Figure 2.11-b and c). In terms of emission behavior, the unfused derivatives **61**, **78**, and **87** exhibit emission maxima at λ_{em} 438 nm, λ_{em} 450 nm, and λ_{em} 435 nm, respectively, in DCM solution (Figure 2.11-a, b, and c).

Fusion of unsubstituted bianthracene **61** leads to a significant red-shift in both the absorption and emission maxima ($\lambda_{abs}/\lambda_{em}$ = 554/568 nm) (Figure 2.11-d), and the effect is particularly noticeable when

the phenyl groups are introduced. The absorption and emission spectra for the fused anthracene-toluene **85** and fused anthracene-anisole **86** are very similar with a maximum absorption at λ_{abs} 564 nm and with a maximum emission at λ_{em} 580 nm (Figure 2.11-e and f). As mentioned at the introduction chapter, it was believed that by fusing the aromatic rings the absorption and emission spectra would be red-shifted due to a smaller HOMO and LUMO energy gap. The observable red-shift of fused anthracene precursors in the absorption and fluorescence spectra compared to that of unfused anthracene precursors demonstrates the successfully extended π-conjugated systems in the resulting cyclized products.

The photophysical properties of di-substituted fused derivatives **88** and **89** display that they have similar or little shifted maximum absorption wavelengths but have significantly longer maximum emission wavelengths from those of unsubstituted fused derivatives ($\lambda_{abs}/\lambda_{em}$ = 562/610 nm for **88** and $\lambda_{abs}/\lambda_{em}$ = 580/625 nm for **89**). Moreover, it can be noted that fused derivatives containing two donor substituents show a broader absorption band than those of unsubstituted fused derivatives (Figure 2.11-g and h).

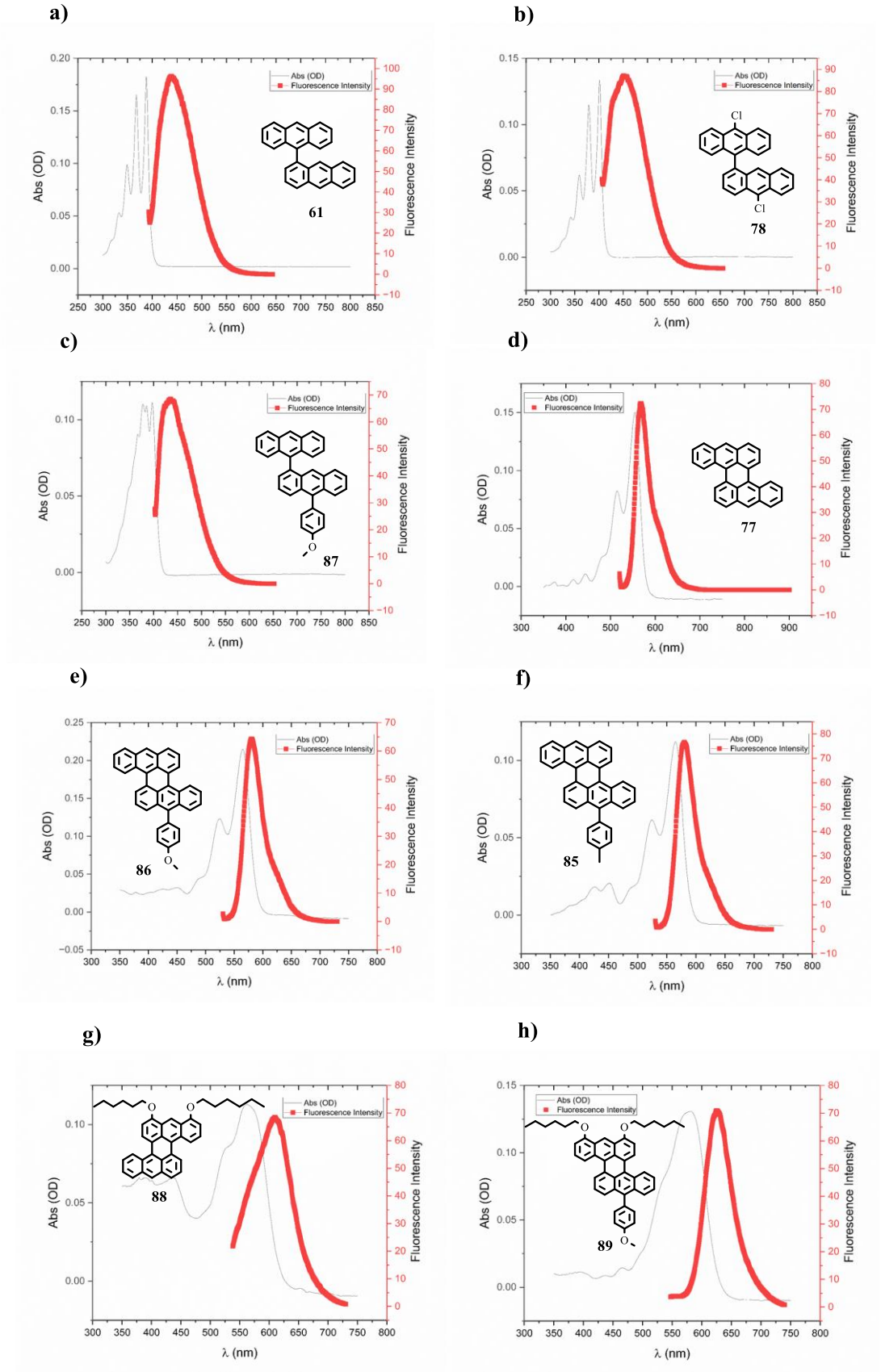

Figure 2.11: Absorption (grey line) and emission (red line) spectra for unfused and fused anthracene compounds **61** (a), **78** (b), **87** (c), **77** (d), **86** (e), **85** (f), **88** (g), and **89** (h) in DCM.

2.9 Conclusion

In summary, the boronate and halide partners that were needed for cross-coupling were successfully synthesized. Different strategies were investigated in order to improve the reaction yield for the cross-coupling. The synthesis of cross-coupled bianthracenes using palladium-catalysed Suzuki cross-coupling reactions required the optimization of a modified synthetic procedure. This modification was necessary to counteract the relatively low reactivity of the bromide coupling partners as well as avoid the competing homo-coupling side-product of the aryl halide and protodeboronation of aryl boronate. The use of iodoanthracene as the halide coupling partner along with $Pd(PPh_3)_4$ as the palladium catalyst source was more favourable for the cross-coupling reaction than their bromoanthracene and $Pd(dppf)Cl_2$ counterparts. This allowed the useful synthesis of unfunctionalized and functionalized bianthracene derivatives.

A variety of reaction conditions were attempted to achieve the oxidative cyclodehydrogenation. The use of $FeCl_3$ proved to be unsuccessful due to high competition between oxidative cyclodehydrogenation and chlorination. $FeBr_3$ was ineffective giving **77** with an inseparable starting material. No reactions occurred when the $AlCl_3$/NaCl and $K_3Fe(CN)_6$ /DCM systems were applied. With DDQ/MsOH as the oxidant, only an unidentifiable messy mixture was detected. Finally, the oxidative cyclodehydrogenation was successfully achieved by the treatment of **61** with DDQ in DCM/ TfOH, which was proved to be the best oxidant reagent for the desired transformation.

The substrate scope of unfunctionalized bianthracene **61** was explored to assess the applicability and generality of the Scholl reaction of functionalized bianthracene components **73** and **41**.

The incorporation of phenyl rings, that was designed to enhance the stability and efficiency of the target fused anthracenes, at the central 10`-position had little impact on the yield for both unsubstituted and disubstituted moieties. However, this approach still did not show a significant variation in the yield.

The MALDI-TOF MS analysis revealed that the conversion of the target mono-hexyloxy fused anthracene precursors **42** and **93** was too slow. Unfortunately, the inclusion of electron withdrawing

acetate group was clearly noted as an obstacle. The structures of the synthesized unfused and fused anthracene were effectively characterized using NMR spectroscopy, MALDI-TOF MS, single-crystal X-ray diffraction, UV–vis, and emission spectroscopy.

2.10 Future work

This area of investigation has promising prospects for future work. The oxidative cyclodehyrogenation of the unsubstituted bianthracene **61** opens the door for promising strategies to expand the π-systems. Future work in this regard will pertain to functionalizing the fused anthracene with halogens in the most reactive sites (central rings), and thus rebuilding larger extended π-conjugated systems by the SMC and Scholl reactions. This can also help to reduce the number of steps required to install functional groups prior to cross coupling since this strategy requires no prefunctionalization on the anthracene units. Furthermore, studying the variation of the fused formed products in the UV/vis spectrum over time at room temperature upon light and air and understanding the stability for each precursor.

Experimental Section

3.1 Reagents and Instrumentation

All reagents and solvents were purchased from commercially available sources. Most reactions were carried out under nitrogen or argon and monitored using TLC plates. All material performed in a glove box were in a controlled atmosphere whose argon atmosphere was constantly circulated through a purification system and continuously monitored for moisture and oxygen content which was kept at a level of ~l ppm. TLC analysis was performed on aluminium backed sheets (Merck Silica Gel 60F245) by using 254 nm UV light. Column chromatography was cried out by utilizing 60 A 40-63 micron at ambient temperature. Evaporating the solvents of prepared compounds was performed using a Buchi Rotavapor.

^{1}H and ^{13}C spectroscopic measurements for all compounds were recorded using a 400 MHz and 500 MHz NMR spectrometers. Mass spectra measurements were recorded using MALDI-MS and no matrix was used. Melting points were recorded on a Reichart Thermovar microscope with a thermopar based temperature control. Ultraviolet-Visible absorption spectra were measured on a Perkin Elmer Lamda 365 UV/VIS instrument. Fluorescence spectra were obtained on a Perkin Elmer LS55 spectrometer over a 300 - 800 nm range using DCM solutions. Samples were taken at room temperature in quartz cuvettes of path length 1 cm.

3.2 Preparation of 1-Bromoanthracene

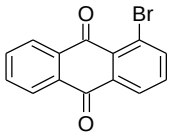

1-Bromoanthracene-9,10-Dione[125] **(56):** To a 250 mL rb flask, copper (II) bromide (2.51 g, 11.23 mmol) was dissolved in *tert*-butyl nitrite (1.6 mL, 13.4 mmol) and 40 mL of acetonitrile with stirring under argon gas. To this stirred solution at 65 °C, 1-aminoanthracene-9,10-dione **55** (1.98 g, 8.87 mmol) was added in 20 portions in 1 h, and the temperature was increased to 90 °C for 3 h. The mixture was then cooled to 25 °C and diluted with 100 mL of 1 M of hydrochloric acid. The mixture was filtered, washed

with 20 mL of 1 M HCl and 50 mL of H_2O. The crude solid was dried on air overnight. The solid was dissolved in 250 mL of DCM and dried over $MgSO_4$. The resulting solution was concentrated to give **56** (1.92 g, 74%) as an orange solid. ^{1}H NMR (500 MHz, Chloroform-*d*) δ 8.38 (dd, *J* = 7.7, 1.3 Hz, 1H), 8.34 – 8.31 (m, 1H), 8.29 – 8.26 (m, 1H), 8.06 (dd, *J* = 7.9, 1.3 Hz, 1H), 7.85 – 7.78 (m, 3H), 7.59 (t, *J* = 7.8 Hz, 1H).

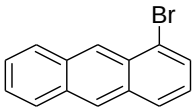

1-Bromoanthracene[125] **(40):** 1-Bromoanthracene-9,10-dione **56** (1.92 g, 6.69 mmol) was dissolved in 35 mL of *i*-PrOH, placed in ice water bath, and 0.56 g of $NaBH_4$ (0.56 g, 14.89 mmol) was added into the stirred solution. After 3 h of stirring, 10 mL of H_2O were added in two portions in a minute, and stirred for additional 3 h, then concentrated to 25 mL under vacuum. The mixture was extracted with 50 mL of toluene, dried by Na_2SO_4, and concentrated under vacuum to give 1.70 g. The residue was dissolved in 90 mL of glacial acetic acid, and $SnCl_2$ (3.01 g, 15.88 mmol) was added in one portion. The solution was heated for 2 h at 100 °C, and cooled to 23 °C. The mixture solution was then diluted with 100 mL of H_2O, extracted wit 150 mL of toluene, dried over Na_2SO_4, and concentrated under vacuum. The crude solid was then isolated through 4-inch silica plug using DCM/pet ether mixture (1:5) to obtain **40** (0.58 g, 34%) as a yellow powder. ^{1}H NMR (500 MHz, Chloroform-*d*) δ 8.82 (s, 1H), 8.44 (s, 1H), 8.13 – 8.08 (m, 1H), 8.05 – 8.00 (m, 1H), 7.98 (d, *J* = 8.6 Hz, 1H), 7.79 (d, *J* = 7.1 Hz, 1H), 7.63 – 7.44 (m, 2H), 7.29 (dd, *J* = 8.40, 7.05 Hz, 1H).

3.3 Preparation of Mono-Hexyloxy-10-Anthracenyl(Pinacol)Boronate Ester

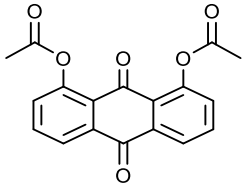

1,8-Diacetoxyanthraquinone[92] **(47):** A mixture of 1,8-dihydroxyanthraquinone **46** (9.22 g, 38.38 mmol), acetic acid, sodium salt (48 mg, 0.58 mmol), and acetic anhydride (70.0 mL, 635 mmol) were placed in a

250 mL rb flask. The solution was refluxed for 16 h at 150 °C. The mixture was then cooled and quenched with 300 mL H_2O and stirred for 30 min at rt. The precipitate was filtered, washed with H_2O (3×30 mL) and dried overnight. 1,8-diacetoxyanthraquinone **47** (12.15 g, 98%) was obtained as a brown-green solid. ^{1}H NMR (500 MHz, Chloroform-*d*) δ 8.23 (dd, *J* = 7.8, 1.3 Hz, 2H), 7.77 (t, *J* = 7.9 Hz, 2H), 7.41 (dd, *J* = 8.0, 1.3 Hz, 2H), 2.45 (s, 6H).

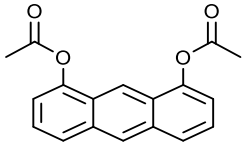

1,8-Diacetoxyanthracene[95,97] **(48):** To a 250 mL three neck rb flask, a mixture of 1,8-diacetoxyanthraquinone **47** (6.5 g, 20.04 mmol), anhydrous sodium acetate (2.46 g, 30.05 mmol), AcOH (70 mL), and $(CH_3CO)_2O$ (176 mL) were added, and heated at 135 °C with stirring under nitrogen gas until the mixture became a clear solution. To this stirring solution, zinc powder (23.6 g, (360.7 mmol) was added portion by portion but heating stopped during the addition. The reaction mixture was kept stirred at 130 °C for 1 h. The solution was then cooled to 25 °C, and filtered to remove the zinc powder. The resulting solution was concentrated, dissolved in DCM, and filtered to remove the zinc salts. The residue was subjected to silica gel chromatography (DCM) to give a non-isolated mixture of 1,8-diacetoxyanthracene and a small amount of 1,8-diacetoxyanthracene-9,10-dihydroanthracene (3.50 g). The crude product was then dissolved in dry dioxane (35 mL), and DDQ (0.60 g, 2.64 mmol) was added in one portion. The resulting mixture was refluxed at 120 °C for 30 min under nitrogen. The reaction mixture was cooled to rt and filtered to remove the hydroquinone. The solid was washed with DCM and the combined filtrates were concentrated to dryness. The crude was then dissolved in DCM and passed through silica gel. The resulting solution was concentrated in vacuum to give a relatively pure 1,8-diacetoxyanthracene **48** (3.14 g, 61%) as a yellow solid. ^{1}H NMR (400 MHz, Chloroform-*d*) δ 8.50 (s, 1H), 8.46 (s, 1H), 7.91 (dd, *J* = 8.5, 0.9 Hz, 2H), 7.48 (dd, *J* = 8.6, 7.3 Hz, 2H), 7.29 (dd, *J* = 7.3, 1.0 Hz, 2H), 2.53 (s, 6H).

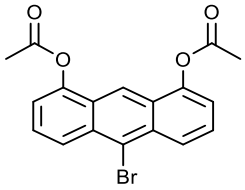

1,8-Diacetoxy-10-Bromoanthracene[98] **(49):** A DMF solution (43 mL) of NBS (5.10 g, 28.68 mmol) was dropwise added at 0 °C to a DMF solution (84 mL) of 1,8-diacetoxyanthracene **48** (4.22 g, 14.34 mmol), and the resulting mixture was stirred overnight at 10-15 °C under nitrogen. The reaction was monitored by TLC and NMR analysis. The resulting mixture was poured into an aqueous solution of Na_2SO_3 (2 wt%, 850 mL), and stirred at 10 °C for 30 min. The precipitate filtered, washed with water, dried in vacuum, and recrystallized with *i*-PrOH to afford 1,8-diacetoxy-10-bromoanthracene **49** (3.32 g, 62%) as a green solid. ^{1}H NMR (400 MHz, Chloroform-*d*) δ 8.54 (s, 1H), 8.43 (dd, *J* = 9.0, 1.0 Hz, 2H), 7.61 (dd, *J* = 9.0, 7.3 Hz, 2H), 7.35 (d, *J* = 7.2 Hz, 2H), 2.53 (s, 6H).

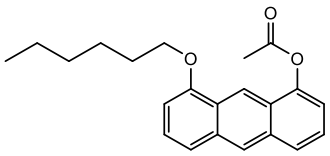

1-Hexyloxy-8-Acetoxyanthracene (54): 1,8-diacetoxyanthracene **48** (50 mg, 0.170 mmol), Cs_2CO_3 (2 equiv.), and 1-bromohexane (8 equiv.) were added to dried acetone (5 mL), and the solution was refluxed at 68 °C for 24 h under argon. The reaction was monitored by TLC (DCM). The reaction mixture was cooled to rt, filtered through 4-inch silica plug using DCM to remove the caesium carbonate salts, and the filtrate was evaporated. The crude solid was washed with a small quantity of cool pet ether and dried under vacuum at 70 °C for 1 h. The residue was subjected to silica gel chromatography (1:1 Pet ether: DCM) to give **54** (20 mg, 35%) as a yellow solid. ^{1}H NMR (400 MHz, Chloroform-*d*) δ 8.88 (s, 1H), 8.40 (s, 1H), 7.89 (d, *J* = 8.6 Hz, 1H), 7.57 (d, *J* = 8.6 Hz, 1H), 7.45 (dd, *J* = 8.6, 7.2 Hz, 1H), 7.38 (dd, *J* = 8.6, 7.4 Hz, 1H), 7.25 (d, *J* = 8.6 Hz, 1H), 6.74 (d, *J* = 8.6 Hz, 1H), 4.20 (t, *J* = 6.3 Hz, 2H), 2.55 (s, 3H), 2.09 – 1.92 (m, 2H), 1.72 – 1.59 (m, 2H), 1.52 – 1.35 (m, 4H), 0.96 (t, *J* = 6.9 Hz, 3H).

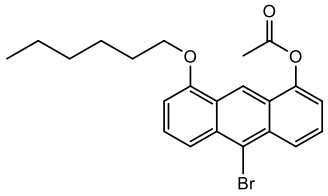

1-Hexyloxy-8-Acetoxy-10-Bromoanthracene (50): 1,8-diacetoxy-10-bromoanthracene **49** (0.54 g, 1.54 mmol), Cs_2CO_3 (7 equiv.), and 1-bromohexane (9 equiv.) were added to dried acetone (50 mL), and the solution was refluxed at 68 °C for 8 h under nitrogen. The reaction was monitored by TLC (DCM). The reaction mixture was cooled to rt, filtered through 4-inch silica plug using DCM to remove the caesium carbonate salts, and the filtrate was evaporated. The resultant residue was then dissolved in DCM and subjected to silica gel chromatography pet ether/ DCM mixture (2:1). The crude solid was washed with a small quantity of cool pet ether and dried under vacuum at 70 °C for 2 h to give **50** (0.33 g, 57%) as a yellow solid. ^{1}H NMR (400 MHz, Chloroform-*d*) δ 8.94 (s, 1H), 8.40 (d, *J* = 9.0 Hz, 1H), 8.03 (d, *J* = 8.9 Hz, 1H), 7.57 (dd, *J* = 8.9, 7.3 Hz, 1H), 7.48 (dd, *J* = 9.0, 7.4 Hz, 1H), 7.28 (d, *J* = 7.3 Hz, 1H),), 6.75 (d, *J* = 7.4 Hz, 1H), 4.18 (t, *J* = 6.3 Hz, 2H), 2.54 (s, 3H), 2.04 – 1.93 (m, 2H), 1.67 – 1.61 (m, 2H), 1.47 – 1.36 (m, 4H), 0.95 (t, *J* = 6.9 Hz, 3H). ^{13}C NMR (101 MHz, Chloroform-*d*) δ 169.34, 154.90, 147.02, 131.86, 131.67, 127.89, 126.44, 125.80, 125.77, 125.30, 122.24, 119.56, 116.99, 115.41, 103.03, 68.36, 31.70, 29.24, 26.07, 22.72, 20.96, 14.11. MP: 123 – 126 °C. MS (MALDI-TOF): m/z = 415.14 $[M]^+$. Chemical formula and calcd for $C_{22}H_{23}BrO_3$: 414.08 g.mol$^-$.

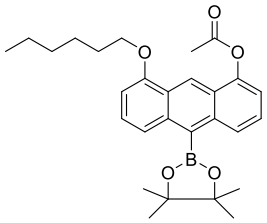

1-Hexyloxy-8-Acetoxy-10-(4,4,5,5-Tetramethyl-1,3,2-Dioxaborolan-2-yl)Anthracene[88] (39): Compound **50** (1.11 g, 2.78 mmol), bis(pinacolato)diboron (1.06 g, 4.17 mmol), potassium acetate (0.95 g, 9.73 mmol), and $Pd(dppf)Cl_2$ (0.11 g, 0.14 mmol) were taken in a 25 mL 2 neck rb flask. Dry 1,4-dioxane (11 mL) was added under nitrogen gas and the reaction mixture was stirred at 90 °C overnight.

The reaction mixture was cooled to rt, filtered through 4-inch silica plug using DCM, and the filtrate was evaporated. The resultant residue was then dissolved in DCM and subjected to silica gel chromatography DCM/pet ether mixture (2:1) to give **39** (0.71 g, 55%) as a green solid. ^{1}H NMR (500 MHz, Chloroform-*d*) δ 9.00 (s, 1H), 8.29 (d, *J* = 8.8, 1.0 Hz, 1H), 7.95 (d, *J* = 8.8, 0.9 Hz, 1H), 7.46 (dd, *J* = 7.5, 7.4 Hz, 1H), 7.38 (dd, *J* = 8.8, 7.4 Hz, 1H), 7.22 (d, *J* = 7.3, 1H), 6.72 (d, *J* = 7.3 Hz, 1H), 4.19 (t, *J* = 6.3 Hz, 2H), 2.52 (s, 3H), 2.03 – 1.94 (m, 2H), 1.69 – 1.59 (m, 2H), 1.53 (s, 12H), 1.43 – 1.35 (m, 4H), 0.94 (t, *J* = 7.1 Hz, 3H). ^{13}C NMR (101 MHz, Chloroform-*d*) δ 169.44, 155.11, 147.28, 136.96, 136.78, 126.40, 126.33, 125.07, 124.80, 124.42, 120.27, 117.43, 116.24, 102.44, 84.46, 68.05, 31.73, 29.71, 29.30, 26.09, 25.18, 22.71, 20.99, 14.11, 1.03. MP: 124 – 127 °C. MS (MALDI-TOF): m/z = 463.21 $[M]^{+}$. Chemical formula and calcd for $C_{28}H_{35}BO_5$: 462.26 g.mol^{-}.

3.4 Synthesis of Di-Hexyloxy-10-Anthracenyl(Pinacol)Boronate Ester

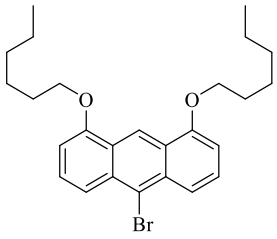

1,8-Dihexyloxy-10-Bromoanthracene (71): Compound **49** (0.57 g, 1.53 mmol), Cs_2CO_3 (7 equiv.), and 1-bromohexane (9 equiv.) were added to dried acetone (60 mL), and the solution was refluxed at 68 °C for 17 days under nitrogen. The reaction was monitored by TLC (DCM). The reaction mixture was cooled to rt, filtered through 4-inch silica plug using DCM to remove the caesium carbonate salts, and the filtrate was evaporated. The resultant residue was then dissolved in DCM and subjected to silica gel chromatography pet ether/ DCM mixture (5:1). The crude solid was washed with a small quantity of cool pet ether and dried under vacuum at 70 °C for 2 h to give **71** (357 mg, 51%) as a yellow solid. ^{1}H NMR (400 MHz, Chloroform-*d*) δ 7.43 (dd, *J* = 7.9, 0.9 Hz, 2H), 6.84 (t, *J* = 8.0 Hz, 2H), 6.40 (dd, *J* = 8.3, 0.9 Hz, 2H), 6.21 (s, 1H), 3.93 – 3.77 (m, 4H), 2.04 – 1.82 (m, 4H), 1.71 – 1.60 (m, 4H), 1.49 – 1.37 (m, 8H), 1.01 – 0.93 (t, *J* = 7.24 Hz, 6H), 0.93 – 0.80 (m, 4H). ^{13}C NMR (101 MHz, Chloroform-*d*) δ 154.91, 145.19, 127.78, 126.61, 119.51, 109.40, 74.83, 68.26, 52.29, 31.78, 29.62, 25.97, 22.76, 14.22. MP: 96 –

98 °C. MS (MALDI-TOF): m/z = 457.04 $[M]^+$. Chemical formula and calcd for $C_{26}H_{33}BrO_2$: 456.17 $g.mol^-$.

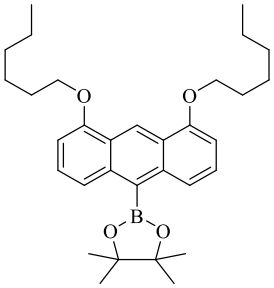

1,8-Dihexyloxy-10-Anthracenyl(Pinacol)Boronate Ester (72): In a glovebox, compound **71** (1.75 g, 3.82 mmol), bis(pinacolato)diboron (1.45 g, 5.74 mmol), potassium acetate (1.31 g, 13.37 mmol), and $Pd(dppf)Cl_2$ (0.15 g, 0.19 mmol) were taken in a 40 mL sealed tube. Dry 1,4-dioxane (15 mL) was added under nitrogen gas and the reaction mixture was stirred at 90 °C for 48 h. The reaction mixture was cooled to rt, filtered through 4-inch silica plug using DCM, and the filtrate was evaporated. The resultant residue was then dissolved in DCM and subjected to silica gel chromatography pet ether/DCM mixture (9:1 to 1:1) to give **72** (1.23 g, 64%) as a green solid. ^{1}H NMR (400 MHz, Chloroform-*d*) δ 9.44 (s, 1H), 7.91 (d, *J* = 8.9, Hz, 2H), 7.36 (dd, *J* = 8.8, 7.4 Hz, 2H), 6.69 (d, *J* = 7.4 Hz, 2H), 4.19 (t, *J* = 6.4 Hz, 4H), 2.05 – 1.93 (m, 4H), 1.71 – 1.56 (m, 4H), 1.56 (s, 12H), 1.48 – 1.35 (m, 8H), 0.94 (t, *J* = 8.8 Hz, 3H). ^{13}C NMR (101 MHz, Chloroform-*d*) δ 155.59, 136.92, 129.36, 126.05, 124.12, 120.10, 118.54, 116.15, 101.92, 84.27, 68.09, 31.73, 29.33, 26.03, 25.20, 22.67, 14.09. MP: 98 – 101 °C. MS (MALDI-TOF): m/z = 505.14 $[M]^+$. Chemical formula and calcd for $C_{32}H_{45}BO_4$: 504.34 $g.mol^-$.

3.5 Synthesis of 1-Iodoanthracene

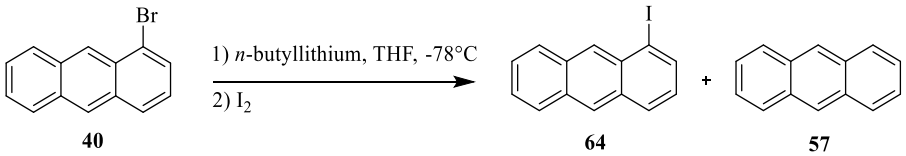

3.5.1 Preparation of 1-Iodoanthracene (64) from 1-Bromoanthracene[99] (40):

In a 250 mL 3 neck rb flask, *n*-butyllithium (2.5 M in hexane, 1.55 mL, 3.87 mmol) was added dropwise to a solution of 1-bromoanthracene **40** (905 mg, 3.52 mmol) in dry THF (40 mL) at -78 °C under

nitrogen. The reaction mixture was stirred at -78 °C for 1 h (reaction monitored by TLC). A solution of iodine (1.05 g, 4.15 mmol) in dry THF (15 mL) was added dropwise at -78 °C and the reaction mixture was stirred overnight. After the addition of water (50 mL), the layers were separated and the aqueous layer extracted with DCM (3 x 25 mL). The combined organic layers were washed with aqueous sodium metabisulphite (10%, 2 x 50 mL) and water (50 mL), dried over $MgSO_4$, filtered and the solvent evaporated under reduced pressure to give a yellow solid containing the desired product **64** (863 mg, 73%, 85% by ^{1}H NMR) as an inseparable mixture with the anthracene **57** (15% by ^{1}H NMR). ^{1}H NMR (400 MHz, Chloroform-*d*) (peaks belonging to **64** only).

3.5.2 Preparation of Iodoanthracene (64) from 1-Amino-9,10-Anthraquinone (55):

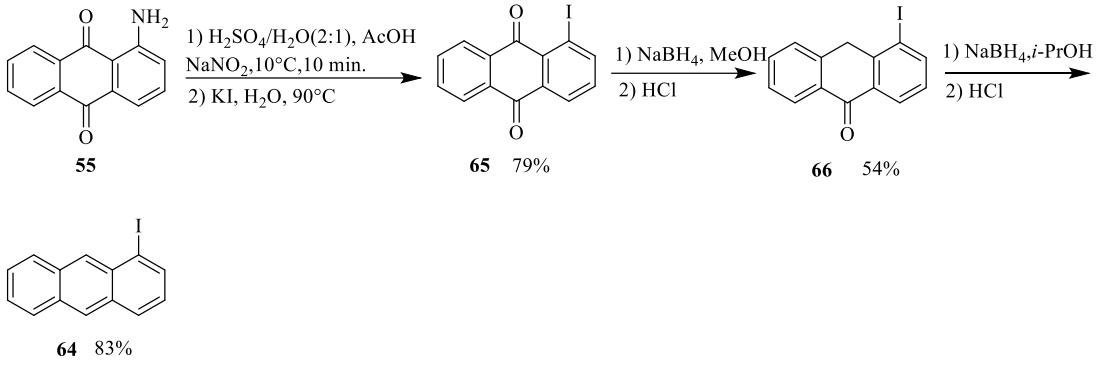

55 **65** 79% **66** 54% **64** 83%

Preparation of Iodoanthracene-9,10-Dione[100] **(65):** To a solution of aminoanthracene-9,10-dione **55** (7 g, 31.36 mmol) in AcOH (200 mL) was slowly added diluted H_2SO_4 (112 mL of conc. H_2SO_4 and 56 mL of water) under nitrogen. The salt solution was filtered to remove precipitated solids and 350 mL of H_2O was added to the red solution. Afterwards, the solution was cooled to 10 °C and diazotized slowly with a solution of $NaNO_2$ (6.5 g, 94.07 mmol) in mL of H_2O for 15 min. In a 2 L rb flask, the diazonium solution was quickly poured into a solution of KI (23.43 g, 141.12 mmol) in 500 mL of H_2O at 90 °C and vigorously stirred for 1:30 h. The mixture then was cooled to 25 °C, filtered, washed with water, and dried overnight. Purification by column chromatography pet ether/DCM mixture (1:1) afforded iodinated product **65** (8.24 g, 79%) as an orange solid. ^{1}H NMR (400 MHz, Chloroform-*d*) δ 8.45 (dd, *J* = 7.8, 1.3 Hz, 1H), 8.41 (dd, *J* = 7.7, 1.3 Hz, 1H), 8.37 – 8.26 (m, 2H), 7.85 – 7.77 (m, 2H), 7.40 (t, *J* = 7.8 Hz, 1H).

Preparation of 5-Iodo-9-Anthrone[102] **(66):** To a stirred solution of **65** (5.20 g, 15.56 mmol) in MeOH (332 mL) was added $NaBH_4$ (2.94 g, 77.82 mmol) with small portions (portion by portion) at rt. over 4 h (ca. 0.73 g every 1 h) under nitrogen. The reaction mixture was further stirred for 1 h at rt. to give a clear yellow solution. The mixture was carefully quenched with HCl (1:1 v/v, 50 mL) and subsequently refluxed at 60 °C for 1 h. The reaction mixture was cooled to rt., neutralized with $NaHCO_3$ (sat. aq.), extracted with DCM (3 x 50 mL), dried over $MgSO_4$, filtered and the solvent concentrated under reduced pressure. The crude solid product was separated by column chromatography pet ether/DCM mixture (5:1 to 1:1) to give **66** (2.67 g, 54%) as a beige solid. ^{1}H NMR (400 MHz, Chloroform-*d*) δ 8.41 (d, *J* = 7.8 Hz, 1H), 8.34 (d, *J* = 7.8 Hz, 1H), 8.18 – 8.11 (d, *J* = 7.8 Hz, 1H), 7.68 – 7.44 (m, 3H), 7.24 (dd, *J* = 13.8, 5.4 Hz, 2H), 4.24 (s, 2H).

Preparation of 1-Iodoanthracene[102] **(64):** To a stirred solution of **66** (1.24 g, 3.87 mmol) in *i*-PrOH (78 mL) was added $NaBH_4$ (0.73 g, 19.37 mmol) portionwise at rt. over 2 h (ca. 0.03 g every 5 min). The mixture was further stirred for 1 h at rt to give a clear orange solution. After addition of conc. HCI (11 mL), the mixture was refluxed for 1 h. The formed solid was collected by filtration, washed with H_2O (100 mL), and air-dried. The crude solid product was separated by column chromatography pet ether/DCM mixture (5:1 to 1:1) to give **64** (0.98 g, 83%) as a bright yellow solid with the recovery of the starting material **66** (75 mg, 6%). ^{1}H NMR (400 MHz, Chloroform-*d*) δ 8.67 (s, 1H), 8.37 (s, 1H), 8.15 – 8.08 (m, 2H), 8.08 – 7.97 (m, 2H), 7.61 – 7.47 (m, 2H), 7.15 (dd, *J* = 8.5, 7.0 Hz, 1H).

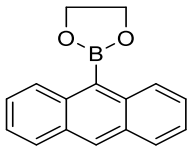

Preparation of 9-Anthracenyl(Ethylene Glycol)Boronate Ester[99] **(70):** A solution of 9-anthracenyl boronic acid **69** (5 g, 22.52 mmol), ethylene glycol (1.68 mL, 27.02 mmol) and toluene (65 mL) was heated under reflux for 2 h with azeotropic removal of water using a Dean-Stark type separator (The reaction was monitored by TLC). The solvent was removed under reduced pressure to give the crude boronate **70** (5.40g, 97%) as a yellow solid. Recrystallization from EtOH afforded yellow crystals of **70**.

^{1}H NMR (400 MHz, Chloroform-*d*) δ 8.52 (s, 1H), 8.45 (dd, *J* = 8.8, 1.0 Hz, 2H), 8.05 – 7.98 (m, 2H), 7.54 – 7.42 (m, 4H), 4.65 (s, 4H).

3.6 Preparation of Unsubstituted 1-Anthracenyl Boronic Acid:

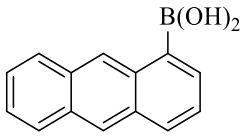

Preparation of 1-Anthracenyl Boronic Acid[105] (74):

To a solution of 1-bromoantharcene **40** (0.47 g, 1.83 mmol) in anhydrous THF (4 mL) kept at −78 °C was added dropwise *n*-BuLi (1.6 mL, 2.5 M, 4.02 mmol). After the resultant orange solution was stirred for 1 h at the same temperature, a solution of trimethylborate (0.57 g, 5.49 mmol) in anhydrous THF (2 mL) was added slowly and the reaction mixture was further stirred for 3 h allowing the temperature to rise to rt.. The resulting solution was then quenched with a saturated aqueous NH_4Cl (10 mL). The organic material was extracted with ethyl acetate, washed with brine, dried over $MgSO_4$, filtered, and evaporated. The required product **74** (0.18 g, 46%) was obtained after recrystallization from DCM as a yellow solid. ^{1}H NMR (400 MHz, Acetone-d_6) δ 9.21 (s, 1H), 8.51 (s, 1H), 8.12 – 8.03 (m, 3H), 7.90 (dd, *J* = 6.6, 1.3 Hz, 1H), 7.50 – 7.44 (m, 3H). ^{13}C NMR (101 MHz, Acetone-d_6) δ 134.06, 132.72, 131.89, 131.72, 131.29, 130.10, 128.55, 127.80, 127.59, 126.36, 125.30, 125.15, 124.66, 115.20. MP: >350 °C. MS (MALDI-TOF): m/z = 223.07 $[M]^+$. Chemical formula and calcd for $C_{14}H_{11}BO_2$: 222.09 g.mol^{-}.

3.7 Synthesis of Suzuki Reactions

3.7.1 Preparation of 9-(1-Naphthalenyl)Anthracene (63)

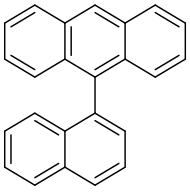

3.7.1.1 Use of Boronate Ester 59 and Bromonaphthalene 62:

a. *With $Pd(dppf)Cl_2$ and Na_2CO_3 / dioxane:*

Quantities: **59** (0.22 g, 0.72 mmol), **62** (0.1 g, 0.48 mmol), $Pd(dppf)Cl_2$ (0.016 g, 0.02 mmol), dioxane (1.8 mL), and saturated Na_2CO_3 aqueous solution (0.39 mL) were stirred and heated at 75 °C for 2 days under nitrogen. The reaction mixture was cooled to rt, diluted with H_2O (10 mL) and extracted with EtOAc (30 mL). The combined organic layers were dried over ($MgSO_4$) and the solvent removed under reduced pressure. The resultant residue was subjected to silica gel chromatography pet ether / DCM mixture (5:1) but no evidence for the formation of the desired compound **63** was made by ^1H NMR spectroscopy and TLC analysis (deboronated product **57**, unreactive halide **62**, and homo-coupled product **58**).

b. *With $Pd(dppf)Cl_2$ and CsF / DME at elevated temperatures:*

Quantities: **59** (0.38 g, 1.25 mmol), **62** (0.26 g, 1.25 mmol), $Pd(dppf)Cl_2$ (0.05 g, 0.06 mmol), CsF (0.38 g, 2.50 mmol), and DME (4 mL) were stirred and refluxed for 24 h under nitrogen. The reaction mixture was cooled to rt, filtered through 4-inch silica plug using DCM, and the filtrate was evaporated. The resultant residue was subjected to silica gel chromatography pet ether / DCM mixture (5:1) but no evidence for the formation of the desired compound **63** was made by ^1H NMR spectroscopy and TLC analysis (deboronated product **57**).

Quantities: **59** (0.30 g, 1.00 mmol), **62** (0.21 g, 1.00 mmol), $Pd(dppf)Cl_2$ (0.04 g, 0.05 mmol), CsF (0.30 g, 2.00 mmol), and DME (4 mL) were placed in a sealed tube, stirred, and heated at 90 °C for 24 h under nitrogen. The reaction mixture was cooled to rt, filtered through 4-inch silica plug using DCM, and the filtrate was evaporated. The resultant residue was subjected to silica gel chromatography pet ether / DCM mixture (5:1) but no evidence for the formation of the desired compound **63** was made by ^1H NMR spectroscopy and TLC analysis (deboronated product **57** and unreactive halide **62**).

c. *With $Pd(dppf)Cl_2$ and Cs_2CO_3 / dioxane / H_2O:*

Quantities: **59** (76 mg, 0.25 mmol), **62** (60 mg, 0.29 mmol), $Pd(dppf)Cl_2$ (5.00 mg, 6.10 μmol), Cs_2CO_3 (0.23 g, 0.75 mmol), dioxane (1 mL), and H_2O (1.8 mL) were stirred and heated at 65 °C for 5 h under nitrogen. The reaction mixture was cooled to rt, diluted with H_2O (10 mL) and extracted with EtOAc (30

mL). The combined organic layers were dried over ($MgSO_4$) and the solvent removed under reduced pressure. The resultant residue was subjected to silica gel chromatography pet ether / DCM mixture (5:1) but no evidence for the formation of the desired compound **63** was made by ^{1}H NMR and TLC analysis (deboronated product **57** and unreactive halide **62**).

d. *With Pd(dppf)Cl_2 and NaOH / THF / H_2O:*

Quantities: **59** (60 mg, 0.21 mmol), **62** (50 mg, 0.25 mmol), Pd(dppf)Cl_2 (3.40 mg, 4.00 μmol), NaOH (17.0 mg, 0.42 mmol), THF (1 mL), and H_2O (1.8 mL) were stirred and heated at 55 °C for 18 h under nitrogen. The reaction mixture was cooled to rt, diluted with H_2O (10 mL) and extracted with EtOAc (30 mL). The combined organic layers were dried over ($MgSO_4$) and the solvent removed under reduced pressure. The resultant residue was subjected to silica gel chromatography pet ether / DCM mixture (5:1) but no evidence for the formation of the desired compound **63** was made by ^{1}H NMR spectroscopy and TLC analysis (deboronated product **57** and unreactive halide **62**).

e. *With Pd(dppf)Cl_2 and CsF / DME at room temperature:*

Quantities: **59** (0.23 g, 0.75 mmol), **62** (0.15 g, 0.75 mmol), Pd(dppf)Cl_2 (0.01 g, 0.01 mmol), CsF (0.23 g, 1.50 mmol), and DME (2 mL) were stirred for 48 h under nitrogen at 25 °C. The reaction mixture was filtered through 4-inch silica plug using DCM, and the filtrate was evaporated. The resultant residue was subjected to silica gel chromatography pet ether / DCM mixture (5:1) but no evidence for the formation of the desired compound **63** was made by ^{1}H NMR spectroscopy and TLC analysis (deboronated product **57**).

f. *With Pd(dppf)Cl_2 and Na_2CO_3 / ethanol/toluene:*

According to the experimental procedure described by Babudri for the synthesis of aryl and vinyl substituents,[73] In a 25 mL microwave vial, **62** (0.10 g, 0.48 mmol), and Pd(dppf)Cl_2 (19 mg, 24.0 μmol) were degassed by bubbling N_2 for 1h. The solids were kept unstirred and heated at 70 °C for 1 h. A solution of **59** (0.14 g, 0.45 mmol), toluene (8.8 mL), and EtOH (2.2 mL) was degassed by bubbling N_2 for 1h. A 2 M Na_2CO_3 aqueous solution (5.7 mL) was degassed by bubbling N_2 for 1h. The degassed

solutions were added into the vial and the mixture was stirred and heated at 80 °C for 30 mins under nitrogen. The reaction mixture was cooled to rt, diluted with H_2O (10 mL) and extracted with EtOAc (30 mL). The combined organic layers were dried ($MgSO_4$) and the solvent removed under reduced pressure. The resultant residue was subjected to silica gel chromatography pet ether / DCM = (25:1 to 5:1) to give the desired product **63** (55 mg, 35%) as a yellow solid. ^{1}H NMR (500 MHz, Chloroform-*d*) δ 8.59 (s, 1H), 8.09 (d, *J* = 8.8 Hz, 2H), 8.05 (d, *J* = 8.2 Hz, 1H), 8.00 (d, *J* = 8.2 Hz, 1H), 7.69 (dd, *J* = 8.3, 6.9 Hz, 1H), 7.52 (dd, *J* = 6.9, 1.2 Hz, 1H), 7.48 – 7.43 (m, 3H), 7.40 (dd, *J* = 9.0, 1.0 Hz, 2H), 7.25 – 7.22 (m, 2H), 7.20 – 7.17 (m, 1H), 7.07 (dd, *J* = 8.5, 1.0 Hz, 1H).

3.7.1.2 Use of Boronate Ester 59 and Iodoonaphthalene 68:
Quantities: A 25 mL microwave vial charged with **59** (0.29 g, 0.95 mmol), $Pd(dppf)Cl_2$ (15 mg, 17 μmol), and CsF (0.29 g, 1.90 mmol) was evacuated and refilled with nitrogen for 3 times and a degassed DME solution (1 mL) of **68** (0.16 g, 0.63 mmol) was added to the vial. Dry DME (5 mL) was added to the mixture solution, stirred and heated at 90 °C for 24 h under nitrogen. The reaction mixture was cooled to rt, filtered through 4-inch silica plug using DCM, and the filtrate was evaporated. The resultant residue was subjected to silica gel chromatography pet ether / DCM mixture (25:1 to 5:1) to give the desired product **63** (57 mg, 30%) as a yellow solid.

3.7.2 Preparation of 1,9`-Bianthracene (61)

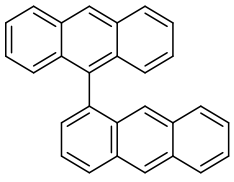

3.7.2.1 Use of Boronate Ester /Boronic Acid and 1-Bromoanthracene 40:

*a) With 9-anthracenyl(pinacol)boronate ester **59**, $Pd(dppf)Cl_2$ and Na_2CO_3 / dioxane:*

Quantities: **59** (0.14 g, 0.47 mmol), **40** (0.1 g, 0.39 mmol), $Pd(dppf)Cl_2$ (0.016 g, 0.02 mmol), dioxane (1.5 mL), and saturated Na_2CO_3 aqueous solution (0.31 mL) were stirred and heated at 75 °C for 2 days under nitrogen. The reaction mixture was cooled to rt, diluted with H_2O (10 mL) and extracted with EtOAc (30 mL). The combined organic layers were dried over ($MgSO_4$) and the solvent removed under

reduced pressure. The resultant residue was subjected to silica gel chromatography pet ether / DCM mixture (5:1) but no evidence for the formation of the desired compound **61** was made by ^{1}H NMR spectroscopy and TLC analysis (deboronated product **57**, unreactive halide **40**, and homo-coupled product **58**).

*b) With **59**, Pd(dppf)Cl$_2$ and CsF / DME:*

Quantities: **59** (0.14 g, 0.47 mmol), **40** (0.1 g, 0.39 mmol), Pd(dppf)Cl$_2$ (0.016 g, 0.02 mmol), CsF (0.12 g, 0.78 mmol), and DME (1.8 mL) were stirred and heated at 70 °C for 24 h under nitrogen. The reaction mixture was cooled to rt, filtered through 4-inch silica plug using DCM, and the filtrate was evaporated. The resultant residue was subjected to silica gel chromatography pet ether / DCM mixture (5:1) but no evidence for the formation of the desired compound **61** was made by ^{1}H NMR spectroscopy and TLC analysis (deboronation occurred already after 3 hours).

Quantities: **59** (0.23 g, 0.77 mmol), **40** (0.1 g, 0.39 mmol), Pd(dppf)Cl$_2$ (0.01 g, 0.012 mmol), CsF (0.18 g, 1.17 mmol), and DME (10 mL) were stirred and heated at 80 °C for 24 h under nitrogen. The reaction mixture was cooled to rt, filtered through 4-inch silica plug using DCM, and the filtrate was evaporated. The resultant residue was subjected to silica gel chromatography pet ether / DCM mixture (5:1) but no evidence for the formation of the desired compound **61** was made by ^{1}H NMR spectroscopy and TLC analysis (deboronation occurred already after 5 hours).

*c) With **59**, Pd(dppf)Cl$_2$ and Na$_2$CO$_3$ / ethanol/toluene at 80 °C:*

According to the experimental procedure described by Babudri for the synthesis of aryl and vinyl substituents,[73] inf a 25 mL microwave vial, **40** (0.1 g, 0.39 mmol), and Pd(dppf)Cl$_2$ (16 mg, 0.02 mmol) were degassed by bubbling N_2 for 1h. The solids were kept unstirred and heated at 60 °C for 1 h. A solution of **59** (0.11 g, 0.37 mmol), toluene (7.2 mL), and EtOH (1.8 mL) was degassed by bubbling N_2 for 1h. A 2 M Na$_2$CO$_3$ aqueous solution (4.7 mL) was degassed by bubbling N_2 for 1h. The degassed solutions were added into the vial and the mixture was stirred and heated at 80 °C for 30 mins under nitrogen. The reaction mixture was cooled to rt, diluted with H_2O (10 mL) and extracted with EtOAc (30

mL). The combined organic layers were dried over ($MgSO_4$) and the solvent removed under reduced pressure. The resultant residue was subjected to silica gel chromatography pet ether / DCM = (25:1 to 5:1) to give 11 mg (8%) of an inseparable mixture of the desired product **61** (50% by ^{1}H NMR spectroscopy) with the homo-coupled product 1,1'-bianthracene **58** (50% by ^{1}H NMR spectroscopy).

*d) With **59**, $Pd(dppf)Cl_2$ and Na_2CO_3 / ethanol/toluene at room temperature:*

Quantities: In a 25 mL microwave vial, **40** (0.1 g, 0.39 mmol), and $Pd(dppf)Cl_2$ (0.016 g, 0.05 mmol) were degassed by bubbling N_2 for 1h. A 2 M Na_2CO_3 aqueous solution (4.7 mL), degassed by bubbling N_2 for 1h, was added into the vial. A mixture of **59** (0.11 g, 0.37 mmol), toluene (7.2 mL), and EtOH (1.8 mL), degassed by bubbling N_2 for 1h, was dropwise added at 25 °C to the solution. The mixture was stirred at rt for 21 h under nitrogen. The reaction mixture was diluted with H_2O (10 mL) and extracted with EtOAc (30 mL). The combined organic layers were dried over ($MgSO_4$) and the solvent removed under reduced pressure. The resultant residue was subjected to silica gel chromatography pet ether / DCM = (25:1 to 5:1) to give the desired product **61** (8 mg, 6%, 50% ^{1}H NMR spectroscopy) as an inseparable mixture with **58** (50% ^{1}H NMR spectroscopy).

*e) With **59**, $Pd(dppf)Cl_2$ and CsF / DME using a Schlenk line:*

Quantities: A 25 mL microwave vial charged with **40** (0.1 g, 0.39 mmol), $Pd(dppf)Cl_2$ (0.01 g, 0.012 mmol), and CsF (0.13 g, 0.85 mmol) was evacuated and refilled with nitrogen for 3 times and a degassed DME (4 mL) was added. A DME solution (2 mL) of **59** (0.14 g, 0.47 mmol) dropwise added to the DME mixture solution, stirred and heated at 90 °C for 48 h under nitrogen. The reaction mixture was cooled to rt, filtered through 4-inch silica plug using DCM, and the filtrate was evaporated. The resultant residue was subjected to silica gel chromatography pet ether / DCM mixture (25:1 to 5:1) to give the desired product **61** (14 mg, 10%, 55% ^{1}H NMR spectroscopy) as an inseparable mixture with **58** (45% ^{1}H NMR spectroscopy) (deboronated product **57** and unreactive halide **40**).

*f) With **59**, $Pd(dppf)Cl_2$ and CsF / DME using a glovebox:*

Quantities: In a glovebox, a solution of **59** (0.35 g, 1.17 mmol), **40** (0.20 g, 0.78 mmol), Pd(dppf)Cl_2 (32.0 mg, 39.0 μmol), and CsF (0.62 g, 4.09 mmol) in dry DME (9 mL) was added in a sealed tube. The mixture was stirred and heated at 90 °C for 72 h in oil bath. The reaction mixture was cooled to rt, filtered through 4-inch silica plug using DCM, and the filtrate was evaporated. The resultant residue was subjected to silica gel chromatography pet ether / DCM mixture (30:1 to 5:1) to give the desired product **61** (128 mg, 46%, 68% ^{1}H NMR spectroscopy) as an inseparable mixture with **58** (32% ^{1}H NMR spectroscopy).

*g) With 9- anthracenyl boronic acid **69,** Pd(dppf)Cl_2 and CsF / DME using a glovebox:*

Quantities: In a glovebox, a solution of **69** (0.26 g, 1.17 mmol), **40** (0.20 g, 0.78 mmol), Pd(dppf)Cl_2 (32.0 mg, 39.0 μmol), and CsF (0.62 g, 4.09 mmol) in dry DME (9 mL) was added in a sealed tube. The mixture was stirred and heated at 90 °C for 72 h in oil bath. The reaction mixture was cooled to rt, filtered through 4-inch silica plug using DCM, and the filtrate was evaporated. The resultant residue was subjected to silica gel chromatography pet ether/DCM mixture (30:1 to 5:1) to give the desired product **61** (104 mg, 38%, 66% ^{1}H NMR spectroscopy) as an inseparable mixture with **58** (34% ^{1}H NMR spectroscopy).

*h) With 9-Anthracenyl(Ethylene Glycol)Boronate Ester **70,** Pd(dppf)Cl_2 and CsF / DME using a glovebox:*

Quantities: In a glovebox, a solution of **70** (0.29 g, 1.17 mmol), **40** (0.20 g, 0.78 mmol), Pd(dppf)Cl_2 (32.0 mg, 39.0 μmol), and CsF (0.62 g, 4.09 mmol) in dry DME (9 mL) was added in a sealed tube. The mixture was stirred and heated at 90 °C for 72 h in oil bath. The reaction mixture was cooled to rt, filtered through 4-inch silica plug using DCM, and the filtrate was evaporated. The resultant residue was subjected to silica gel chromatography pet ether/DCM mixture (30:1 to 5:1) to give the desired product **61** (110 mg, 40%, 69% ^{1}H NMR spectroscopy) as an inseparable mixture with **58** (31% ^{1}H NMR spectroscopy).

3.7.2.2 Use of Boronate Ester/Boronic Acid and Iodoanthracene 64:

*a) With **59,** $Pd(dppf)Cl_2$ and $Ba(OH)_2$ / ethanol/toluene at 75 °C:*

Quantities: In a 25 mL rb 2 neck flask, **59** (0.30 g, 1.31 mmol), $Ba(OH)_2$ (0.17 g, 0.99 mmol), and $Pd(dppf)Cl_2$ (27 mg, 30 μmol) were degassed by bubbling N_2, and the solids were kept unstirred and heated at 60 °C for 1 h. On the other hand, in a 25 mL rb flask, a solution of **64** (0.20 g, 0.66 mmol), toluene (4 mL), EtOH (4 mL), and water (1.3 mL) was degassed by bubbling N_2 and kept unstirred and unheated for 1h. The degassed solution was added into the solids and the mixture was stirred and heated at 75 °C for 30 mins under nitrogen (The reaction was monitored by TLC until one of the starting materials disappeared). The reaction mixture was cooled to rt, diluted with H_2O (25 mL) and extracted with DCM (3 x 25 mL). The combined organic layers were dried over ($MgSO_4$) and the solvent removed under reduced pressure. The resultant residue was subjected to silica gel chromatography pet ether / DCM = (30:1 to 5:1) to give the desired product **61** (102 mg, 44%, 52% ^{1}H NMR spectroscopy) as an inseparable mixture with the homo-coupled product 1,1'-bianthracene **58** (48% ^{1}H NMR spectroscopy).

*b) With **59,** $Pd(dppf)Cl_2$ and CsF / DME using a Schlenk line:*

Quantities: A 25 mL rb 3 neck charged with **59** (0.30 g, 0.99 mmol), $Pd(dppf)Cl_2$ (0.02 g, 24 μmol), and CsF (0.30 g, 1.96 mmol) was evacuated and refilled with nitrogen for 3 times. Degassed DME solution (5.5 mL) of **64** (0.15 g, 0.49 mmol) was added to the solid mixture, stirred and heated at 90 °C for 48 h under nitrogen. The reaction mixture was cooled to rt, filtered through 4-inch silica plug using DCM, and the filtrate was evaporated. The resultant residue was subjected to silica gel chromatography pet ether / DCM mixture (30:1 to 5:1) to give the desired product **61** (17 mg, 10%, 53% ^{1}H NMR) as an inseparable mixture with **58** (47% ^{1}H NMR spectroscopy) (deboronated product **57** and unreactive boronate **59**).

*c) With **59,** $Pd(dppf)Cl_2$ and CsF / DME using a glovebox:*

Quantities: In a glovebox, a solution of **59** (0.30 g, .98 mmol), **64** (0.20 g, 0.66 mmol), $Pd(dppf)Cl_2$ (27.0 mg, 33.0 μmol), and CsF (0.52 g, 3.43 mmol) in dry DME (9 mL) was added in a sealed tube. The mixture was stirred and heated at 90 °C for 72 h in oil bath. The reaction mixture was cooled to rt, filtered through 4-inch silica plug using DCM, and the filtrate was evaporated. The resultant residue was

subjected to silica gel chromatography pet ether / DCM mixture (30:1 to 5:1) to give the desired product **61** (121 mg, 52%, 80% ^{1}H NMR spectroscopy) as an inseparable mixture with **58** (20% ^{1}H NMR spectroscopy).

*d) With **29,** Pd(dppf)Cl$_2$ and CsF / DME using a glovebox:*

Quantities: In a glovebox, a solution of **69** (0.23 g, 1.06 mmol), **64** (0.16 g, 0.53 mmol), Pd(dppf)Cl$_2$ (22.0 mg, 26.5 μmol), and CsF (0.64 g, 4.24 mmol) in dry DME (6 mL) was added in a sealed tube. The mixture was stirred and heated at 90 °C for 72 h in oil bath. The reaction mixture was cooled to rt, filtered through 4-inch silica plug using DCM, and the filtrate was evaporated. The resultant residue was subjected to silica gel chromatography pet ether / DCM mixture (30:1 to 5:1) to give the desired product **61** (66 mg, 37%, 76% ^{1}H NMR) as an inseparable mixture with the homo-coupled product 1,1'-bianthracene **58** (24% ^{1}H NMR spectroscopy).

*e) With **70,** Pd(dppf)Cl$_2$ and CsF / DME using a glovebox:*

Quantities: In a glovebox, a solution of **70** (0.24 g, 0.98 mmol), **64** (0.15 g, 0.49 mmol), Pd(dppf)Cl$_2$ (20.0 mg, 24.0 μmol), and CsF (0.59 g, 3.92 mmol) in dry DME (5.5 mL) was added in a sealed tube. The mixture was stirred and heated at 90 °C for 72 h in oil bath. The reaction mixture was cooled to rt, filtered through 4-inch silica plug using DCM, and the filtrate was evaporated. The resultant residue was subjected to silica gel chromatography pet ether / DCM mixture (30:1 to 5:1) to give the desired product **61** (59 mg, 35%, 73% ^{1}H NMR spectroscopy) as an inseparable mixture with **58** (27% ^{1}H NMR spectroscopy).

*f) With **59,** Pd(PPh$_3$)$_4$ and CsF / DME using a glovebox:*

Quantities: In a glovebox, a solution of **59** (0.30 g, .98 mmol), **64** (0.20 g, 0.66 mmol), Pd(PPh$_3$)$_4$ (23.0 mg, 19.8 μmol), and CsF (0.53 g, 3.46 mmol) in dry DME (8 mL) was added in a sealed tube. The mixture was stirred and heated at 85 °C for 72 h in oil bath. The reaction mixture was cooled to rt, filtered through 4-inch silica plug using DCM, and the filtrate was evaporated. The resultant residue was

subjected to silica gel chromatography pet ether / DCM mixture (30:1 to 5:1) to give the desired product **61** (174 mg, 75%) as a yellow solid.

*g) With **69,** $Pd(PPh_3)_4$ and CsF / DME using a glovebox:*

Quantities: In a glovebox, a solution of **69** (0.18 g, .79 mmol), **64** (0.20 g, 0.66 mmol), $Pd(PPh_3)_4$ (23.0 mg, 19.8 μmol), and CsF (0.36 g, 2.37 mmol) in dry DME (8 mL) was added in a sealed tube. The mixture was stirred and heated at 85 °C for 72 h in oil bath. The reaction mixture was cooled to rt, filtered through 4-inch silica plug using DCM, and the filtrate was evaporated. The resultant residue was subjected to silica gel chromatography pet ether / DCM mixture (30:1 to 5:1) to give the desired product **61** (190 mg, 81%) as a yellow solid.

*h) With **70,** $Pd(PPh_3)_4$ and CsF / DME using a glovebox:*

Quantities: In a glovebox, a solution of **70** (0.20 g, .79 mmol), **64** (0.20 g, 0.66 mmol), $Pd(PPh_3)_4$ (23.0 mg, 19.8 μmol), and CsF (0.36 g, 2.37 mmol) in dry DME (8 mL) was added in a sealed tube. The mixture was stirred and heated at 85 °C for 72 h in oil bath. The reaction mixture was cooled to rt, filtered through 4-inch silica plug using DCM, and the filtrate was evaporated. The resultant residue was subjected to silica gel chromatography pet ether / DCM mixture (30:1 to 5:1) to give the desired product **61** (196 mg, 84%) as a yellow solid. ^{1}H NMR (400 MHz, Methylene Chloride-d_2) δ 8.66 (s, 1H), 8.62 (s, 1H), 8.25 (d, *J* = 8.7 Hz, 1H), 8.15 (d, *J* = 8.5 Hz, 2H), 8.03 (d, *J* = 8.7 Hz, 1H), 7.70 (dd, *J* = 8.6, 6.7 Hz, 1H), 7.61 (s, 1H), 7.51 (dd, *J* = 6.7, 1.2 Hz, 1H), 7.50 – 7.39 (m, 6H), 7.27 (ddd, *J* = 8.5, 6.5, 1.2 Hz, 1H), 7.22 (ddd, *J* = 8.9, 6.5, 1.3 Hz, 2H). ^{13}C NMR (101 MHz, Chloroform-*d*) δ 136.71, 135.09, 131.97, 131.80, 131.67, 131.53, 131.14, 128.63, 128.55, 128.45, 128.42, 127.86, 127.01, 126.64, 125.60, 125.55, 125.25, 125.20, 125.10. MP: 253 – 258 °C. MS (MALDI-TOF): m/z = 355.05 $[M]^+$. Chemical formula and calcd for $C_{28}H_{18}$: 354.14 g.mol$^-$. UV-Vis, (DCM)/nm: 317, 333, 349, 368, 388. Fluorometry (DCM) λmax/nm: 438.

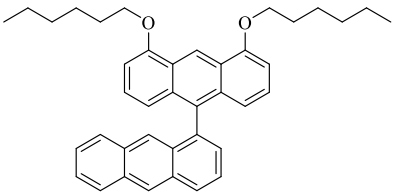

3.7.3 Preparation of 4',5'-Dihexyloxy-1,9'-bianthracene (73):

Quantities: In a glovebox, a solution of **72** (135.0 mg, .0.27 mmol), **64** (68.0 mg, 0.22 mmol), $Pd(PPh_3)_4$ (7.60 mg, 6.70 μmol), and CsF (142.0 mg, 0.94 mmol) in dry DME (3.5 mL) was added in a sealed tube. The mixture was stirred and heated at 85 °C for 72 h in oil bath. The reaction mixture was cooled to rt, filtered through 4-inch silica plug using DCM, and the filtrate was evaporated. The resultant residue was subjected to silica gel chromatography pet ether / DCM mixture (30:1 to 5:1) to give the desired product **73** (80.6 mg, 65%) as a beige solid. ^{1}H NMR (500 MHz, Methylene Chloride-d_2) δ 9.55 (s, 1H), 8.60 (s, 1H), 8.22 (d, *J* = 8.9 Hz, 1H), 8.03 (d, *J* = 8.8 Hz, 1H), 7.68 (dd, *J* = 8.6, 6.6 Hz, 1H), 7.60 (s, 1H), 7.51 – 7.46 (m, 2H), 7.43 – 7.38 (m, 1H), 7.29 – 7.24 (m, 1H), 7.11 (dd, *J* = 8.8, 7.3 Hz, 2H), 6.90 (d, *J* = 8.9, 2H), 6.74 (d, *J* = 7.3 Hz, 2H), 4.27 (t, *J* = 6.4 Hz, 4H), 2.10 – 2.03 (m, 4H), 1.77 – 1.67 (m, 4H), 1.51 – 1.39 (m, 8H), 0.98 (t, *J* = 7.1 Hz, 6H). ^{13}C NMR (101 MHz, Chloroform-*d*) δ 155.43, 137.49, 133.71, 133.24, 132.31, 131.97, 131.72, 131.60, 128.60, 128.47, 128.15, 127.82, 126.46, 125.74, 125.68, 125.46, 125.11, 125.04, 124.47, 118.85, 116.35, 102.06, 68.23, 31.74, 29.39, 26.10, 22.74, 14.15. MP: 153 – 156 °C. MS (MALDI-TOF): m/z = 555.14 $[M]^+$. Chemical formula and calcd for $C_{40}H_{42}O_2$: 554.32 g.mol$^-$.

3.7.4 Preparation of 4'-Acetyloxy-5'-hexyloxy-1,9'-bianthracene (41)

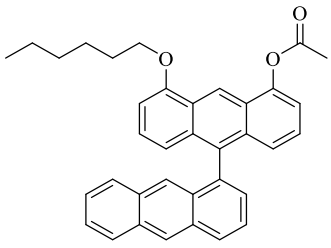

3.7.4.1 Use of 1-Hexyloxy-8-Acetyloxy-10-Anthracenyl(Pinacol)Boronate Ester 39 and 1-Bromoanthracene 40:

Quantities: Compound **39** (40.0 mg, 86.5 μmol), **40** (18.5 mg, 72.1 μmol), Pd(dppf)Cl_2 (5.9 mg, 72.2 μmol), dioxane (1.5 mL), and saturated Na_2CO_3 aqueous solution (0.15 mL) were stirred and heated at 75 °C for 2 days under nitrogen. The reaction mixture was cooled to rt, diluted with H_2O (10 mL) and extracted with EtOAc (25 mL). The combined organic layers were dried over ($MgSO_4$) and the solvent removed under reduced pressure. The resultant residue was subjected to silica gel chromatography pet ether / DCM mixture (5:1) but no evidence for the formation of the desired compound **41** was made by ^{1}H NMR and TLC analysis (deboronated product **57**, and homo-coupled product **58**).

3.7.4.2 Use of 1-Hexyloxy-8-Acetyloxy-10-Anthracenyl(Pinacol)Boronate Ester 39 and Iodooanthracene 64:

a) With Pd(dppf)Cl_2 and CsF / DME using a glovebox:

Quantities: In a glovebox, a solution of **39** (0.27 g, .59 mmol), **64** (0.15 mg, 0.49 mmol), Pd(dppf)Cl_2 (20.0 mg, 24.5 μmol), and CsF (0.36 g, 2.36 mmol) in dry DME (5.5 mL) was added in a sealed tube. The mixture was stirred and heated at 95 °C for 72 h in oil bath. The reaction mixture was cooled to rt, filtered through 4-inch silica plug using DCM, and the filtrate was evaporated. The resultant residue was subjected to silica gel chromatography pet ether/ DCM mixture (30:1 to 5:1) to give the desired product **41** (15 mg, 9%) as a green solid.

b) With Pd(PPh_3)$_4$ and CsF / DME using a glovebox:

Quantities: In a glovebox, a solution of **39** (0.33 g, 0.72 mmol), **64** (0.18 g, 0.60 mmol), Pd(PPh_3)$_4$ (21.0 mg, 18.0 μmol), and CsF (0.38 g, 2.52 mmol) in dry DME (8 mL) was added in a sealed tube. The mixture was stirred and heated at 85 °C for 72 h in oil bath. The reaction mixture was cooled to rt, filtered through 4-inch silica plug using DCM, and the filtrate was evaporated. The resultant residue was subjected to silica gel chromatography pet ether/ EtOAc mixture (20:1 to 10:1) to give the desired product **41** (135 mg, 45%) as a green solid. ^{1}H NMR (400 MHz, Methylene Chloride-d_2) δ 9.13 (s, 1H), 8.61 (s, 1H), 8.24 (d, J = 8.64 Hz, 1H), 8.04 (d, J = 8.52 Hz, 1H), 7.69 (dd, J = 8.6, 6.7 Hz, 1H), 7.62 (s, 2H),

7.55 – 7.47 (m, 2H), 7.47 – 7.38 (m, 1H), 7.34 – 7.28 (m, 2H), 7.23 – 7.19 (m, 2H), 7.14 (dd, *J* = 8.9, 7.4 Hz, 1H), 6.93 (dd, *J* = 8.8, 1.0 Hz, 1H), 6.77 (d, *J* = 7.3 Hz, 1H), 4.27 (t, *J* = 6.3 Hz, 2H), 2.59 (s, 3H), 2.10 – 2.02 (m, 2H), 1.72 (p, *J* = 7.3 Hz, 2H), 1.54 – 1.39 (m, 4H), 0.99 (t, *J* = 7.1 Hz, 3H). ^{13}C NMR (101 MHz, Chloroform-*d*) δ 169.76, 154.97, 147.16, 136.79, 134.92, 132.36, 132.31, 131.90, 131.83, 131.79, 131.66, 128.58, 128.56, 128.46, 127.81, 126.58, 126.11, 125.61, 125.59, 125.24, 125.22, 125.17, 125.05, 124.82, 124.76, 119.02, 116.60, 115.26, 102.62, 68.20, 31.76, 29.37, 26.17, 22.77, 21.07, 14.14. MP: 152 – 155 °C. MS (MALDI-TOF): m/z = 513.17 $[M]^+$. Chemical formula and calcd for $C_{36}H_{32}O_3$: 512.24 g.mol$^-$.

3.8 Synthesis of Scholl Reactions

3.8.1 Synthesis of Non-cyclized Bianthracene

3.8.1.1 Preparation of 9,10′-Dichloro-10,8′-bianthracene (78)

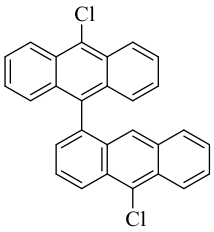

According to the modified literature method,[88] to a 500 mL Schlenk flask, a solution of **61** (0.1 g, 0.28 mmol) in dry DCM (250 mL) was purged with nitrogen for 30 min. A solution of $FeCl_3$ (0.27 g, 1.68 mmol, 5 eq.) in nitromethane (2 mL) was then added dropwise at 0 °C. The reaction mixture was stirred at 0 °C for 1:30 h then at rt for 3:30 h with a constant nitrogen flow bubbling through the mixture. The reaction was quenched by adding methanol (3 mL), washed with aq. NH_4Cl (100 mL) and water (50 mL) and extracted with DCM (3 x 30 mL), dried over $MgSO_4$ and concentrated under vacuum. The resultant residue was subjected to silica gel chromatography pet ether to afford the desired product **78** (23 mg, 20%) as a yellow solid. ^{1}H NMR (400 MHz, Toluene-d_8) δ 8.77 (dt, *J* = 8.9, 1.1 Hz, 1H), 8.70 (dt, *J* = 8.9, 1.0 Hz, 2H), 8.46 (dq, *J* = 8.9, 0.9 Hz, 1H), 7.67 (s, 1H), 7.50 – 7.42 (m, 3H), 7.28 (ddd, *J* = 8.9, 6.5, 1.2 Hz, 2H), 7.23 (dd, *J* = 6.7, 1.1 Hz, 1H), 7.17 (ddd, *J* = 9.0, 6.5, 1.3 Hz, 1H), 6.96 (ddd, *J* = 8.9, 6.5,

1.2 Hz, 2H), 6.84 (ddd, *J* = 8.6, 6.5, 1.1 Hz, 1H), 6.75 (dp, *J* = 8.6, 0.7 Hz, 1H). ^{13}C NMR (101 MHz, Chloroform-*d*) δ 136.56, 134.22, 132.10, 132.01, 129.42, 129.17, 129.13, 129.10, 128.90, 128.69, 127.22 (d, *J* = 8.4 Hz), 126.77, 126.44, 126.00, 125.65, 125.28, 125.16, 125.00, 124.60. MP: 273 – 276 °C. MS (MALDI-TOF): m/z = 421.45 $[M]^+$. Chemical formula and calcd for $C_{28}H_{16}Cl_2$: 422.06 g.mol$^-$. UV-Vis, (DCM)/nm: 326, 342, 360, 379, 401. Fluorometry (DCM) λmax/nm: 450.

3.8.1.2 Preparation of Preparation of 9,9`,10′-trichloro-10,8′-bianthracene (80)

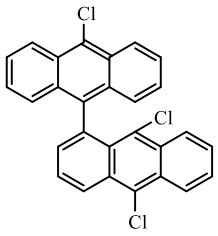

According to the modified literature method,[88] to a 250 mL Schlenk flask, a solution of $FeCl_3$ (0.36 g, 2.22 mmol, 8 eq.) in dry DCM (120 mL) was purged with nitrogen for 20 min. A solution of **61** (0.1 g, 0.28 mmol) in dry DCM (10 mL) was then added dropwise at -10 °C. The reaction mixture was allowed to warm at room temperature and further stirred overnight with a constant nitrogen flow bubbling through the mixture. The reaction was quenched by adding methanol (3 mL), washed with aq. NH_4Cl (100 mL) and water (50 mL) and extracted with DCM (3 x 30 mL), dried over $MgSO_4$ and concentrated under vacuum. The resultant residue was subjected to silica gel chromatography pet ether to afford the desired product **80** (32 mg) as an inseparable mixture with **79** in a ratio of 1:0.89 as identified by ^{1}H NMR spectroscopy.

3.8.1.3 Preparation of 10′-Anisole-10,8′-bianthracene (87)

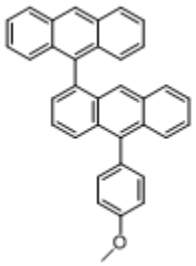

According to the modified literature method,[68,114,115] in a 250 mL Schlenk flask, a solution of **61** (0.1 g, 0.28 mmol) and DDQ (96 mg, 0.42 mmol) in dry DCM (100 mL) was stirred at rt. Then, dry anisole (1

mL) was added and the solution colour changed from yellow to black and purged with nitrogen for 30 min. After the addition of TfOH (0.30 mL) in one portion giving a dark green colour, the reaction mixture was stirred in dark at rt for 1 h. The reaction mixture was then poured into $NaHCO_3$ (sat. aq.) to give brown-red colour and extracted with DCM (3 x 30 mL). The combined organic layer was dried over $MgSO_4$ and evaporated to dryness. The crude product was purified by column chromatography pet ether/ DCM mixture (5:1 to 2:1) to give **87** as a yellow solid (52 mg, 40%) with the recovery of the starting material **61** (4 mg, 4%). ^{1}H NMR (400 MHz, Methylene Chloride-d_2) δ 8.64 (s, 1H), 8.27 (d, *J* = 8.6 Hz, 1H), 8.06 (d, *J* = 8.5 Hz, 1H), 7.83 (d, *J* = 8.9 Hz, 2H), 7.76 – 7.70 (m, 2H), 7.60 – 7.52 (m, 3H), 7.49 (s, 1H), 7.48 – 7.41 (m, 3H), 7.38 – 7.26 (m, 3H), 7.26 – 7.16 (m, 4H), 3.99 (s, 3H). ^{13}C NMR (101 MHz, Methylene Chloride-d_2) δ 132.43, 128.81, 128.41, 128.19, 127.84, 127.15, 126.94, 126.68, 125.63, 125.37, 125.23, 125.18, 125.16, 125.00, 113.91. MP: 315 °C. MS (MALDI-TOF): m/z = 459.42 $[M]^+$. Chemical formula and calcd for $C_{35}H_{24}O$: 460.18 g.mol$^-$. UV-Vis, (DCM)/nm: 332, 350, 367, 378, 385, 397. Fluorometry (DCM) λmax/nm: 435.

3.8.2 Synthesis of Cyclized Bianthracene

3.8.2.1 Preparation of 1,2,7,8-Dibenzoperylene (77)

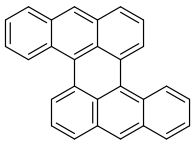

3.8.2.1.1 Use of 1,9`-bianthracene 61 and DDQ/MsOH:

Following the modified literature method,[115] to a 250 mL Schlenk flask, a solution of **61** (35 mg, 0.10 mmol) and DDQ (25 mg, 0.11 mmol) in dry DCM (50 mL) was stirred at 0 °C and purged with nitrogen for 30 min. After the addition of MsOH (1 mL) in one portion giving a dark green colour, the reaction mixture was stirred at rt for 16 h. The reaction mixture was then poured into $NaHCO_3$ (sat. aq.) and extracted with DCM (3 x 30 mL). The combined organic layer was dried over $MgSO_4$, evaporated to dryness, and passed through a short pad of Celite using pet ether/ EtOAc mixture (40:1). After removal of

the solvent by rotary evaporation, the product was collected after recrystallization from methanol/*n*-hexane to give unknown species with the recovery of the starting material **61**.

3.8.2.1.2 Use of 1,9`-bianthracene 61 and DDQ/ TfOH:

This novel compound was prepared according to the modified literature method.[68,114,115] In a 250 mL Schlenk flask, a solution of **61** (0.1 g, 0.28 mmol) and DDQ (96 mg, 0.42 mmol) in dry DCM (100 mL) was stirred at rt and purged with nitrogen for 30 min. After the addition of TfOH (0.30 mL) in one portion giving a dark green colour, the reaction mixture was stirred in dark at rt for 5 h. The reaction mixture was then poured into $NaHCO_3$ (sat. aq.) to give light-purple colour and extracted with DCM (3 x 30 mL) in dark. The combined organic layer was dried over $MgSO_4$, evaporated to dryness, and passed through a short pad of Celite using pet ether/ EtOAc mixture (40:1) in dark. After removal of the solvent by rotary evaporation, the product was collected after recrystallization from methanol/*n*-hexane in dark to give **77** as light-purple solid (24 mg, 16%). ^{1}H NMR (400 MHz, Chloroform-*d*) δ 8.88 – 8.80 (m, 2H), 8.34 (s, 2H), 8.23 (d, *J* = 7.2 Hz, 2H), 8.10 – 8.01 (m, 2H), 7.93 (d, *J* = 8.3 Hz, 2H), 7.61 (dd, *J* = 8.4, 7.3 Hz, 2H), 7.57 – 7.47 (m, 4H). ^{13}C NMR (101 MHz, Chloroform-*d*) δ 133.41, 131.30, 130.83, 128.99, 128.83, 128.67, 128.05, 127.68, 127.21, 127.05, 126.76, 125.98, 125.64, 125.60. MP: 250 °C. MS (MALDI-TOF): m/z = 351.62 $[M]^+$. Chemical formula and calcd for $C_{28}H_{16}$: 352.13 g.mol$^-$. UV-Vis, (DCM)/nm: 416, 444, 481, 515, 555. Fluorometry (DCM) λmax/nm: 568.

3.8.2.1.3 Use of 1,9`-bianthracene 61 and $FeBr_3$:

In a 250 mL Schlenk flask, a solution of $FeBr_3$ (0.25 g, 0.85 mmol, 3 eq.) in dry DCM (150 mL) was purged with nitrogen for 20 min. A solution of **61** (0.1 g, 0.28 mmol) in dry DCM (10 mL) was then added dropwise at 0 °C. The reaction mixture was allowed to warm at room temperature and further stirred for 72 h with a constant nitrogen flow bubbling through the mixture. The reaction was monitored by TLC. The resulting solution was quenched by adding methanol (3 mL), washed with aq. NH_4Cl (100 mL) and water (50 mL) and extracted with DCM (3 x 30 mL), dried over $MgSO_4$ and concentrated under vacuum. The resultant residue was subjected to silica gel chromatography pet ether / DCM mixture (1:0 to 5:1) to afford the desired product **77** (24 mg) as an inseparable mixture with the starting material **61**.

3.8.2.2 Preparation of 9,10′-dichloro-anthracene-fused-anthracene (79)

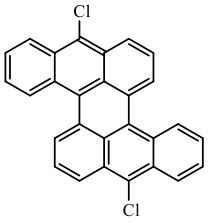

According to the modified literature method,[88] to a 250 mL Schlenk flask, a solution of $FeCl_3$ (0.13 g, 0.80 mmol, 8 eq.) in dry DCM (110 mL) was purged with nitrogen for 30 min. A solution of **61** (35 mg, 0.10 mmol) in dry DCM (10 mL) was then added dropwise at 0 °C. The reaction mixture was stirred at 0 °C for 30 min with a constant nitrogen flow bubbling through the mixture. The reaction was quenched by adding methanol (3 mL), washed with aq. NH_4Cl (60 mL) and water (2 x 50 mL) and extracted with DCM (3 x 30 mL), dried over $MgSO_4$ and concentrated under vacuum. The resultant residue was subjected to silica gel chromatography pet ether to afford the desired product **79** (trace amount) as purple solid. ^{1}H NMR (400 MHz, Chloroform-*d*) δ 8.74 (d, *J* = 8.7 Hz, 2H), 8.61 (d, *J* = 8.9, 1.1 Hz, 2H), 8.47 (d, *J* = 8.7, 0.8 Hz, 2H), 8.16 (d, *J* = 7.2 Hz, 2H), 7.72 (dd, *J* = 8.7, 7.3 Hz, 1H), 7.68 – 7.63 (m, 2H), 7.60 – 7.55 (m, 2H).

3.8.2.3 Preparation of 3-Toluene-1,2,7,8-dibenzoperylene (85)

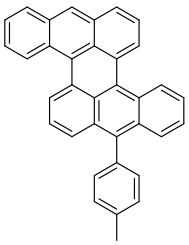

This novel compound was prepared according to the modified literature method.[68,114,115] In a 250 mL Schlenk flask, a solution of **61** (0.1 g, 0.28 mmol) and DDQ (96 mg, 0.42 mmol) in dry DCM (100 mL) was stirred at rt. Then, dry toluene (0.05 mL) was added and the solution colour changed from yellow to red and purged with nitrogen for 30 min. After the addition of TfOH (0.30 mL) in one portion giving a dark green colour, the reaction mixture was stirred in dark at rt for 4 h. The reaction mixture was then

poured into $NaHCO_3$ (sat. aq.) to give dark-purple colour and extracted with DCM (3 x 30 mL). The combined organic layer was dried over $MgSO_4$ and evaporated to dryness. The crude product was purified by column chromatography pet ether/ DCM mixture (15:1 to 7:1) in dark and recrystalized from methanol/*n*-hexane in dark to give **85** as a purple solid (26 mg, 21%). ^{1}H NMR (400 MHz, Chloroform-*d*) δ 8.88 (d, *J* = 8.8 Hz, 1H), 8.85 – 8.81 (m, 1H), 8.35 (s, 1H), 8.22 (dd, *J* = 7.2, 4.0 Hz, 2H), 8.11 – 8.03 (m, 1H), 7.95 (d, *J* = 8.4 Hz, 1H), 7.80 – 7.72 (m, 1H), 7.69 – 7.59 (m, 2H), 7.56 – 7.48 (m, 4H), 7.47 – 7.41 (m, 4H), 7.41 – 7.36 (m, 1H), 2.56 (s, 3H). ^{13}C NMR (101 MHz, Chloroform-*d*) δ 137.24, 136.49, 135.90, 133.48, 132.21, 131.30, 131.23, 130.78, 130.56, 130.04, 129.29, 129.03, 128.84, 128.52, 128.25, 127.90, 127.81, 127.68, 127.50, 127.30, 127.26, 126.90, 126.69, 126.37, 126.01, 125.85, 125.64, 125.48, 125.28, 22.67, 21.45. MP: 240 °C. MS (MALDI-TOF): m/z = 441.20 $[M]^+$. Chemical formula and calcd for $C_{35}H_{22}$: 442.17 g.mol$^-$. UV-Vis, (DCM)/nm: 426, 452, 490, 524, 565. Fluorometry (DCM) λmax/nm: 580.

3.8.2.4 Preparation of 3-Anisole-1,2,7,8-dibenzoperylene (86)

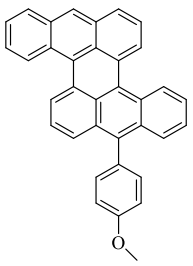

This novel compound was prepared according to the modified literature method.[68,114,115] In a 250 mL Schlenk flask, a solution of **61** (0.05 g, 0.14 mmol) and DDQ (52 mg, 0.23 mmol) in dry DCM (80 mL) was stirred at rt. Then, dry anisole (0.03 mL) was added and the solution colour changed from yellow to black and purged with nitrogen for 30 min. After the addition of TfOH (0.15 mL) in one portion giving a dark green colour, the reaction mixture was stirred in dark overnight at rt. The reaction mixture was then poured into $NaHCO_3$ (sat. aq.) to give dark-purple colour and extracted with DCM (3 x 30 mL). The combined organic layer was dried over $MgSO_4$ and evaporated to dryness. The crude product was purified by column chromatography pet ether/ DCM mixture (5:1) in dark and recrystalized from methanol/*n*-hexane in dark to give **86** as a purple solid (16 mg, 25%). ^{1}H NMR (400 MHz, Methylene

Chloride-d_2) δ 8.80 (d, *J* = 8.9 Hz, 1H), 8.77 – 8.74 (m, 1H), 8.31 (s, 1H), 8.15 (d, *J* = 7.2 Hz, 2H), 8.05 – 7.98 (m, 1H), 7.91 (d, *J* = 8.4 Hz, 1H), 7.68 (d, *J* = 8.7 Hz, 1H), 7.62 – 7.54 (m, 2H), 7.51 – 7.39 (m, 4H), 7.39 – 7.28 (m, 3H), 7.14 – 7.06 (m, 2H), 3.89 (s, 3H). ^{13}C NMR (101 MHz, Chloroform-*d*) δ 159.13, 136.17, 133.48, 132.51, 131.22, 131.03, 130.57, 129.04, 128.85, 128.24, 127.89, 127.68, 127.49, 127.31, 127.25, 126.90, 126.70, 126.37, 125.99, 125.85, 125.64, 125.51, 125.30, 114.05, 55.43. MP: 300 °C. MS (MALDI-TOF): m/z = 457.46 $[M]^+$. Chemical formula and calcd for $C_{35}H_{22}O$: 458.17 g.mol$^-$. UV-Vis, (DCM)/nm: 426, 452, 490, 524, 565. Fluorometry (DCM) λmax/nm: 580.

3.8.2.5 Preparation of 1,15-Dihexyloxy-dibenzo[a,j]perylene (88)

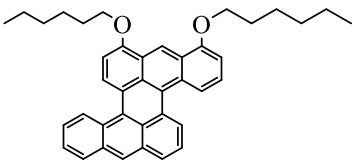

This novel compound was prepared according to the modified literature method.[68,114,115] In a 250 mL Schlenk flask, a solution of **73** (0.15 g, 0.27 mmol) and DDQ (0.09 g, 0.40 mmol) in dry DCM (115 mL) was stirred in an ice bath at 0 °C and purged with nitrogen for 30 min. After the addition of TfOH (0.2 mL) in one portion giving a dark green colour, the reaction mixture was stirred in dark at 0 °C for 50 min. The reaction mixture was then poured into $NaHCO_3$ (sat. aq.) to give dark-purple colour and extracted with DCM (3 x 30 mL). The combined organic layer was dried over $MgSO_4$ and evaporated to dryness. The crude product was purified by column chromatography pet ether/ DCM mixture (6:1) in dark and recrystalized from methanol/*n*-hexane in dark to give **88** as a purple solid (13 mg, 9%). ^{1}H NMR (400 MHz, Chloroform-*d*) δ 9.27 (s, 1H), 8.81 – 8.74 (m, 1H), 8.43 (d, *J* = 8.8 Hz, 1H), 8.21 (d, *J* = 6.2 Hz, 2H), 8.13 (d, *J* = 8.1 Hz, 1H), 8.04 – 7.97 (m, 1H), 7.86 (d, *J* = 8.4 Hz, 1H), 7.55 (t, *J* = 7.8 Hz, 1H), 7.49 – 7.44 (m, 2H), 7.42 (dd, *J* = 8.8, 7.5 Hz, 1H), 6.91 (dd, *J* = 17.9, 9.2 Hz, 1H), 6.80 (d, *J* = 7.4 Hz, 1H), 4.31 (t, *J* = 6.3 Hz, 2H), 4.26 (t, *J* = 6.3 Hz, 2H), 2.12 – 1.99 (m, 4H), 1.70 (p, *J* = 7.3 Hz, 4H), 1.51 – 1.37 (m, 8H), 0.97 (t, *J* = 7.0 Hz, 6H). MP: 88 – 90 °C. MS (MALDI-TOF): m/z = 551.56 $[M]^+$. Chemical formula and calcd for $C_{40}H_{40}O_2$: 552.30 g.mol$^-$. UV-Vis, (DCM)/nm: 437, 527, 562. Fluorometry (DCM) λmax/nm: 610.

3.8.2.6 Preparation of 1,15-Dihexyloxy8-anisole-dibenzo[a,j]perylene (89)

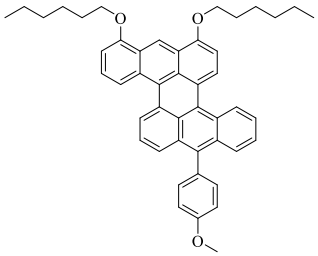

This novel compound was prepared according to the modified literature method.[68,114,115] In a 250 mL Schlenk flask, a solution of **73** (0.15 g, 0.27 mmol), DDQ (0.09 g, 0.40 mmol) and dry anisole (0.04 mL) in dry DCM (115 mL) was stirred in an ice bath at 0 °C and purged with nitrogen for 30 min. After the addition of TfOH (0.2 mL) in one portion giving a dark green colour, the reaction mixture was stirred in dark at 0 °C for 1 h. The reaction mixture was then poured into $NaHCO_3$ (sat. aq.) to give dark-purple colour and extracted with DCM (3 x 30 mL). The combined organic layer was dried over $MgSO_4$ and evaporated to dryness. The crude product was purified by column chromatography pet ether/ DCM mixture (5:1) in dark and recrystalized from methanol/*n*-hexane in dark to give **89** as a purple solid (21 mg, 12%). ^{1}H NMR (400 MHz, Chloroform-*d*) δ 9.29 (s, 1H), 8.82 (d, *J* = 8.7 Hz, 1H), 8.43 (d, *J* = 8.9 Hz, 0H), 8.21 (d, *J* = 7.2 Hz, 1H), 8.14 (d, *J* = 8.0 Hz, 1H), 7.73 (d, *J* = 8.8 Hz, 1H), 7.60 (d, *J* = 8.8 Hz, 1H), 7.50 – 7.31 (m, 6H), 7.20 – 7.14 (m, 2H), 6.96 (d, *J* = 8.1 Hz, 1H), 6.81 (d, *J* = 7.4 Hz, 1H), 4.33 (t, *J* = 6.4 Hz, 2H), 4.26 (t, *J* = 6.4 Hz, 2H), 3.97 (s, 3H), 2.05 (dt, *J* = 14.0, 6.9 Hz, 4H), 1.77 – 1.64 (m, 4H), 1.54 – 1.43 (m, 8H), 0.97 (t, *J* = 7.0, 6H).

^{13}C NMR (101 MHz, Chloroform-*d*) δ 158.99, 155.70, 154.76, 132.61, 130.34, 129.09, 128.49, 127.58, 127.22, 127.00, 126.94, 125.56, 125.30, 125.15, 123.54, 118.95, 114.03, 103.57, 103.08. MP: 128 – 133 °C. MS (MALDI-TOF): m/z = 657.49 $[M]^+$. Chemical formula and calcd for $C_{47}H_{46}O_3$: 658.34 g.mol$^-$. UV-Vis, (DCM)/nm: 437, 465, 498, 535, 581. Fluorometry (DCM) λmax/nm: 625.

References

(1) Korfmacher, W. A.; Wehry, E. L.; Mamantov, G.; Natusch, D. F. S. Resistance to Photochemical Decomposition of Polycyclic Aromatic Hydrocarbons Vapor-Adsorbed on Coal Fly Ash. *Environ. Sci. Technol.* **1980**, *14* (9), 1094–1099. https://doi.org/10.1021/es60169a019.

(2) Wang, C.; Dong, H.; Hu, W.; Liu, Y.; Zhu, D. Semiconducting π-Conjugated Systems in Field-Effect Transistors: A Material Odyssey of Organic Electronics. *Chem. Rev.* **2012**, *112* (4), 2208–2267. https://doi.org/10.1021/cr100380z.

(3) Facchetti, A. π-Conjugated Polymers for Organic Electronics and Photovoltaic Cell Applications. *Chem. Mater.* **2011**, *23* (3), 733–758. https://doi.org/10.1021/cm102419z.

(4) Chen, X.; Tan, D.; Yang, D. T. Multiple-Boron-Nitrogen (Multi-BN) Doped π-Conjugated Systems for Optoelectronics. *J. Mater. Chem. C* **2022**, *10* (37), 13499–13532. https://doi.org/10.1039/d2tc01106a.

(5) Wang, Y.; Fang, D.; Fu, T.; Ali, M. U.; Shi, Y.; He, Y.; Hu, Z.; Yan, C.; Mei, Z.; Meng, H. Anthracene Derivative Based Multifunctional Liquid Crystal Materials for Optoelectronic Devices. *Mater. Chem. Front.* **2020**, *4* (12), 3546–3555. https://doi.org/10.1039/d0qm00038h.

(6) Jin, T.; Terada, M. Recent Topics on Synthesis of π-Extended Polycycles by Cascade Annulations. *Tetrahedron Lett.* **2020**, *61* (8), 151514. https://doi.org/10.1016/j.tetlet.2019.151514.

(7) Islam, K.; Narjinari, H.; Kumar, A. Polycyclic Aromatic Hydrocarbons Bearing Polyethynyl Bridges: Synthesis, Photophysical Properties, and Their Applications. *Asian J. Org. Chem.* **2021**, *10* (7), 1544–1566. https://doi.org/10.1002/ajoc.202100134.

(8) Ghosh, S.; Shankar, S.; Philips, D. S.; Ajayaghosh, A. Diketopyrrolopyrrole-Based Functional Supramolecular Polymers: Next-Generation Materials for Optoelectronic Applications. *Mater. Today Chem.* **2020**, *16*, 100242. https://doi.org/10.1016/j.mtchem.2020.100242.

(9) Ito, H.; Ozaki, K.; Itami, K. Annulative π-Extension (APEX): Rapid Access to Fused Arenes,

Heteroarenes, and Nanographenes. *Angew. Chemie - Int. Ed.* **2017**, *56* (37), 11144–11164. https://doi.org/10.1002/anie.201701058.

(10) Anthony, J. E. The Larger Acenes: Versatile Organic Semiconductors. *Angew. Chemie - Int. Ed.* **2008**, *47* (3), 452–483. https://doi.org/10.1002/anie.200604045.

(11) Pramanik, C.; Miller, G. P. An Improved Synthesis of Pentacene: Rapid Access to a Benchmark Organic Semiconductor. *Molecules* **2012**, *17* (4), 4625–4633. https://doi.org/10.3390/molecules17044625.

(12) Mondal, R.; Adhikari, R. M.; Shah, B. K.; Neckers, D. C. Revisiting the Stability of Hexacenes. *Org. Lett.* **2007**, *9* (13), 2505–2508. https://doi.org/10.1021/ol0709376.

(13) Hiruta, K.; Tokita, S.; Nishimoto, K. Precise PPP Molecular Orbital Calculations of Excitation Energies of Polycyclic Aromatic Hydrocarbons. Part 1. on the Correlation between the Chemical Softness and the Absolute Hardness. *J. Chem. Soc. Perkin Trans. 2* **1995**, No. 7, 1443–1448.

(14) Hsu, C. S.; Lobodin, V. V.; Rodgers, R. P.; McKenna, A. M.; Marshall, A. G. Compositional Boundaries for Fossil Hydrocarbons. *Energy and Fuels* **2011**, *25* (5), 2174–2178. https://doi.org/10.1021/ef2004392.

(15) A. G. G. M. Tielens. *The Physics and Chemistry of the Interstellar Medium*; Cambridge, UK, 2005.

(16) Clar, E. *The Aromatic Sextet*; Wiley, New York, 1972.

(17) Solà, M. Forty Years of Clar's Aromatic π-Sextet Rule. *Front. Chem.* **2013**, *1* (October), 4–11. https://doi.org/10.3389/fchem.2013.00022.

(18) Ruiz-Morales, Y. The Agreement between Clar Structures and Nucleus-Independent Chemical Shift Values in Pericondensed Benzenoid Polycyclic Aromatic Hydrocarbons: An Application of the Y-Rule. *J. Phys. Chem. A* **2004**, *108* (49), 10873–10896. https://doi.org/10.1021/jp040179q.

(19) Allouche, A. Software News and Updates Gabedit — A Graphical User Interface for

Computational Chemistry Softwares. *J. Comput. Chem.* **2012**, *32*, 174–182. https://doi.org/10.1002/jcc.

(20) Klauk, H.; Zschieschang, U.; Weitz, R. T.; Meng, H.; Sun, F.; Nunes, G.; Keys, D. E.; Fincher, C. R.; Xiang, Z. Organic Transistors Based on Di(Phenylvinyl)Anthracene: Performance and Stability. *Adv. Mater.* **2007**, *19* (22), 3882–3887. https://doi.org/10.1002/adma.200701431.

(21) Okamoto, H.; Kawasaki, N.; Kaji, Y.; Kubozono, Y.; Fujiwara, A.; Yamaji, M. Air-Assisted High-Performance Field-Effect Transistor with Thin Films of Picene. *J. Am. Chem. Soc.* **2008**, *130* (32), 10470–10471. https://doi.org/10.1021/ja803291a.

(22) Clar, E. : : 12-2 : 3-10 : **1861**, No. 11, 1861–1865.

(23) Martín-Martínez, F. J.; Fias, S.; Van Lier, G.; De Proft, F.; Geerlings, P. Electronic Structure and Aromaticity of Graphene Nanoribbons. *Chem. - A Eur. J.* **2012**, *18* (20), 6183–6194. https://doi.org/10.1002/chem.201103977.

(24) Ciesielski, A.; Krygowski, T. M.; Cyrański, M. K.; Balaban, A. T. Defining Rules of Aromaticity: A Unified Approach to the Hückel, Clar and Randić Concepts. *Phys. Chem. Chem. Phys.* **2011**, *13* (9), 3737–3747. https://doi.org/10.1039/c0cp01446j.

(25) Poater, J.; Fradera, X.; Duran, M.; Solà, M. The Delocalization Index as an Electronic Aromaticity Criterion: Application to a Series of Planar Polycyclic Aromatic Hydrocarbons. *Chem. - A Eur. J.* **2003**, *9* (2), 400–406. https://doi.org/10.1002/chem.200390041.

(26) Portella, G.; Poater, J.; Bofill, J. M.; Alemany, P.; Solà, M. Local Aromaticity of [n]Acenes, [n]Phenacenes, and [n]Helicenes (n = 1-9). *J. Org. Chem.* **2005**, *70* (7), 2509–2521. https://doi.org/10.1021/jo0480388.

(27) Krygowski, T. M. Crystallographic Studies of Inter- and Intramolecular Interactions Reflected in Aromatic Character of π-Electron Systems. *J. Chem. Inf. Comput. Sci.* **1993**, *33* (1), 70–78. https://doi.org/10.1021/ci00011a011.

(28) Anthony, J. E. Functionalized Acenes and Heteroacenes for Organic Electronics. *Chem. Rev.* **2006**, *106* (12), 5028–5048. https://doi.org/10.1021/cr050966z.

(29) Wu, M. X.; Li, Y.; Liu, P.; Shi, X.; Kang, H.; Zhao, X. L.; Xu, L.; Li, X.; Fang, J.; Fang, Z.; et al. Functionalization of Pentacene: A Facile and Versatile Approach to Contorted Polycyclic Aromatic Hydrocarbons. *Angew. Chemie - Int. Ed.* **2023**, *200241*. https://doi.org/10.1002/anie.202309619.

(30) Kim, K. H.; Jahan, S. A.; Kabir, E.; Brown, R. J. C. A Review of Airborne Polycyclic Aromatic Hydrocarbons (PAHs) and Their Human Health Effects. *Environ. Int.* **2013**, *60*, 71–80. https://doi.org/10.1016/j.envint.2013.07.019.

(31) Li, R.; Cai, J.; Li, J.; Wang, Z.; Pei, P.; Zhang, J.; Krebs, P. Characterizing the Long-Term Occurrence of Polycyclic Aromatic Hydrocarbons and Their Driving Forces in Surface Waters. *J. Hazard. Mater.* **2022**, *423* (PA), 127065. https://doi.org/10.1016/j.jhazmat.2021.127065.

(32) Sajid, M.; Nazal, M. K.; Ihsanullah, I. Novel Materials for Dispersive (Micro) Solid-Phase Extraction of Polycyclic Aromatic Hydrocarbons in Environmental Water Samples: A Review. *Anal. Chim. Acta* **2021**, *1141*, 246–262. https://doi.org/10.1016/j.aca.2020.07.064.

(33) Li, X.; Liu, Z.; Li, C.; Gao, R.; Qi, Y.; Ren, Y. Synthesis and Photophysical Properties of Carbazole-Functionalized Diazaphosphepines via Sequent P − N Chemistry. **2023**. https://doi.org/10.1021/acs.joc.3c01351.

(34) Tsurusaki, A.; Kamikawa, K. Multiple Helicenes Featuring Synthetic Approaches and Molecular Structures. *Chem. Lett.* **2021**, *50* (11), 1913–1932. https://doi.org/10.1246/cl.210409.

(35) Aumaitre, C.; Morin, J. F. Polycyclic Aromatic Hydrocarbons as Potential Building Blocks for Organic Solar Cells. *Chem. Rec.* **2019**, *19* (6), 1142–1154. https://doi.org/10.1002/tcr.201900016.

(36) Matsuoka, W.; Ito, H.; Itami, K. Rapid Access to Nanographenes and Fused Heteroaromatics by Palladium-Catalyzed Annulative π-Extension Reaction of Unfunctionalized Aromatics with Diiodobiaryls. *Angew. Chemie - Int. Ed.* **2017**, *56* (40), 12224–12228.

https://doi.org/10.1002/anie.201707486.

(37) Rieger, R.; Müllen, K. Forever Young: Polycyclic Aromatic Hydrocarbons as Model Cases for Structural and Optical Studies. *J. Phys. Org. Chem.* **2010**, *23* (4), 315–325. https://doi.org/10.1002/poc.1644.

(38) Chen, L.; Hernandez, Y.; Feng, X.; Müllen, K. From Nanographene and Graphene Nanoribbons to Graphene Sheets: Chemical Synthesis. *Angew. Chemie - Int. Ed.* **2012**, *51* (31), 7640–7654. https://doi.org/10.1002/anie.201201084.

(39) Mori, H.; Tanaka, T.; Osuka, A. Fused Porphyrinoids as Promising Near-Infrared Absorbing Dyes. *J. Mater. Chem. C* **2013**, *1* (14), 2500–2519. https://doi.org/10.1039/c3tc00932g.

(40) Yamaguchi, J.; Yamaguchi, A. D.; Itami, K. C À H Bond Functionalization : Emerging Synthetic Tools for Natural Products and Pharmaceuticals Angewandte. **2012**, 8960–9009. https://doi.org/10.1002/anie.201201666.

(41) Lehnherr, D.; Gao, J.; Hegmann, F. A.; Tykwinski, R. R. Synthesis and Electronic Properties of Conjugated Pentacene Dimers. *Org. Lett.* **2008**, *10* (21), 4779–4782. https://doi.org/10.1021/ol801886h.

(42) Sun, Z.; Ye, Q.; Chi, C.; Wu, J. *Low Band Gap Polycyclic Hydrocarbons: From Closed-Shell near Infrared Dyes and Semiconductors to Open-Shell Radicals*; 2012; Vol. 41. https://doi.org/10.1039/c2cs35211g.

(43) Liu, K.; Jiang, Z.; Lalancette, R. A.; Tang, X.; Jäkle, F. Near-Infrared-Absorbing B-N Lewis Pair-Functionalized Anthracenes: Electronic Structure Tuning, Conformational Isomerism, and Applications in Photothermal Cancer Therapy. *J. Am. Chem. Soc.* **2022**, *144* (41), 18908–18917. https://doi.org/10.1021/jacs.2c06538.

(44) Chung, C. Y. S.; Li, S. P. Y.; Morris, J. A.; Sale, D.; Yam, V. W. W. Induced Self-Assembly and Disassembly of Water-Soluble Alkynylplatinum(Ii) Terpyridyl Complexes with “Switchable” near-

Infrared (NIR) Emission Modulated by Metal-Metal Interactions over Physiological PH: Demonstration of PH-Responsive NIR Luminescent Prob. *Chem. Sci.* **2013**, *4* (6), 2453–2462. https://doi.org/10.1039/c3sc50196e.

(45) Yao, L.; Zhang, S.; Wang, R.; Li, W.; Shen, F.; Yang, B.; Ma, Y. Highly Efficient Near-Infrared Organic Light-Emitting Diode Based on a Butterfly-Shaped Donor-Acceptor Chromophore with Strong Solid-State Fluorescence and a Large Proportion of Radiative Excitons. *Angew. Chemie - Int. Ed.* **2014**, *53* (8), 2119–2123. https://doi.org/10.1002/anie.201308486.

(46) Wang, T.; Zhao, Q. J.; Hu, H. G.; Yu, S. C.; Liu, X.; Liu, L.; Wu, Q. Y. Spirolactonized Si-Rhodamine: A Novel NIR Fluorophore Utilized as a Platform to Construct Si-Rhodamine-Based Probes. *Chem. Commun.* **2012**, *48* (70), 8781–8783. https://doi.org/10.1039/c2cc34159j.

(47) Fabian, J.; Nakazumi, H.; Matsuoka, M. Near-Infrared Absorbing Dyes. *Chem. Rev.* **1992**, *92* (6), 1197–1226. https://doi.org/10.1021/cr00014a003.

(48) Qi, J.; Qiao, W.; Wang, Z. Y. Advances in Organic Near-Infrared Materials and Emerging Applications. *Chem. Rec.* **2016**, 1531–1548. https://doi.org/10.1002/tcr.201600013.

(49) Guo, C.; Xia, D.; Yang, Y.; Zuo, X. Synthesis of π-Conjugated Benzocyclotrimers. *Chem. Rec.* **2019**, *19* (10), 2143–2156. https://doi.org/10.1002/tcr.201800160.

(50) Heravi, M. M.; Hashemi, E.; Nazari, N. Negishi Coupling: An Easy Progress for C-C Bond Construction in Total Synthesis. *Mol. Divers.* **2014**, *18* (2), 441–472. https://doi.org/10.1007/s11030-014-9510-1.

(51) Heravi, M. M.; Hashemi, E.; Azimian, F. Recent Developments of the Stille Reaction as a Revolutionized Method in Total Synthesis. *Tetrahedron* **2014**, *70* (1), 7–21. https://doi.org/10.1016/j.tet.2013.07.108.

(52) Bakherad, M. Recent Progress and Current Applications of Sonogashira Coupling Reaction in Water. *Appl. Organomet. Chem.* **2013**, *27* (3), 125–140. https://doi.org/10.1002/aoc.2931.

(53) Kumar, A.; Kumar Rao, G.; Singh, A. K. Organochalcogen Ligands and Their Palladium(II) Complexes: Synthesis to Catalytic Activity for Heck Coupling. *RSC Adv.* **2012**, *2* (33), 12552–12574. https://doi.org/10.1039/c2ra20508d.

(54) Martin, R.; Buchwald, S. L. Palladium-Catalyzed Suzuki-Miyaura Cross-Coupling Reactions Employing Dialkylbiaryl Phosphine Ligands. *Acc. Chem. Res.* **2008**, *41* (11), 1461–1473. https://doi.org/10.1021/ar800036s.

(55) Miyaura, N.; Suzuki, A. Palladium-Catalyzed Cross-Coupling Reactions of Organoboron Compounds. *Chem. Rev.* **1995**, *95* (7), 2457–2483. https://doi.org/10.1021/cr00039a007.

(56) Miyaura, N.; Yamada, K.; Suzuki, A. Our Continuous Discovered. *Tetrahedron Lett.* **1979**, *20* (36), 3437–3440.

(57) Hall, D. G. *Structure, Properties, and Preparation of Boronic Acid Derivatives. Overview of Their Reactions and Applications*; Wiley-VCH GmbH: Weinheim, 2005.

(58) Lennox, A. J. J.; Lloyd-Jones, G. C. Selection of Boron Reagents for Suzuki-Miyaura Coupling. *Chem. Soc. Rev.* **2014**, *43* (1), 412–443. https://doi.org/10.1039/c3cs60197h.

(59) Suzuki, A. Cross-Coupling Reactions of Organoboranes: An Easy Way to Construct C-C Bonds (Nobel Lecture). *Angew. Chemie - Int. Ed.* **2011**, *50* (30), 6723–6733. https://doi.org/10.1002/anie.201101379.

(60) Suzuki, A. Recent Advances in the Cross-Coupling Reactions of Organoboron derivatives with Organic Electrophiles. *J. Organomet. Chem.* **1999**, *576*, 147-168.

(61) Lu, G.; Franzén, R.; Zhang, Q.; Xu, Y. Palladium Charcoal-Catalyzed, Ligandless Suzuki Reaction by Using Tetraarylborates in Water. *Tetrahedron Lett.* **2005**, *46* (24), 4255–4259. https://doi.org/10.1016/j.tetlet.2005.04.022.

(62) Leclerc, M.; Morin, JF. *Synthetic Methods for Conjugated Polymer and Carbon Materials*; Wiley-VCH: Weinheim, **2017**.

(63) Kotha, S.; Lahiri, K.; Kashinath, D. Recent Applications of the Suzuki-Miyaura Cross-Coupling Reaction in Organic Synthesis. *Tetrahedron* **2002**, *58* (48), 9633–9695. https://doi.org/10.1016/S0040-4020(02)01188-2.

(64) Aliprantis, A. O.; Canary, J. W. Observation of Catalytic Intermediates in the Suzuki Reaction by Electrospray Mass Spectrometry. *J. Am. Chem. Soc.* **1994**, *116* (15), 6985–6986. https://doi.org/10.1021/ja00094a083.

(65) Jolly, A.; Miao, D.; Daigle, M.; Morin, J. Emerging Bottom-Up Strategies for the Synthesis of Graphene Nanoribbons and Related Structures. *Angew. Chemie* **2020**, *132* (12), 4652–4661. https://doi.org/10.1002/ange.201906379.

(66) Hein, S. J.; Lehnherr, D.; Arslan, H.; Uribe-Romo, F. J.; Dichtel, W. R. Alkyne Benzannulation Reactions for the Synthesis of Novel Aromatic Architectures. *Acc. Chem. Res.* **2017**, *50* (11), 2776–2788. https://doi.org/10.1021/acs.accounts.7b00385.

(67) Tsefrikas, V. M.; Scott, L. T. Geodesic Polyarenes by Flash Vacuum Pyrolysis. *Chem. Rev.* **2006**, *106* (12), 4868–4884. https://doi.org/10.1021/cr050553y.

(68) Zhang, Y.; Pun, S. H.; Miao, Q. The Scholl Reaction as a Powerful Tool for Synthesis of Curved Polycyclic Aromatics. *Chem. Rev.* **2022**, *122* (18), 14554–14593. https://doi.org/10.1021/acs.chemrev.2c00186.

(69) Scholl R, Mansfeld J. meso-Benzdianthron (Helianthron), meso-Naphthodianthron, und ein neuer Weg zum Flavanthren. *Ber. Dtsch. Chem. Ges*. **1910**, 43: 1734.

(70) Narita, A.; Feng, X.; Hernandez, Y.; Jensen, S. A.; Bonn, M.; Yang, H.; Verzhbitskiy, I. A.; Casiraghi, C.; Hansen, M. R.; Koch, A. H. R.; et al. Synthesis of Structurally Well-Defined and Liquid-Phase-Processable Graphene Nanoribbons. *Nat. Chem.* **2014**, *6* (2), 126–132. https://doi.org/10.1038/nchem.1819.

(71) Zhai, L.; Shukla, R.; Rathore, R. Oxidative C - C Bond Formation (Scholl Reaction) with DDQ as

an Efficient and Easily Recyclable Oxidant. *Org. Lett.* **2009**, *11* (15), 3474–3477. https://doi.org/10.1021/ol901331p.

(72) Zhai, L.; Shukla, R.; Wadumethrige, S. H.; Rathore, R. Probing the Arenium-Ion (ProtonTransfer) versus the Cation-Radical (Electron Transfer) Mechanism of Scholl Reaction Using DDQ as Oxidant. *J. Org. Chem.* **2010**, *75* (14), 4748–4760. https://doi.org/10.1021/jo100611k.

(73) Horibe, T.; Ohmura, S.; Ishihara, K. Structure and Reactivity of Aromatic Radical Cations Generated by FeCl3. *J. Am. Chem. Soc.* **2019**, *141* (5), 1877–1881. https://doi.org/10.1021/jacs.8b12827.

(74) Jassas, R. S.; Mughal, E. U.; Sadiq, A.; Alsantali, R. I.; Al-Rooqi, M. M.; Naeem, N.; Moussa, Z.; Ahmed, S. A. Scholl Reaction as a Powerful Tool for the Synthesis of Nanographenes: A Systematic Review. *RSC Adv.* **2021**, *11* (51), 32158–32202. https://doi.org/10.1039/d1ra05910f.

(75) Grzybowski, M.; Sadowski, B.; Butenschön, H.; Gryko, D. T. Synthetic Applications of Oxidative Aromatic Coupling—From Biphenols to Nanographenes. *Angew. Chemie - Int. Ed.* **2020**, *59* (8), 2998–3027. https://doi.org/10.1002/anie.201904934.

(76) Kumar, S.; Huang, D. C.; Venkateswarlu, S.; Tao, Y. T. Nonlinear Polyfused Aromatics with Extended -Conjugation from Phenanthrotriphenylene, Tetracene, and Pentacene: Syntheses, Crystal Packings, and Properties. *J. Org. Chem.* **2018**, *83* (19), 11614–11622. https://doi.org/10.1021/acs.joc.8b01582.

(77) Han, Y.; Xue, Z.; Li, G.; Gu, Y.; Ni, Y.; Dong, S.; Chi, C. Formation of Azulene-Embedded Nanographene: Naphthalene to Azulene Rearrangement During the Scholl Reaction. *Angew. Chemie* **2020**, *132* (23), 9111–9116. https://doi.org/10.1002/ange.201915327.

(78) Beil, S. B.; Franzmann, P.; Müller, T.; Hielscher, M. M.; Prenzel, T.; Pollok, D.; Beiser, N.; Schollmeyer, D.; Waldvogel, S. R. Investigations on Isomerization and Rearrangement of Polycyclic Arenes under Oxidative Conditions – Anodic versus Reagent-Mediated Reactions.

Electrochim. Acta **2019**, *302*, 310–315. https://doi.org/10.1016/j.electacta.2019.02.041.

(79) Krzeszewski, M.; Sahara, K.; Poronik, Y. M.; Kubo, T.; Gryko, D. T. Unforeseen 1,2-Aryl Shift in Tetraarylpyrrolo[3,2- b] Pyrroles Triggered by Oxidative Aromatic Coupling. *Org. Lett.* **2018**, *20* (6), 1517–1520. https://doi.org/10.1021/acs.orglett.8b00223.

(80) Ponugoti, N.; Parthasarathy, V. Rearrangements in Scholl Reaction. *Chem. - A Eur. J.* **2022**, *28* (17). https://doi.org/10.1002/chem.202103530.

(81) He, J.; Mathew, S.; Kinney, Z. J.; Warrell, R. M.; Molina, J. S.; Hartley, C. S. Tetrabenzanthanthrenes by Mitigation of Rearrangements in the Planarization of Ortho-Phenylene Hexamers. *Chem. Commun.* **2015**, *51* (33), 7245–7248. https://doi.org/10.1039/c5cc00826c.

(82) Israr, H.; Kousar, S.; Rasool, N.; Ahmad, G.; Mubin, M. N. Metal Catalyzed Suzuki-Miyaura Cross-Coupling – Efficient Methodology for Synthesis the Natural and Non-Natural Biological Active Molecules. **2017**, No. May, 1–31. https://doi.org/10.20944/preprints201705.0115.v1.

(83) Taheri Kal Koshvandi, A.; Heravi, M. M.; Momeni, T. Current Applications of Suzuki–Miyaura Coupling Reaction in The Total Synthesis of Natural Products: An Update. *Appl. Organomet. Chem.* **2018**, *32* (3), 1–59. https://doi.org/10.1002/aoc.4210.

(84) Hooshmand, S. E.; Heidari, B.; Sedghi, R.; Varma, R. S. Recent Advances in the Suzuki-Miyaura Cross-Coupling Reaction Using Efficient Catalysts in Eco-Friendly Media. *Green Chem.* **2019**, *21* (3), 381–405. https://doi.org/10.1039/c8gc02860e.

(85) Wu, W.; Liu, Y.; Zhu, D. π-Conjugated Molecules with Fused Rings for Organic Field-Effect Transistors: Design, Synthesis and Applications. *Chem. Soc. Rev.* **2010**, *39* (5), 1489–1502. https://doi.org/10.1039/b813123f.

(86) Wegner, H. A.; Reisch, H.; Rauch, K.; Demeter, A.; Zachariasse, K. A.; De Meijere, A.; Scott, L. T. Oligoindenopyrenes: A New Class of Polycyclic Aromatics. *J. Org. Chem.* **2006**, *71* (24), 9080–9087. https://doi.org/10.1021/jo0613939.

(87) Kawasumi, K.; Zhang, Q.; Segawa, Y.; Scott, L. T.; Itami, K. A Grossly Warped Nanographene and the Consequences of Multiple Odd-Membered-Ring Defects. *Nat. Chem.* **2013**, *5* (9), 739–744. https://doi.org/10.1038/nchem.1704.

(88) Yang, X.; Hoffmann, M.; Rominger, F.; Kirschbaum, T.; Dreuw, A.; Mastalerz, M. Functionalized Contorted Polycyclic Aromatic Hydrocarbons by a One-Step Cyclopentannulation and Regioselective Triflyloxylation. *Angew. Chemie - Int. Ed.* **2019**, *58* (31), 10650–10654. https://doi.org/10.1002/anie.201905666.

(89) Koga, Y.; Kaneda, T.; Saito, Y.; Murakami, K.; Itami, K. Synthesis of Partially and Fully Fused Polyaromatics by Annulative Chlorophenylene Dimerization. *Science (80).* **2018**, *359* (6374), 435–439. https://doi.org/10.1126/science.aap9801.

(90) Toyota, S.; Ban, S.; Hara, M.; Kawamura, M.; Ikeda, H.; Tsurumaki, E. Synthesis and Properties of Rubicene-Based Aromatic π-Conjugated Compounds as Five-Membered Ring Embedded Planar Nanographenes. *Chem. - A Eur. J.* **2023**, *29* (49). https://doi.org/10.1002/chem.202301346.

(91) Davis, N. K. S.; Pawlicki, M.; Anderson, H. L. Expanding the Porphyrin π-System by Fusion with Anthracene. *Org. Lett.* **2008**, *10* (18), 3945–3947. https://doi.org/10.1021/ol801500b.

(92) Prinzisky, C.; Meyenburg, I.; Jacob, A.; Heidelmeier, B.; Schröder, F.; Heimbrodt, W.; Sundermeyer, J. Optical and Electrochemical Properties of Anthraquinone Imine Based Dyes for Dye-Sensitized Solar Cells. *European J. Org. Chem.* **2016**, *2016* (4), 756–767. https://doi.org/10.1002/ejoc.201501309.

(93) Kissel, P.; Weibel, F.; Federer, L.; Sakamoto, J.; Schlüter, A. D. An Easy and Multigram Scale Synthesis of Anthracene-1,8-Ditriflate. *Synlett.* **2008**, 12, 1793–1796. https://doi.org/10.1055/s-2008-1078499.

(94) Brockmann, Buddc. Spectroscopic Identification of the Parent Hydrocarbon of Polynuclear Oxyquinones. *Chem. Ber*. **1952**, 86, 432–433.

(95) Liebermann, C. Ueber die der Chrysazinreihe angehörigen Anthracenverbindungen. *Chem. Ber.* **1879**, 1, 182-188.

(96) Zhang, W.; Ma, H.; Zhou, L.; Miao, H.; Xu, J. Oxidative Dehydrogenation of 9, 10-Dihydroanthracene Catalyzed by 2, 3-Dichloro-5, 6-Dicyano-1, 4-Benzoquinone/NaNO2. *Cuihua Xuebao / Chinese J. Catal.* **2009**, *30* (2), 86–88. https://doi.org/10.1016/s1872-2067(08)60090-x.

(97) Servalli, M.; Trapp, N.; Wörle, M.; Klärner, F. G. Anthraphane: An Anthracene-Based, Propeller-Shaped D3h-Symmetric Hydrocarbon Cyclophane and Its Layered Single Crystal Structures. *J. Org. Chem.* **2016**, *81* (6), 2572–2580. https://doi.org/10.1021/acs.joc.6b00209.

(98) Leung, F. K. C.; Ishiwari, F.; Kajitani, T.; Shoji, Y.; Hikima, T.; Takata, M.; Saeki, A.; Seki, S.; Yamada, Y. M. A.; Fukushima, T. Supramolecular Scaffold for Tailoring the Two-Dimensional Assembly of Functional Molecular Units into Organic Thin Films. *J. Am. Chem. Soc.* **2016**, *138* (36), 11727–11733. https://doi.org/10.1021/jacs.6b05513.

(99) Cammidge, A. N.; Crépy, K. V. L. Synthesis of Chiral Binaphthalenes Using the Asymmetric Suzuki Reaction. *Tetrahedron* **2004**, *60* (20), 4377–4386. https://doi.org/10.1016/j.tet.2003.11.095.

(100) Ivashkina, N. V.; Romanov, V. S.; Moroz, A. A.; Shvartsberg, M. S. 5-Arylethynyl-1,4-Naphthoquinones. *Bull. Acad. Sci. USSR Div. Chem. Sci.* **1984**, *33* (11), 2345–2348. https://doi.org/10.1007/BF00948851.

(101) Šalitroš, I.; Fuhr, O.; Gál, M.; Valášek, M.; Ruben, M. Photoisomerization of Bis(Tridentate) 2,6-Bis(1H-Pyrazol-1-Yl)Pyridine Ligands Exhibiting a Multi-Anthracene Skeleton. *Chem. - A Eur. J.* **2017**, *23* (42), 10100–10109. https://doi.org/10.1002/chem.201700825.

(102) Goichi, M.; Segawa, K.; Suzuki, S.; Toyota, S. Improved Synthesis of 1,8-Diiodoanthracene and Its Application to the Synthesis of Multiple Phenylethynyl-Substituted Anthracenes. *Synthesis (Stuttg).* **2005**, No. 13, 2116–2118. https://doi.org/10.1055/s-2005-869999.

(103) Roy, P.; Al-Kahtani, F.; Cammidge, A. N.; Meech, S. R. Solvent Tuning Excited State Structural

Dynamics in a Novel Bianthryl. *J. Phys. Chem. Lett.* **2023**, *14* (1), 253–259. https://doi.org/10.1021/acs.jpclett.2c03469.

(104) Teng, C.; Yang, X.; Yang, C.; Li, S.; Cheng, M.; Hagfeldt, A.; Sun, L. Molecular Design of Anthracene-Bridged Metal-Free Organic Dyes for Efficient Dye-Sensitized Solar Cells. *J. Phys. Chem. C* **2010**, *114* (19), 9101–9110. https://doi.org/10.1021/jp101238k.

(105) Jacobse, P. H.; van den Hoogenband, A.; Moret, M. E.; Klein Gebbink, R. J. M.; Swart, I. Aryl Radical Geometry Determines Nanographene Formation on Au(111). *Angew. Chemie - Int. Ed.* **2016**, *55* (42), 13052–13055. https://doi.org/10.1002/anie.201606440.

(106) Davis, N. K. S.; Thompson, A. L.; Anderson, H. L. A Porphyrin Fused to Four Anthracenes. *J. Am. Chem. Soc.* **2011**, *133* (1), 30–31. https://doi.org/10.1021/ja109671f.

(107) Dou, C.; Saito, S.; Matsuo, K.; Hisaki, I.; Yamaguchi, S. A Boron-Containing PAH as a Substructure of Boron-Doped Graphene. *Angew. Chemie* **2012**, *124* (49), 12372–12376. https://doi.org/10.1002/ange.201206699.

(108) Dorel, R.; Manzano, C.; Grisolia, M.; Soe, W. H.; Joachim, C.; Echavarren, A. M. Tetrabenzocircumpyrene: A Nanographene Fragment with an Embedded Peripentacene Core. *Chem. Commun.* **2015**, *51* (32), 6932–6935. https://doi.org/10.1039/c5cc00693g.

(109) Tanaka, M.; Hayashi, S.; Eu, S.; Umeyama, T.; Matano, Y.; Imahori, H. Novel Unsymmetrically π-Elongated Porphyrin for Dye-Sensitized TiO 2 Cells. *Chem. Commun.* **2007**, *3* (20), 2069–2071. https://doi.org/10.1039/b702501g.

(110) Yao, J. H.; Chi, C.; Wu, J.; Loh, K. P. Bisanthracene Bis(Dicarboxylic Imide)s as Soluble and Stable NIR Dyes. *Chem. - A Eur. J.* **2009**, *15* (37), 9299–9302. https://doi.org/10.1002/chem.200901398.

(111) Chaolumen; Stepek, I. A.; Yamada, K. E.; Ito, H.; Itami, K. Construction of Heptagon-Containing Molecular Nanocarbons. *Angew. Chemie - Int. Ed.* **2021**, *60* (44), 23508–23532.

https://doi.org/10.1002/anie.202100260.

(112) Jørgensen, K. B. Photochemical Oxidative Cyclisation of Stilbenes and Stilbenoids-the Mallory-Reaction. *Molecules* **2010**, *15* (6), 4334–4358. https://doi.org/10.3390/molecules15064334.

(113) Grzybowski, M.; Skonieczny, K.; Butenschön, H.; Gryko, D. T. Comparison of Oxidative Aromatic Coupling and the Scholl Reaction. *Angew. Chemie - Int. Ed.* **2013**, *52* (38), 9900–9930. https://doi.org/10.1002/anie.201210238.

(114) Kawamura, M.; Tsurumaki, E.; Toyota, S. Facile Synthesis of Rubicenes by Scholl Reaction. *Synth.* **2018**, *50* (1), 134–138. https://doi.org/10.1055/s-0036-1588570.

(115) Dumslaff, T.; Yang, B.; Maghsoumi, A.; Velpula, G.; Mali, K. S.; Castiglioni, C.; De Feyter, S.; Tommasini, M.; Narita, A.; Feng, X.; et al. Adding Four Extra K-Regions to Hexa-Peri-Hexabenzocoronene. *J. Am. Chem. Soc.* **2016**, *138* (14), 4726–4729. https://doi.org/10.1021/jacs.6b01976.

(116) Cammidge, A. N.; Gopee, H. Macrodiscotic Triphenylenophthalocyanines. *Chem. Commun.* **2002**, *2* (9), 966–967. https://doi.org/10.1039/b200978a.

(117) Cammidge, A. N.; Gopee, H. Structural Factors Controlling the Transition between Columnar-Hexagonal and Helical Mesophase in Triphenylene Liquid Crystals. *J. Mater. Chem.* **2001**, *11* (11), 2773–2783. https://doi.org/10.1039/b103450m.

(118) Zhou, Y.; Liu, W. J.; Zhang, W.; Cao, X. Y.; Zhou, Q. F.; Ma, Y.; Pei, J. Selective Oxidative Cyclization by $FeCl_3$ in the Construction of 10H-Indeno[1,2-b]Triphenylene Skeletons in Polycyclic Aromatic Hydrocarbons. *J. Org. Chem.* **2006**, *71* (18), 6822–6828. https://doi.org/10.1021/jo0609172.

(119) Rempala, P.; Kroulik, J.; King, B. T. Investigation of the Mechanism of the Intramolecular Scholl Reaction of Contiguous Phenylbenzenes. *J. Org. Chem.* **2006**, *71* (14), 5067–5081. https://doi.org/10.1021/jo0526744.

(120) Eberson, L.; Hartshorn, M. P.; Persson, O. Formation and EPR Spectra of Radical Species Derived from the Oxidation of the Spin Trap, α-Phenyl-N-Tert-Butylnitrone (PBN), and Some of Its Derivatives in 1,1,1,3,3,3-Hexafluoropropan-2-Ol. Formation of Isoxazolidine Radical Cations. *J. Chem. Soc. Perkin Trans. 2* **1997**, No. 2, 195–201. https://doi.org/10.1039/a606004h.

(121) Camargo Solórzano, P.; Baumgartner, M. T.; Puiatti, M.; Jimenez, L. B. Arenium Cation or Radical Cation? An Insight into the Cyclodehydrogenation Reaction of 2-Substituted Binaphthyls Mediated by Lewis Acids. *RSC Adv.* **2020**, *10* (37), 21974–21985. https://doi.org/10.1039/d0ra04213g.

(122) Alsharif, M. A.; Raja, Q. A.; Majeed, N. A.; Jassas, R. S.; Alsimaree, A. A.; Sadiq, A.; Naeem, N.; Mughal, E. U.; Alsantali, R. I.; Moussa, Z.; et al. DDQ as a Versatile and Easily Recyclable Oxidant: A Systematic Review. *RSC Adv.* **2021**, *11* (47), 29826–29858. https://doi.org/10.1039/d1ra04575j.

(123) Izquierdo-García, P.; Fernández-García, J. M.; Perles, J.; Fernández, I.; Martín, N. Electronic Control of the Scholl Reaction: Selective Synthesis of Spiro vs Helical Nanographenes. *Angew. Chemie* **2023**, *135* (7). https://doi.org/10.1002/ange.202215655.

(124) Li, H.; Chen, Q.; Lu, Z.; Li, A. Total Syntheses of Aflavazole and 14-Hydroxyaflavinine. *J. Am. Chem. Soc.* **2016**, *138* (48), 15555–15558. https://doi.org/10.1021/jacs.6b10880.

(125) Tsvetkov, N. P.; Gonzalez-Rodriguez, E.; Hughes, A.; dos Passos Gomes, G.; White, F. D.; Kuriakose, F.; Alabugin, I. V. Radical Alkyne Peri-Annulation Reactions for the Synthesis of Functionalized Phenalenes, Benzanthrenes, and Olympicene. *Angew. Chemie - Int. Ed.* **2018**, *57* (14), 3651–3655. https://doi.org/10.1002/anie.201712783.

Appendix

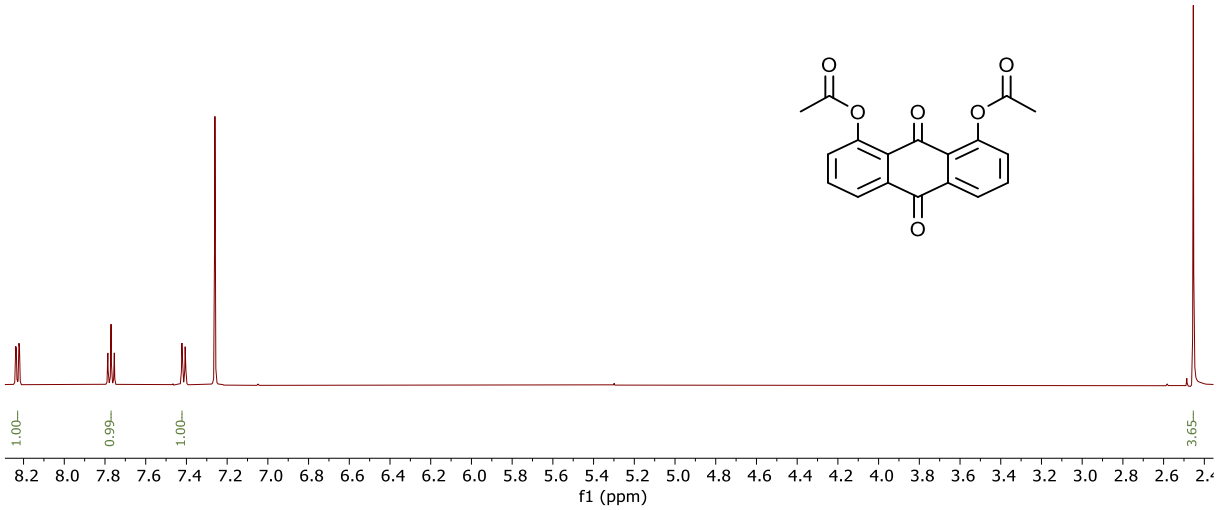

Figure 0.1: ^{1}H NMR spectrum of compound **47**.

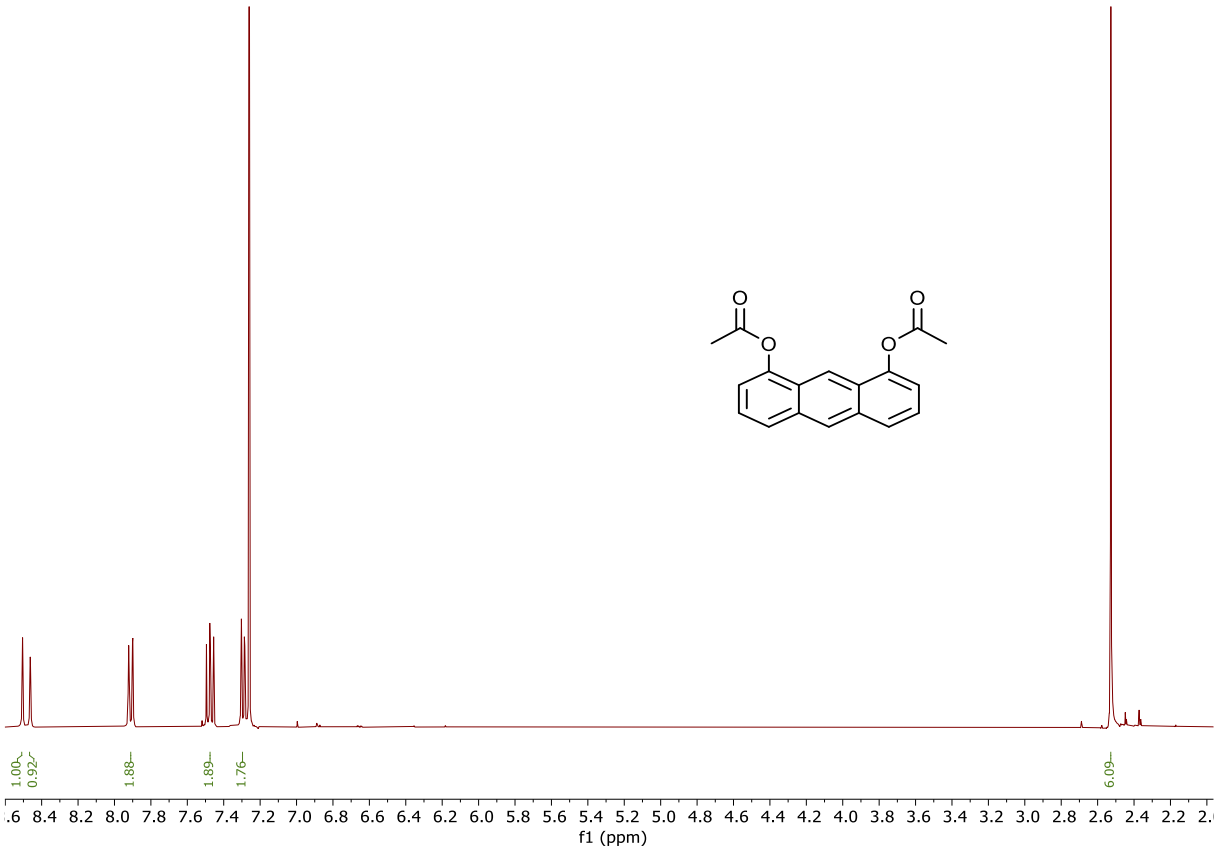

Figure 0.2: ^{1}H NMR spectrum of compound **48**.

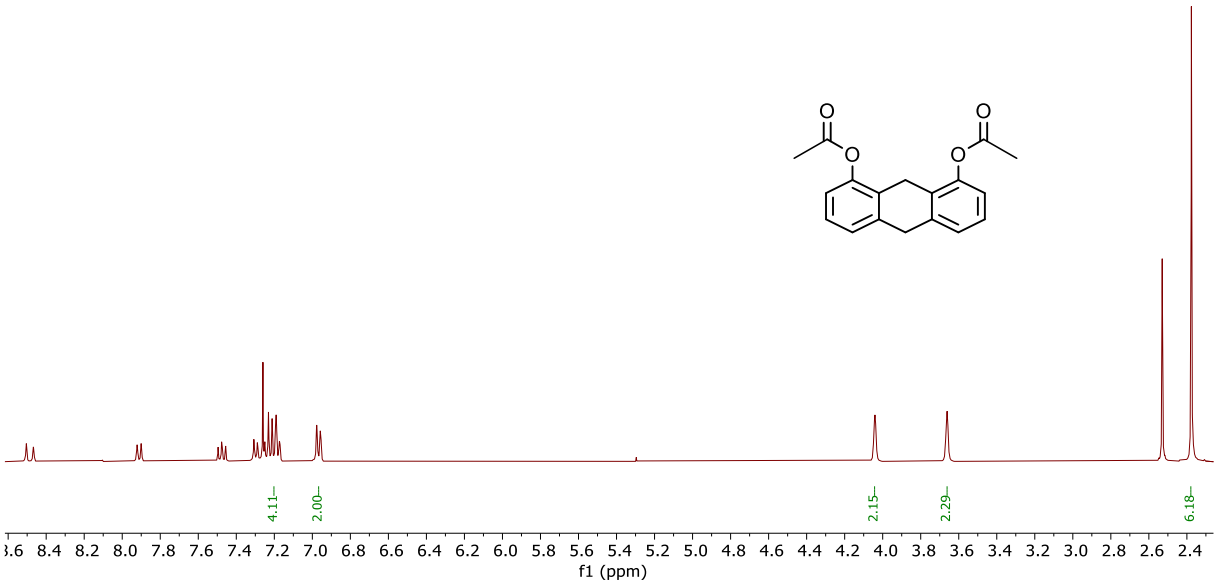

Figure 0.3: ^{1}H NMR spectrum of compound **51**.

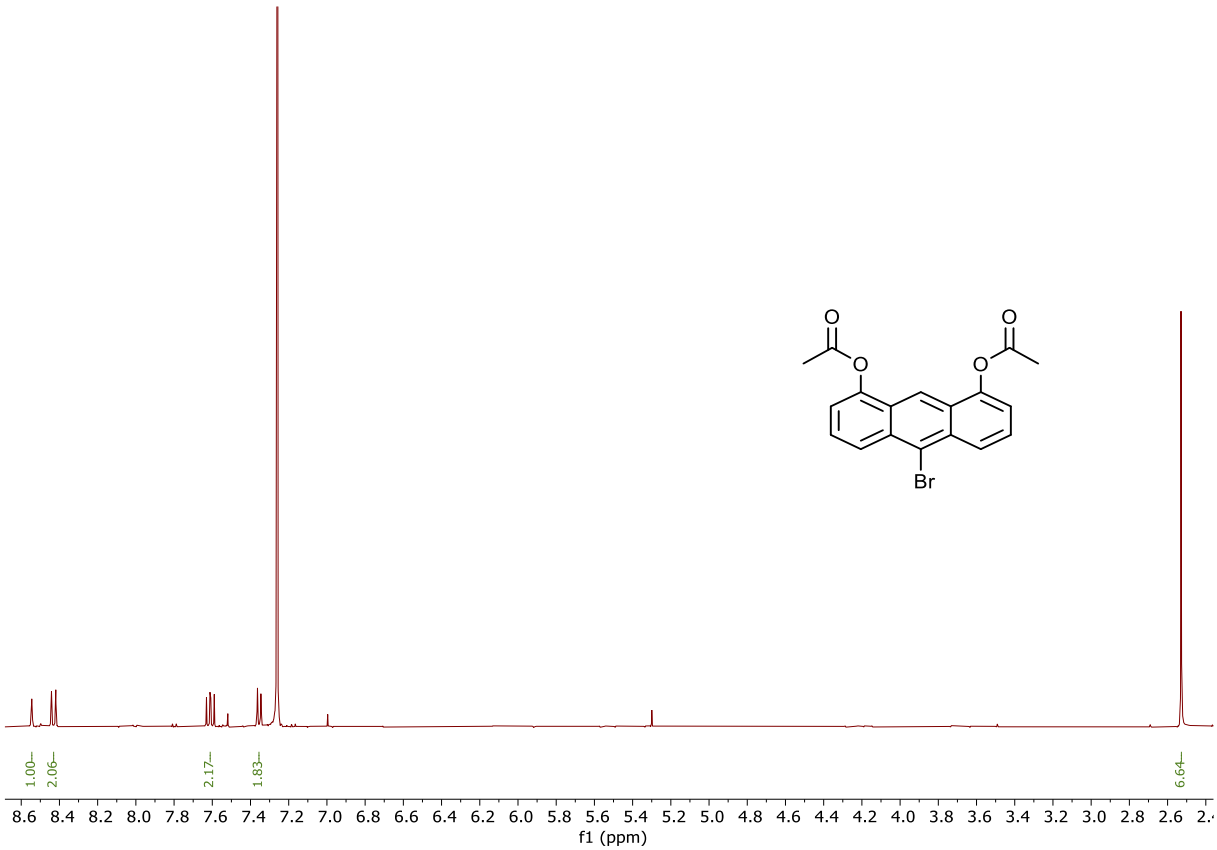

Figure 0.4: ^{1}H NMR spectrum of compound **49**.

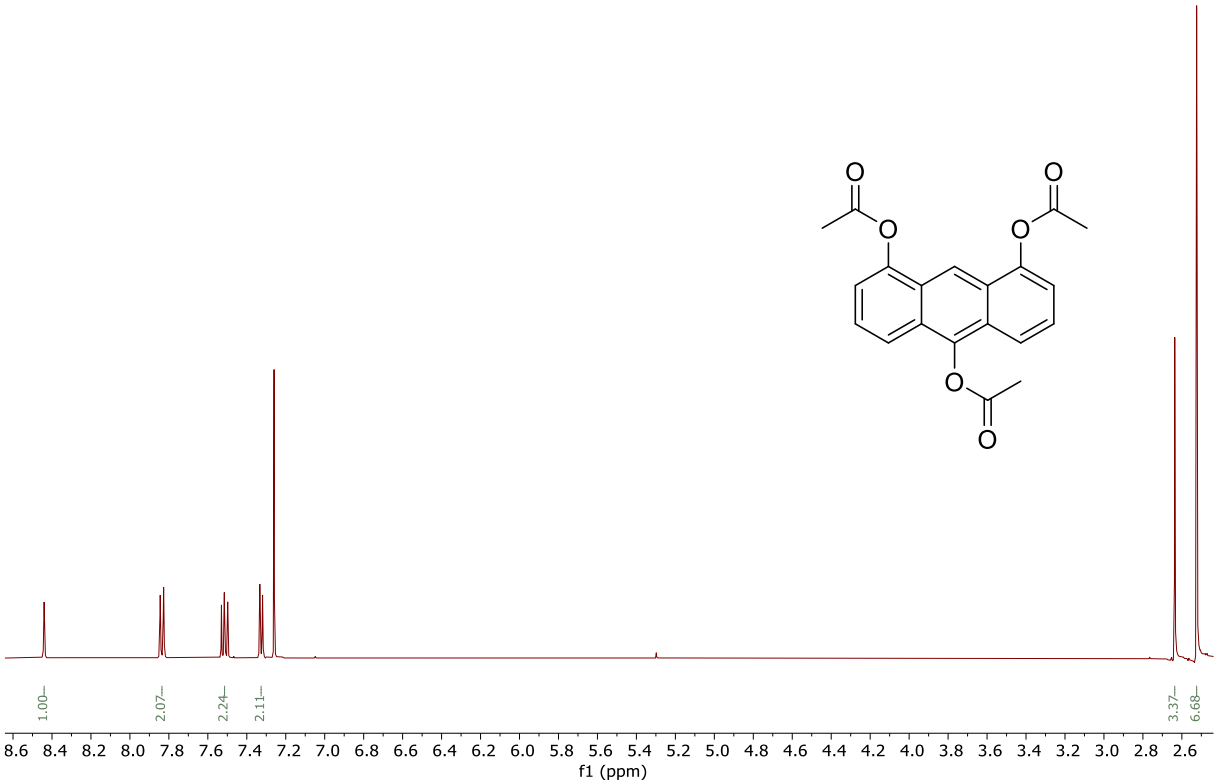

Figure 0.5: ^{1}H NMR spectrum of compound **52**.

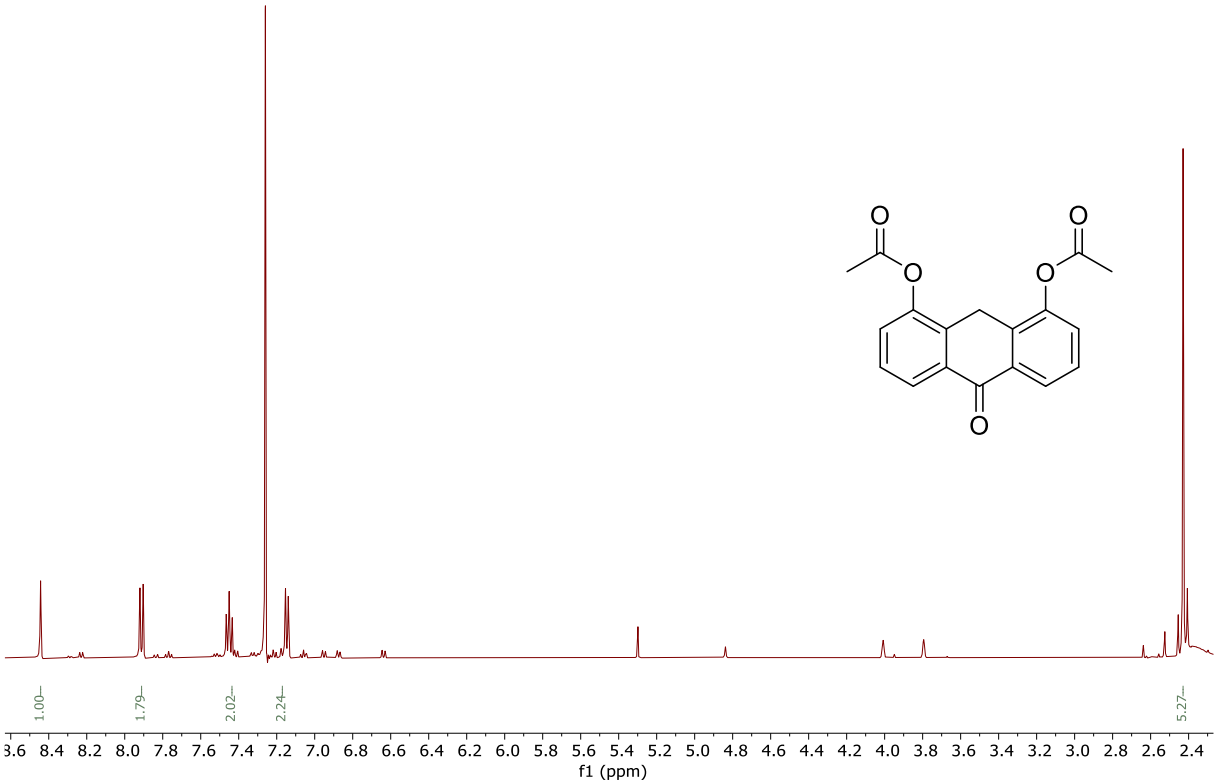

Figure 0.6: ^{1}H NMR spectrum of compound **53**.

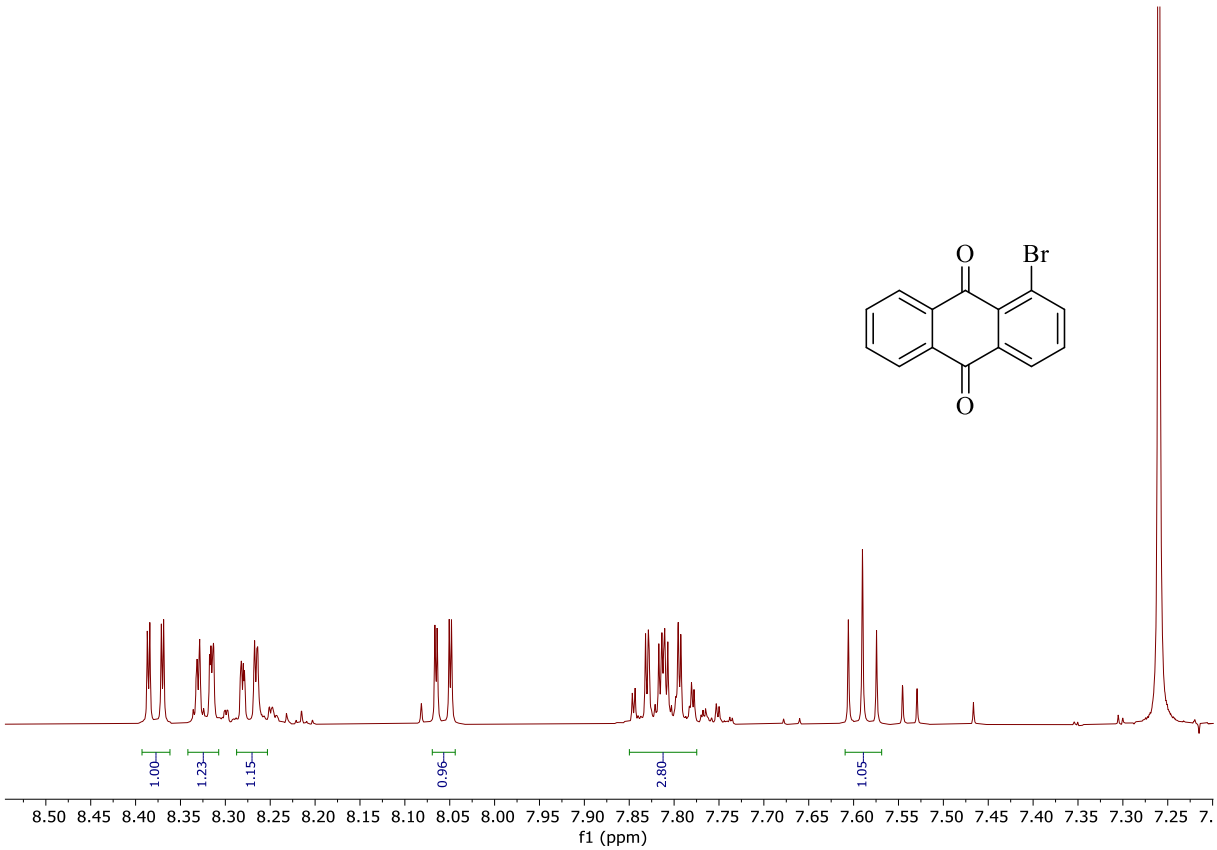

Figure 0.7: ^{1}H NMR spectrum of compound **56**.

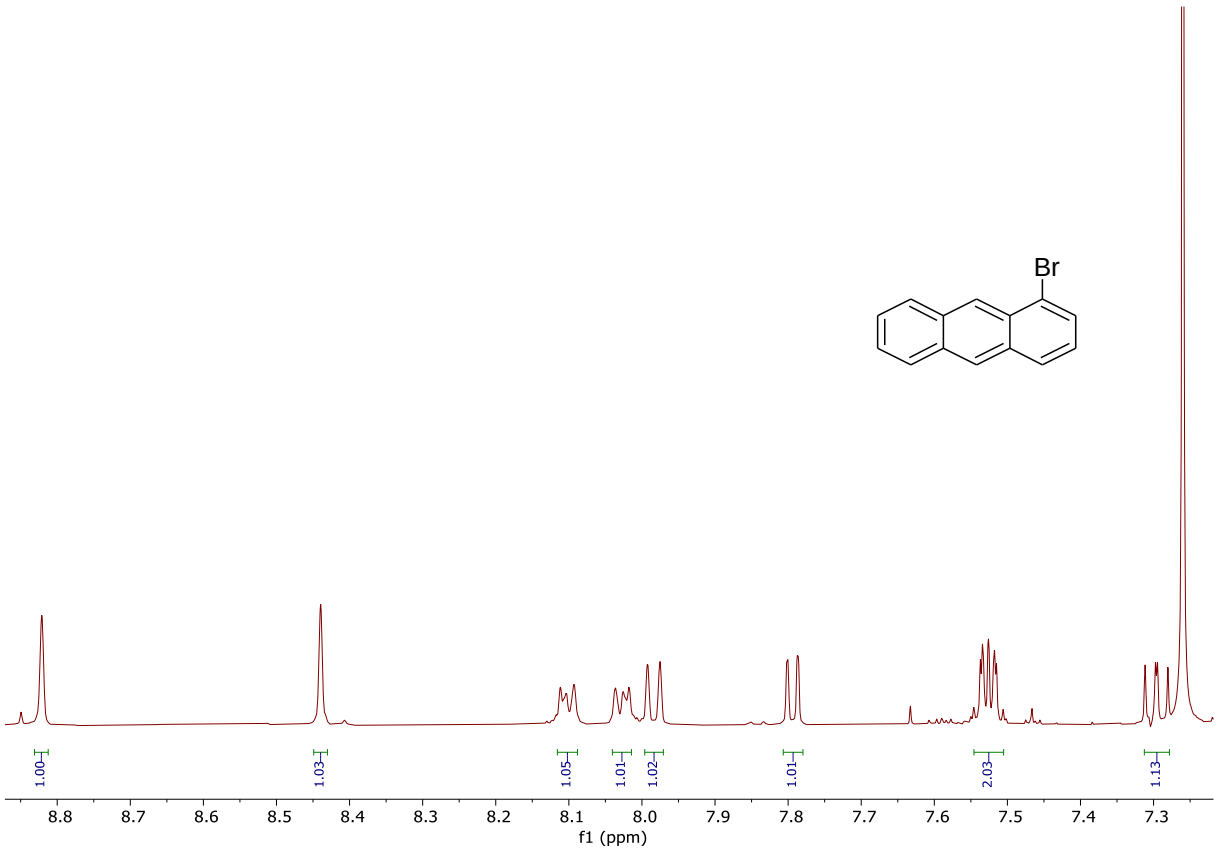

Figure 0.8: ^{1}H NMR spectrum of compound **40**.

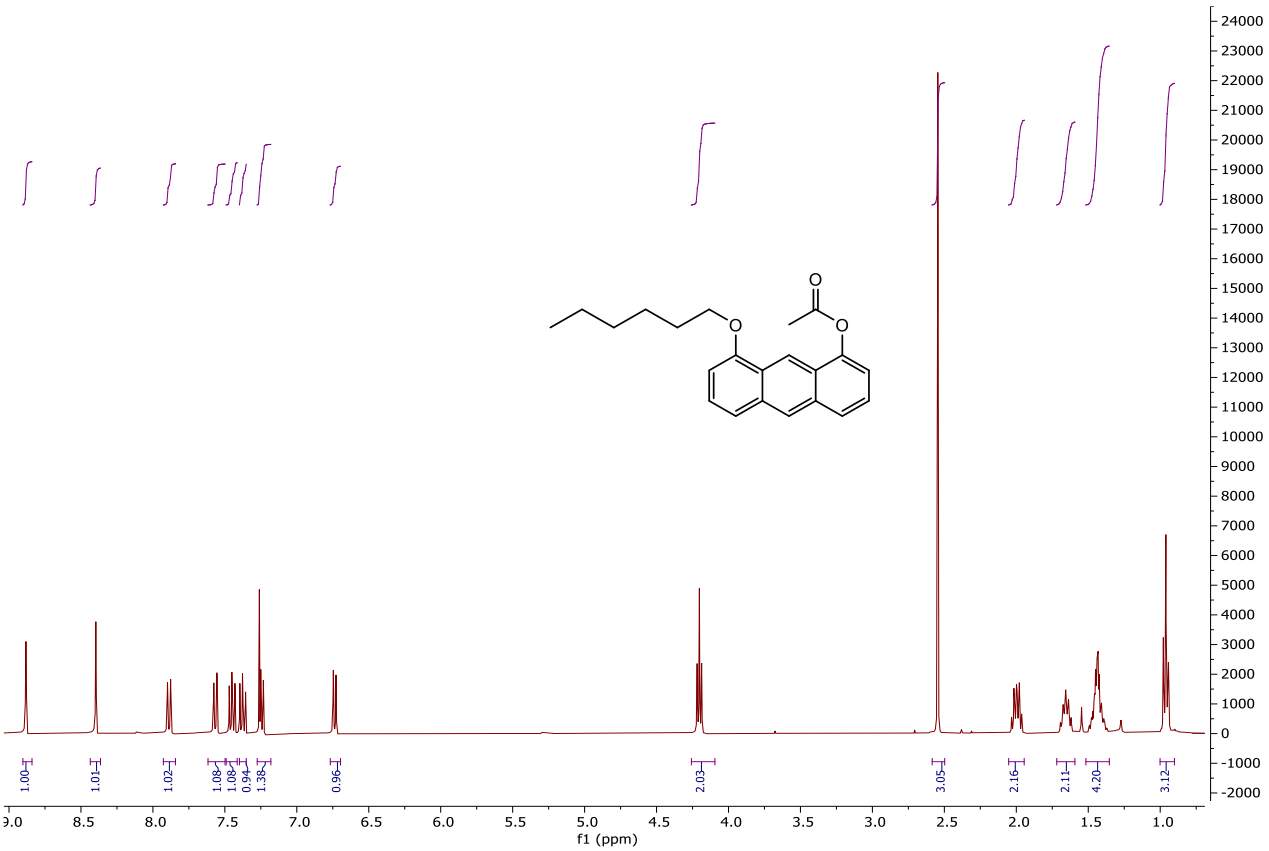

Figure 0.9: ^{1}H NMR spectrum of compound **54**.

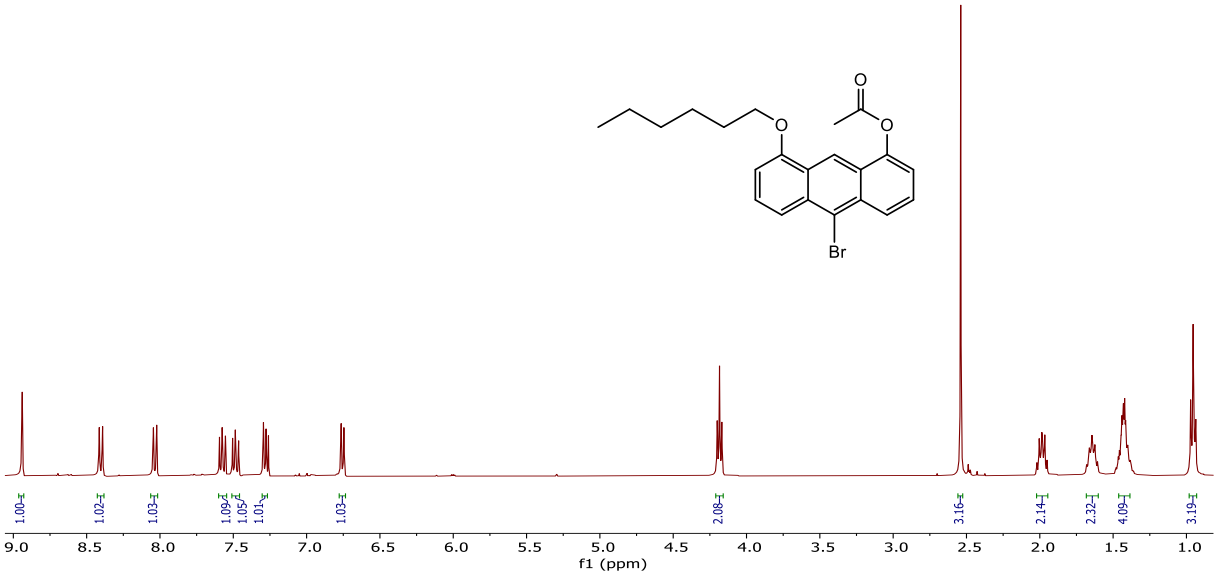

Figure 0.10: ^{1}H NMR spectrum of compound **50**.

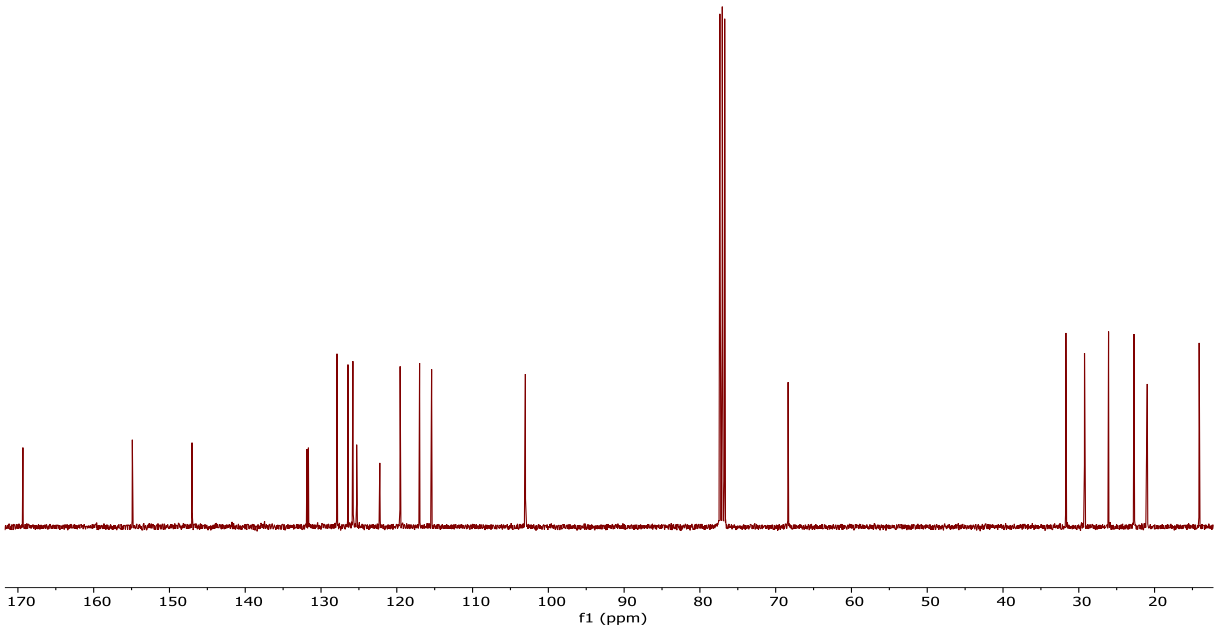

Figure 0.11: ^{13}C NMR spectrum of compound **50**.

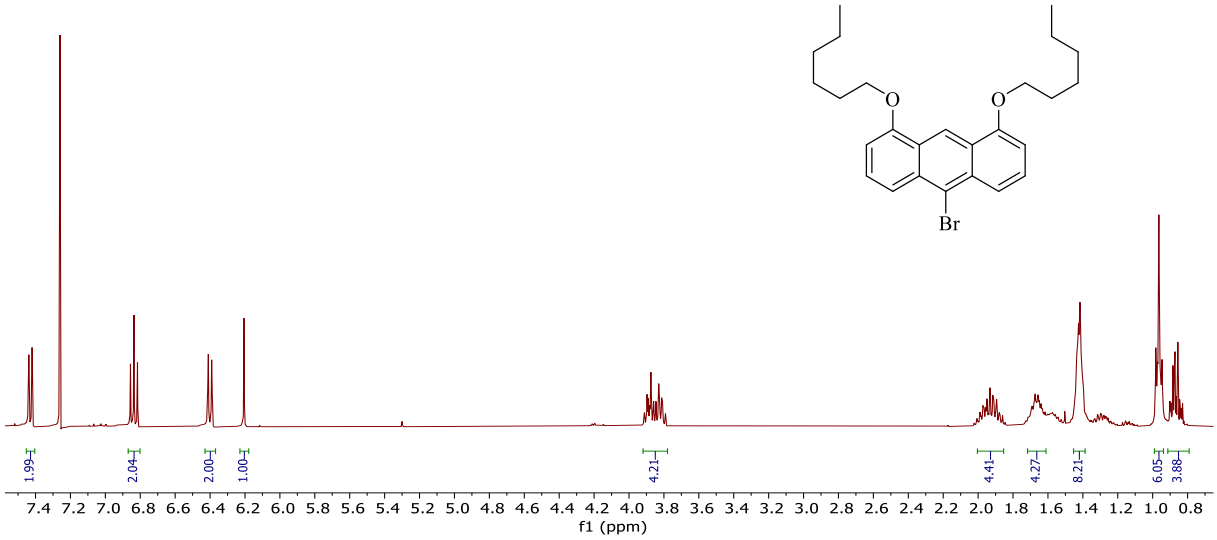

Figure 0.12: ^{1}H NMR spectrum of compound **71**.

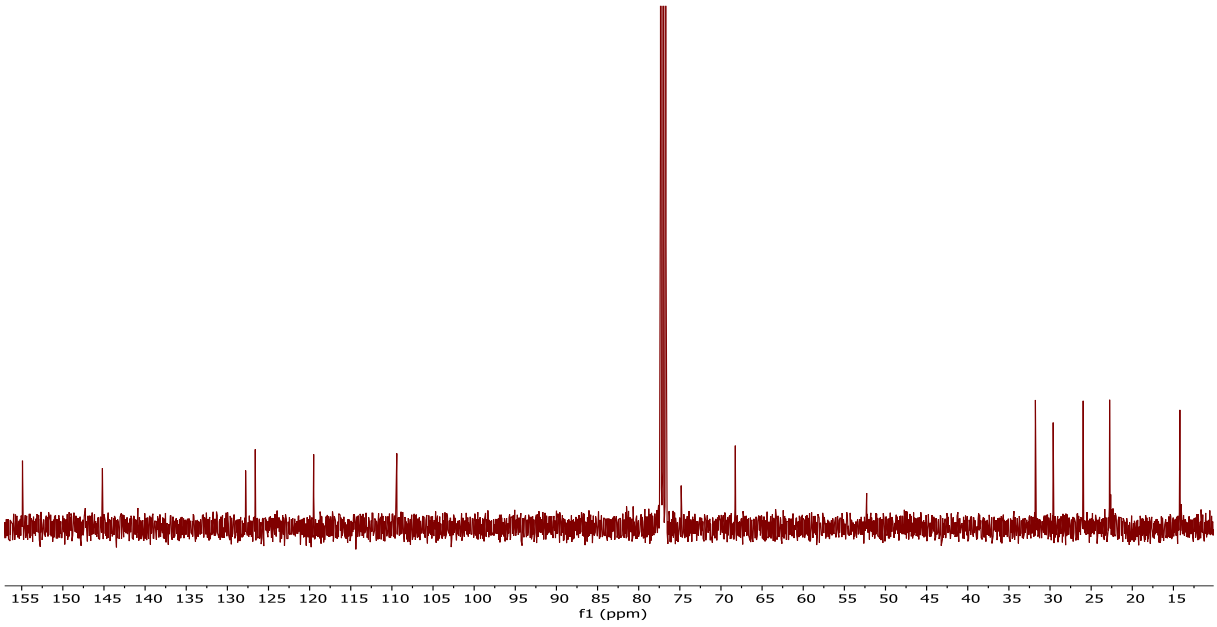

Figure 0.13: ^{13}C NMR spectrum of compound **71**.

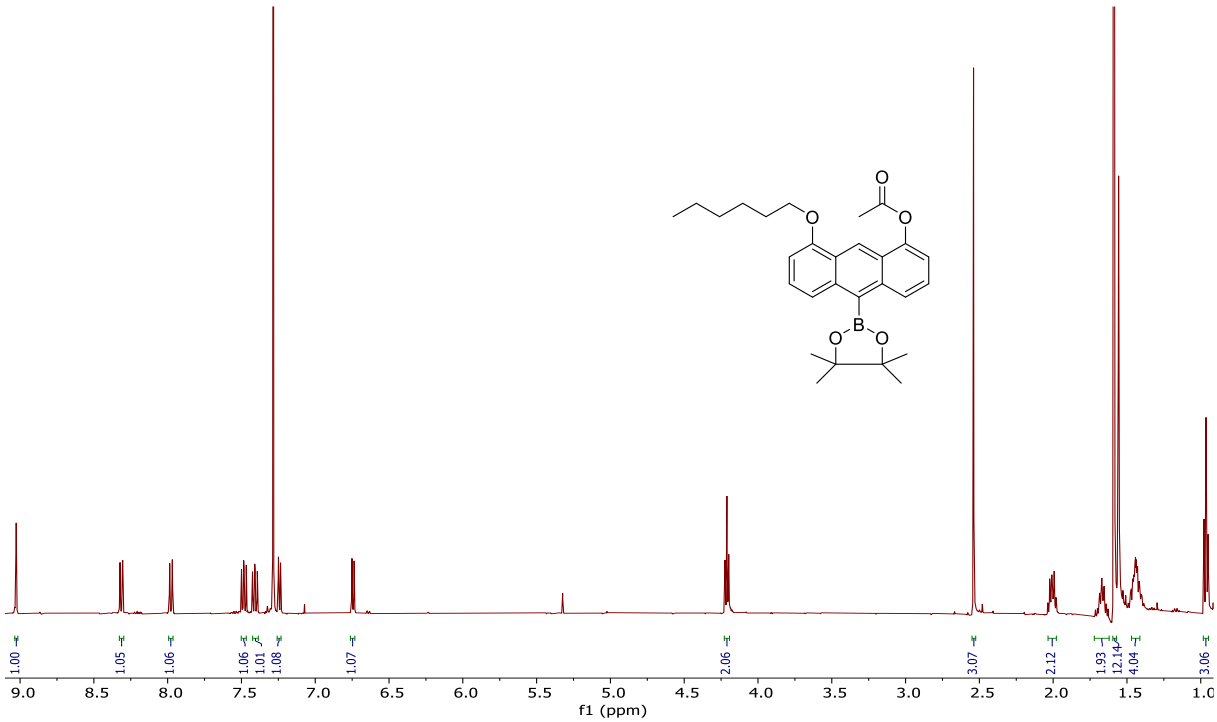

Figure 0.14: ^{1}H NMR spectrum of compound **39**.

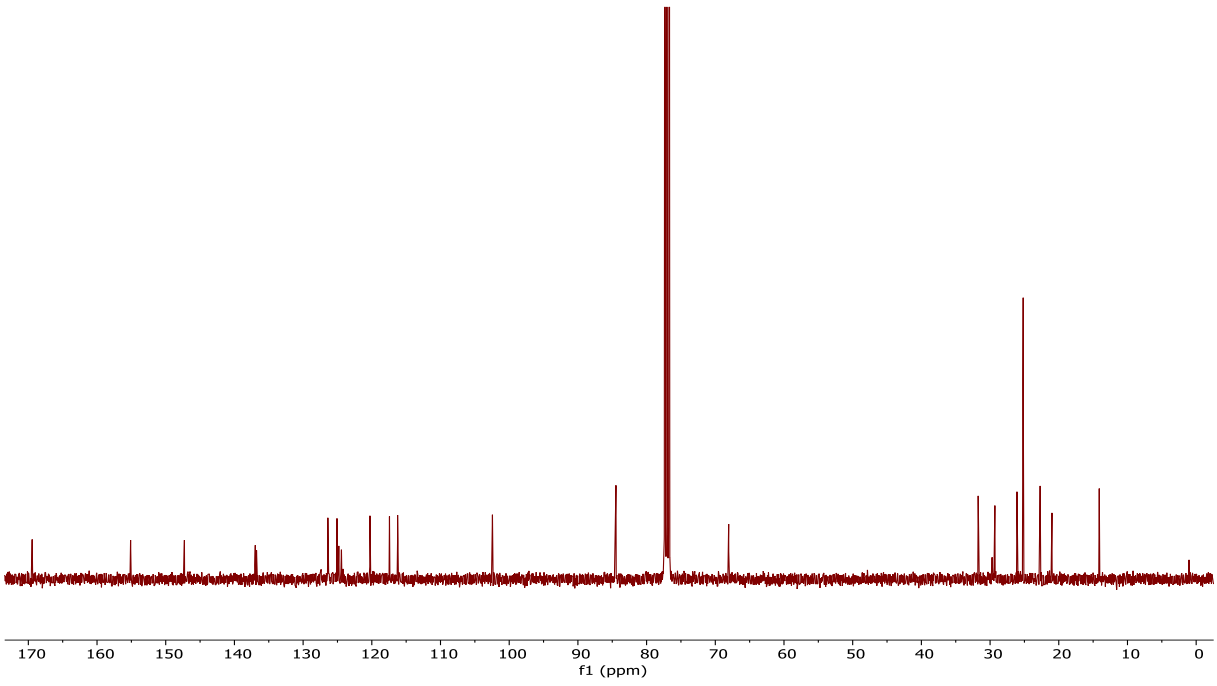

Figure 0.15: ^{13}C NMR spectrum of compound **39**.

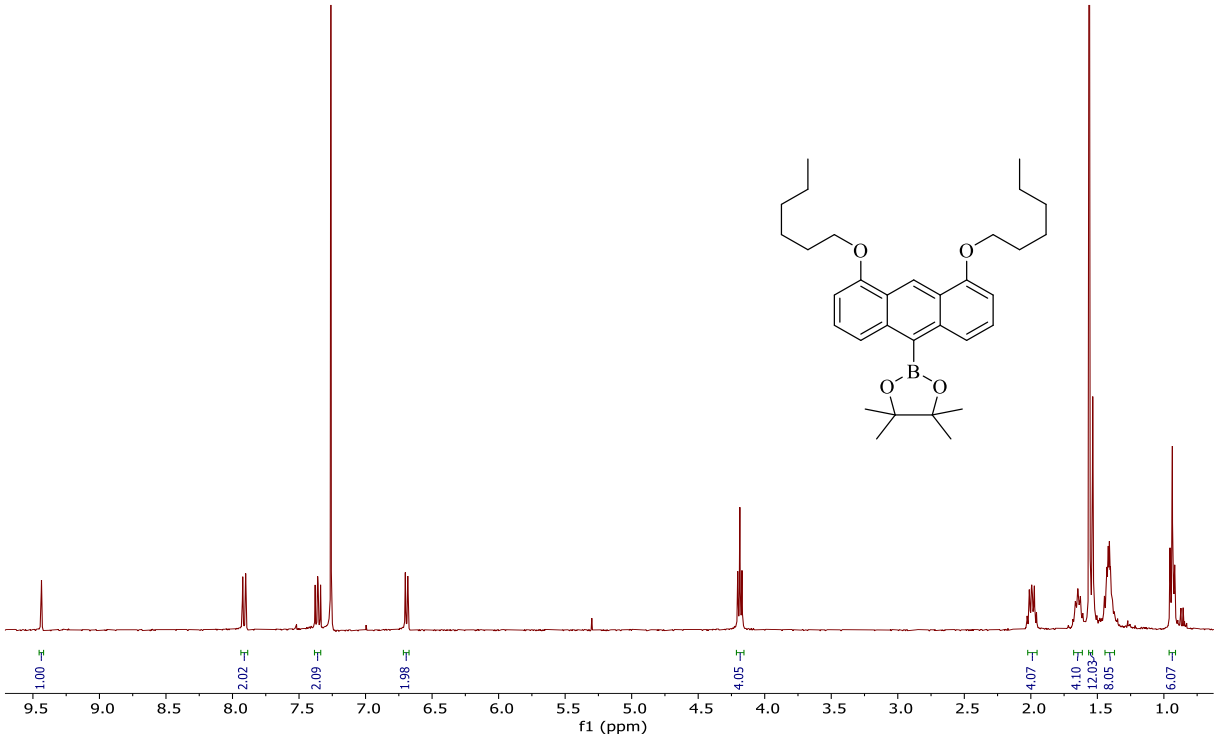

Figure 0.16: ^{1}H NMR spectrum of compound **72**.

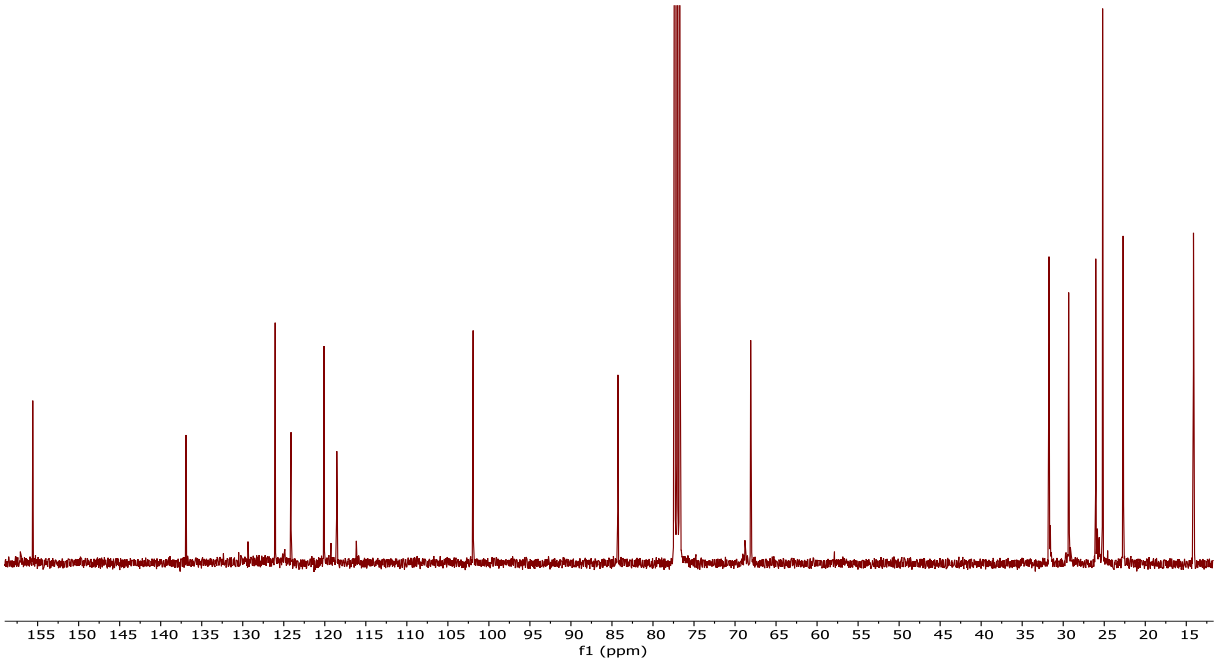

Figure 0.17: ^{13}C NMR spectrum of compound **72**.

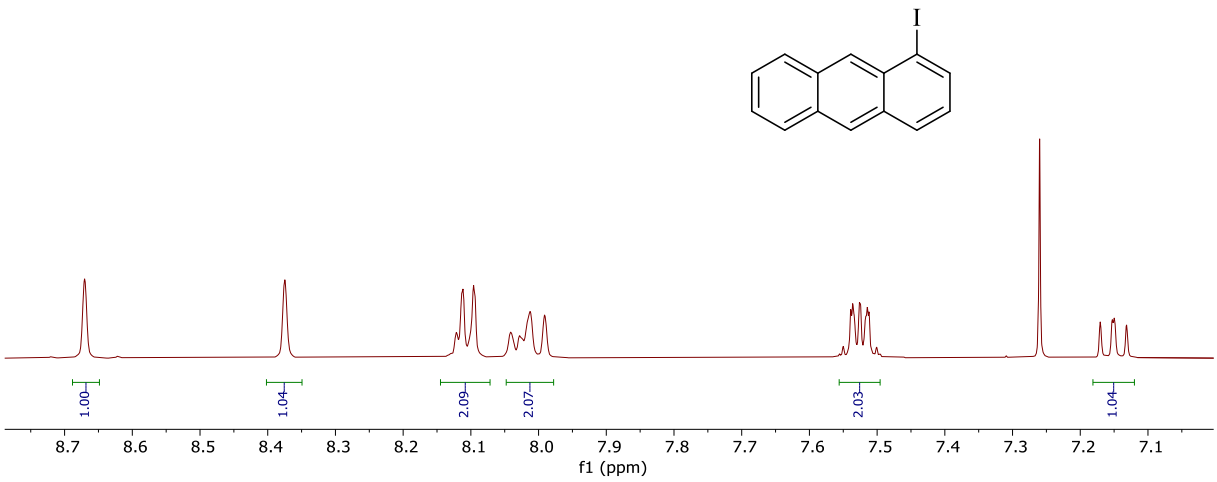

Figure 0.18: ^{1}H NMR spectrum of compound **64**.

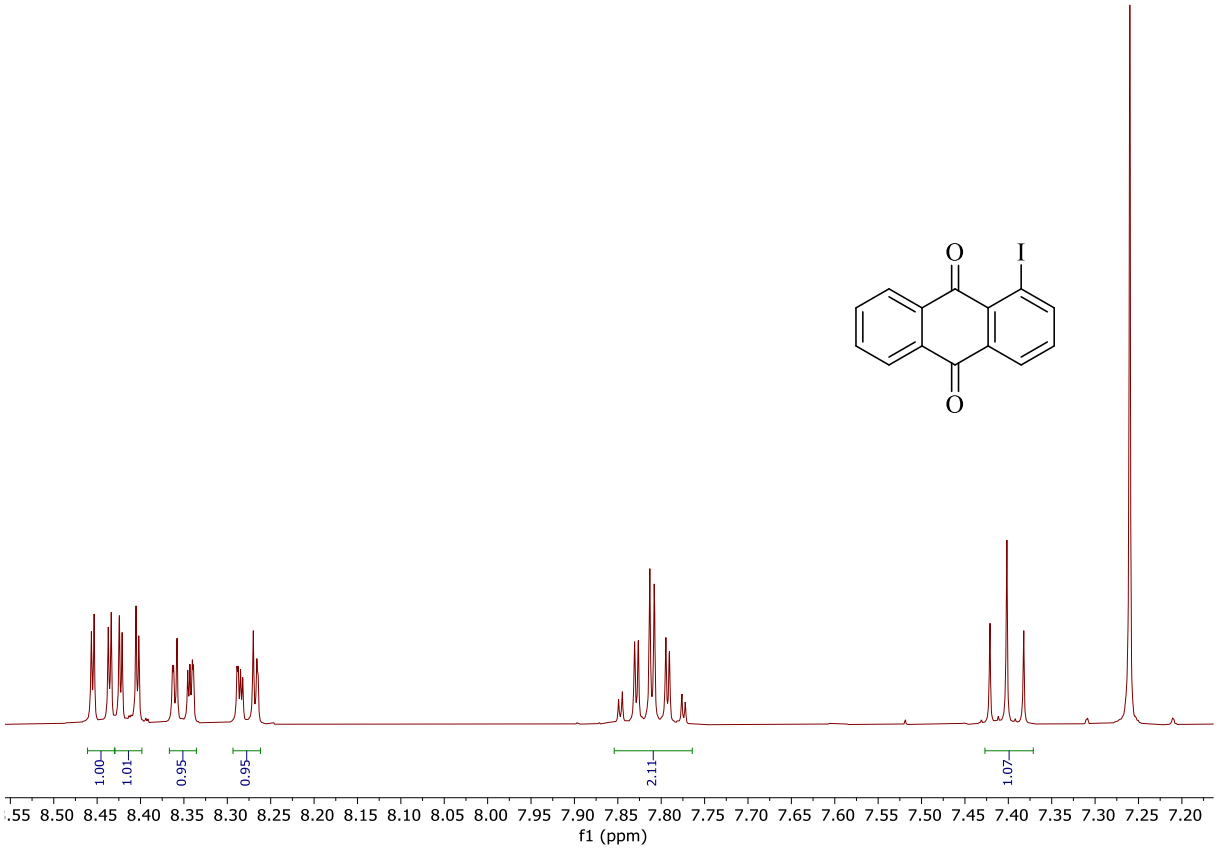

Figure 0.19: ^{1}H NMR spectrum of compound **65**.

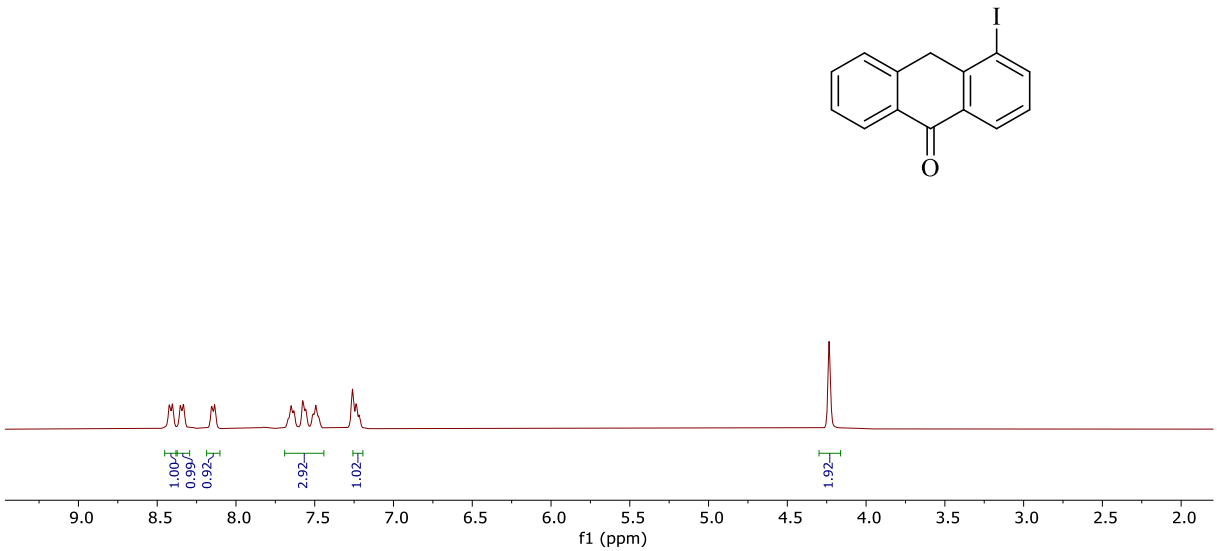

Figure 0.20: ^{1}H NMR spectrum of compound **66**.

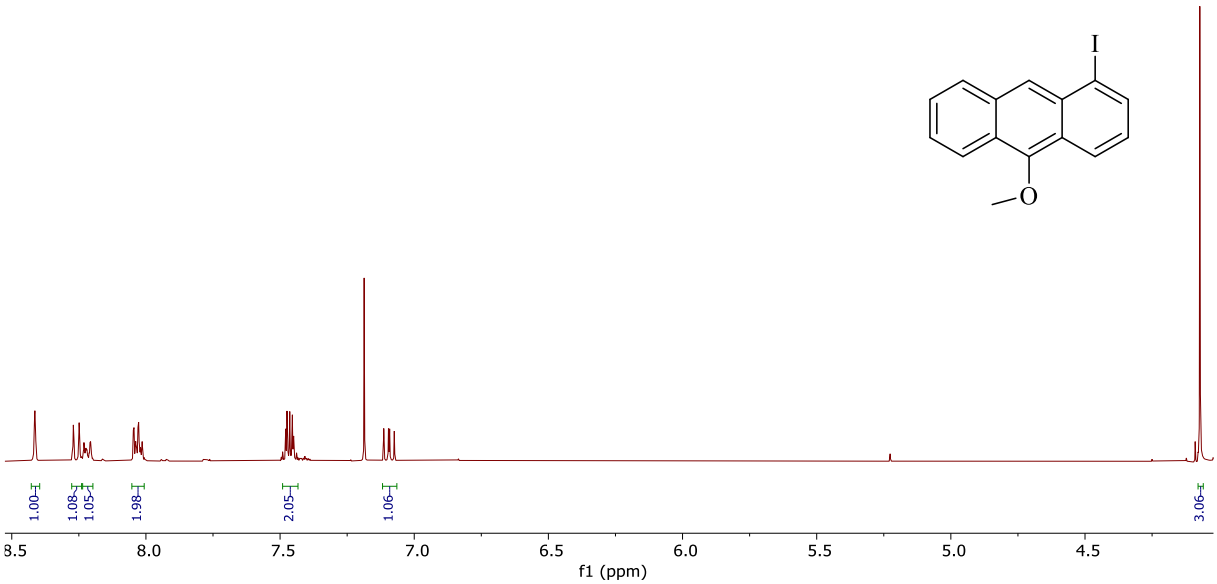

Figure 0.21: ^{1}H NMR spectrum of compound **67**.

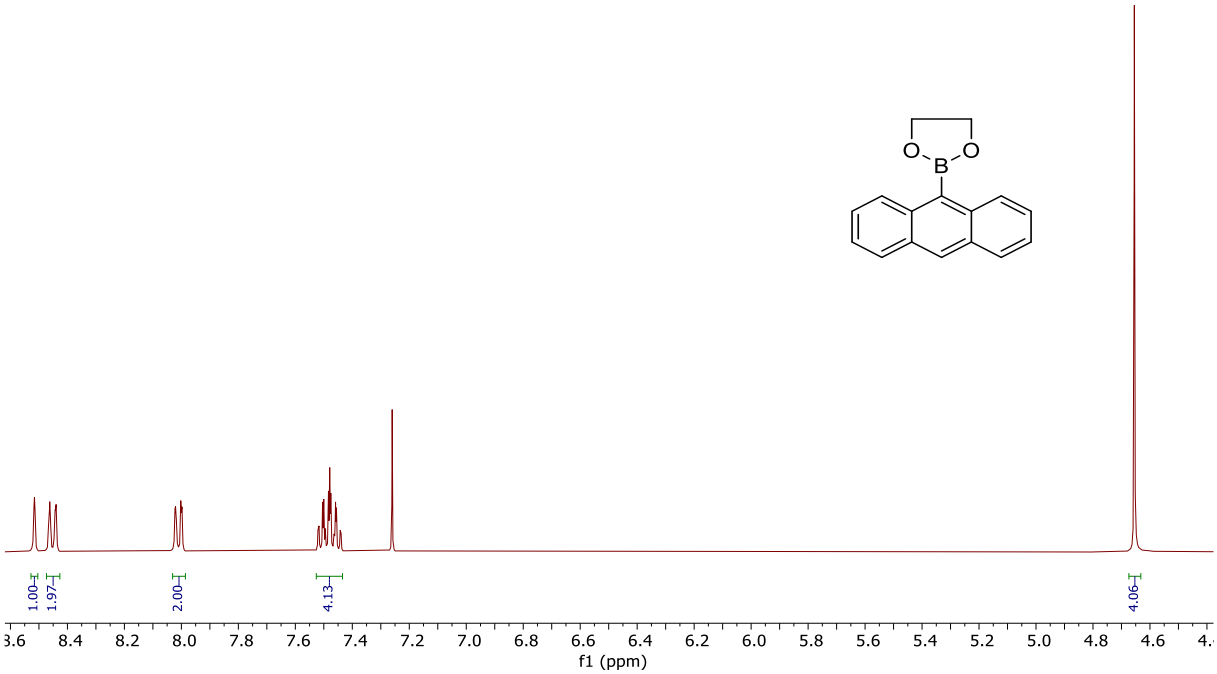

Figure 0.22: ^{1}H NMR spectrum of compound **70**.

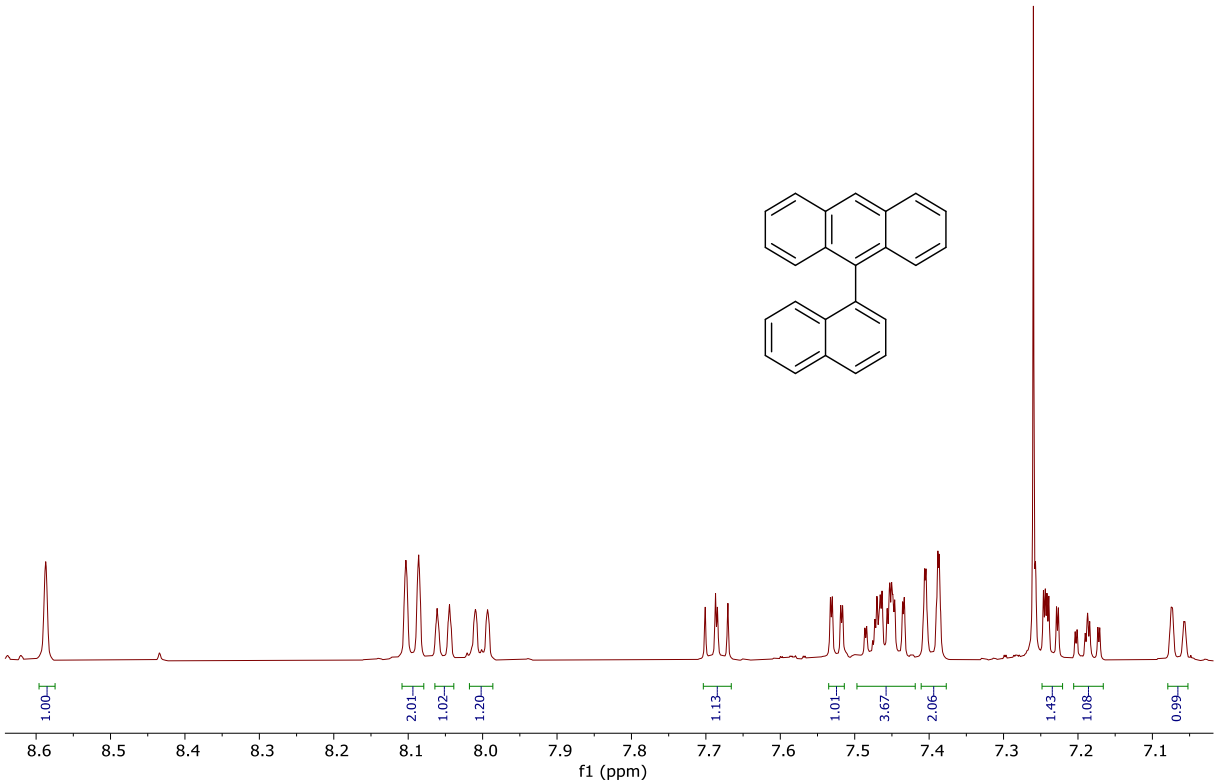

Figure 0.23: ^{1}H NMR spectrum of compound **63**.

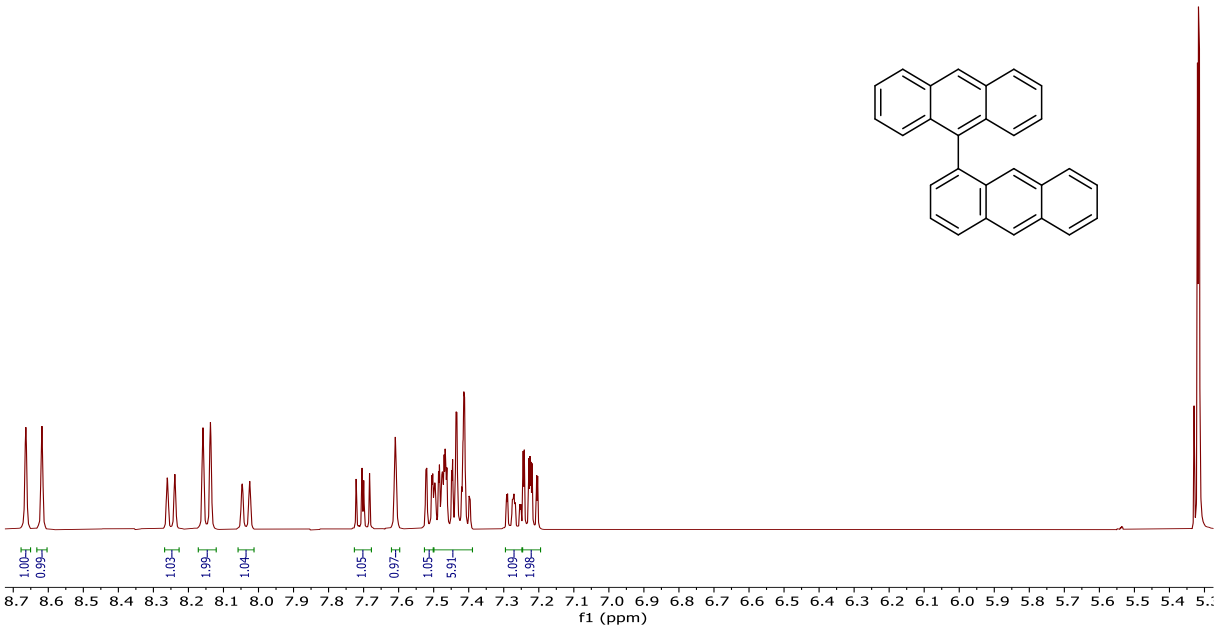

Figure 0.24: ^{1}H NMR spectrum of compound **61**.

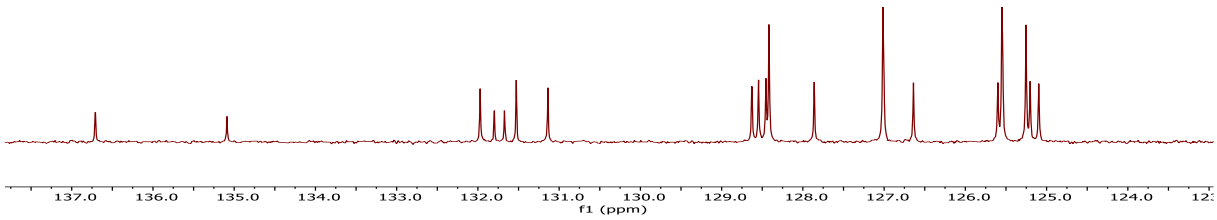

Figure 0.25: ^{13}C NMR spectrum of compound **61**.

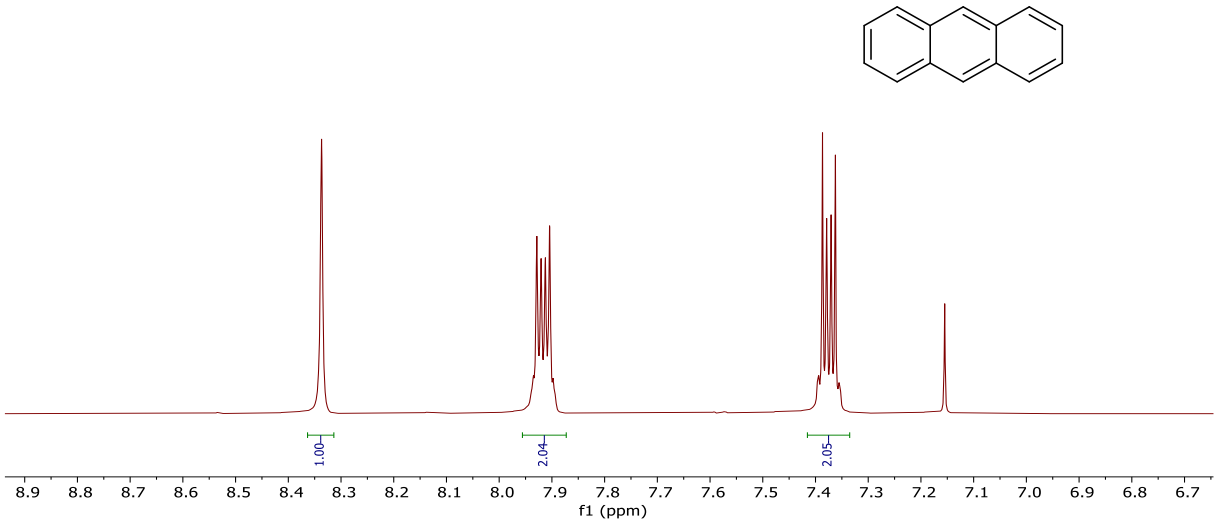

Figure 0.26: ^{1}H NMR spectrum of compound **57**.

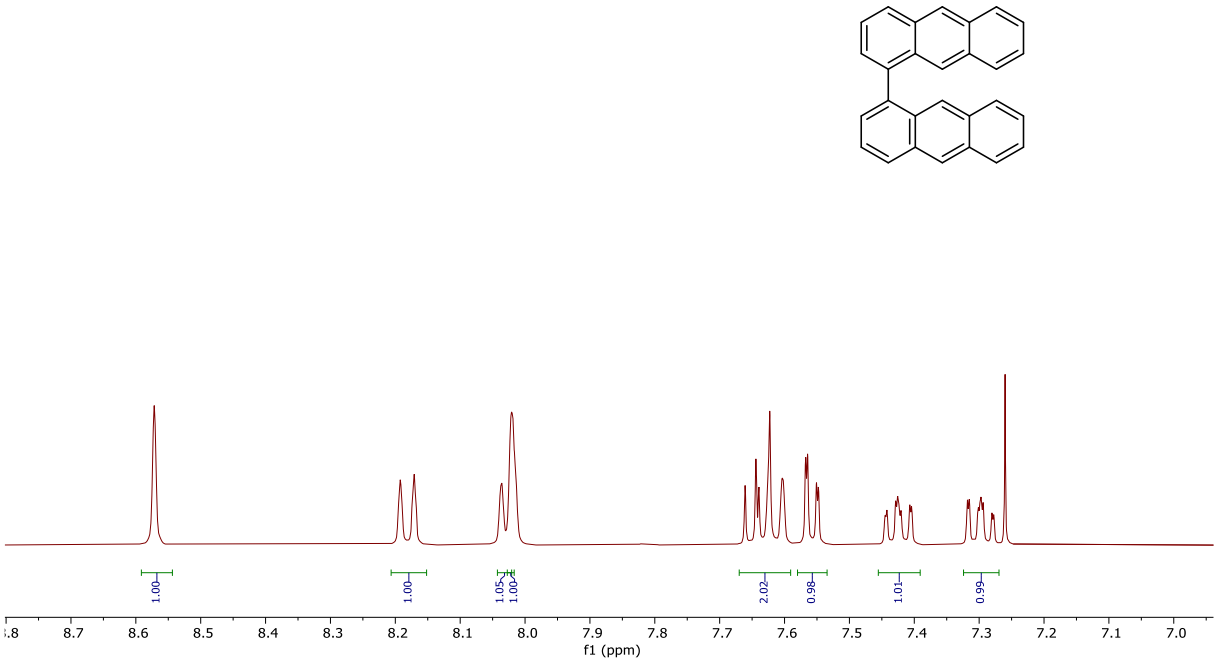

Figure 0.27: ^{1}H NMR spectrum of compound **58**.

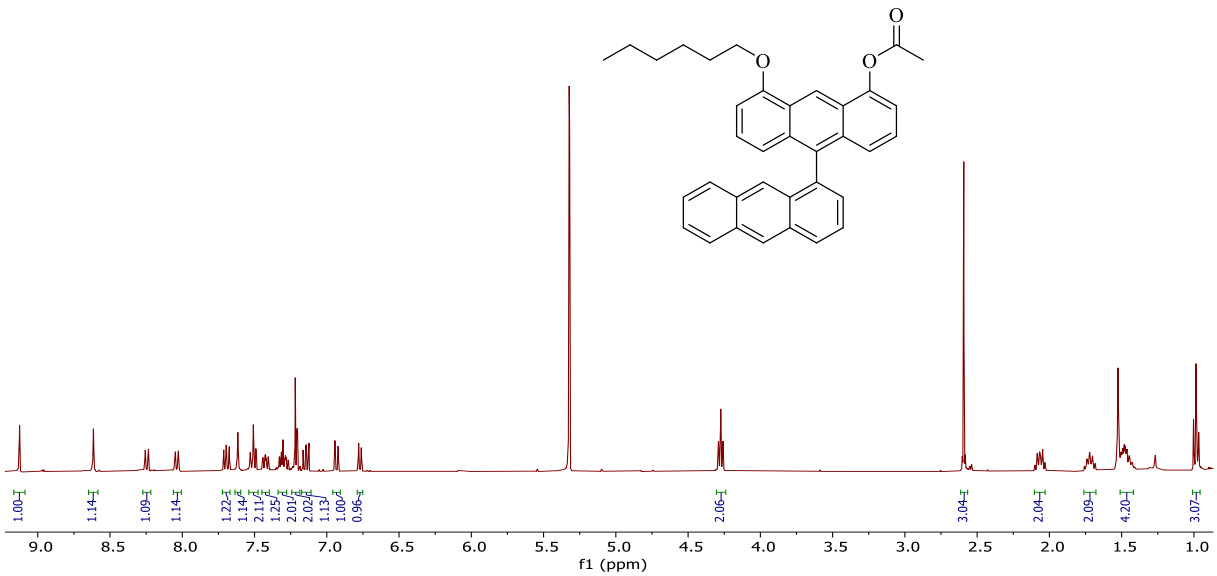

Figure 0.28: ^{1}H NMR spectrum of compound **41**.

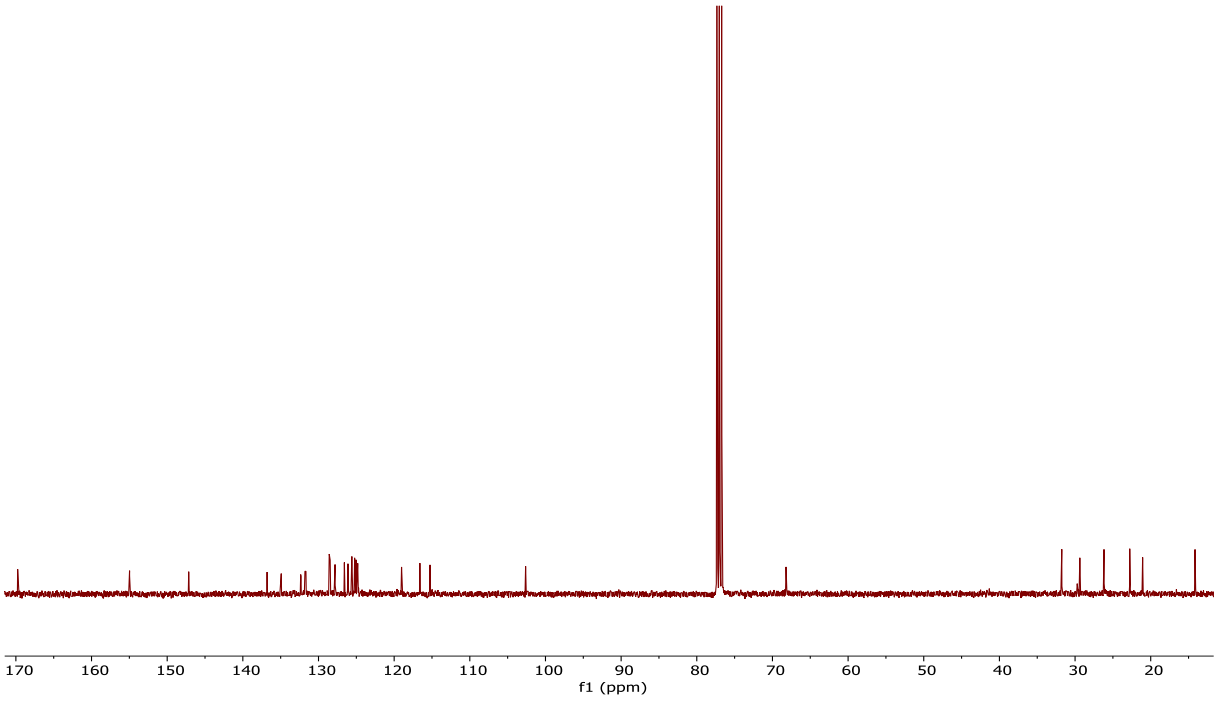

Figure 0.29: ^{13}C NMR spectrum of compound **41**.

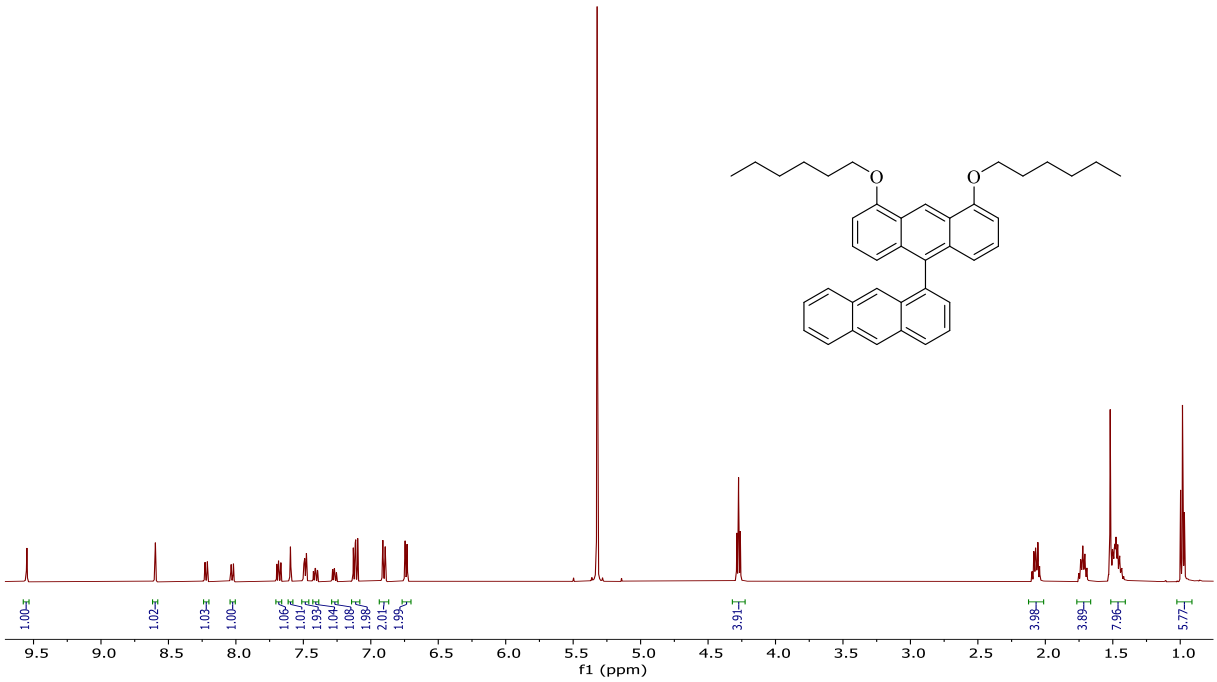

Figure 0.30: ^{1}H NMR spectrum of compound **73**.

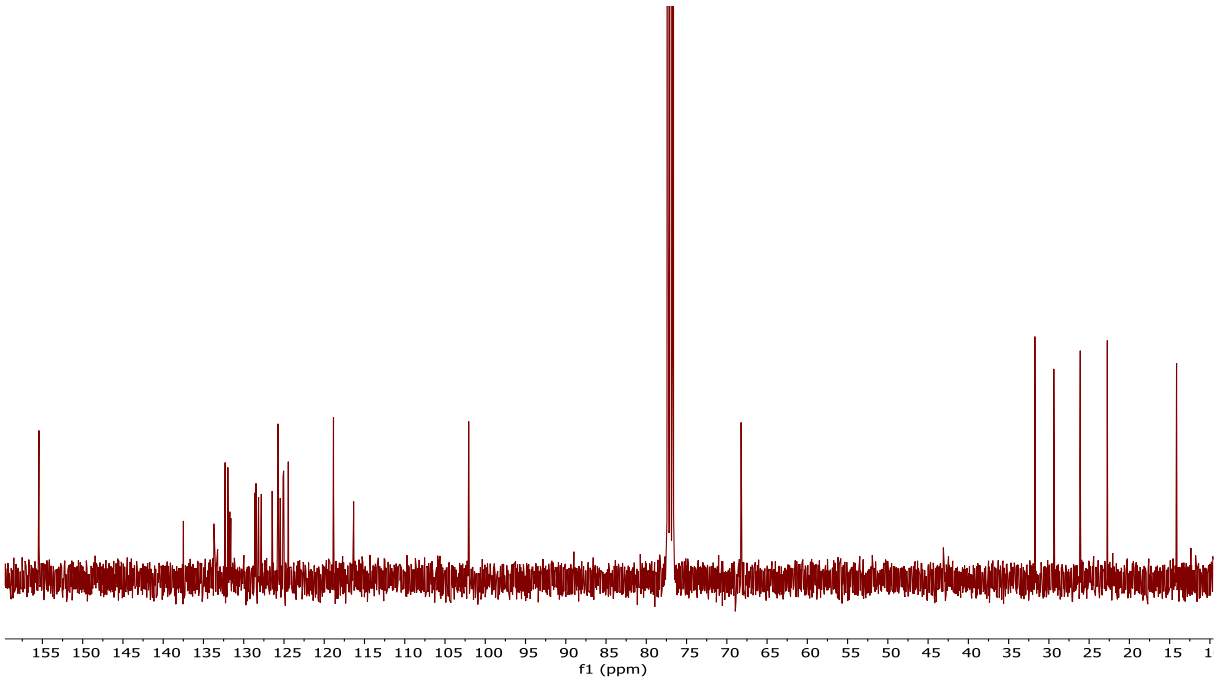

Figure 0.31: ^{13}C NMR spectrum of compound **73**.

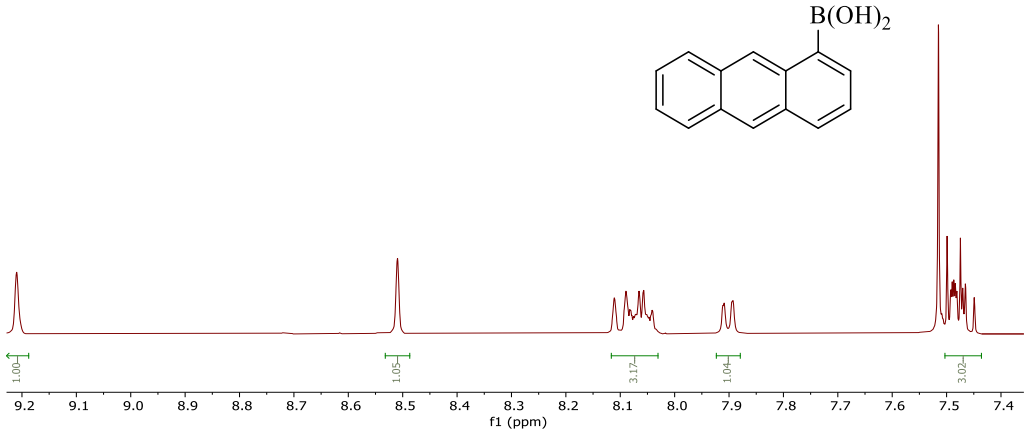

Figure 0.32: ^{1}H NMR spectrum of compound **74**.

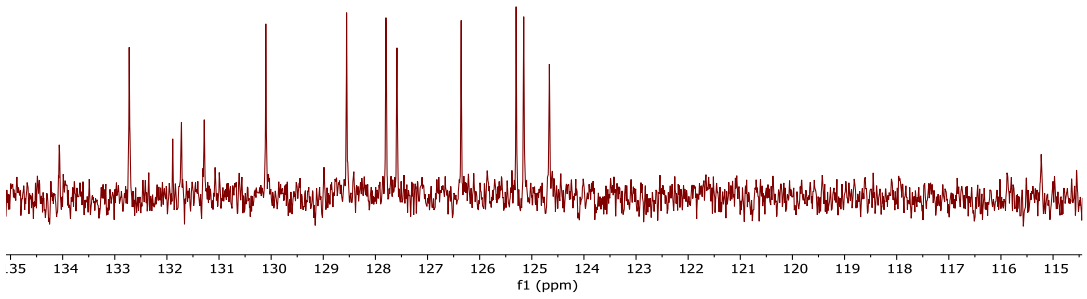

Figure 0.33: ^{13}C NMR spectrum of compound **74**.

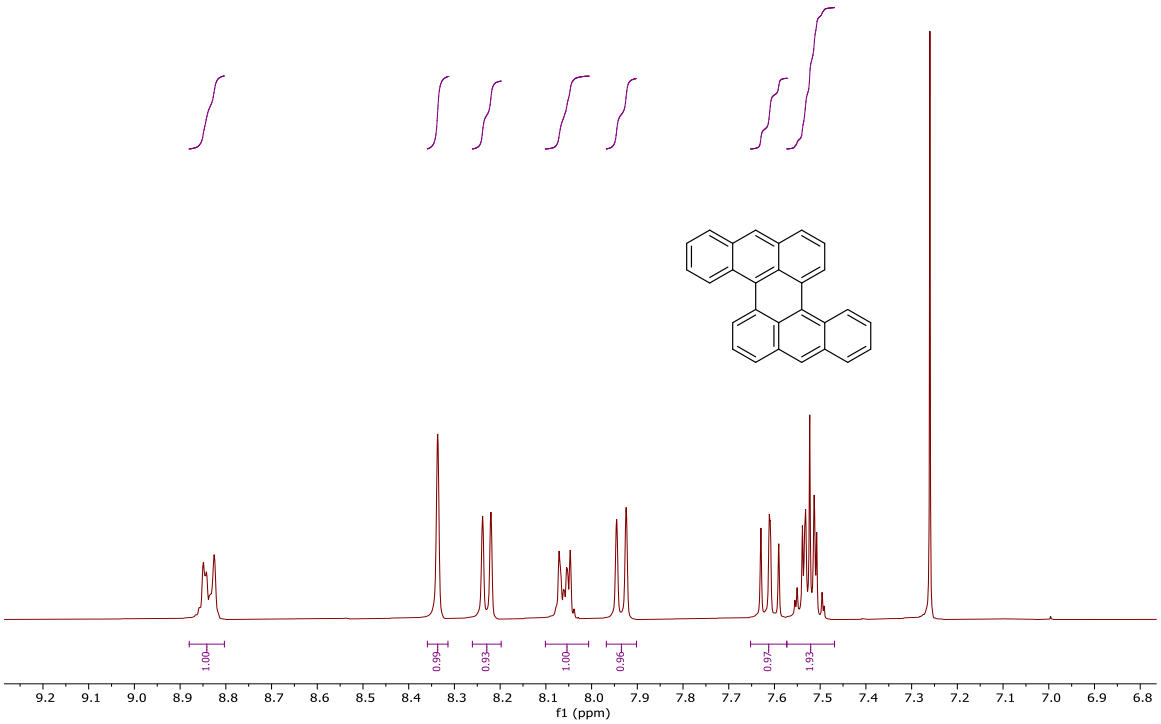

Figure 0.34: ^{1}H NMR spectrum of compound **77**.

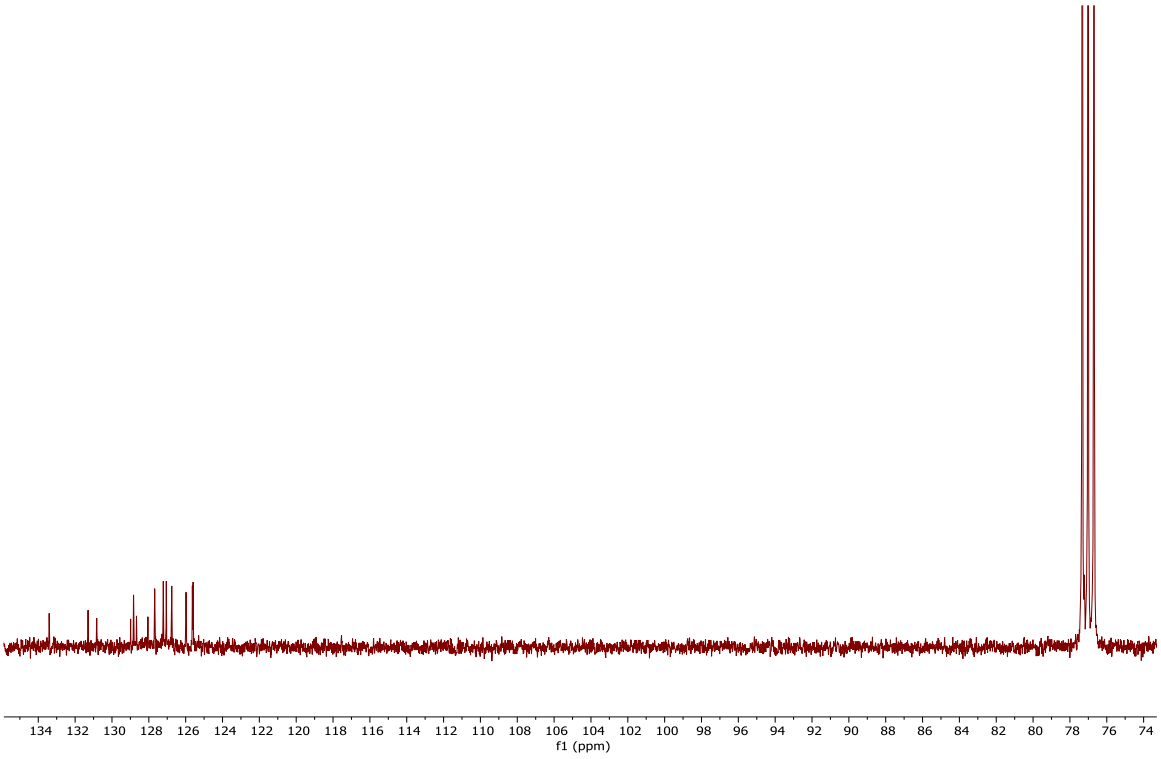

Figure 0.35: ^{13}C NMR spectrum of compound **77**.

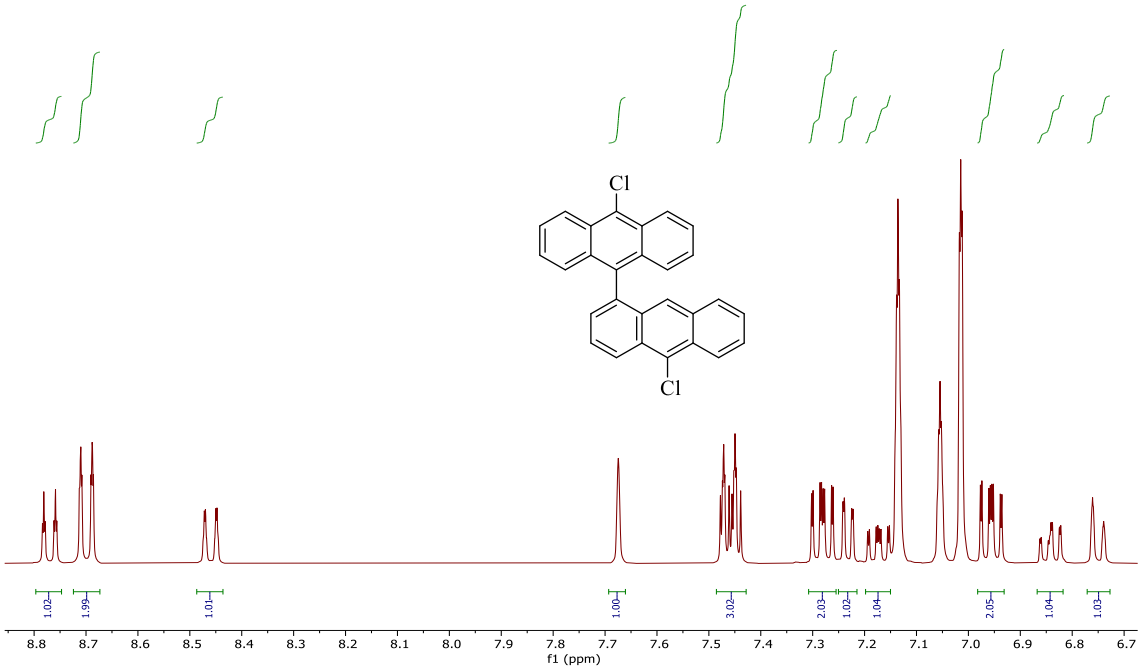

Figure 0.36: ^{1}H NMR spectrum of compound **78**.

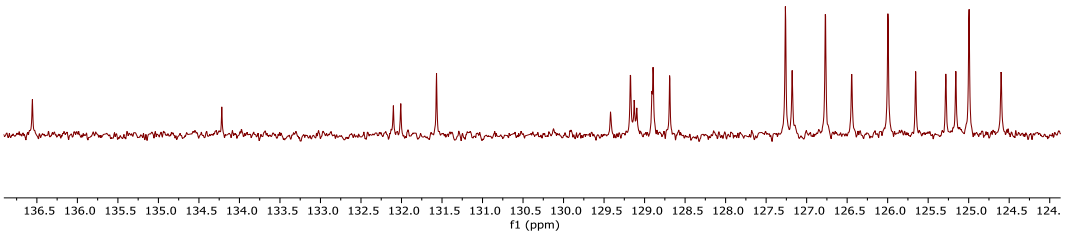

Figure 0.37: ^{13}C NMR spectrum of compound **78**.

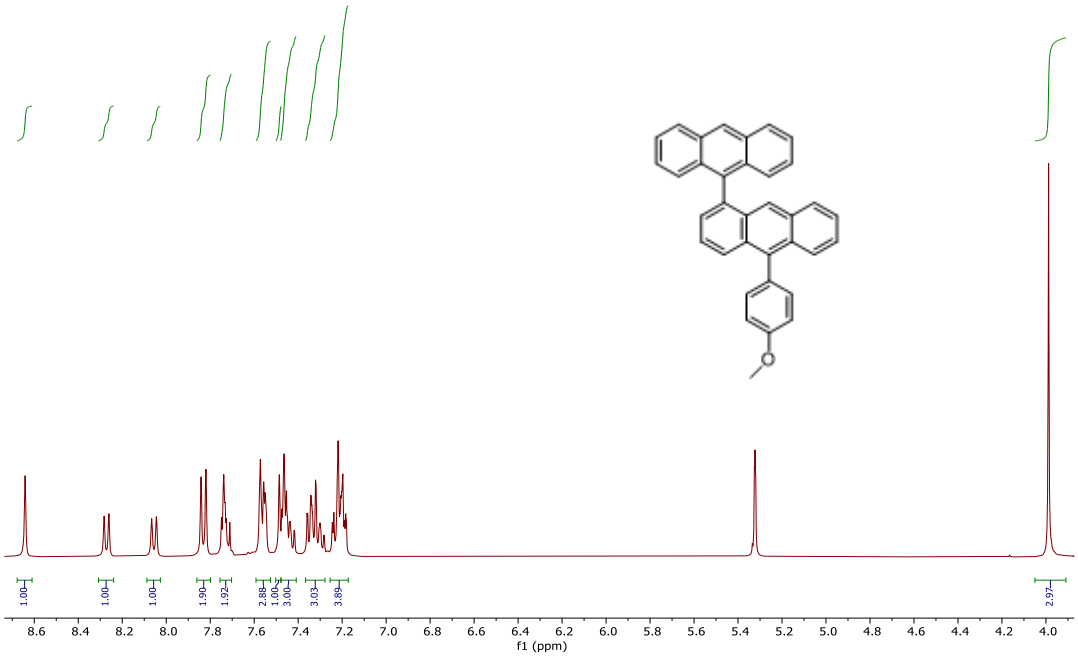

Figure 0.38: ^{1}H NMR spectrum of compound **87**.

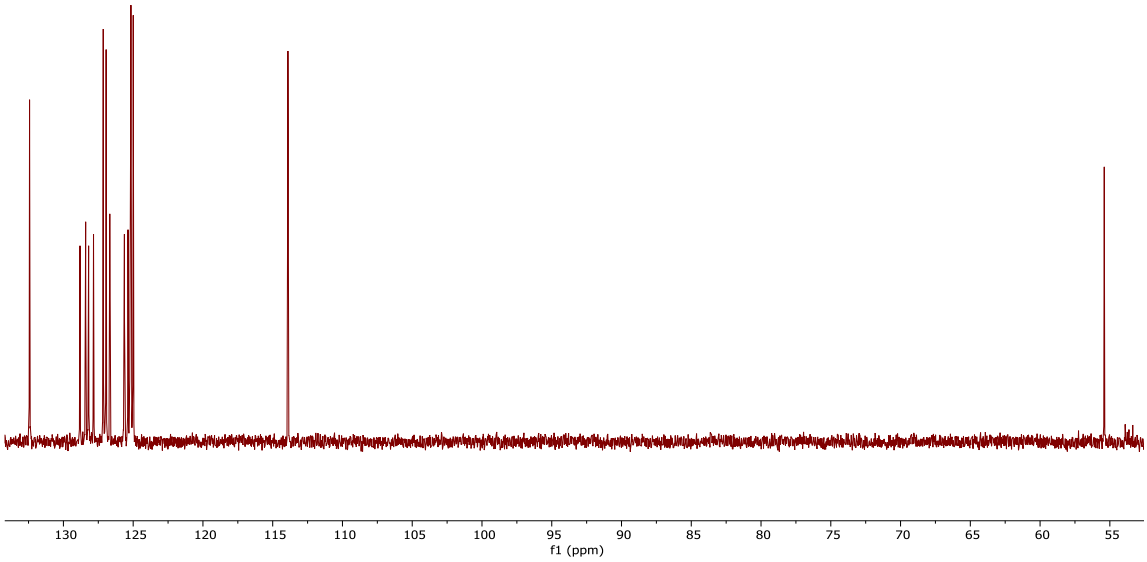

Figure 0.39: ^{13}C NMR spectrum of compound **87**.

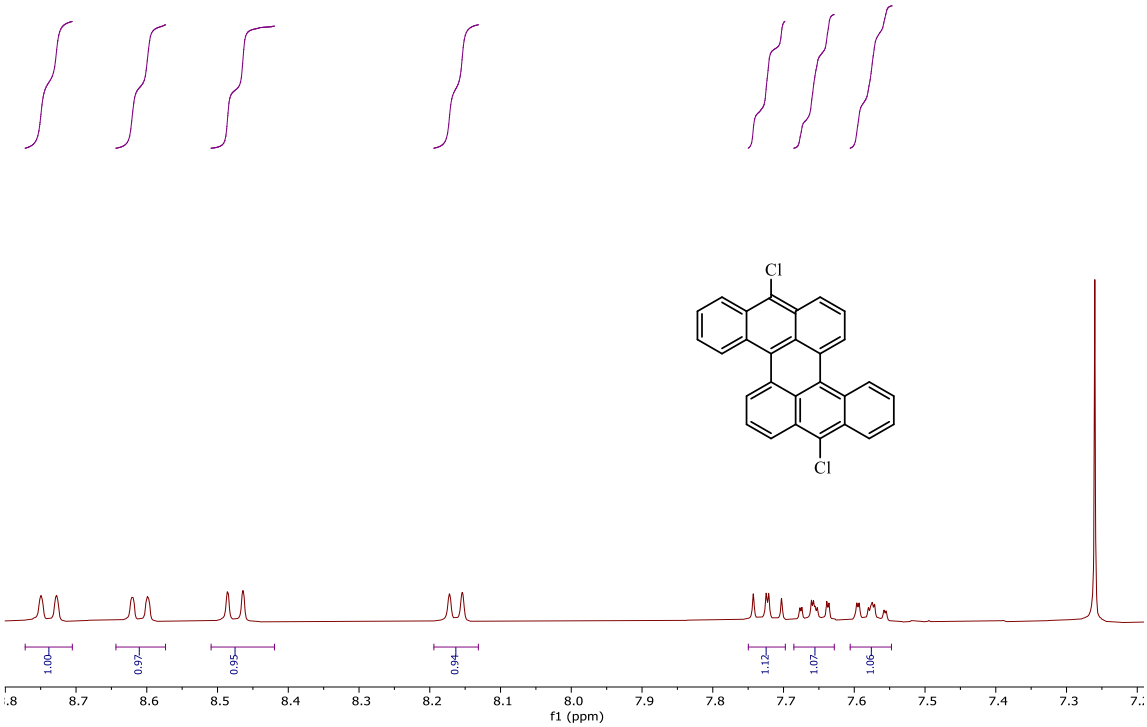

Figure 0.40: ^{1}H NMR spectrum of compound **79**.

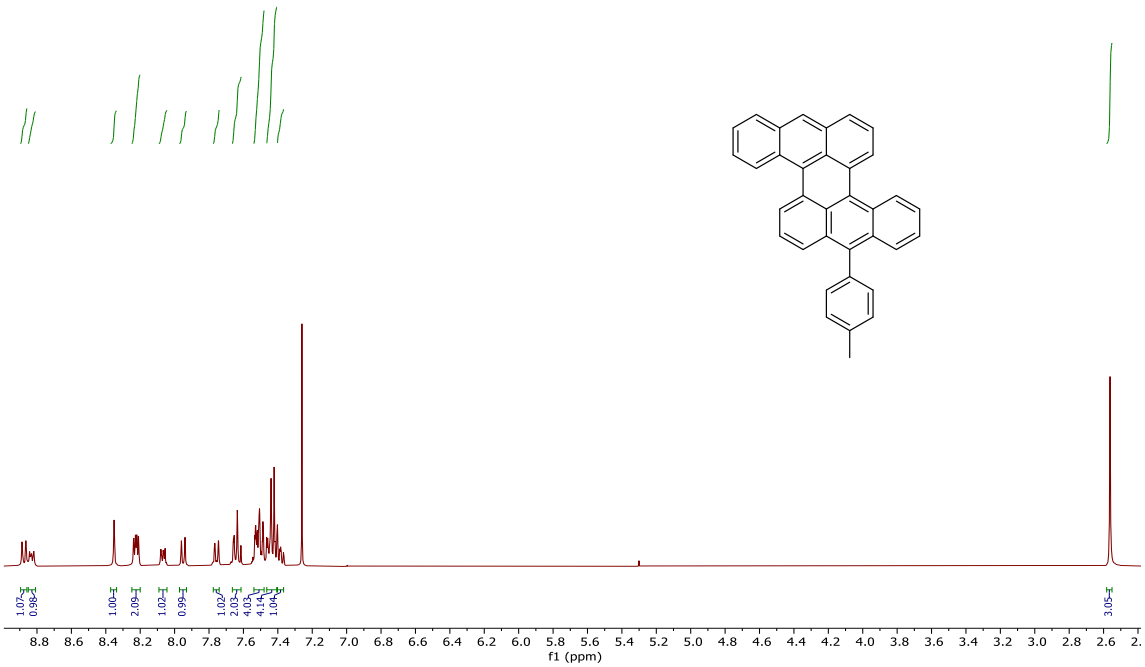

Figure 0.41: ^{1}H NMR spectrum of compound **85**.

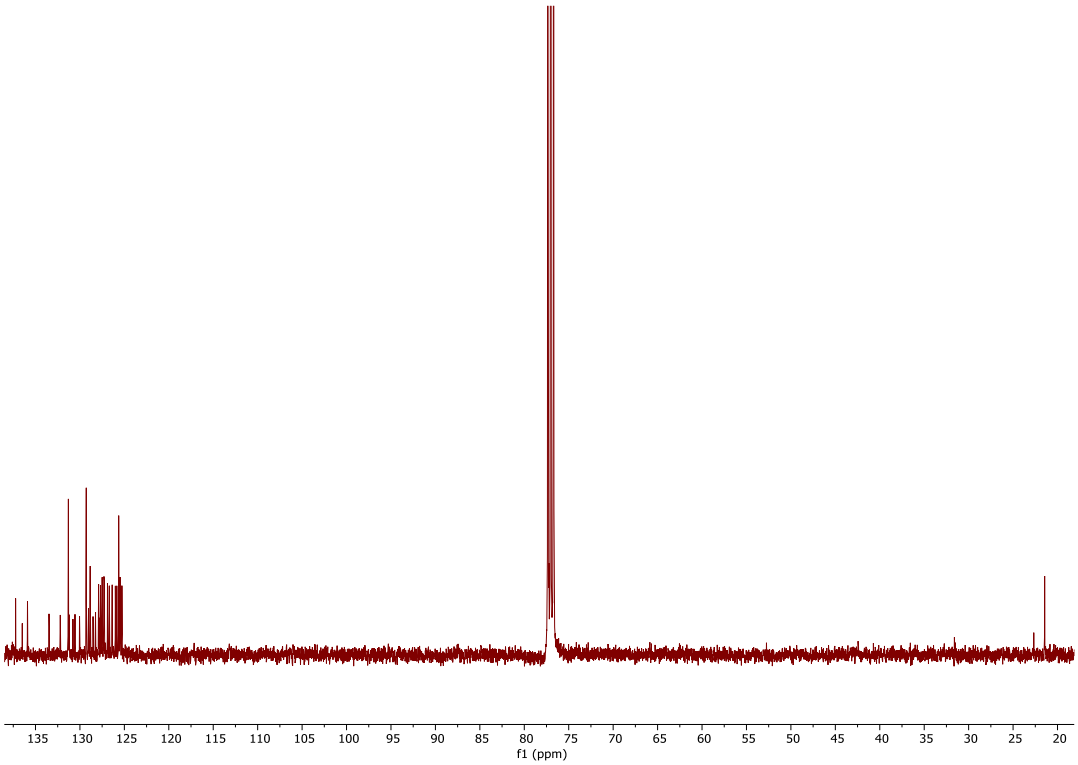

Figure 0.42: ^{13}C NMR spectrum of compound **85**.

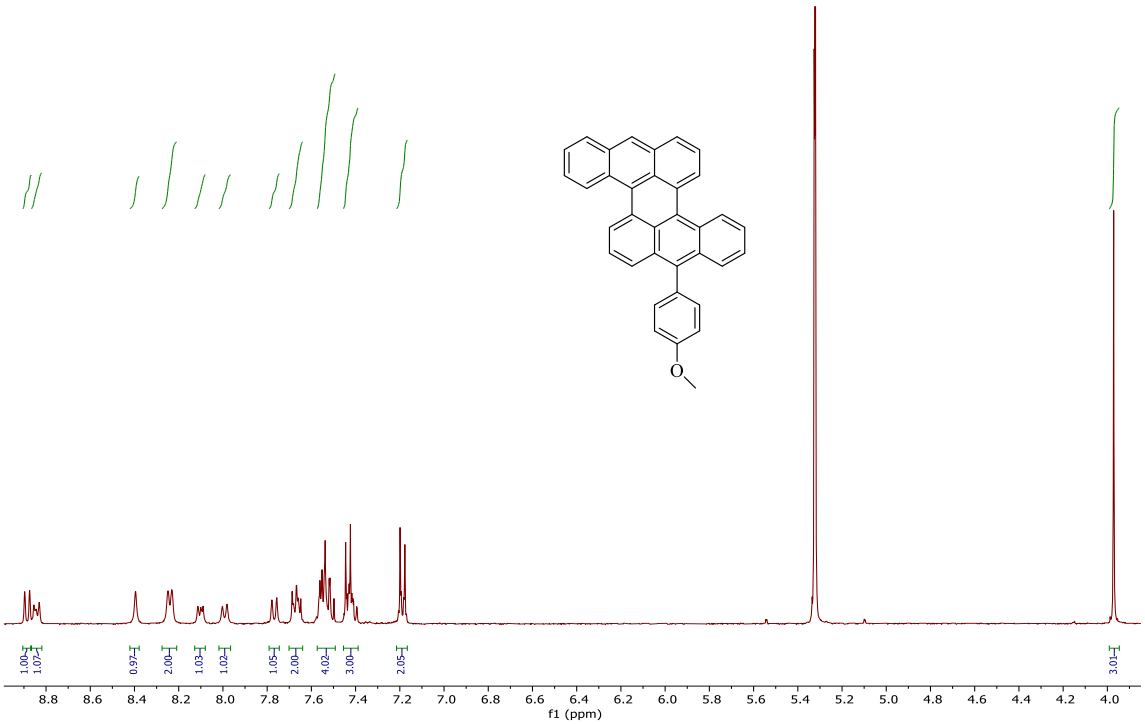

Figure 0.43: ^{1}H NMR spectrum of compound **86**.

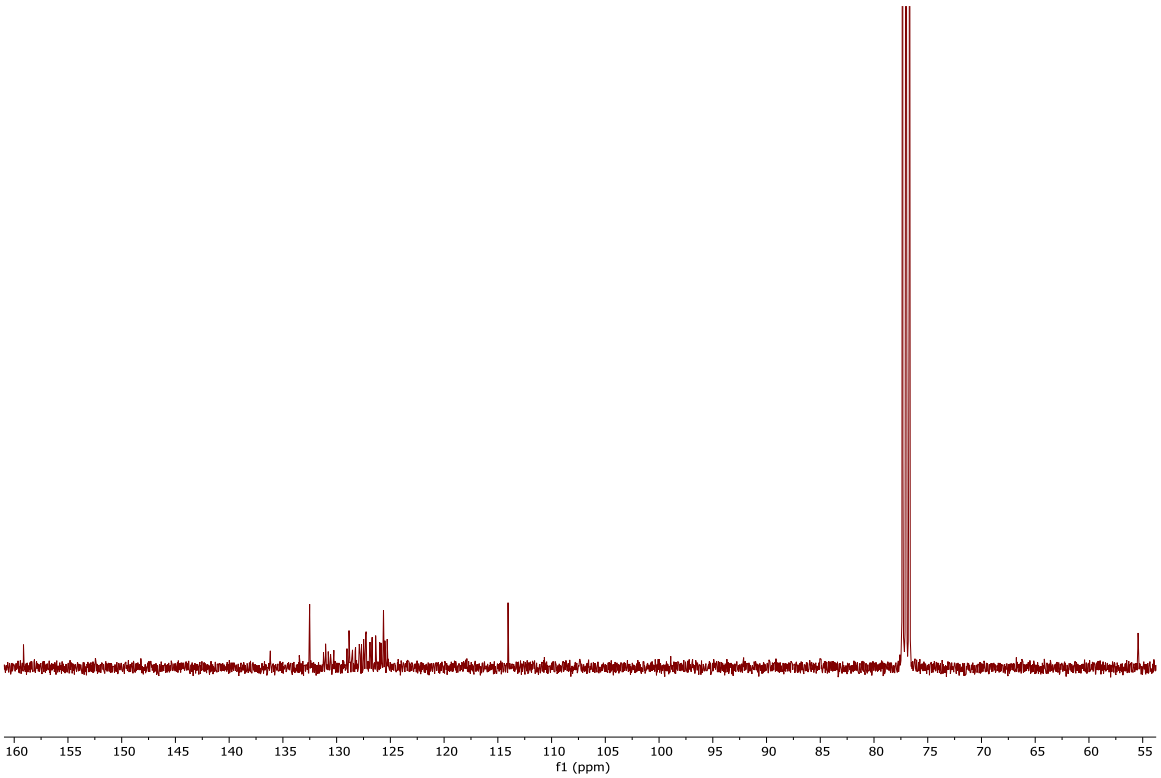

Figure 0.44: ^{13}C NMR spectrum of compound **86**.

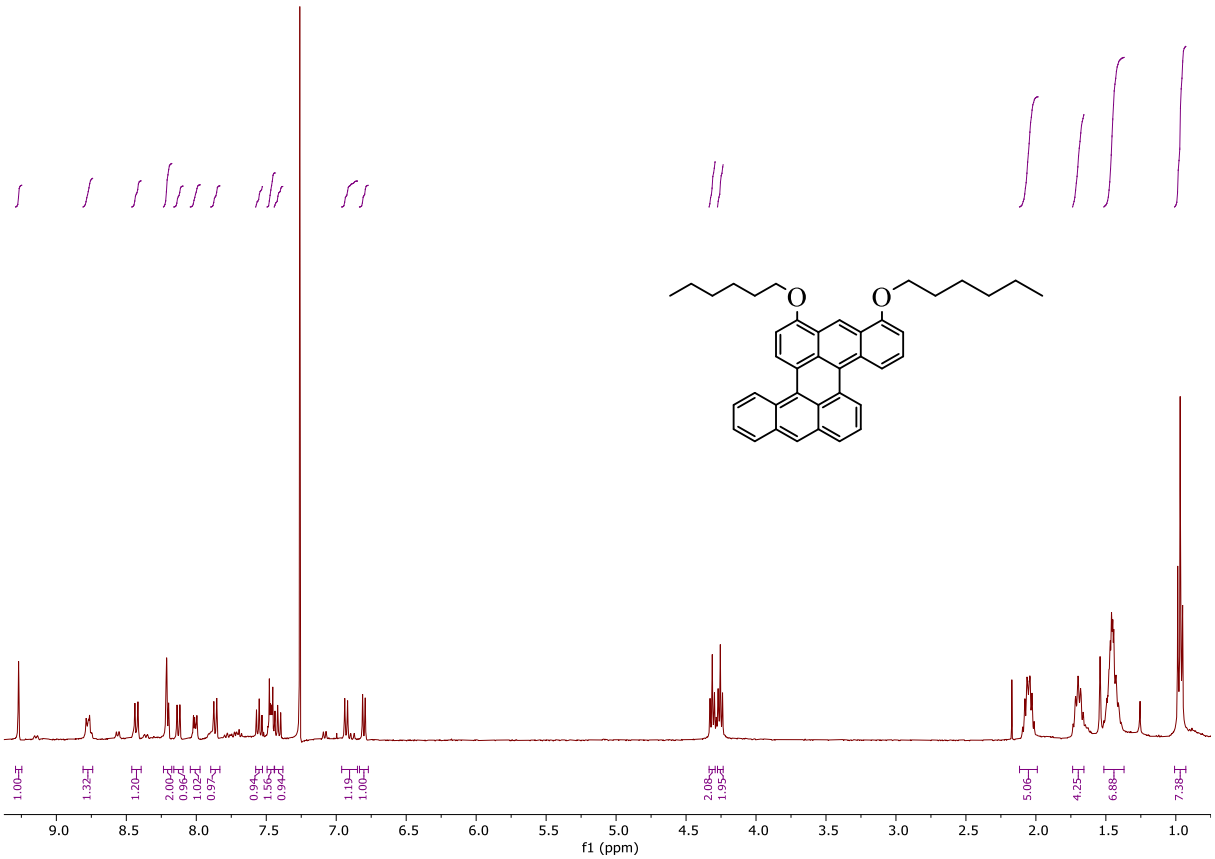

Figure 0.45: ^{1}H NMR spectrum of compound **88**.

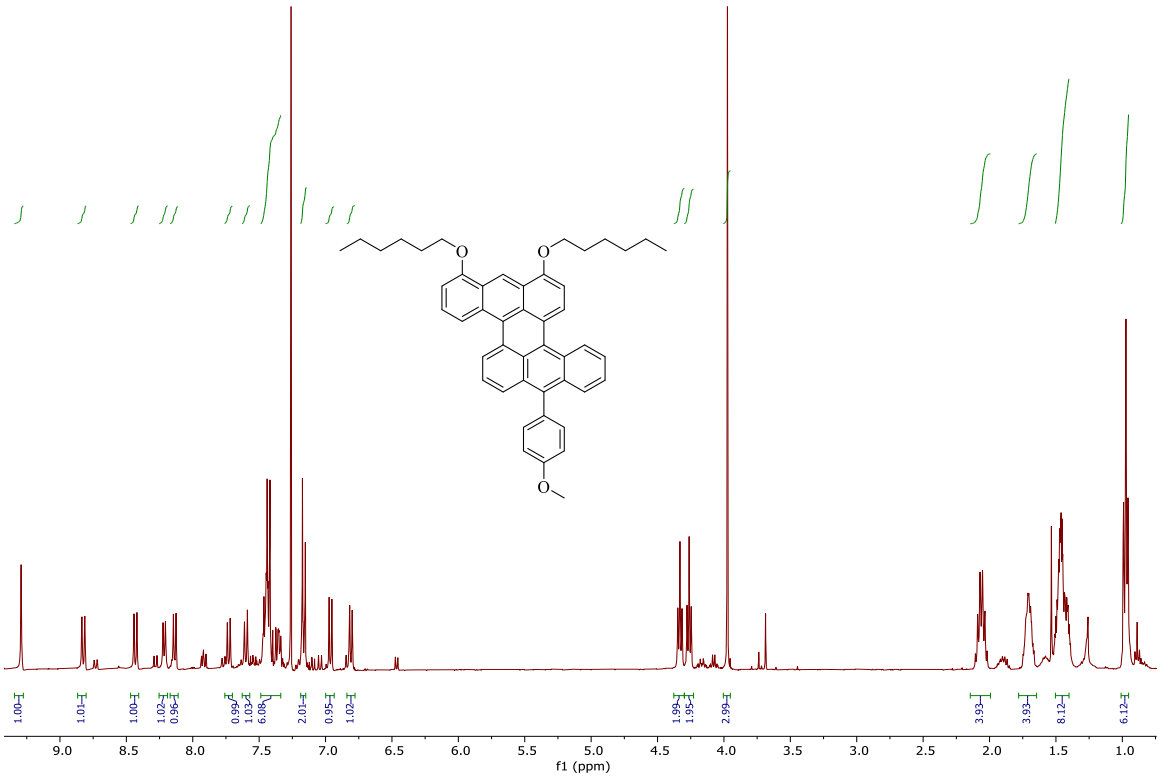

Figure 0.46: ^{1}H NMR spectrum of compound **89**.

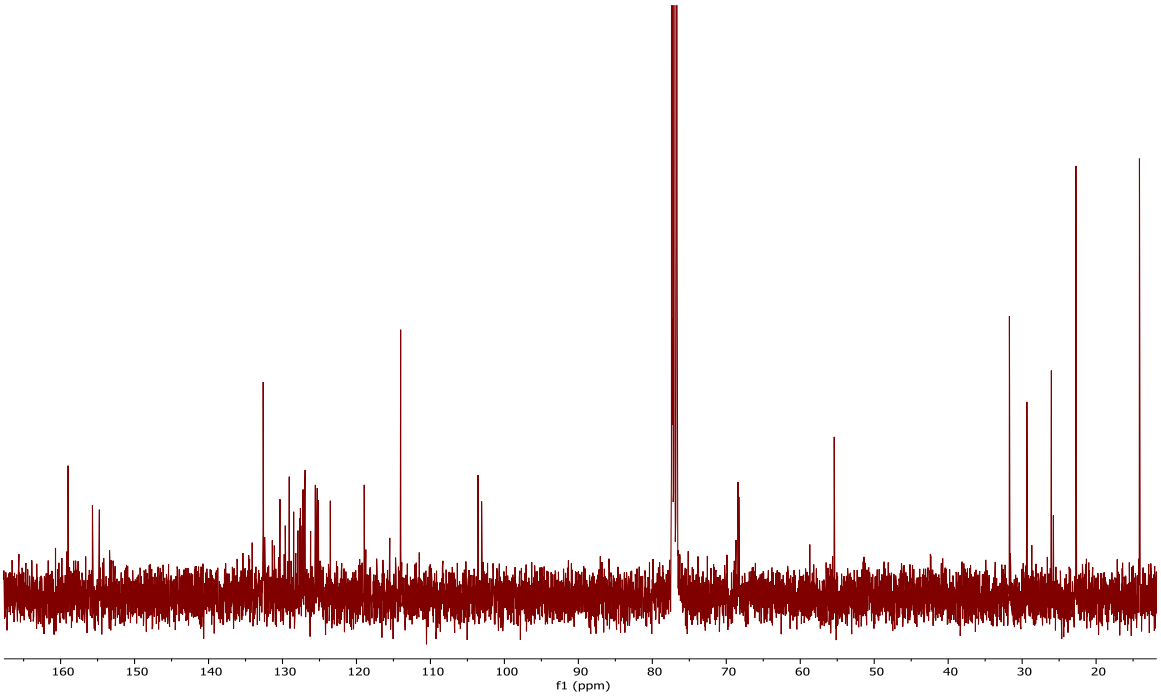

Figure 0.47: ^{13}C NMR spectrum of compound **89**.

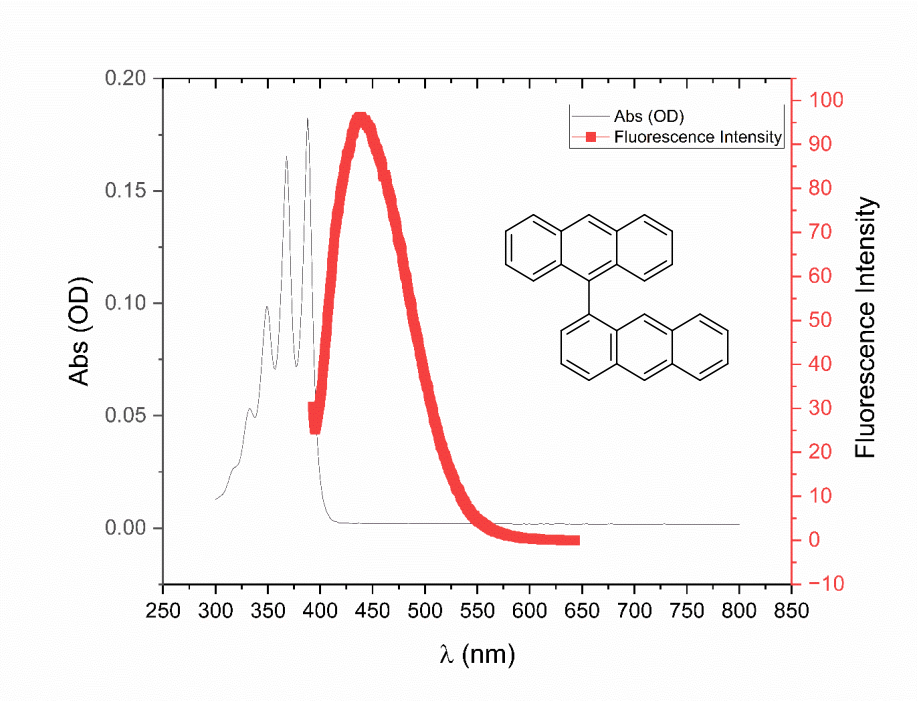

Figure 0.48: Absorption and emission spectrum of compound **61**.

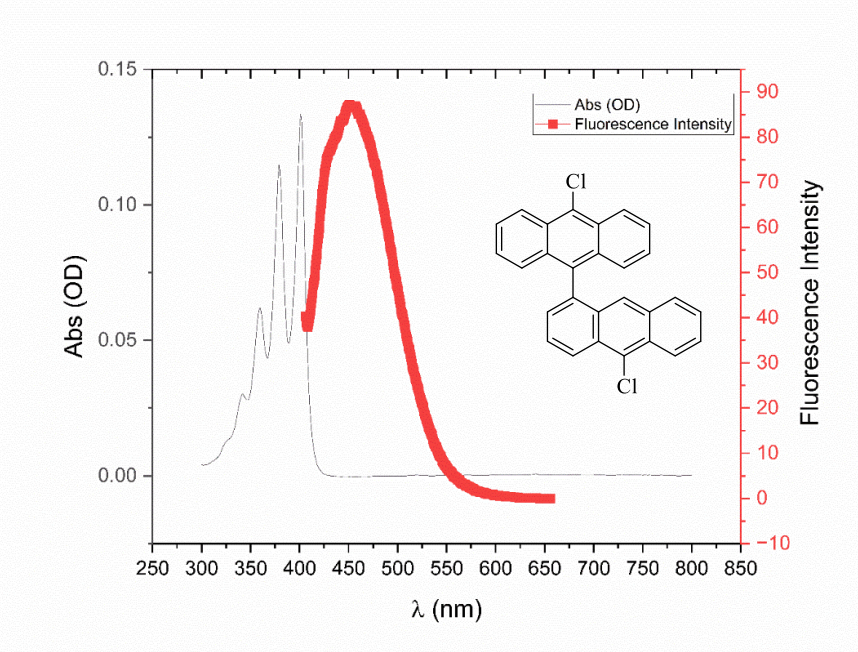

Figure 0.49: Absorption and emission spectrum of compound **78**.

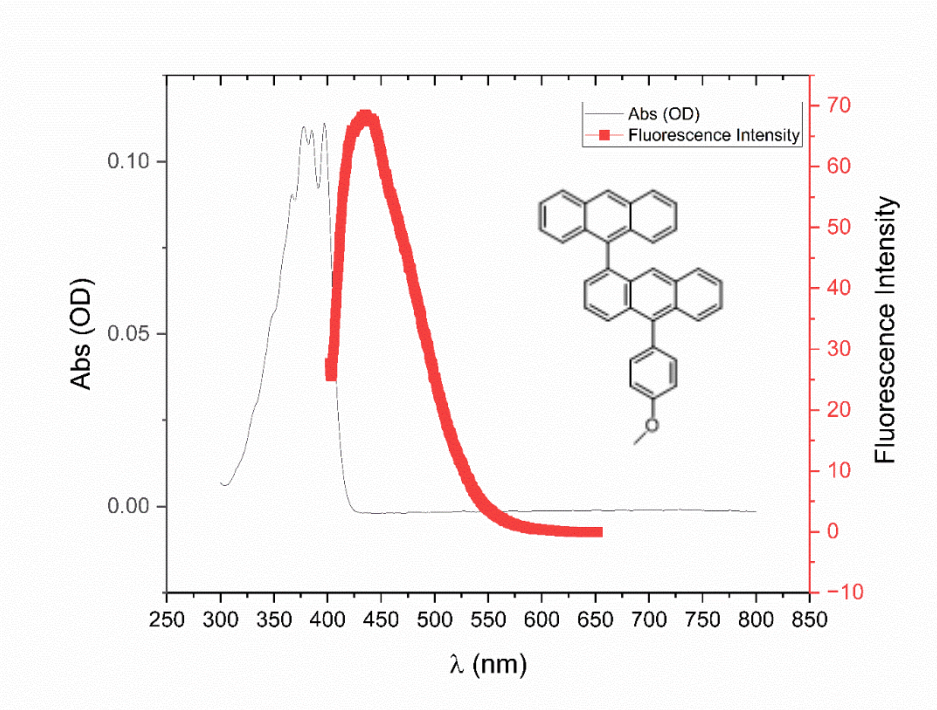

Figure 0.50: Absorption and emission spectrum of compound **87**.

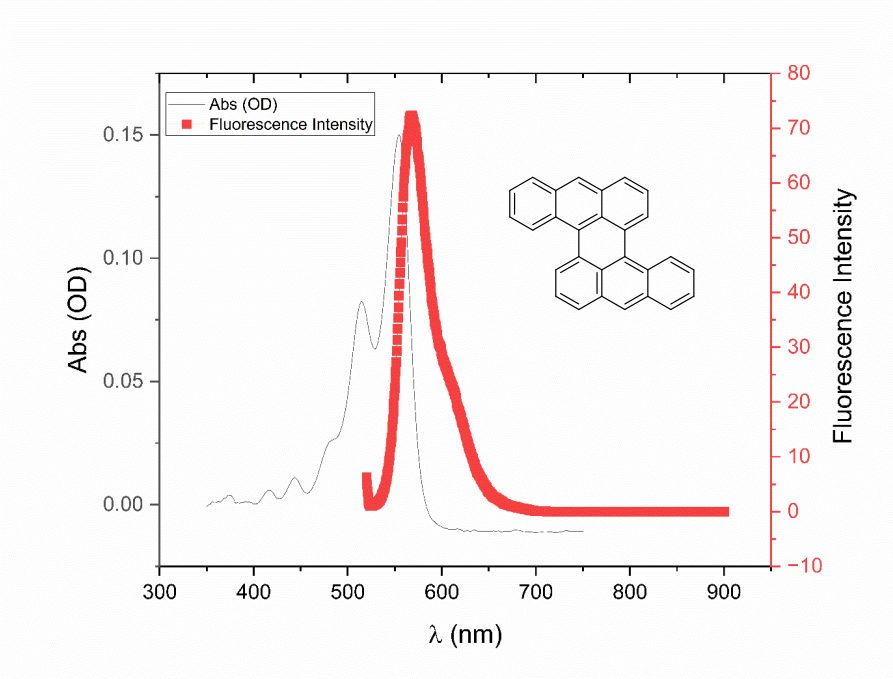

Figure 0.51: Absorption and emission spectrum of compound **77**.

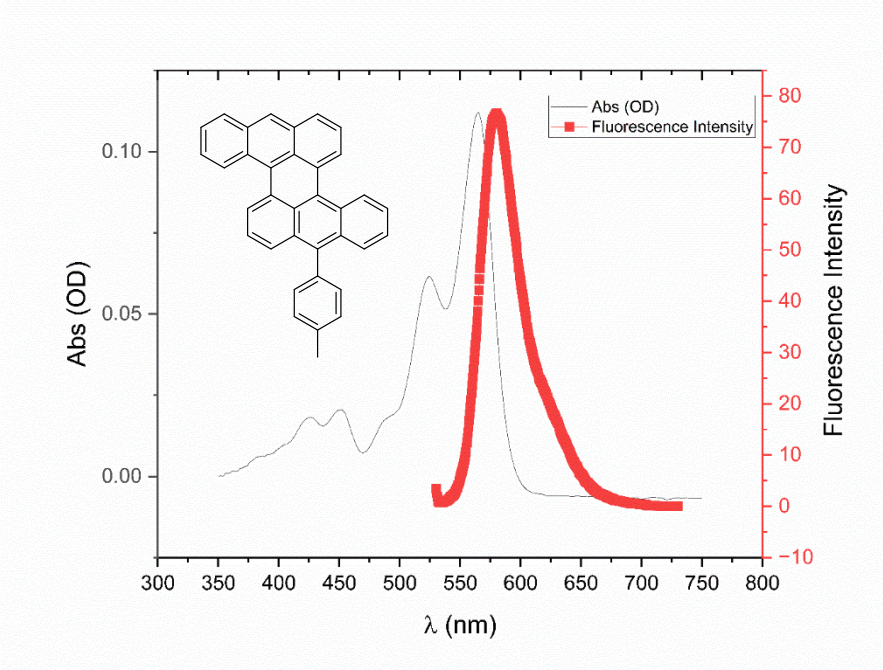

Figure 0.52: Absorption and emission spectrum of compound **85**.

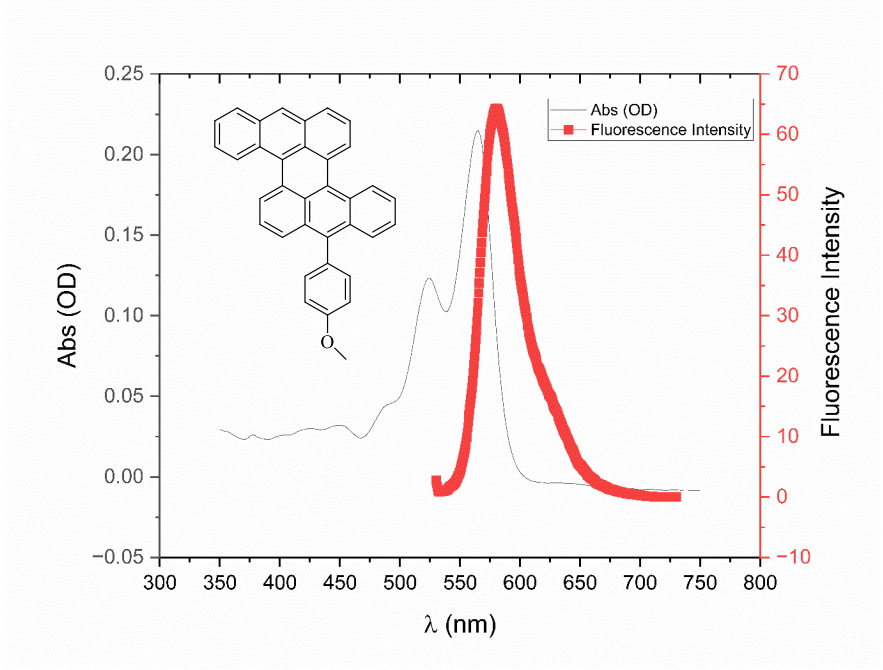

Figure 0.53: Absorption and emission spectrum of compound **86**.

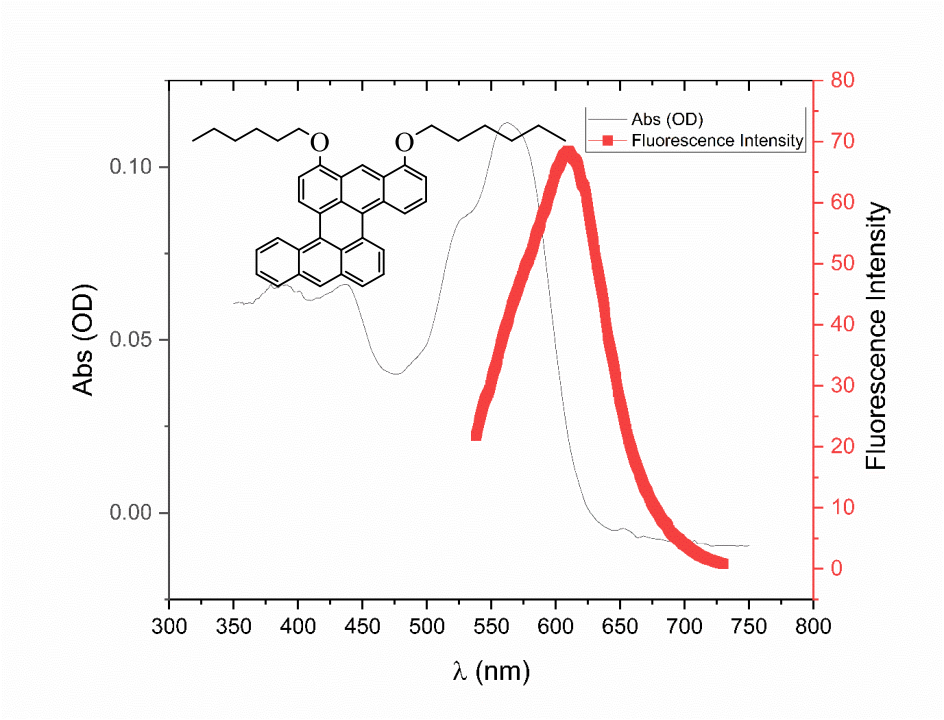

Figure 0.54: Absorption and emission spectrum of compound **88**.

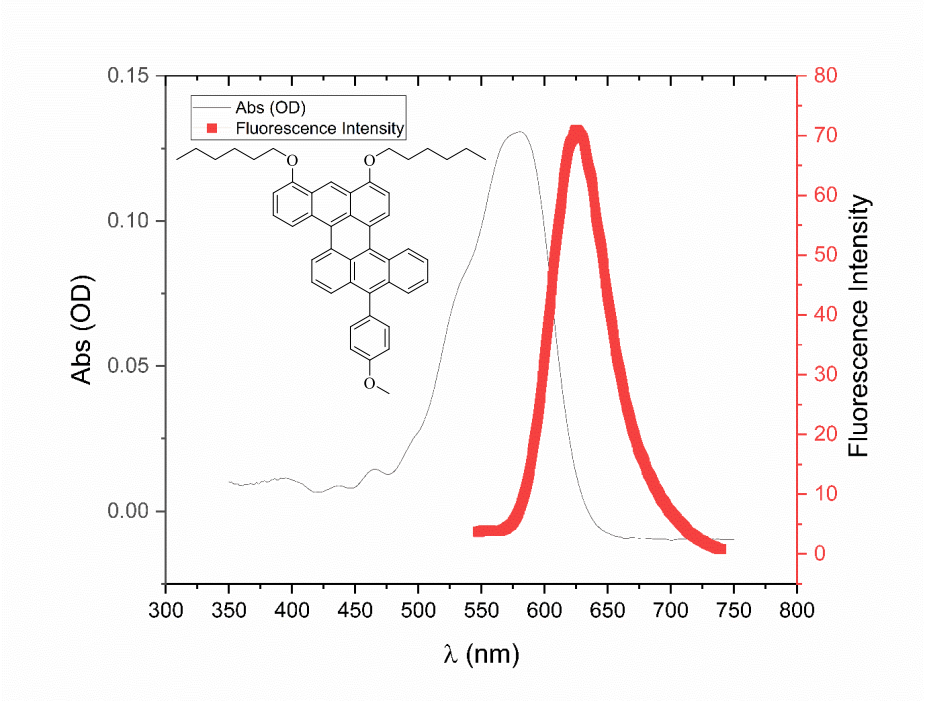

Figure 0.55: Absorption and emission spectrum of compound **89**.

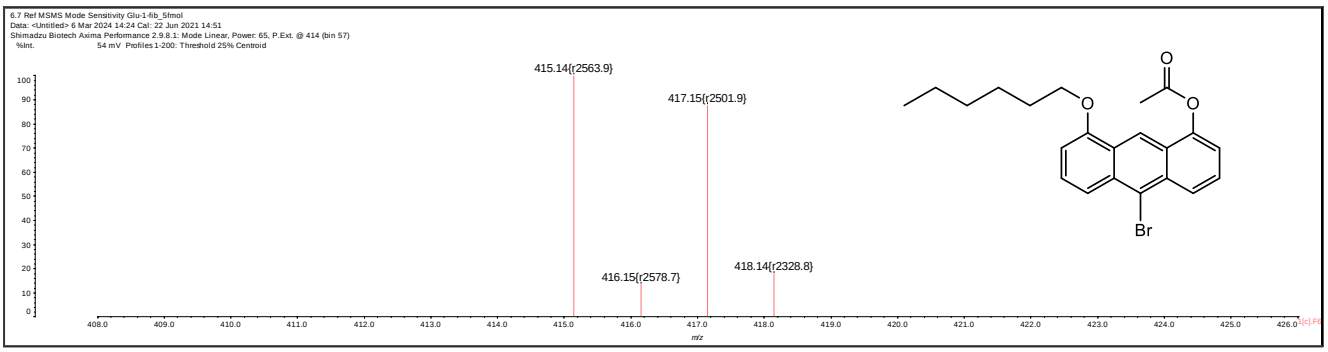

Figure 0.56: MALDI-TOF MS spectrum of **50**.

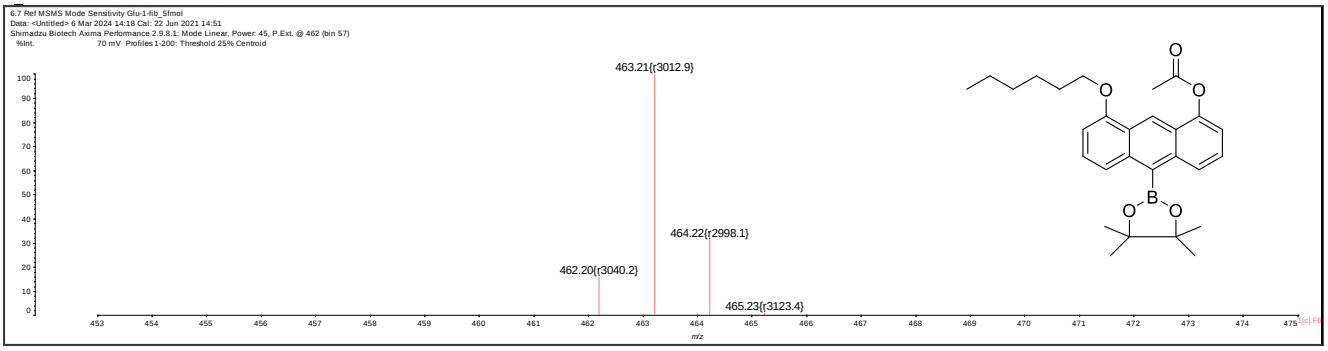

Figure 0.57: MALDI-TOF MS spectrum of **39**.

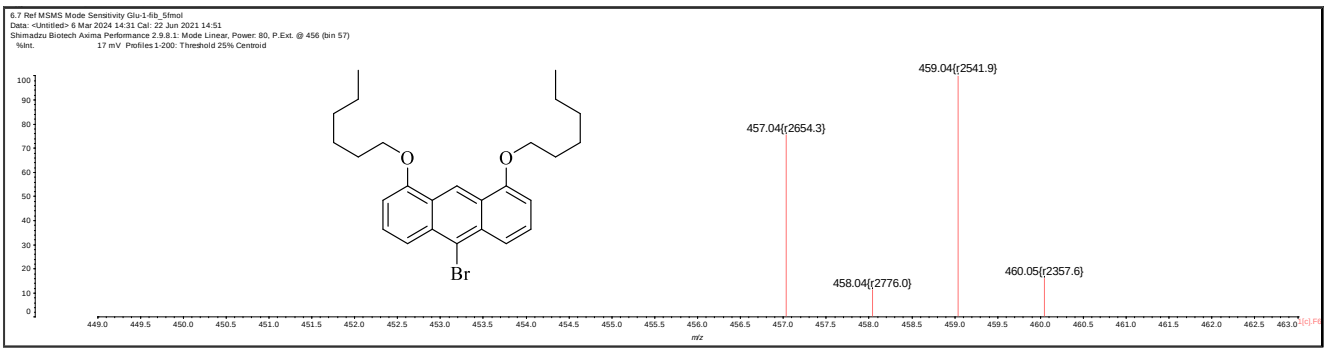

Figure 0.58: MALDI-TOF MS spectrum of **71**.

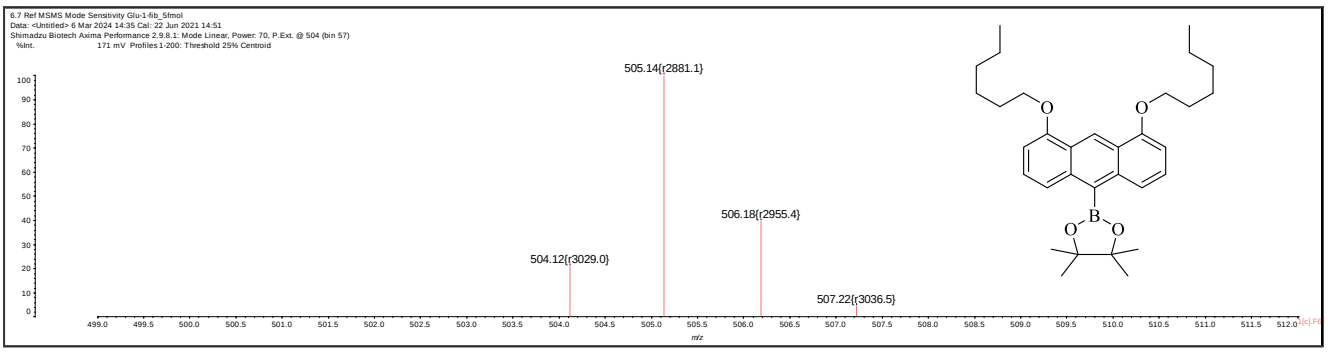

Figure 0.59: MALDI-TOF MS spectrum of **72**.

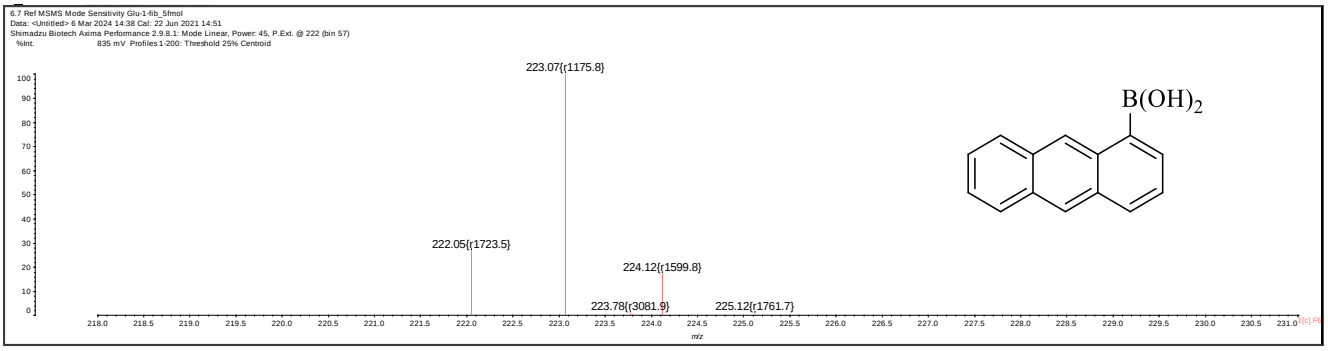

Figure 0.60: MALDI-TOF MS spectrum of **74**.

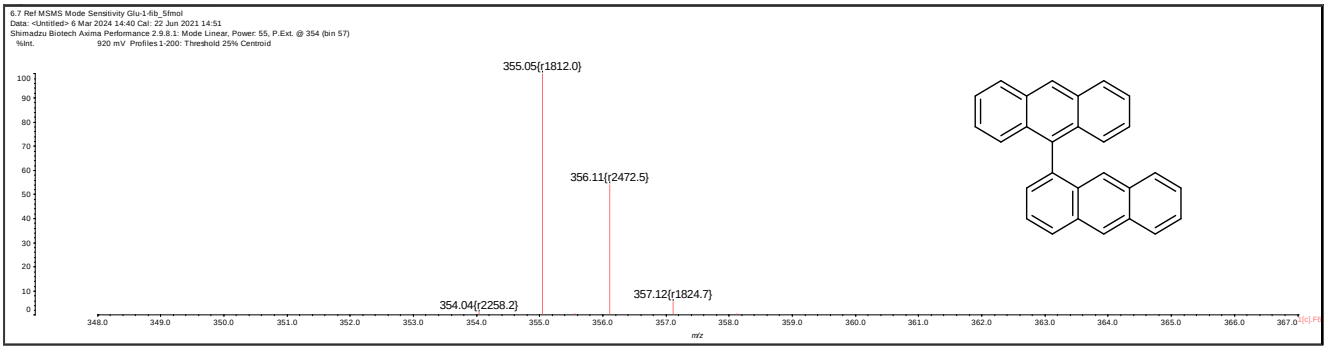

Figure 0.61: MALDI-TOF MS spectrum of **61**.

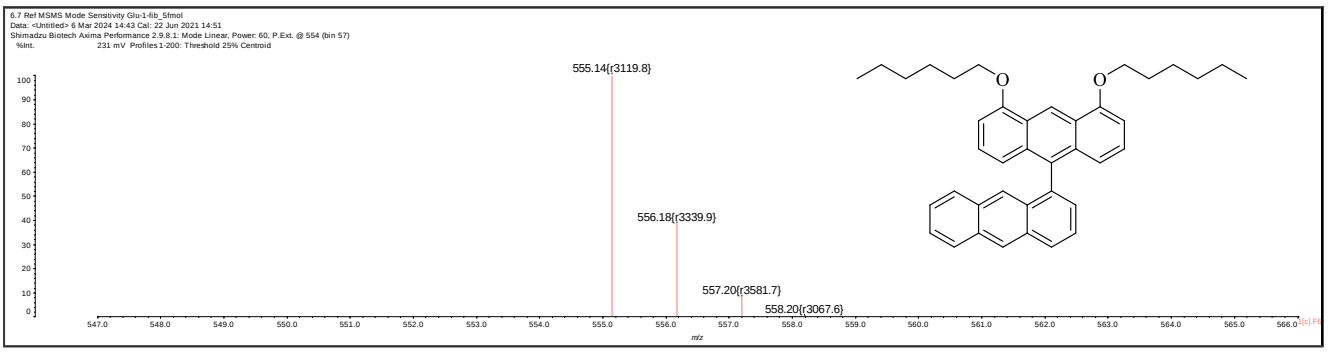

Figure 0.62: MALDI-TOF MS spectrum of **73**.

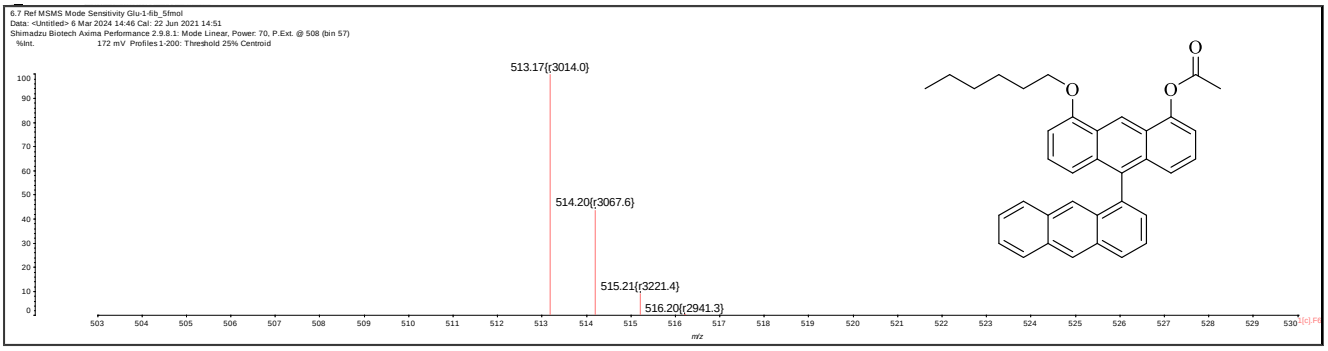

Figure 0.63: MALDI-TOF MS spectrum of **41**.

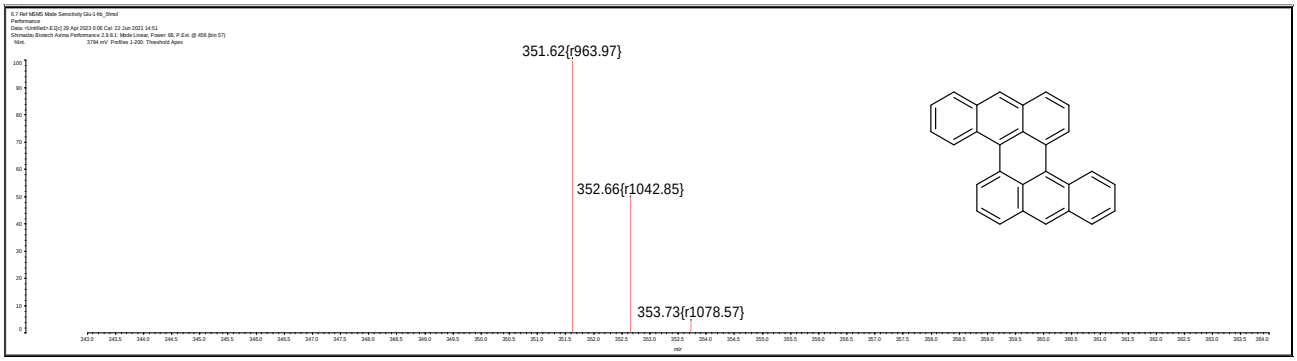

Figure 0.64: MALDI-TOF MS spectrum of **77**.

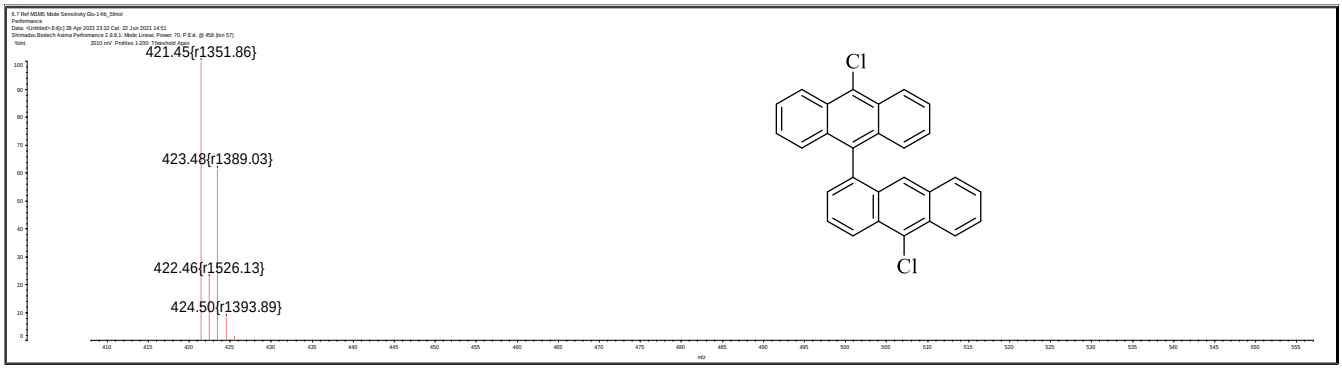

Figure 0.65: MALDI-TOF MS spectrum of **78**.

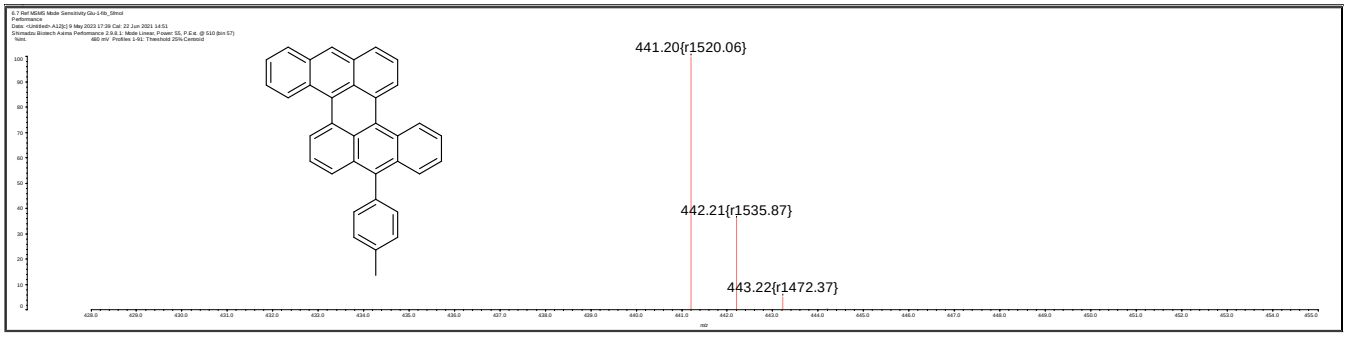

Figure 0.66: MALDI-TOF MS spectrum of **85**.

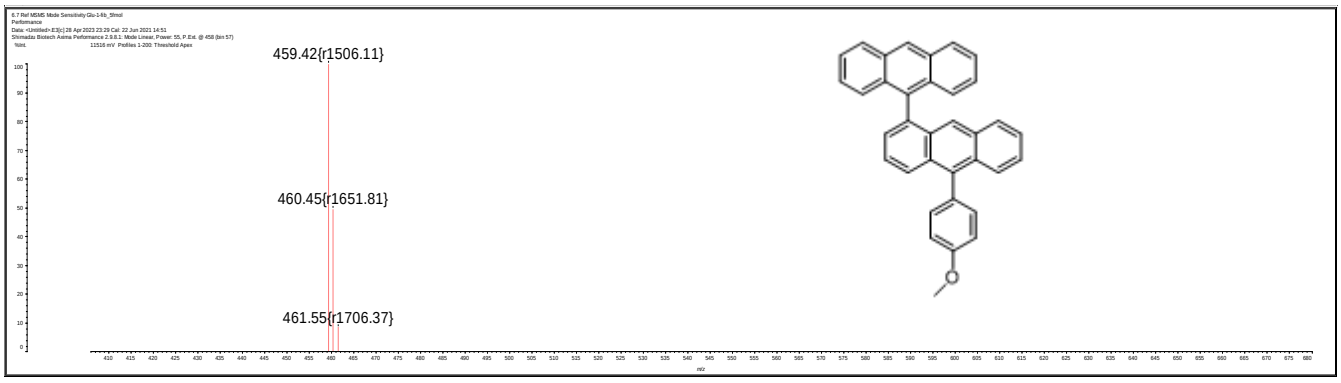

Figure 0.66**:** MALDI-TOF MS spectrum of **87**.

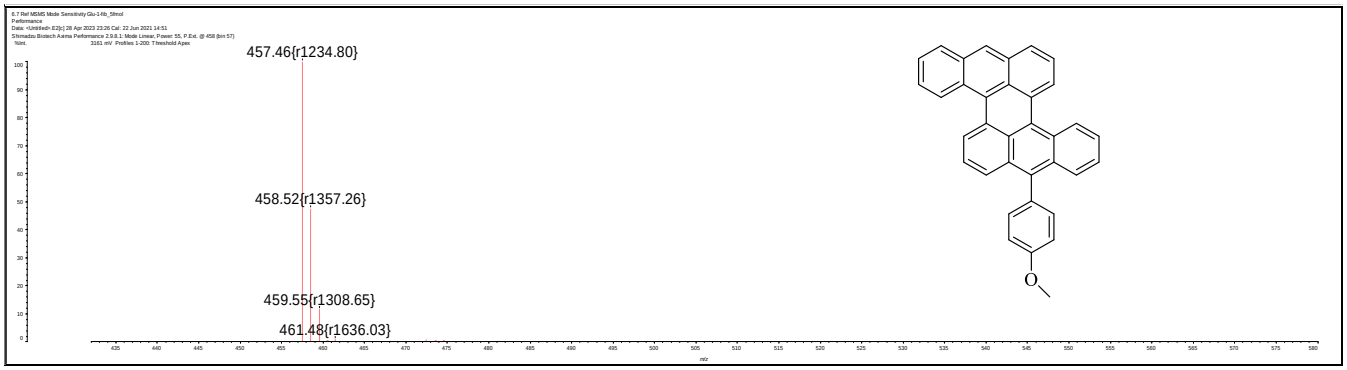

Figure 0.67**:** MALDI-TOF MS spectrum of **86**.

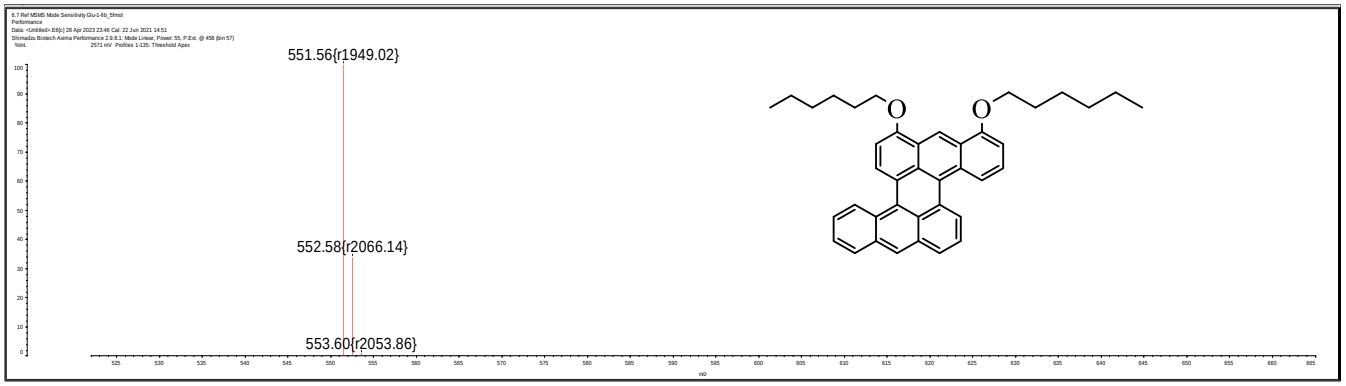

Figure 0.68**:** MALDI-TOF MS spectrum of **88**.

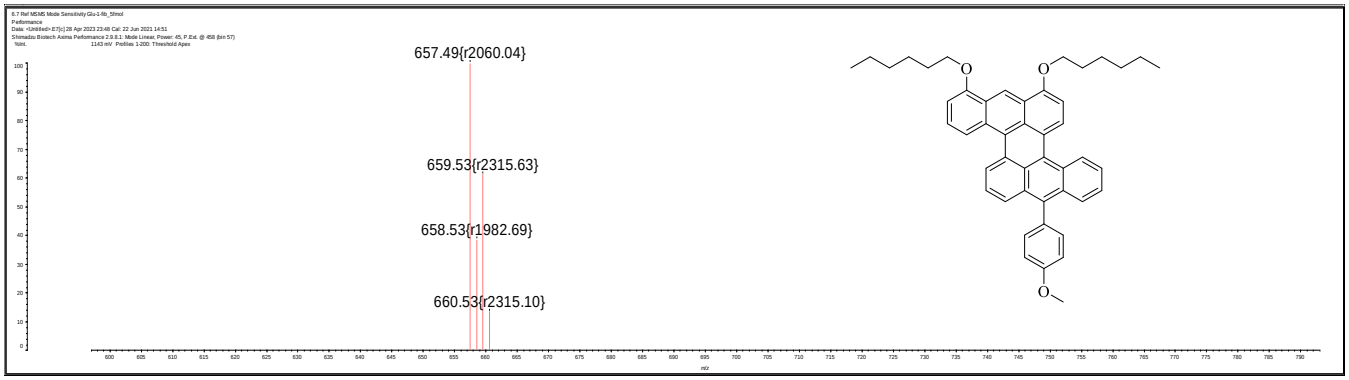

Figure 0.70: MALDI-TOF MS spectrum of **89**.

Crystal data and structure refinement for bis-anthracene (**61**)

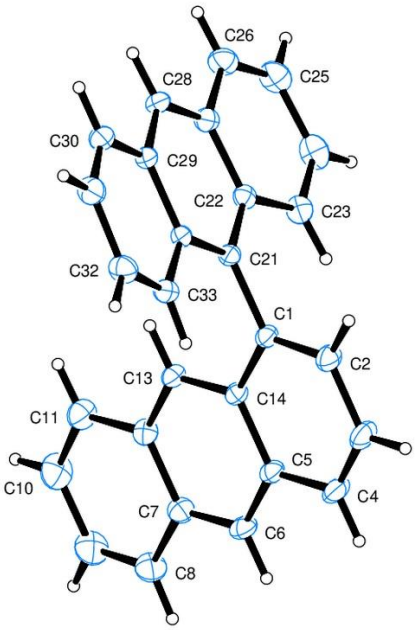

Identification code	isabf1170
Elemental formula	C28 H18
Formula weight	354.42
Crystal system, space group	Orthorhombic, $P2_12_12_1$ (no. 19)
Unit cell dimensions	a = 7.23695(12) Å α = 90 ° b = 8.40965(15) Å β = 90 ° c = 31.3804(5) Å γ = 90 °
Volume	1909.84(6) $Å^3$
Z, Calculated density	4, 1.233 Mg/m^3
F(000)	744
Absorption coefficient	0.530 mm^{-1}
Temperature	295(2) K
Wavelength	1.54184 Å
Crystal colour, shape	yellow block
Crystal size	0.18 x 0.15 x 0.08 mm

Crystal mounting: on a small loop, in oil, fixed in cold N_2 stream

On the diffractometer:

Theta range for data collection	7.723 to 69.947 °
Limiting indices	-4<=h<=8, -10<=k<=10, -38<=l<=32

Completeness to theta = 67.684	99.2 %
Absorption correction	Semi-empirical from equivalents
Max. and min. transmission	1.00000 and 0.57032
Reflections collected (not including absences)	7367
No. of unique reflections	3276 [R(int) for equivalents = 0.039]
No. of 'observed' reflections ($I > 2\sigma_I$)	3032
Structure determined by:	dual methods, in SHELXT
Refinement:	Full-matrix least-squares on F^2, in SHELXL
Data / restraints / parameters	3276 / 0 / 253
Goodness-of-fit on F^2	1.078
Final R indices ('observed' data)	R_1 = 0.040, wR_2 = 0.094
Final R indices (all data)	R_1 = 0.043, wR_2 = 0.097
Reflections weighted: $w = [\sigma^2(Fo^2)+(0.0429P)^2+0.1248P]^{-1}$ where $P=(Fo^2+2Fc^2)/3$	
Absolute structure parameter	0.2(10)
Extinction coefficient	n/a
Largest diff. peak and hole	0.12 and -0.20 e.Å^{-3}
Location of largest difference peak	near H(2)

Table 1. Atomic coordinates (x 10^4) and equivalent isotropic displacement parameters ($Å^2$ x 10^4). U(eq) is defined as one third of the trace of the orthogonalized Uij tensor. E.s.ds are in parentheses.

	x	y	z	U(eq)
C(1)	5559(3)	4396(3)	3914.9(6)	378(4)
C(2)	3927(3)	4636(3)	4122.3(7)	516(6)
C(3)	2463(3)	5511(4)	3935.6(8)	598(7)
C(4)	2643(3)	6125(3)	3542.8(8)	554(6)
C(5)	4301(3)	5906(3)	3303.1(7)	419(5)
C(6)	4510(3)	6527(3)	2896.0(7)	483(5)
C(7)	6118(3)	6325(3)	2661.6(6)	478(5)
C(8)	6350(4)	6966(4)	2243.9(7)	641(7)
C(9)	7907(5)	6718(4)	2022.0(8)	763(9)
C(10)	9379(4)	5845(4)	2199.6(8)	747(9)
C(11)	9255(4)	5222(4)	2600.7(7)	598(7)
C(12)	7613(3)	5441(3)	2846.7(6)	436(5)
C(13)	7418(3)	4826(3)	3256.9(6)	395(4)
C(14)	5793(3)	5028(2)	3491.7(6)	358(4)
C(21)	7104(3)	3514(3)	4127.7(6)	357(4)
C(22)	7533(3)	1954(3)	3999.7(6)	390(5)
C(23)	6464(4)	1110(3)	3695.0(7)	503(6)
C(24)	6883(4)	-410(3)	3582.8(8)	643(7)
C(25)	8414(4)	-1195(3)	3767.4(9)	658(7)
C(26)	9464(4)	-452(3)	4059.0(8)	582(6)
C(27)	9058(3)	1137(3)	4193.9(6)	434(5)
C(28)	10039(3)	1871(3)	4518.1(7)	441(5)
C(29)	9563(3)	3368(3)	4666.0(6)	390(4)
C(30)	10469(3)	4076(3)	5019.4(7)	505(6)
C(31)	9989(4)	5519(3)	5167.9(8)	575(6)
C(32)	8583(4)	6402(3)	4960.9(8)	565(6)
C(33)	7681(3)	5786(3)	4619.4(7)	452(5)
C(34)	8084(3)	4235(2)	4463.2(6)	351(4)

Table 2. Molecular dimensions. Bond lengths are in Ångstroms, angles in degrees. E.s.ds are in parentheses.

C(1)-C(2)	1.363(3)	C(21)-C(22)	1.407(3)
C(1)-C(14)	1.440(3)	C(21)-C(34)	1.407(3)
C(1)-C(21)	1.499(3)	C(22)-C(23)	1.420(3)
C(2)-C(3)	1.417(3)	C(22)-C(27)	1.436(3)
C(3)-C(4)	1.343(3)	C(23)-C(24)	1.361(4)
C(4)-C(5)	1.428(3)	C(24)-C(25)	1.414(4)
C(5)-C(6)	1.388(3)	C(25)-C(26)	1.343(4)
C(5)-C(14)	1.436(3)	C(26)-C(27)	1.432(3)
C(6)-C(7)	1.387(3)	C(27)-C(28)	1.386(3)
C(7)-C(8)	1.427(3)	C(28)-C(29)	1.385(3)
C(7)-C(12)	1.435(3)	C(29)-C(30)	1.419(3)
C(8)-C(9)	1.341(4)	C(29)-C(34)	1.443(3)
C(9)-C(10)	1.409(5)	C(30)-C(31)	1.345(4)
C(10)-C(11)	1.367(4)	C(31)-C(32)	1.417(4)
C(11)-C(12)	1.429(3)	C(32)-C(33)	1.357(3)
C(12)-C(13)	1.394(3)	C(33)-C(34)	1.424(3)
C(13)-C(14)	1.398(3)		

C(2)-C(1)-C(14)	119.17(18)		
C(2)-C(1)-C(21)	120.43(18)	C(22)-C(21)-C(34)	120.27(18)
C(14)-C(1)-C(21)	120.39(16)	C(22)-C(21)-C(1)	119.98(17)
C(1)-C(2)-C(3)	121.8(2)	C(34)-C(21)-C(1)	119.73(18)
C(4)-C(3)-C(2)	120.5(2)	C(21)-C(22)-C(23)	122.51(19)
C(3)-C(4)-C(5)	121.0(2)	C(21)-C(22)-C(27)	119.67(18)
C(6)-C(5)-C(4)	121.84(19)	C(23)-C(22)-C(27)	117.8(2)
C(6)-C(5)-C(14)	119.39(19)	C(24)-C(23)-C(22)	121.5(2)
C(4)-C(5)-C(14)	118.77(19)	C(23)-C(24)-C(25)	120.5(2)
C(7)-C(6)-C(5)	122.21(19)	C(26)-C(25)-C(24)	120.4(2)
C(6)-C(7)-C(8)	122.6(2)	C(25)-C(26)-C(27)	121.2(2)
C(6)-C(7)-C(12)	118.78(18)	C(28)-C(27)-C(26)	121.9(2)
C(8)-C(7)-C(12)	118.6(2)	C(28)-C(27)-C(22)	119.5(2)
C(9)-C(8)-C(7)	121.1(3)	C(26)-C(27)-C(22)	118.6(2)
C(8)-C(9)-C(10)	120.7(2)	C(29)-C(28)-C(27)	121.58(19)
C(11)-C(10)-C(9)	121.0(3)	C(28)-C(29)-C(30)	121.9(2)
C(10)-C(11)-C(12)	120.2(3)	C(28)-C(29)-C(34)	119.72(19)
C(13)-C(12)-C(11)	122.4(2)	C(30)-C(29)-C(34)	118.4(2)
C(13)-C(12)-C(7)	119.28(19)	C(31)-C(30)-C(29)	122.0(2)
C(11)-C(12)-C(7)	118.4(2)	C(30)-C(31)-C(32)	119.9(2)
C(12)-C(13)-C(14)	121.78(18)	C(33)-C(32)-C(31)	120.5(2)
C(13)-C(14)-C(5)	118.55(17)	C(32)-C(33)-C(34)	121.5(2)
C(13)-C(14)-C(1)	122.68(18)	C(21)-C(34)-C(33)	123.28(18)
C(5)-C(14)-C(1)	118.77(17)	C(21)-C(34)-C(29)	119.10(18)
		C(33)-C(34)-C(29)	117.61(18)

Table 3. Anisotropic displacement parameters ($Å^2$ x 10^4) for the expression:

$$\exp\{-2\pi^2(h^2a^{*2}U_{11} + \ldots + 2hka^*b^*U_{12})\}$$

E.s.ds are in parentheses.

	U_{11}	U_{22}	U_{33}	U_{23}	U_{13}	U_{12}
C(1)	323(9)	437(11)	375(9)	21(9)	-36(8)	9(9)
C(2)	398(11)	683(15)	468(11)	99(11)	47(9)	36(11)
C(3)	333(11)	827(18)	635(14)	94(14)	68(10)	125(12)
C(4)	350(10)	697(16)	614(13)	70(13)	-53(10)	126(11)
C(5)	370(10)	458(11)	428(10)	2(9)	-95(8)	28(9)
C(6)	456(11)	541(13)	451(11)	39(11)	-151(9)	59(11)
C(7)	528(12)	532(13)	374(10)	28(10)	-106(9)	-40(11)
C(8)	730(16)	778(18)	415(12)	120(13)	-101(12)	-46(16)
C(9)	870(20)	1020(20)	400(12)	162(15)	-20(13)	-110(20)
C(10)	726(18)	1030(20)	488(13)	26(15)	197(13)	-44(18)
C(11)	546(14)	757(17)	490(13)	15(12)	81(11)	44(13)
C(12)	442(11)	501(12)	366(10)	-34(9)	-8(9)	-27(11)
C(13)	349(9)	456(11)	379(10)	10(9)	-47(8)	33(9)
C(14)	337(9)	390(10)	347(9)	-14(8)	-49(7)	3(8)
C(21)	338(9)	411(10)	321(9)	62(8)	5(7)	3(9)
C(22)	398(10)	436(11)	336(9)	27(9)	48(8)	-17(10)
C(23)	536(13)	542(14)	430(11)	-25(10)	-9(10)	-49(11)
C(24)	788(18)	595(16)	546(14)	-159(12)	49(13)	-148(15)
C(25)	773(18)	487(14)	715(16)	-112(13)	148(14)	42(14)
C(26)	618(14)	457(13)	672(15)	-17(12)	102(12)	115(12)
C(27)	423(11)	439(11)	440(10)	35(10)	69(9)	42(9)
C(28)	359(10)	459(12)	504(12)	97(10)	-26(9)	77(9)
C(29)	337(9)	429(11)	404(10)	85(9)	-23(8)	-9(9)
C(30)	473(12)	521(13)	520(12)	87(11)	-160(10)	-47(11)
C(31)	651(15)	550(14)	523(13)	12(12)	-207(12)	-133(13)
C(32)	674(15)	420(12)	601(13)	-57(11)	-71(12)	-41(12)
C(33)	463(11)	402(11)	489(11)	38(9)	-41(10)	6(10)
C(34)	325(9)	372(10)	356(9)	61(8)	17(8)	-17(8)

Table 4. Hydrogen coordinates (x 10^4) and isotropic displacement parameters (Å^2 x 10^3). All hydrogen atoms were included in idealised positions with U(iso)'s set at 1.2*U(eq) of the parent carbon atoms.

	x	y	z	U(iso)
H(2)	3770	4213	4394	62
H(3)	1370	5661	4086	72
H(4)	1672	6702	3425	66
H(6)	3539	7097	2776	58
H(8)	5404	7566	2124	77
H(9)	8017	7127	1748	92
H(10)	10452	5691	2042	90
H(11)	10242	4653	2714	72
H(13)	8395	4266	3378	47
H(23)	5455	1609	3569	60
H(24)	6156	-937	3383	77
H(25)	8696	-2230	3686	79
H(26)	10474	-980	4175	70
H(28)	11040	1346	4639	53
H(30)	11423	3527	5152	61
H(31)	10579	5937	5406	69
H(32)	8276	7410	5060	68
H(33)	6779	6392	4484	54

Table 5. Torsion angles, in degrees. E.s.ds are in parentheses.

C(14)-C(1)-C(2)-C(3)	-1.0(4)		
C(21)-C(1)-C(2)-C(3)	177.8(2)	C(14)-C(1)-C(21)-C(34)	107.1(2)
C(1)-C(2)-C(3)-C(4)	0.5(4)	C(34)-C(21)-C(22)-C(23)	173.15(18)
C(2)-C(3)-C(4)-C(5)	0.4(4)	C(1)-C(21)-C(22)-C(23)	-5.1(3)
C(3)-C(4)-C(5)-C(6)	179.8(2)	C(34)-C(21)-C(22)-C(27)	-4.1(3)
C(3)-C(4)-C(5)-C(14)	-0.7(4)	C(1)-C(21)-C(22)-C(27)	177.70(17)
C(4)-C(5)-C(6)-C(7)	179.7(2)	C(21)-C(22)-C(23)-C(24)	-178.6(2)
C(14)-C(5)-C(6)-C(7)	0.2(3)	C(27)-C(22)-C(23)-C(24)	-1.3(3)
C(5)-C(6)-C(7)-C(8)	-179.6(2)	C(22)-C(23)-C(24)-C(25)	-0.3(4)
C(5)-C(6)-C(7)-C(12)	0.1(3)	C(23)-C(24)-C(25)-C(26)	0.6(4)
C(6)-C(7)-C(8)-C(9)	-178.5(3)	C(24)-C(25)-C(26)-C(27)	0.6(4)
C(12)-C(7)-C(8)-C(9)	1.8(4)	C(25)-C(26)-C(27)-C(28)	174.8(2)
C(7)-C(8)-C(9)-C(10)	-1.4(5)	C(25)-C(26)-C(27)-C(22)	-2.2(3)
C(8)-C(9)-C(10)-C(11)	0.4(5)	C(21)-C(22)-C(27)-C(28)	2.7(3)
C(9)-C(10)-C(11)-C(12)	0.3(5)	C(23)-C(22)-C(27)-C(28)	-174.63(19)
C(10)-C(11)-C(12)-C(13)	179.9(3)	C(21)-C(22)-C(27)-C(26)	179.81(19)
C(10)-C(11)-C(12)-C(7)	0.0(4)	C(23)-C(22)-C(27)-C(26)	2.4(3)
C(6)-C(7)-C(12)-C(13)	-0.7(3)	C(26)-C(27)-C(28)-C(29)	-175.7(2)
C(8)-C(7)-C(12)-C(13)	179.1(2)	C(22)-C(27)-C(28)-C(29)	1.2(3)
C(6)-C(7)-C(12)-C(11)	179.2(2)	C(27)-C(28)-C(29)-C(30)	175.0(2)
C(8)-C(7)-C(12)-C(11)	-1.0(3)	C(27)-C(28)-C(29)-C(34)	-3.8(3)
C(11)-C(12)-C(13)-C(14)	-179.0(2)	C(28)-C(29)-C(30)-C(31)	-178.9(2)
C(7)-C(12)-C(13)-C(14)	0.9(3)	C(34)-C(29)-C(30)-C(31)	-0.1(3)
C(12)-C(13)-C(14)-C(5)	-0.5(3)	C(29)-C(30)-C(31)-C(32)	-2.2(4)
C(12)-C(13)-C(14)-C(1)	179.7(2)	C(30)-C(31)-C(32)-C(33)	1.6(4)
C(6)-C(5)-C(14)-C(13)	-0.1(3)	C(31)-C(32)-C(33)-C(34)	1.3(4)
C(4)-C(5)-C(14)-C(13)	-179.6(2)	C(22)-C(21)-C(34)-C(33)	-177.70(18)
C(6)-C(5)-C(14)-C(1)	179.8(2)	C(1)-C(21)-C(34)-C(33)	0.5(3)
C(4)-C(5)-C(14)-C(1)	0.3(3)	C(22)-C(21)-C(34)-C(29)	1.6(3)
C(2)-C(1)-C(14)-C(13)	-179.6(2)	C(1)-C(21)-C(34)-C(29)	179.78(17)
C(21)-C(1)-C(14)-C(13)	1.6(3)	C(32)-C(33)-C(34)-C(21)	175.8(2)
C(2)-C(1)-C(14)-C(5)	0.6(3)	C(32)-C(33)-C(34)-C(29)	-3.4(3)
C(21)-C(1)-C(14)-C(5)	-178.25(19)	C(28)-C(29)-C(34)-C(21)	2.4(3)
C(2)-C(1)-C(21)-C(22)	106.5(2)	C(30)-C(29)-C(34)-C(21)	-176.49(18)
C(14)-C(1)-C(21)-C(22)	-74.7(3)	C(28)-C(29)-C(34)-C(33)	-178.34(19)
C(2)-C(1)-C(21)-C(34)	-71.7(3)	C(30)-C(29)-C(34)-C(33)	2.8(3)

Crystal data and structure refinement for Cl-$C_{14}H_8$-$C_{14}H_8$-Cl (**78**)

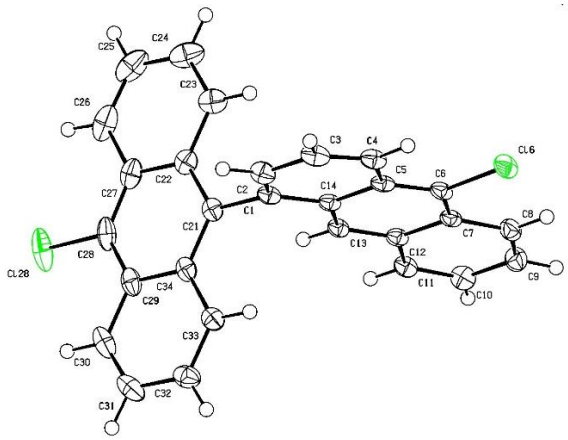

Identification code	isabf1341
Elemental formula	C28 H16 Cl2
Formula weight	423.31
Crystal system, space group	Monoclinic, C 2/c (no. 15)
Unit cell dimensions	a = 31.8679(4) Å α = 90 ° b = 9.02744(12) Å β = 90.2226(10) ° c = 13.5896(2) Å γ = 90 °
Volume	3909.48(9) $Å^3$
Z, Calculated density	8, 1.438 Mg/m^3
F(000)	1744
Absorption coefficient	3.071 mm^{-1}
Temperature	99.90(18) K
Wavelength	1.54184 Å
Crystal colour, shape	pale yellow plate
Crystal size	0.12 x 0.08 x 0.02 mm
Crystal mounting:	on a small loop, in oil, fixed in cold N_2 stream
On the diffractometer:	
Theta range for data collection	8.278 to 72.487 °
Limiting indices	-34<=h<=39, -11<=k<=10, -15<=l<=16
Completeness to theta = 67.684	99.6 %
Absorption correction	Semi-empirical from equivalents
Max. and min. transmission	1.00000 and 0.79350

Reflections collected (not including absences) 14249

No. of unique reflections 3788 [R(int) for equivalents = 0.042]

No. of 'observed' reflections ($I > 2\sigma_I$) 3491

Structure determined by: dual methods, in SHELXT

Refinement: Full-matrix least-squares on F^2, in SHELXL

Data / restraints / parameters 3788 / 0 / 271

Goodness-of-fit on F^2 1.041

Final R indices ('observed' data) $R_1 = 0.035$, $wR_2 = 0.087$

Final R indices (all data) $R_1 = 0.037$, $wR_2 = 0.089$

Reflections weighted:
$w = [\sigma^2(Fo^2)+(0.0375P)^2+3.4554P]^{-1}$ where $P=(Fo^2+2Fc^2)/3$

Extinction coefficient n/a

Largest diff. peak and hole 0.21 and -0.44 e.$Å^{-3}$

Location of largest difference peak near Cl(28)

Table 1. Atomic coordinates (x 10^5) and equivalent isotropic displacement parameters ($Å^2$ x 10^4). U(eq) is defined as one third of the trace of the orthogonalized Uij tensor. E.s.ds are in parentheses.

	x	y	z	U(eq)
C(1)	62951(5)	57173(16)	65807(10)	212(3)
C(2)	61339(5)	64409(17)	73775(11)	260(3)
C(3)	63900(5)	73731(17)	79695(11)	270(3)
C(4)	68002(5)	75976(16)	77457(10)	238(3)
C(5)	69887(5)	68445(15)	69335(10)	201(3)
C(6)	74134(5)	69830(15)	66900(10)	206(3)
C(7)	76034(4)	61740(15)	59326(10)	198(3)
C(8)	80415(5)	62311(17)	57126(11)	244(3)
C(9)	82051(5)	53600(18)	49946(12)	276(3)
C(10)	79471(5)	44044(18)	44255(11)	272(3)
C(11)	75287(5)	43404(17)	45979(10)	227(3)
C(12)	73411(4)	52033(15)	53599(10)	193(3)
C(13)	69144(4)	50960(15)	55650(10)	191(3)
C(14)	67318(4)	58702(15)	63437(10)	190(3)
C(21)	60120(4)	48119(17)	59335(10)	215(3)
C(22)	58062(4)	55092(18)	51439(10)	242(3)
C(23)	58727(5)	70418(19)	49331(11)	301(4)
C(24)	56712(6)	77210(20)	41785(12)	386(4)
C(25)	53877(6)	69200(30)	35794(13)	438(5)
C(26)	53159(5)	54590(30)	37424(12)	386(4)
C(27)	55269(5)	46840(20)	45179(11)	287(4)
C(28)	54749(5)	31770(20)	47117(11)	307(4)
C(29)	56683(5)	24540(18)	55029(11)	267(3)
C(30)	55980(5)	9340(20)	57442(13)	340(4)
C(31)	58012(6)	2780(19)	65085(13)	353(4)
C(32)	60947(5)	10855(18)	70816(12)	299(3)
C(33)	61598(5)	25507(17)	69004(11)	247(3)
C(34)	59488(4)	32983(17)	61182(10)	222(3)
Cl(6)	77232(2)	81924(4)	73785(3)	271,6(11)
Cl(28)	51574(2)	21408(6)	39165(3)	483.0(16)

Table 2. Molecular dimensions. Bond lengths are in Ångstroms, angles in degrees. E.s.ds are in parentheses.

C(1)-C(2)	1.367(2)	C(21)-C(34)	1.404(2)
C(1)-C(14)	1.436(2)	C(21)-C(22)	1.404(2)
C(1)-C(21)	1.500(2)	C(22)-C(23)	1.429(2)
C(2)-C(3)	1.420(2)	C(22)-C(27)	1.437(2)
C(3)-C(4)	1.358(2)	C(23)-C(24)	1.355(2)
C(4)-C(5)	1.431(2)	C(24)-C(25)	1.413(3)
C(5)-C(6)	1.400(2)	C(25)-C(26)	1.357(3)
C(5)-C(14)	1.443(2)	C(26)-C(27)	1.431(2)
C(6)-C(7)	1.402(2)	C(27)-C(28)	1.396(3)
C(6)-Cl(6)	1.7421(14)	C(28)-C(29)	1.399(2)
C(7)-C(8)	1.430(2)	C(28)-Cl(28)	1.7486(16)
C(7)-C(12)	1.438(2)	C(29)-C(30)	1.429(2)
C(8)-C(9)	1.359(2)	C(29)-C(34)	1.440(2)
C(9)-C(10)	1.419(2)	C(30)-C(31)	1.358(3)
C(10)-C(11)	1.356(2)	C(31)-C(32)	1.417(2)
C(11)-C(12)	1.429(2)	C(32)-C(33)	1.361(2)
C(12)-C(13)	1.393(2)	C(33)-C(34)	1.426(2)
C(13)-C(14)	1.3970(19)		

C(2)-C(1)-C(14)	119.96(13)	C(34)-C(21)-C(22)	120.40(13)
C(2)-C(1)-C(21)	119.87(13)	C(34)-C(21)-C(1)	120.80(13)
C(14)-C(1)-C(21)	120.13(12)	C(22)-C(21)-C(1)	118.80(13)
C(1)-C(2)-C(3)	121.00(14)	C(21)-C(22)-C(23)	121.21(14)
C(4)-C(3)-C(2)	120.87(14)	C(21)-C(22)-C(27)	120.42(14)
C(3)-C(4)-C(5)	120.61(14)	C(23)-C(22)-C(27)	118.36(14)
C(6)-C(5)-C(4)	123.31(13)	C(24)-C(23)-C(22)	121.34(17)
C(6)-C(5)-C(14)	118.04(13)	C(23)-C(24)-C(25)	120.29(18)
C(4)-C(5)-C(14)	118.64(13)	C(26)-C(25)-C(24)	120.76(16)
C(5)-C(6)-C(7)	123.21(13)	C(25)-C(26)-C(27)	121.08(17)
C(5)-C(6)-Cl(6)	118.39(11)	C(28)-C(27)-C(26)	124.03(16)
C(7)-C(6)-Cl(6)	118.39(11)	C(28)-C(27)-C(22)	117.86(14)
C(6)-C(7)-C(8)	124.03(13)	C(26)-C(27)-C(22)	118.11(16)
C(6)-C(7)-C(12)	117.60(13)	C(27)-C(28)-C(29)	123.20(14)
C(8)-C(7)-C(12)	118.35(13)	C(27)-C(28)-Cl(28)	118.28(13)
C(9)-C(8)-C(7)	120.45(14)	C(29)-C(28)-Cl(28)	118.52(13)
C(8)-C(9)-C(10)	121.35(14)	C(28)-C(29)-C(30)	123.76(15)
C(11)-C(10)-C(9)	119.98(14)	C(28)-C(29)-C(34)	118.04(15)
C(10)-C(11)-C(12)	121.09(14)	C(30)-C(29)-C(34)	118.20(15)
C(13)-C(12)-C(11)	121.24(13)	C(31)-C(30)-C(29)	121.32(15)
C(13)-C(12)-C(7)	120.02(13)	C(30)-C(31)-C(32)	120.53(15)
C(11)-C(12)-C(7)	118.73(13)	C(33)-C(32)-C(31)	120.09(16)
C(12)-C(13)-C(14)	121.77(13)	C(32)-C(33)-C(34)	121.53(15)
C(13)-C(14)-C(1)	121.90(13)	C(21)-C(34)-C(33)	121.77(13)
C(13)-C(14)-C(5)	119.27(13)	C(21)-C(34)-C(29)	120.03(14)
C(1)-C(14)-C(5)	118.83(13)	C(33)-C(34)-C(29)	118.20(14)

Table 3. Anisotropic displacement parameters ($Å^2$ x 10^4) for the expression:

$$\exp\{-2\pi^2(h^2a^{*2}U_{11} + \ldots + 2hka^*b^*U_{12})\}$$

E.s.ds are in parentheses.

	U_{11}	U_{22}	U_{33}	U_{23}	U_{13}	U_{12}
C(1)	286(7)	168(7)	182(6)	27(5)	3(5)	-5(6)
C(2)	313(8)	234(8)	232(7)	6(6)	59(6)	-4(6)
C(3)	419(9)	208(7)	185(7)	-22(6)	47(6)	30(6)
C(4)	370(8)	174(7)	170(7)	-16(5)	-32(6)	5(6)
C(5)	311(8)	140(7)	151(6)	20(5)	-32(5)	14(5)
C(6)	301(8)	146(7)	171(7)	21(5)	-71(5)	-31(5)
C(7)	263(7)	149(7)	181(6)	35(5)	-38(5)	-12(5)
C(8)	268(7)	230(8)	235(7)	47(6)	-39(6)	-55(6)
C(9)	240(7)	291(8)	298(8)	36(6)	19(6)	-28(6)
C(10)	302(8)	267(8)	248(7)	-16(6)	51(6)	1(6)
C(11)	293(7)	199(7)	191(6)	-11(5)	1(5)	-17(6)
C(12)	260(7)	160(7)	158(6)	26(5)	-19(5)	-1(5)
C(13)	251(7)	159(7)	163(6)	1(5)	-22(5)	-11(5)
C(14)	265(7)	146(7)	159(6)	28(5)	-22(5)	5(5)
C(21)	210(7)	242(8)	192(7)	-25(6)	51(5)	-12(6)
C(22)	229(7)	308(8)	190(7)	-4(6)	55(5)	14(6)
C(23)	370(9)	318(9)	216(7)	26(6)	67(6)	41(7)
C(24)	510(11)	415(10)	233(8)	88(7)	81(7)	140(8)
C(25)	383(10)	706(14)	226(8)	134(8)	36(7)	169(9)
C(26)	247(8)	709(14)	203(7)	24(8)	10(6)	17(8)
C(27)	197(7)	475(10)	191(7)	-6(7)	52(5)	-9(7)
C(28)	204(7)	493(11)	225(7)	-75(7)	54(6)	-121(7)
C(29)	219(7)	322(9)	259(7)	-67(6)	76(6)	-73(6)
C(30)	322(8)	339(9)	359(9)	-114(7)	104(7)	-149(7)
C(31)	411(9)	226(8)	423(10)	-42(7)	150(8)	-90(7)
C(32)	346(8)	229(8)	322(8)	2(6)	92(6)	19(6)
C(33)	256(7)	227(8)	257(7)	-29(6)	50(6)	-11(6)
C(34)	204(7)	250(8)	213(7)	-39(6)	73(5)	-33(6)
Cl(6)	346(2)	225(2)	243(2)	-41.7(13)	-83.6(14)	-60.6(14)
Cl(28)	368(2)	774(4)	307(2)	-88(2)	-7(2)	-321(2)

Table 4. Hydrogen coordinates (x 10^4) and isotropic displacement parameters (Å^2 x 10^3). All hydrogen atoms were included in idealised positions with U(iso)'s set at 1.2*U(eq) of the parent carbon atoms.

	x	y	z	U(iso)
H(2)	5846	6319	7538	31
H(3)	6273	7846	8529	32
H(4)	6963	8261	8132	29
H(8)	8219	6883	6071	29
H(9)	8498	5391	4871	33
H(10)	8068	3810	3924	33
H(11)	7357	3711	4206	27
H(13)	6743	4480	5164	23
H(23)	6062	7596	5330	36
H(24)	5721	8741	4052	46
H(25)	5246	7410	3057	53
H(26)	5122	4942	3335	46
H(30)	5405	371	5362	41
H(31)	5746	-731	6660	42
H(32)	6246	604	7593	36
H(33)	6350	3087	7305	30

Table 5. Torsion angles, in degrees. E.s.ds are in parentheses.

C(14)-C(1)-C(2)-C(3)	1.3(2)		
C(21)-C(1)-C(2)-C(3)	-176.37(14)	C(14)-C(1)-C(21)-C(22)	-89.53(17)
C(1)-C(2)-C(3)-C(4)	1.6(2)	C(34)-C(21)-C(22)-C(23)	-178.81(13)
C(2)-C(3)-C(4)-C(5)	-2.9(2)	C(1)-C(21)-C(22)-C(23)	2.0(2)
C(3)-C(4)-C(5)-C(6)	-177.34(14)	C(34)-C(21)-C(22)-C(27)	0.3(2)
C(3)-C(4)-C(5)-C(14)	1.5(2)	C(1)-C(21)-C(22)-C(27)	-178.92(13)
C(4)-C(5)-C(6)-C(7)	175.88(13)	C(21)-C(22)-C(23)-C(24)	-179.28(15)
C(14)-C(5)-C(6)-C(7)	-2.9(2)	C(27)-C(22)-C(23)-C(24)	1.6(2)
C(4)-C(5)-C(6)-Cl(6)	-2.78(19)	C(22)-C(23)-C(24)-C(25)	0.1(3)
C(14)-C(5)-C(6)-Cl(6)	178.41(10)	C(23)-C(24)-C(25)-C(26)	-0.7(3)
C(5)-C(6)-C(7)-C(8)	-175.95(13)	C(24)-C(25)-C(26)-C(27)	-0.5(3)
Cl(6)-C(6)-C(7)-C(8)	2.71(19)	C(25)-C(26)-C(27)-C(28)	-178.50(16)
C(5)-C(6)-C(7)-C(12)	2.5(2)	C(25)-C(26)-C(27)-C(22)	2.2(2)
Cl(6)-C(6)-C(7)-C(12)	-178.81(10)	C(21)-C(22)-C(27)-C(28)	-1.2(2)
C(6)-C(7)-C(8)-C(9)	176.94(14)	C(23)-C(22)-C(27)-C(28)	177.97(14)
C(12)-C(7)-C(8)-C(9)	-1.5(2)	C(21)-C(22)-C(27)-C(26)	178.17(13)
C(7)-C(8)-C(9)-C(10)	1.8(2)	C(23)-C(22)-C(27)-C(26)	-2.7(2)
C(8)-C(9)-C(10)-C(11)	-0.4(2)	C(26)-C(27)-C(28)-C(29)	-176.78(15)
C(9)-C(10)-C(11)-C(12)	-1.2(2)	C(22)-C(27)-C(28)-C(29)	2.5(2)
C(10)-C(11)-C(12)-C(13)	-177.40(14)	C(26)-C(27)-C(28)-Cl(28)	4.0(2)
C(10)-C(11)-C(12)-C(7)	1.4(2)	C(22)-C(27)-C(28)-Cl(28)	-176.70(11)
C(6)-C(7)-C(12)-C(13)	0.18(19)	C(27)-C(28)-C(29)-C(30)	176.10(15)
C(8)-C(7)-C(12)-C(13)	178.75(13)	Cl(28)-C(28)-C(29)-C(30)	-4.7(2)
C(6)-C(7)-C(12)-C(11)	-178.59(13)	C(27)-C(28)-C(29)-C(34)	-2.8(2)
C(8)-C(7)-C(12)-C(11)	-0.02(19)	Cl(28)-C(28)-C(29)-C(34)	176.35(11)
C(11)-C(12)-C(13)-C(14)	176.31(13)	C(28)-C(29)-C(30)-C(31)	178.55(15)
C(7)-C(12)-C(13)-C(14)	-2.4(2)	C(34)-C(29)-C(30)-C(31)	-2.5(2)
C(12)-C(13)-C(14)-C(1)	-177.54(13)	C(29)-C(30)-C(31)-C(32)	-0.9(2)
C(12)-C(13)-C(14)-C(5)	2.0(2)	C(30)-C(31)-C(32)-C(33)	3.3(2)
C(2)-C(1)-C(14)-C(13)	176.88(14)	C(31)-C(32)-C(33)-C(34)	-2.1(2)
C(21)-C(1)-C(14)-C(13)	-5.5(2)	C(22)-C(21)-C(34)-C(33)	178.62(13)
C(2)-C(1)-C(14)-C(5)	-2.7(2)	C(1)-C(21)-C(34)-C(33)	-2.2(2)
C(21)-C(1)-C(14)-C(5)	174.99(13)	C(22)-C(21)-C(34)-C(29)	-0.6(2)
C(6)-C(5)-C(14)-C(13)	0.62(19)	C(1)-C(21)-C(34)-C(29)	178.55(13)
C(4)-C(5)-C(14)-C(13)	-178.25(12)	C(32)-C(33)-C(34)-C(21)	179.43(14)
C(6)-C(5)-C(14)-C(1)	-179.82(12)	C(32)-C(33)-C(34)-C(29)	-1.3(2)
C(4)-C(5)-C(14)-C(1)	1.32(19)	C(28)-C(29)-C(34)-C(21)	1.9(2)
C(2)-C(1)-C(21)-C(34)	-91.07(18)	C(30)-C(29)-C(34)-C(21)	-177.15(13)
C(14)-C(1)-C(21)-C(34)	91.26(16)	C(28)-C(29)-C(34)-C(33)	-177.44(13)
C(2)-C(1)-C(21)-C(22)	88.14(17)	C(30)-C(29)-C(34)-C(33)	3.

Crystal data and structure refinement for 8,16-dichloro-dibenzo[A,J]perylene (**79**)

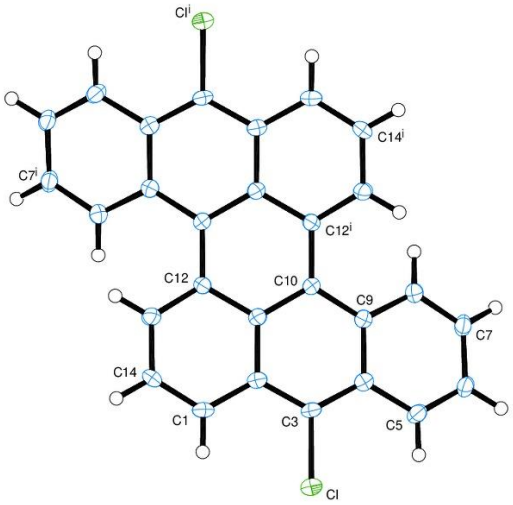

Identification code	isabf1377
Elemental formula	C28 H14 Cl2
Formula weight	421.29
Crystal system, space group	Orthorhombic, Iba2 (no. 45)
Unit cell dimensions	a = 20.7702(14) Å α = 90 ° b = 11.6284(7) Å β = 90 ° c = 7.5051(6) Å γ = 90 °
Volume	1812.7(2) Å^3
Z, Calculated density	4, 1.544 Mg/m^3
F(000)	864
Absorption coefficient	3.311 mm^{-1}
Temperature	100(2) K
Wavelength	1.54184 Å
Crystal colour, shape	purple needle
Crystal size	0.69 x 0.06 x 0.04 mm
Crystal mounting:	on a small loop, in oil, fixed in cold N_2 stream
On the diffractometer:	
Theta range for data collection	8.223 to 69.868 °
Limiting indices	-25<=h<=14, -11<=k<=14, -8<=l<=7
Completeness to theta = 67.684	98.8 %
Absorption correction	Semi-empirical from equivalents

Max. and min. transmission	1.00000 and 0.46450
Reflections collected (not including absences)	2823
No. of unique reflections	1287 [R(int) for equivalents = 0.055]
No. of 'observed' reflections ($I > 2\sigma_I$)	1204
Structure determined by:	dual methods, in SHELXT
Refinement:	Full-matrix least-squares on F^2, in SHELXL
Data / restraints / parameters	1287 / 1 / 136
Goodness-of-fit on F^2	1.087
Final R indices ('observed' data)	R_1 = 0.056, wR_2 = 0.155
Final R indices (all data)	R_1 = 0.058, wR_2 = 0.156
Reflections weighted: $w = [\sigma^2(Fo^2)+(0.1048P)^2+1.2336P]^{-1}$ where $P=(Fo^2+2Fc^2)/3$	
Absolute structure parameter	0.00(4)
Extinction coefficient	n/a
Largest diff. peak and hole	0.34 and -0.54 e.Å^{-3}
Location of largest difference peak	near the Cl atom

Table 1. Atomic coordinates (x 10^4) and equivalent isotropic displacement parameters ($Å^2$ x 10^4). U(eq) is defined as one third of the trace of the orthogonalized Uij tensor. E.s.ds are in parentheses.

	x	y	z	U(eq)
C(1)	4849(2)	8199(4)	3877(10)	286(13)
C(2)	5341(2)	7377(4)	4227(9)	223(11)
C(3)	5993(2)	7683(4)	4350(9)	251(13)
C(4)	6477(2)	6898(4)	4835(7)	217(12)
C(5)	7126(2)	7245(4)	5136(8)	253(12)
C(6)	7567(2)	6503(4)	5804(9)	251(12)
C(7)	7378(2)	5366(5)	6273(8)	229(11)
C(8)	6774(2)	4982(5)	5886(8)	220(11)
C(9)	6302(2)	5716(4)	5091(8)	201(11)
C(10)	5665(2)	5346(4)	4664(7)	198(11)
C(11)	5177(2)	6188(4)	4440(7)	191(11)
C(12)	4510(2)	5854(4)	4402(8)	185(12)
C(13)	4051(2)	6691(4)	3976(8)	215(10)
C(14)	4223(2)	7843(4)	3733(8)	247(12)
Cl	6198.6(5)	9125.1(9)	4063(3)	362(5)

Table 2. Molecular dimensions. Bond lengths are in Ångstroms, angles in degrees. E.s.ds are in parentheses.

C(1)-C(14)	1.369(7)	C(6)-C(7)	1.424(8)
C(1)-C(2)	1.422(7)	C(7)-C(8)	1.363(7)
C(2)-C(3)	1.404(6)	C(8)-C(9)	1.430(7)
C(2)-C(11)	1.432(6)	C(9)-C(10)	1.429(7)
C(3)-C(4)	1.405(7)	C(10)-C(11)	1.419(7)
C(3)-Cl	1.744(5)	C(10)-C(12)#1	1.455(6)
C(4)-C(5)	1.425(7)	C(11)-C(12)	1.439(7)
C(4)-C(9)	1.435(7)	C(12)-C(13)	1.400(7)
C(5)-C(6)	1.354(8)	C(13)-C(14)	1.399(7)
C(14)-C(1)-C(2)	119.5(4)	C(10)-C(9)-C(8)	123.3(5)
C(3)-C(2)-C(1)	122.3(4)	C(10)-C(9)-C(4)	119.5(5)
C(3)-C(2)-C(11)	117.8(4)	C(8)-C(9)-C(4)	117.0(4)
C(1)-C(2)-C(11)	119.9(4)	C(11)-C(10)-C(9)	118.7(4)
C(2)-C(3)-C(4)	122.9(4)	C(11)-C(10)-C(12)#1	117.9(5)
C(2)-C(3)-Cl	118.2(4)	C(9)-C(10)-C(12)#1	123.3(4)
C(4)-C(3)-Cl	118.8(4)	C(10)-C(11)-C(2)	120.6(4)
C(3)-C(4)-C(5)	122.3(4)	C(10)-C(11)-C(12)	120.2(4)
C(3)-C(4)-C(9)	118.4(4)	C(2)-C(11)-C(12)	119.1(4)
C(5)-C(4)-C(9)	119.3(4)	C(13)-C(12)-C(11)	118.2(4)
C(6)-C(5)-C(4)	121.2(5)	C(13)-C(12)-C(10)#1	121.9(4)
C(5)-C(6)-C(7)	119.8(4)	C(11)-C(12)-C(10)#1	119.7(4)
C(8)-C(7)-C(6)	120.3(5)	C(14)-C(13)-C(12)	121.4(4)
C(7)-C(8)-C(9)	121.6(5)	C(1)-C(14)-C(13)	121.5(4)

Symmetry transformation used to generate equivalent atoms:
#1 : 1-x, 1-y, z

Table 3. Anisotropic displacement parameters ($Å^2$ x 10^4) for the expression:
$\exp \{-2\pi^2(h^2a^{*2}U_{11} + ... + 2hka^*b^*U_{12})\}$
E.s.ds are in parentheses.

	U_{11}	U_{22}	U_{33}	U_{23}	U_{13}	U_{12}
C(1)	260(20)	132(19)	470(40)	30(30)	-30(30)	-36(17)
C(2)	200(20)	160(20)	310(30)	0(20)	20(20)	-32(17)
C(3)	210(20)	140(20)	400(40)	-20(20)	30(20)	-51(17)
C(4)	200(20)	180(20)	270(30)	-10(20)	-10(20)	-20(20)
C(5)	190(30)	220(20)	340(30)	-40(20)	40(20)	-54(19)
C(6)	150(20)	240(20)	360(30)	-60(20)	40(20)	-20(20)
C(7)	150(20)	260(30)	270(30)	-30(20)	-10(20)	10(18)
C(8)	180(20)	200(20)	280(30)	-20(20)	20(20)	20(20)
C(9)	170(20)	180(20)	250(30)	-20(20)	-20(20)	1(18)
C(10)	160(20)	160(20)	270(30)	11(19)	-4(19)	-14(18)
C(11)	170(20)	166(19)	230(30)	-2(19)	20(20)	-11(17)
C(12)	180(20)	150(20)	230(30)	-2(19)	30(20)	7(16)
C(13)	200(20)	176(19)	270(30)	30(20)	-30(20)	-14(16)
C(14)	230(20)	150(20)	370(30)	20(20)	0(20)	39(17)
Cl	236(6)	175(6)	674(11)	24(7)	26(8)	-39(4)

Table 4. Hydrogen coordinates (x 10^4) and isotropic displacement parameters ($Å^2$ x 10^3). All hydrogen atoms were included in idealised positions with U(iso)'s set at 1.2*U(eq) of the parent carbon atoms.

	x	y	z	U(iso)
H(1)	4955	8989	3744	34
H(5)	7252	8010	4863	30
H(6)	8001	6741	5959	30
H(7)	7675	4872	6859	27
H(8)	6664	4208	6152	26
H(13)	3612	6472	3849	26
H(14)	3899	8392	3463	30

Table 5. Torsion angles, in degrees. E.s.ds are in parentheses.

C(14)-C(1)-C(2)-C(3)	178.5(7)		
C(14)-C(1)-C(2)-C(11)	-0.5(10)		
C(1)-C(2)-C(3)-C(4)	174.7(7)		
C(11)-C(2)-C(3)-C(4)	-6.2(9)	C(8)-C(9)-C(10)-C(11)	159.6(5)
C(1)-C(2)-C(3)-Cl	0.1(9)	C(4)-C(9)-C(10)-C(11)	-16.1(8)
C(11)-C(2)-C(3)-Cl	179.2(4)	C(8)-C(9)-C(10)-C(12)#1	-22.0(9)
C(2)-C(3)-C(4)-C(5)	-173.3(6)	C(4)-C(9)-C(10)-C(12)#1	162.4(5)
Cl-C(3)-C(4)-C(5)	1.3(8)	C(9)-C(10)-C(11)-C(2)	14.5(8)
C(2)-C(3)-C(4)-C(9)	4.6(9)	C(12)#1-C(10)-C(11)-C(2)	-164.0(6)
Cl-C(3)-C(4)-C(9)	179.2(4)	C(9)-C(10)-C(11)-C(12)	-166.2(5)
C(3)-C(4)-C(5)-C(6)	172.1(6)	C(12)#1-C(10)-C(11)-C(12)	15.2(7)
C(9)-C(4)-C(5)-C(6)	-5.7(9)	C(3)-C(2)-C(11)-C(10)	-3.5(9)
C(4)-C(5)-C(6)-C(7)	-2.1(9)	C(1)-C(2)-C(11)-C(10)	175.5(6)
C(5)-C(6)-C(7)-C(8)	6.7(9)	C(3)-C(2)-C(11)-C(12)	177.2(5)
C(6)-C(7)-C(8)-C(9)	-3.3(9)	C(1)-C(2)-C(11)-C(12)	-3.7(9)
C(7)-C(8)-C(9)-C(10)	179.9(5)	C(10)-C(11)-C(12)-C(13)	-172.8(5)
C(7)-C(8)-C(9)-C(4)	-4.3(8)	C(2)-C(11)-C(12)-C(13)	6.4(8)
C(3)-C(4)-C(9)-C(10)	6.8(8)	C(10)-C(11)-C(12)-C(10)#1	2.4(8)
C(5)-C(4)-C(9)-C(10)	-175.3(5)	C(2)-C(11)-C(12)-C(10)#1	-178.4(5)
C(3)-C(4)-C(9)-C(8)	-169.1(5)	C(11)-C(12)-C(13)-C(14)	-5.1(9)
C(5)-C(4)-C(9)-C(8)	8.8(8)	C(10)#1-C(12)-C(13)-C(14)	179.8(6)
		C(2)-C(1)-C(14)-C(13)	2.0(11)
		C(12)-C(13)-C(14)-C(1)	0.9(10)

Crystal data and structure refinement for
9,10,10'-trichloro-1,9'-bianthracene
(**80**)

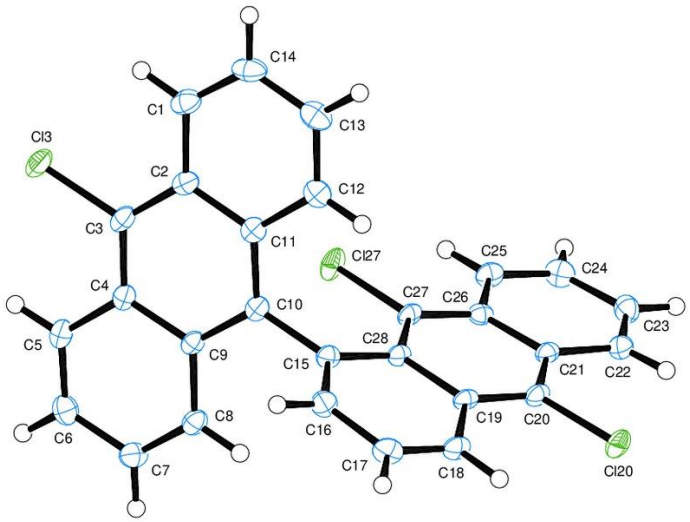

Identification code	isabf1379
Elemental formula	C28 H15 Cl3
Formula weight	457.75
Crystal system, space group	Monoclinic, $P2_1/c$ (no. 14)
Unit cell dimensions	a = 8.2784(2) Å α = 90 ° b = 30.1787(5) Å β = 113.645(2) ° c = 8.7775(2) Å γ = 90 °
Volume	2008.80(8) $Å^3$
Z, Calculated density	4, 1.514 Mg/m^3
F(000)	936
Absorption coefficient	4.231 mm^{-1}
Temperature	100(2) K
Wavelength	1.54184 Å
Crystal colour, shape	yellow block
Crystal size	0.49 x 0.33 x 0.23 mm
Crystal mounting:	on a small loop, in oil, fixed in cold N_2 stream
On the diffractometer:	
Theta range for data collection	8.055 to 69.983 °
Limiting indices	-10<=h<=10, -36<=k<=32, -7<=l<=10
Completeness to theta = 67.684	99.6 %

Absorption correction	Semi-empirical from equivalents
Max. and min. transmission	1.00000 and 0.44863
Reflections collected (not including absences)	13572
No. of unique reflections	3757 [R(int) for equivalents = 0.050]
No. of 'observed' reflections ($I > 2\sigma_I$)	3464
Structure determined by:	dual methods, in SHELXT
Refinement:	Full-matrix least-squares on F^2, in SHELXL
Data / restraints / parameters	3757 / 0 / 280
Goodness-of-fit on F^2	1.046
Final R indices ('observed' data)	R_1 = 0.039, wR_2 = 0.104
Final R indices (all data)	R_1 = 0.042, wR_2 = 0.106
Reflections weighted: $w = [\sigma^2(Fo^2)+(0.0626P)^2+0.8341P]^{-1}$ where $P=(Fo^2+2Fc^2)/3$	
Extinction coefficient	n/a
Largest diff. peak and hole	0.39 and -0.46 e.Å^{-3}
Location of largest difference peak	near Cl(27)

Table 1. Atomic coordinates (x 10^5) and equivalent isotropic displacement parameters ($Å^2$ x 10^4). U(eq) is defined as one third of the trace of the orthogonalized Uij tensor. E.s.ds are in parentheses.

	x	y	z	U(eq)
C(1)	25640(30)	72177(6)	94190(30)	240(4)
C(2)	40150(30)	69982(6)	92430(20)	187(4)
C(3)	57410(30)	70103(6)	104580(20)	194(4)
C(4)	71370(20)	67784(6)	103160(20)	174(4)
C(5)	88950(30)	67787(6)	115700(20)	214(4)
C(6)	102030(30)	65442(7)	113800(20)	240(4)
C(7)	98510(30)	62884(7)	99230(20)	227(4)
C(8)	81930(30)	62792(6)	87010(20)	196(4)
C(9)	67730(20)	65229(6)	88320(20)	164(4)
C(10)	50510(20)	65034(6)	75860(20)	167(4)
C(11)	36830(20)	67430(6)	77630(20)	175(4)
C(12)	19260(30)	67328(6)	65180(20)	220(4)
C(13)	5720(30)	69438(7)	67340(30)	262(4)
C(14)	9080(30)	71838(7)	82230(30)	272(4)
C(15)	46930(20)	62367(6)	60440(20)	172(4)
C(16)	50940(20)	64368(7)	48360(20)	214(4)
C(17)	47840(30)	62267(7)	33030(20)	225(4)
C(18)	39970(20)	58243(6)	29640(20)	199(4)
C(19)	35100(20)	55976(6)	41430(20)	166(4)
C(20)	26570(20)	51870(6)	37770(20)	182(4)
C(21)	22690(20)	49394(6)	49350(20)	170(4)
C(22)	13760(20)	45214(6)	45560(20)	214(4)
C(23)	11190(30)	42824(6)	57470(30)	234(4)
C(24)	17230(30)	44453(6)	74010(30)	236(4)
C(25)	25220(30)	48466(6)	78000(20)	200(4)
C(26)	28170(20)	51123(6)	65830(20)	165(4)
C(27)	35870(20)	55362(6)	69370(20)	164(4)
C(28)	39400(20)	57946(6)	57710(20)	155(4)
Cl(3)	61730(7)	73268(2)	122524(6)	261.5(15)
Cl(20)	20347(6)	49711(2)	17821(5)	244.5(14)
Cl(27)	41591(6)	57220(2)	89627(5)	234.3(14)

Table 2. Molecular dimensions. Bond lengths are in Ångstroms, angles in degrees. E.s.ds are in parentheses.

C(1)-C(14)	1.356(3)	C(15)-C(16)	1.371(3)
C(1)-C(2)	1.433(3)	C(15)-C(28)	1.451(3)
C(2)-C(3)	1.399(3)	C(16)-C(17)	1.415(3)
C(2)-C(11)	1.439(3)	C(17)-C(18)	1.353(3)
C(3)-C(4)	1.399(3)	C(18)-C(19)	1.427(3)
C(3)-Cl(3)	1.7521(18)	C(19)-C(20)	1.398(3)
C(4)-C(5)	1.430(3)	C(19)-C(28)	1.454(2)
C(4)-C(9)	1.437(2)	C(20)-C(21)	1.399(3)
C(5)-C(6)	1.359(3)	C(20)-Cl(20)	1.7412(17)
C(6)-C(7)	1.420(3)	C(21)-C(26)	1.430(3)
C(7)-C(8)	1.362(3)	C(21)-C(22)	1.432(3)
C(8)-C(9)	1.430(3)	C(22)-C(23)	1.355(3)
C(9)-C(10)	1.408(3)	C(23)-C(24)	1.420(3)
C(10)-C(11)	1.404(3)	C(24)-C(25)	1.357(3)
C(10)-C(15)	1.498(2)	C(25)-C(26)	1.433(3)
C(11)-C(12)	1.427(3)	C(26)-C(27)	1.407(3)
C(12)-C(13)	1.367(3)	C(27)-C(28)	1.407(2)
C(13)-C(14)	1.420(3)	C(27)-Cl(27)	1.7394(17)

C(14)-C(1)-C(2)	120.85(18)	C(16)-C(15)-C(10)	116.11(16)
C(3)-C(2)-C(1)	123.35(17)	C(28)-C(15)-C(10)	124.00(15)
C(3)-C(2)-C(11)	117.99(16)	C(15)-C(16)-C(17)	122.02(18)
C(1)-C(2)-C(11)	118.65(17)	C(18)-C(17)-C(16)	119.94(17)
C(2)-C(3)-C(4)	123.14(16)	C(17)-C(18)-C(19)	121.44(17)
C(2)-C(3)-Cl(3)	118.52(14)	C(20)-C(19)-C(18)	121.44(16)
C(4)-C(3)-Cl(3)	118.34(15)	C(20)-C(19)-C(28)	119.37(16)
C(3)-C(4)-C(5)	123.59(16)	C(18)-C(19)-C(28)	119.19(17)
C(3)-C(4)-C(9)	117.93(17)	C(19)-C(20)-C(21)	123.23(16)
C(5)-C(4)-C(9)	118.48(16)	C(19)-C(20)-Cl(20)	118.78(14)
C(6)-C(5)-C(4)	121.33(17)	C(21)-C(20)-Cl(20)	117.98(14)
C(5)-C(6)-C(7)	120.54(18)	C(20)-C(21)-C(26)	117.93(17)
C(8)-C(7)-C(6)	119.87(18)	C(20)-C(21)-C(22)	123.30(17)
C(7)-C(8)-C(9)	121.85(17)	C(26)-C(21)-C(22)	118.77(17)
C(10)-C(9)-C(8)	121.66(16)	C(23)-C(22)-C(21)	121.01(18)
C(10)-C(9)-C(4)	120.37(16)	C(22)-C(23)-C(24)	120.32(18)
C(8)-C(9)-C(4)	117.93(16)	C(25)-C(24)-C(23)	120.54(18)
C(11)-C(10)-C(9)	120.19(16)	C(24)-C(25)-C(26)	121.21(17)
C(11)-C(10)-C(15)	120.03(16)	C(27)-C(26)-C(21)	119.12(16)
C(9)-C(10)-C(15)	119.76(16)	C(27)-C(26)-C(25)	122.80(16)
C(10)-C(11)-C(12)	121.60(17)	C(21)-C(26)-C(25)	118.06(17)
C(10)-C(11)-C(2)	120.34(17)	C(26)-C(27)-C(28)	123.44(16)
C(12)-C(11)-C(2)	118.05(17)	C(26)-C(27)-Cl(27)	115.61(13)
C(13)-C(12)-C(11)	121.63(19)	C(28)-C(27)-Cl(27)	120.92(14)
C(12)-C(13)-C(14)	119.77(19)	C(27)-C(28)-C(15)	126.16(16)
C(1)-C(14)-C(13)	120.98(18)	C(27)-C(28)-C(19)	116.59(16)
C(16)-C(15)-C(28)	119.88(16)	C(15)-C(28)-C(19)	117.25(15)

Table 3. Anisotropic displacement parameters ($Å^2$ x 10^4) for the expression:

$$\exp\{-2\pi^2(h^2a^{*2}U_{11} + \ldots + 2hka^*b^*U_{12})\}$$

E.s.ds are in parentheses.

	U_{11}	U_{22}	U_{33}	U_{23}	U_{13}	U_{12}
C(1)	305(11)	171(9)	305(10)	5(8)	185(9)	20(8)
C(2)	247(10)	142(8)	215(9)	14(7)	139(8)	1(7)
C(3)	289(10)	140(8)	191(9)	-19(7)	136(8)	-19(7)
C(4)	223(9)	158(8)	149(8)	3(6)	82(7)	-24(7)
C(5)	254(10)	198(9)	175(9)	-29(7)	69(8)	-31(7)
C(6)	217(9)	256(10)	212(9)	10(8)	50(8)	-17(7)
C(7)	221(10)	257(10)	216(9)	6(7)	101(8)	26(7)
C(8)	246(10)	202(9)	159(8)	-5(7)	101(7)	-3(7)
C(9)	215(9)	153(8)	144(8)	4(6)	93(7)	-7(7)
C(10)	232(9)	133(8)	161(8)	18(6)	103(7)	-17(7)
C(11)	226(9)	141(8)	173(9)	40(6)	97(8)	-5(7)
C(12)	230(9)	210(9)	223(9)	39(7)	95(8)	-8(7)
C(13)	213(10)	262(10)	303(11)	77(8)	96(8)	25(8)
C(14)	273(10)	207(10)	411(12)	57(8)	215(10)	66(8)
C(15)	167(8)	215(9)	131(8)	8(7)	56(7)	16(7)
C(16)	222(9)	246(9)	179(9)	8(7)	84(8)	-14(7)
C(17)	243(10)	314(10)	147(9)	65(7)	107(8)	12(8)
C(18)	218(9)	288(10)	97(8)	10(7)	70(7)	36(7)
C(19)	162(8)	229(9)	103(8)	10(7)	51(7)	53(7)
C(20)	183(9)	241(9)	110(8)	-24(7)	45(7)	41(7)
C(21)	154(8)	199(9)	151(9)	-11(7)	56(7)	43(7)
C(22)	181(9)	222(9)	227(9)	-46(7)	70(7)	17(7)
C(23)	209(9)	176(9)	299(10)	-15(7)	83(8)	-6(7)
C(24)	254(10)	213(10)	257(10)	56(7)	121(8)	13(7)
C(25)	236(9)	229(9)	151(8)	30(7)	94(7)	26(7)
C(26)	148(8)	195(9)	151(8)	19(7)	58(7)	36(7)
C(27)	189(9)	209(9)	95(8)	-2(6)	56(7)	29(7)
C(28)	154(8)	206(9)	95(8)	5(6)	40(6)	32(7)
Cl(3)	346(3)	228(3)	239(3)	-89(2)	147(2)	-13(2)
Cl(20)	289(3)	310(3)	128(2)	-71(2)	77(2)	-13(2)
Cl(27)	382(3)	224(2)	109(2)	-18(2)	111(2)	-65(2)

Table 4. Hydrogen coordinates (x 10^4) and isotropic displacement parameters (Å^2 x 10^3). All hydrogen atoms were included in idealised positions with U(iso)'s set at 1.2*U(eq) of the parent carbon atoms.

	x	y	z	U(iso)
H(1)	2765	7389	10386	29
H(5)	9154	6946	12557	26
H(6)	11362	6551	12228	29
H(7)	10771	6124	9801	27
H(8)	7973	6106	7734	24
H(12)	1691	6575	5514	26
H(13)	-589	6930	5892	31
H(14)	-42	7323	8382	33
H(16)	5595	6725	5035	26
H(17)	5127	6368	2512	27
H(18)	3765	5690	1918	24
H(22)	957	4410	3452	26
H(23)	533	4005	5475	28
H(24)	1565	4272	8234	28
H(25)	2893	4953	8907	24

Table 5. Torsion angles, in degrees. E.s.ds are in parentheses.

C(14)-C(1)-C(2)-C(3)	-177.99(18)		
C(14)-C(1)-C(2)-C(11)	0.4(3)		
C(1)-C(2)-C(3)-C(4)	176.86(17)	C(28)-C(15)-C(16)-C(17)	0.5(3)
C(11)-C(2)-C(3)-C(4)	-1.6(3)	C(10)-C(15)-C(16)-C(17)	-178.50(17)
C(1)-C(2)-C(3)-Cl(3)	-2.5(2)	C(15)-C(16)-C(17)-C(18)	3.0(3)
C(11)-C(2)-C(3)-Cl(3)	179.02(13)	C(16)-C(17)-C(18)-C(19)	-1.8(3)
C(2)-C(3)-C(4)-C(5)	-178.22(17)	C(17)-C(18)-C(19)-C(20)	178.35(18)
Cl(3)-C(3)-C(4)-C(5)	1.2(2)	C(17)-C(18)-C(19)-C(28)	-2.8(3)
C(2)-C(3)-C(4)-C(9)	1.1(3)	C(18)-C(19)-C(20)-C(21)	175.32(17)
Cl(3)-C(3)-C(4)-C(9)	-179.45(13)	C(28)-C(19)-C(20)-C(21)	-3.5(3)
C(3)-C(4)-C(5)-C(6)	179.33(18)	C(18)-C(19)-C(20)-Cl(20)	-4.9(2)
C(9)-C(4)-C(5)-C(6)	0.0(3)	C(28)-C(19)-C(20)-Cl(20)	176.22(13)
C(4)-C(5)-C(6)-C(7)	-0.4(3)	C(19)-C(20)-C(21)-C(26)	-1.6(3)
C(5)-C(6)-C(7)-C(8)	0.3(3)	Cl(20)-C(20)-C(21)-C(26)	178.60(13)
C(6)-C(7)-C(8)-C(9)	0.2(3)	C(19)-C(20)-C(21)-C(22)	179.18(17)
C(7)-C(8)-C(9)-C(10)	-178.33(17)	Cl(20)-C(20)-C(21)-C(22)	-0.6(2)
C(7)-C(8)-C(9)-C(4)	-0.7(3)	C(20)-C(21)-C(22)-C(23)	176.23(18)
C(3)-C(4)-C(9)-C(10)	-1.1(3)	C(26)-C(21)-C(22)-C(23)	-2.9(3)
C(5)-C(4)-C(9)-C(10)	178.26(16)	C(21)-C(22)-C(23)-C(24)	0.5(3)
C(3)-C(4)-C(9)-C(8)	-178.84(16)	C(22)-C(23)-C(24)-C(25)	1.7(3)
C(5)-C(4)-C(9)-C(8)	0.6(2)	C(23)-C(24)-C(25)-C(26)	-1.4(3)
C(8)-C(9)-C(10)-C(11)	179.26(16)	C(20)-C(21)-C(26)-C(27)	5.1(3)
C(4)-C(9)-C(10)-C(11)	1.6(3)	C(22)-C(21)-C(26)-C(27)	-175.69(16)
C(8)-C(9)-C(10)-C(15)	-2.6(3)	C(20)-C(21)-C(26)-C(25)	-176.11(16)
C(4)-C(9)-C(10)-C(15)	179.82(16)	C(22)-C(21)-C(26)-C(25)	3.1(3)
C(9)-C(10)-C(11)-C(12)	179.57(16)	C(24)-C(25)-C(26)-C(27)	177.76(18)
C(15)-C(10)-C(11)-C(12)	1.4(3)	C(24)-C(25)-C(26)-C(21)	-1.0(3)
C(9)-C(10)-C(11)-C(2)	-2.1(3)	C(21)-C(26)-C(27)-C(28)	-3.5(3)
C(15)-C(10)-C(11)-C(2)	179.74(16)	C(25)-C(26)-C(27)-C(28)	177.76(17)
C(3)-C(2)-C(11)-C(10)	2.0(3)	C(21)-C(26)-C(27)-Cl(27)	178.50(13)
C(1)-C(2)-C(11)-C(10)	-176.49(16)	C(25)-C(26)-C(27)-Cl(27)	-0.2(2)
C(3)-C(2)-C(11)-C(12)	-179.59(16)	C(26)-C(27)-C(28)-C(15)	178.55(17)
C(1)-C(2)-C(11)-C(12)	1.9(2)	Cl(27)-C(27)-C(28)-C(15)	-3.6(3)
C(10)-C(11)-C(12)-C(13)	175.93(17)	C(26)-C(27)-C(28)-C(19)	-1.6(3)
C(2)-C(11)-C(12)-C(13)	-2.4(3)	Cl(27)-C(27)-C(28)-C(19)	176.28(12)
C(11)-C(12)-C(13)-C(14)	0.6(3)	C(16)-C(15)-C(28)-C(27)	174.91(17)
C(2)-C(1)-C(14)-C(13)	-2.4(3)	C(10)-C(15)-C(28)-C(27)	-6.1(3)
C(12)-C(13)-C(14)-C(1)	1.9(3)	C(16)-C(15)-C(28)-C(19)	-4.9(3)
C(11)-C(10)-C(15)-C(16)	97.0(2)	C(10)-C(15)-C(28)-C(19)	174.00(16)
C(9)-C(10)-C(15)-C(16)	-81.2(2)	C(20)-C(19)-C(28)-C(27)	5.1(2)
C(11)-C(10)-C(15)-C(28)	-82.0(2)	C(18)-C(19)-C(28)-C(27)	-173.83(16)
C(9)-C(10)-C(15)-C(28)	99.9(2)	C(20)-C(19)-C(28)-C(15)	-175.09(16)
		C(18)-C(19)-C(28)-C(15)	6.0(2)

Crystal data and structure refinement for tolyl-anthracenyl-anthracene (**85**)

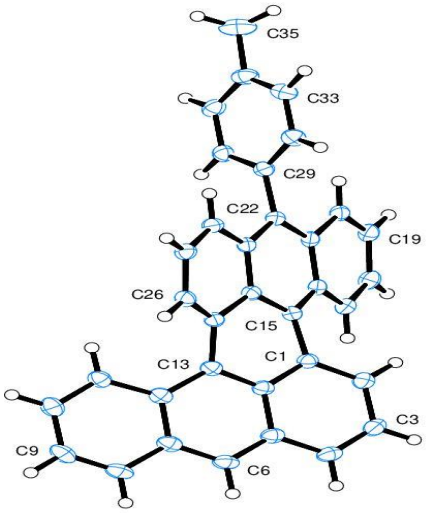

Identification code	isabf1279
Elemental formula	C35 H22
Formula weight	442.52
Crystal system, space group	Orthorhombic, Pbca (no. 61)
Unit cell dimensions	a = 21.3167(8) Å α = 90 ° b = 7.6730(3) Å β = 90 ° c = 26.6217(10) Å γ = 90 °
Volume	4354.3(3) $Å^3$
Z, Calculated density	8, 1.350 Mg/m^3
F(000)	1856
Absorption coefficient	0.076 mm^{-1}
Temperature	100.01(10) K
Wavelength	0.71073 Å
Crystal colour, shape	red block
Crystal size	0.22 x 0.22 x 0.10 mm
Crystal mounting:	on a small loop, in oil, fixed in cold N_2 stream
On the diffractometer:	
Theta range for data collection	3.609 to 27.493 °
Limiting indices	-27<=h<=23, -9<=k<=7, -32<=l<=33
Completeness to theta = 25.242	99.7 %

Absorption correction	Semi-empirical from equivalents
Max. and min. transmission	1.00000 and 0.42041
Reflections collected (not including absences)	22967
No. of unique reflections	4837 [R(int) for equivalents = 0.043]
No. of 'observed' reflections ($I > 2\sigma_I$)	3918
Structure determined by:	dual methods, in SHELXT
Refinement:	Full-matrix least-squares on F^2, in SHELXL
Data / restraints / parameters	4837 / 0 / 317
Goodness-of-fit on F^2	1.047
Final R indices ('observed' data)	R_1 = 0.046, wR_2 = 0.112
Final R indices (all data)	R_1 = 0.059, wR_2 = 0.117
Reflections weighted: $w = [\sigma^2(Fo^2)+(0.0543P)^2+1.6555P]^{-1}$ where $P=(Fo^2+2Fc^2)/3$	
Extinction coefficient	n/a
Largest diff. peak and hole	0.29 and -0.23 e.Å^{-3}
Location of largest difference peak	near C(28)

Table 1. Atomic coordinates (x 10^5) and equivalent isotropic displacement parameters ($Å^2$ x 10^4). U(eq) is defined as one third of the trace of the orthogonalized Uij tensor. E.s.ds are in parentheses.

	x	y	z	U(eq)
C(1)	34469(7)	26450(18)	51137(5)	212(3)
C(2)	33187(7)	9988(19)	49329(6)	255(3)
C(3)	31092(7)	-3541(19)	52514(6)	279(3)
C(4)	30169(7)	-553(19)	57489(6)	268(3)
C(5)	31741(7)	15788(19)	59644(5)	238(3)
C(6)	30995(7)	19213(19)	64756(5)	262(3)
C(7)	32409(7)	35440(20)	66803(5)	254(3)
C(8)	31133(7)	39400(20)	71946(5)	290(3)
C(9)	32167(8)	55480(20)	73869(5)	308(4)
C(10)	34420(7)	68940(20)	70726(5)	292(3)
C(11)	35935(7)	65610(20)	65844(5)	256(3)
C(12)	35189(7)	48698(19)	63696(5)	231(3)
C(13)	36644(7)	44623(18)	58610(5)	214(3)
C(14)	34294(6)	29189(18)	56478(5)	211(3)
C(15)	36196(7)	41213(17)	47915(5)	205(3)
C(16)	34474(7)	42635(17)	42766(5)	209(3)
C(17)	29517(7)	32757(18)	40549(5)	237(3)
C(18)	28032(7)	34426(19)	35580(6)	261(3)
C(19)	31482(7)	45742(18)	32448(5)	251(3)
C(20)	36016(7)	56039(18)	34431(5)	222(3)
C(21)	37481(7)	55517(17)	39692(5)	201(3)
C(22)	41823(7)	67372(17)	41779(5)	199(3)
C(23)	43142(7)	66733(17)	46959(5)	202(3)
C(24)	47659(7)	77947(18)	49213(5)	232(3)
C(25)	48898(7)	76972(19)	54234(5)	239(3)
C(26)	45358(7)	65956(18)	57354(5)	230(3)
C(27)	40713(7)	55411(17)	55443(5)	206(3)
C(28)	39965(7)	54304(17)	50076(5)	197(3)
C(29)	44306(7)	81609(18)	38518(5)	213(3)
C(30)	40172(7)	94740(18)	37039(5)	249(3)
C(31)	42027(8)	107630(19)	33739(5)	276(3)
C(32)	48004(8)	107880(20)	31758(5)	292(3)
C(33)	52198(8)	95230(20)	33354(6)	299(3)
C(34)	50395(7)	82210(20)	36706(5)	266(3)
C(35)	49652(9)	121340(30)	27848(7)	446(5)

Table 2. Molecular dimensions. Bond lengths are in Ångstroms, angles in degrees. E.s.ds are in parentheses.

C(1)-C(2)	1.379(2)	C(16)-C(21)	1.4344(19)
C(1)-C(14)	1.4377(19)	C(17)-C(18)	1.366(2)
C(1)-C(15)	1.4677(18)	C(18)-C(19)	1.411(2)
C(2)-C(3)	1.413(2)	C(19)-C(20)	1.355(2)
C(3)-C(4)	1.358(2)	C(20)-C(21)	1.4357(19)
C(4)-C(5)	1.419(2)	C(21)-C(22)	1.4116(19)
C(5)-C(6)	1.395(2)	C(22)-C(23)	1.4082(18)
C(5)-C(14)	1.4368(19)	C(22)-C(29)	1.4922(18)
C(6)-C(7)	1.392(2)	C(23)-C(24)	1.424(2)
C(7)-C(8)	1.429(2)	C(23)-C(28)	1.4341(19)
C(7)-C(12)	1.439(2)	C(24)-C(25)	1.3646(19)
C(8)-C(9)	1.353(2)	C(25)-C(26)	1.405(2)
C(9)-C(10)	1.414(2)	C(26)-C(27)	1.376(2)
C(10)-C(11)	1.363(2)	C(27)-C(28)	1.4403(18)
C(11)-C(12)	1.427(2)	C(29)-C(34)	1.385(2)
C(12)-C(13)	1.4237(19)	C(29)-C(30)	1.395(2)
C(13)-C(14)	1.4056(19)	C(30)-C(31)	1.381(2)
C(13)-C(27)	1.4656(19)	C(31)-C(32)	1.379(2)
C(15)-C(28)	1.4090(19)	C(32)-C(33)	1.386(2)
C(15)-C(16)	1.4234(19)	C(32)-C(35)	1.508(2)
C(16)-C(17)	1.428(2)	C(33)-C(34)	1.394(2)
C(2)-C(1)-C(14)	118.29(13)	C(18)-C(17)-C(16)	121.45(13)
C(2)-C(1)-C(15)	123.55(13)	C(17)-C(18)-C(19)	120.62(13)
C(14)-C(1)-C(15)	118.13(12)	C(20)-C(19)-C(18)	120.01(13)
C(1)-C(2)-C(3)	121.74(14)	C(19)-C(20)-C(21)	121.26(13)
C(4)-C(3)-C(2)	120.46(14)	C(22)-C(21)-C(16)	120.84(12)
C(3)-C(4)-C(5)	120.61(13)	C(22)-C(21)-C(20)	120.57(12)
C(6)-C(5)-C(4)	122.28(13)	C(16)-C(21)-C(20)	118.58(12)
C(6)-C(5)-C(14)	118.73(13)	C(23)-C(22)-C(21)	119.59(12)
C(4)-C(5)-C(14)	118.98(13)	C(23)-C(22)-C(29)	121.62(12)
C(7)-C(6)-C(5)	121.71(13)	C(21)-C(22)-C(29)	118.39(12)
C(6)-C(7)-C(8)	121.62(14)	C(22)-C(23)-C(24)	121.78(12)
C(6)-C(7)-C(12)	119.77(13)	C(22)-C(23)-C(28)	119.71(12)
C(8)-C(7)-C(12)	118.61(14)	C(24)-C(23)-C(28)	118.51(12)
C(9)-C(8)-C(7)	121.70(14)	C(25)-C(24)-C(23)	120.70(13)
C(8)-C(9)-C(10)	119.84(14)	C(24)-C(25)-C(26)	120.55(13)
C(11)-C(10)-C(9)	120.49(15)	C(27)-C(26)-C(25)	121.44(13)
C(10)-C(11)-C(12)	121.75(14)	C(26)-C(27)-C(28)	118.75(12)
C(13)-C(12)-C(11)	123.81(13)	C(26)-C(27)-C(13)	123.03(12)
C(13)-C(12)-C(7)	118.76(13)	C(28)-C(27)-C(13)	118.16(12)
C(11)-C(12)-C(7)	117.29(13)	C(15)-C(28)-C(23)	120.47(12)
C(14)-C(13)-C(12)	119.44(13)	C(15)-C(28)-C(27)	120.67(12)
C(14)-C(13)-C(27)	117.02(12)	C(23)-C(28)-C(27)	118.86(12)
C(12)-C(13)-C(27)	123.50(13)	C(34)-C(29)-C(30)	118.00(13)
C(13)-C(14)-C(5)	120.07(13)	C(34)-C(29)-C(22)	123.99(13)
C(13)-C(14)-C(1)	120.89(12)	C(30)-C(29)-C(22)	117.95(13)
C(5)-C(14)-C(1)	119.04(13)	C(31)-C(30)-C(29)	121.06(14)
C(28)-C(15)-C(16)	119.05(12)	C(32)-C(31)-C(30)	121.20(14)
C(28)-C(15)-C(1)	117.05(12)	C(31)-C(32)-C(33)	117.95(14)
C(16)-C(15)-C(1)	123.86(12)	C(31)-C(32)-C(35)	119.27(15)
C(15)-C(16)-C(17)	123.24(13)	C(33)-C(32)-C(35)	122.75(16)
C(15)-C(16)-C(21)	119.14(12)	C(32)-C(33)-C(34)	121.36(15)
C(17)-C(16)-C(21)	117.44(12)	C(29)-C(34)-C(33)	120.33(14)

Table 3. Anisotropic displacement parameters ($Å^2$ x 10^4) for the expression:

$$\exp\{-2\pi^2(h^2a^{*2}U_{11} + \ldots + 2hka^*b^*U_{12})\}$$

E.s.ds are in parentheses.

	U_{11}	U_{22}	U_{33}	U_{23}	U_{13}	U_{12}
C(1)	199(7)	204(7)	233(7)	13(5)	13(5)	-1(5)
C(2)	277(8)	239(7)	250(7)	-11(5)	3(6)	-14(6)
C(3)	289(8)	198(7)	350(8)	0(6)	3(6)	-10(6)
C(4)	264(8)	221(7)	318(8)	83(6)	2(6)	0(6)
C(5)	221(7)	232(7)	261(7)	61(5)	-4(6)	23(6)
C(6)	256(8)	287(8)	243(7)	98(6)	21(6)	16(6)
C(7)	240(8)	310(8)	212(7)	59(6)	-9(6)	34(6)
C(8)	275(8)	387(9)	206(7)	85(6)	21(6)	17(7)
C(9)	308(8)	446(9)	171(7)	-3(6)	8(6)	41(7)
C(10)	305(8)	351(8)	221(7)	-39(6)	-19(6)	22(7)
C(11)	267(8)	292(8)	209(7)	11(5)	-8(6)	19(6)
C(12)	226(7)	271(7)	196(7)	27(5)	-23(6)	24(6)
C(13)	217(7)	228(7)	196(7)	29(5)	-16(5)	26(5)
C(14)	197(7)	213(7)	223(7)	37(5)	2(6)	20(5)
C(15)	217(7)	192(7)	206(7)	-2(5)	22(5)	5(5)
C(16)	229(7)	182(6)	216(7)	-29(5)	5(6)	18(5)
C(17)	262(8)	195(7)	255(7)	-11(5)	2(6)	-8(6)
C(18)	264(8)	231(7)	289(8)	-46(6)	-65(6)	-17(6)
C(19)	327(8)	220(7)	207(7)	-13(5)	-53(6)	32(6)
C(20)	271(8)	199(7)	197(7)	-9(5)	-1(6)	19(6)
C(21)	229(7)	177(6)	197(7)	-23(5)	-4(5)	23(5)
C(22)	226(7)	185(6)	187(6)	0(5)	8(5)	0(5)
C(23)	237(7)	186(7)	183(7)	-13(5)	9(5)	9(5)
C(24)	280(8)	210(7)	207(7)	3(5)	13(6)	-37(6)
C(25)	276(8)	224(7)	217(7)	-26(5)	-24(6)	-35(6)
C(26)	276(8)	245(7)	169(7)	-12(5)	-18(6)	12(6)
C(27)	238(7)	193(7)	188(7)	7(5)	8(5)	22(5)
C(28)	213(7)	189(6)	188(6)	2(5)	4(5)	11(5)
C(29)	278(8)	212(7)	148(6)	-14(5)	-24(5)	-29(6)
C(30)	289(8)	234(7)	223(7)	-27(5)	-5(6)	2(6)
C(31)	352(9)	220(7)	255(7)	16(5)	-53(6)	8(6)
C(32)	368(9)	290(8)	216(7)	42(6)	-42(6)	-73(7)
C(33)	282(8)	359(9)	256(8)	20(6)	22(6)	-45(7)
C(34)	266(8)	286(8)	245(7)	21(6)	-13(6)	21(6)
C(35)	450(11)	500(11)	386(10)	192(8)	-37(8)	-99(9)

Table 4. Hydrogen coordinates (x 10^4) and isotropic displacement parameters (Å^2 x 10^3). All hydrogen atoms were included in idealised positions with U(iso)'s set at 1.2*U(eq) or, for the methyl group hydrogen atoms, 1.5*U(eq) of the parent carbon atoms.

	x	y	z	U(iso)
H(2)	3373	768	4585	31
H(3)	3032	-1481	5117	33
H(4)	2846	-948	5954	32
H(6)	2948	1024	6690	31
H(8)	2952	3053	7407	35
H(9)	3138	5770	7732	37
H(10)	3488	8040	7203	35
H(11)	3753	7479	6382	31
H(17)	2720	2485	4257	28
H(18)	2465	2791	3422	31
H(19)	3063	4614	2895	30
H(20)	3827	6375	3230	27
H(24)	4983	8619	4720	28
H(25)	5218	8380	5563	29
H(26)	4619	6578	6086	28
H(30)	3601	9481	3832	30
H(31)	3913	11649	3282	33
H(33)	5639	9544	3214	36
H(34)	5336	7370	3775	32
H(35A)	4609	12293	2556	67
H(35B)	5332	11740	2594	67
H(35C)	5062	13243	2950	67

Table 5. Torsion angles, in degrees. E.s.ds are in parentheses.

C(14)-C(1)-C(2)-C(3)	6.7(2)	C(15)-C(1)-C(2)-C(3)	-175.24(14)
C(1)-C(2)-C(3)-C(4)	1.2(2)		
C(2)-C(3)-C(4)-C(5)	-4.8(2)		
C(3)-C(4)-C(5)-C(6)	-178.51(15)	C(17)-C(16)-C(21)-C(22)	171.46(13)
C(3)-C(4)-C(5)-C(14)	0.4(2)	C(15)-C(16)-C(21)-C(20)	175.83(12)
C(4)-C(5)-C(6)-C(7)	-178.38(14)	C(17)-C(16)-C(21)-C(20)	-8.95(19)
C(14)-C(5)-C(6)-C(7)	2.7(2)	C(19)-C(20)-C(21)-C(22)	-174.43(14)
C(5)-C(6)-C(7)-C(8)	174.47(14)	C(19)-C(20)-C(21)-C(16)	6.0(2)
C(5)-C(6)-C(7)-C(12)	-5.1(2)	C(16)-C(21)-C(22)-C(23)	-1.1(2)
C(6)-C(7)-C(8)-C(9)	-176.12(15)	C(20)-C(21)-C(22)-C(23)	179.37(13)
C(12)-C(7)-C(8)-C(9)	3.5(2)	C(16)-C(21)-C(22)-C(29)	-173.87(12)
C(7)-C(8)-C(9)-C(10)	1.6(2)	C(20)-C(21)-C(22)-C(29)	6.6(2)
C(8)-C(9)-C(10)-C(11)	-4.1(2)	C(21)-C(22)-C(23)-C(24)	177.54(13)
C(9)-C(10)-C(11)-C(12)	1.4(2)	C(29)-C(22)-C(23)-C(24)	-9.9(2)
C(10)-C(11)-C(12)-C(13)	179.35(14)	C(21)-C(22)-C(23)-C(28)	-1.3(2)
C(10)-C(11)-C(12)-C(7)	3.6(2)	C(29)-C(22)-C(23)-C(28)	171.26(13)
C(6)-C(7)-C(12)-C(13)	-2.3(2)	C(22)-C(23)-C(24)-C(25)	-179.39(13)
C(8)-C(7)-C(12)-C(13)	178.10(13)	C(28)-C(23)-C(24)-C(25)	-0.5(2)
C(6)-C(7)-C(12)-C(11)	173.66(14)	C(23)-C(24)-C(25)-C(26)	-5.6(2)
C(8)-C(7)-C(12)-C(11)	-6.0(2)	C(24)-C(25)-C(26)-C(27)	2.3(2)
C(11)-C(12)-C(13)-C(14)	-163.64(14)	C(25)-C(26)-C(27)-C(28)	6.9(2)
C(7)-C(12)-C(13)-C(14)	12.0(2)	C(25)-C(26)-C(27)-C(13)	-175.81(13)
C(11)-C(12)-C(13)-C(27)	18.7(2)	C(14)-C(13)-C(27)-C(26)	-151.03(14)
C(7)-C(12)-C(13)-C(27)	-165.62(13)	C(12)-C(13)-C(27)-C(26)	26.7(2)
C(12)-C(13)-C(14)-C(5)	-14.5(2)	C(14)-C(13)-C(27)-C(28)	26.27(18)
C(27)-C(13)-C(14)-C(5)	163.25(13)	C(12)-C(13)-C(27)-C(28)	-156.03(13)
C(12)-C(13)-C(14)-C(1)	166.22(13)	C(16)-C(15)-C(28)-C(23)	-13.5(2)
C(27)-C(13)-C(14)-C(1)	-15.99(19)	C(1)-C(15)-C(28)-C(23)	164.36(12)
C(6)-C(5)-C(14)-C(13)	7.2(2)	C(16)-C(15)-C(28)-C(27)	166.74(13)
C(4)-C(5)-C(14)-C(13)	-171.72(13)	C(1)-C(15)-C(28)-C(27)	-15.44(19)
C(6)-C(5)-C(14)-C(1)	-173.56(13)	C(22)-C(23)-C(28)-C(15)	8.7(2)
C(4)-C(5)-C(14)-C(1)	7.5(2)	C(24)-C(23)-C(28)-C(15)	-170.21(13)
C(2)-C(1)-C(14)-C(13)	168.31(14)	C(22)-C(23)-C(28)-C(27)	-171.51(13)
C(15)-C(1)-C(14)-C(13)	-9.8(2)	C(24)-C(23)-C(28)-C(27)	9.60(19)
C(2)-C(1)-C(14)-C(5)	-10.9(2)	C(26)-C(27)-C(28)-C(15)	167.06(13)
C(15)-C(1)-C(14)-C(5)	170.93(13)	C(13)-C(27)-C(28)-C(15)	-10.35(19)
C(2)-C(1)-C(15)-C(28)	-152.29(14)	C(26)-C(27)-C(28)-C(23)	-12.74(19)
C(14)-C(1)-C(15)-C(28)	25.74(18)	C(13)-C(27)-C(28)-C(23)	169.84(12)
C(2)-C(1)-C(15)-C(16)	25.4(2)	C(23)-C(22)-C(29)-C(34)	78.73(18)
C(14)-C(1)-C(15)-C(16)	-156.56(13)	C(21)-C(22)-C(29)-C(34)	-108.61(16)
C(28)-C(15)-C(16)-C(17)	-164.00(13)	C(23)-C(22)-C(29)-C(30)	-103.99(16)
C(1)-C(15)-C(16)-C(17)	18.3(2)	C(21)-C(22)-C(29)-C(30)	68.67(17)
C(28)-C(15)-C(16)-C(21)	10.93(19)	C(34)-C(29)-C(30)-C(31)	2.1(2)
C(1)-C(15)-C(16)-C(21)	-166.74(13)	C(22)-C(29)-C(30)-C(31)	-175.36(13)
C(15)-C(16)-C(17)-C(18)	-179.61(13)	C(29)-C(30)-C(31)-C(32)	0.6(2)
C(21)-C(16)-C(17)-C(18)	5.4(2)	C(30)-C(31)-C(32)-C(33)	-2.8(2)
C(16)-C(17)-C(18)-C(19)	1.5(2)	C(30)-C(31)-C(32)-C(35)	175.02(15)
C(17)-C(18)-C(19)-C(20)	-4.9(2)	C(31)-C(32)-C(33)-C(34)	2.5(2)
C(18)-C(19)-C(20)-C(21)	1.0(2)	C(35)-C(32)-C(33)-C(34)	-175.33(15)
C(15)-C(16)-C(21)-C(22)	-3.8(2)	C(30)-C(29)-C(34)-C(33)	-2.5(2)
		C(22)-C(29)-C(34)-C(33)	174.83(13)
		C(32)-C(33)-C(34)-C(29)	0.2(2)

Crystal and structure refinement data for
MeO-,bis($C_6H_{13}O$)-dibenzo-perylene, ca 0.5(CH_2Cl_2)(**89**)

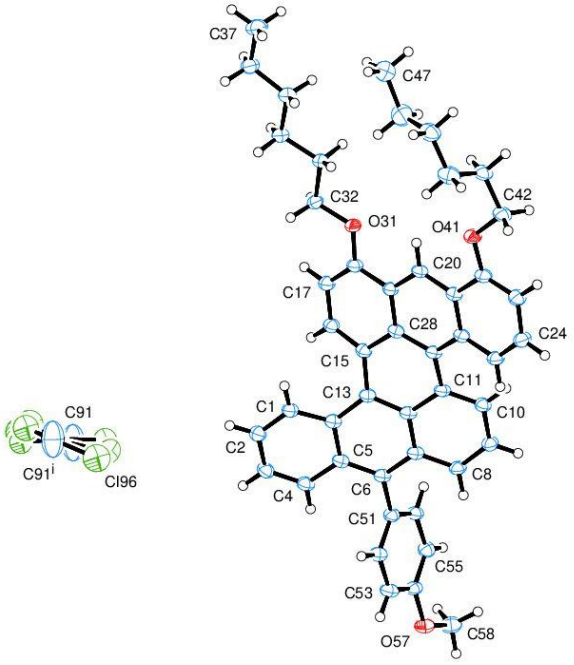

Identification code	isabf1361
Elemental formula	C47 H46 O3, (C0.5 Cl0.9)
Formula weight	696.75
Crystal system, space group	Triclinic, P-1 (no. 1)
Unit cell dimensions	a = 11.7394(4) Å α = 68.631(3) ° b = 12.2856(4) Å β = 84.584(3) ° c = 13.5443(5) Å γ = 86.032(3) °
Volume	1809.74(11) $Å^3$
Z, Calculated density	2, 1.279 Mg/m^3
F(000)	741
Absorption coefficient	1.197 mm^{-1}
Temperature	100(2) K
Wavelength	1.54184 Å
Crystal colour, shape	purple block
Crystal size	0.61 x 0.23 x 0.12 mm

Crystal mounting: on a small loop, in oil, fixed in cold N_2 stream

On the diffractometer:

Theta range for data collection	7.749 to 67.497 °
Limiting indices	-14<=h<=13, -14<=k<=12, -16<=l<=14

Completeness to theta = 67.497	98.7 %
Absorption correction	Semi-empirical from equivalents
Max. and min. transmission	1.00000 and 0.56330
Reflections collected (not including absences)	23118
No. of unique reflections	6447 [R(int) for equivalents = 0.050]
No. of 'observed' reflections ($I > 2\sigma_I$)	5147
Structure determined by:	dual methods, in SHELXT
Refinement:	Full-matrix least-squares on F^2, in SHELXL
Data / restraints / parameters	6447 / 0 / 481
Goodness-of-fit on F^2	1.048
Final R indices ('observed' data)	R^1 = 0.056, wR^2 = 0.150
Final R indices (all data)	R^1 = 0.069, wR^2 = 0.158
Reflections weighted: $w = [\sigma^2(Fo^2)+(0.0969P)^2+0.3145P]^{-1}$ where $P=(Fo^2+2Fc^2)/3$	
Extinction coefficient	n/a
Largest diff. peak and hole	0.29 and -0.33 e.Å^{-3}
Location of largest difference peak	near H(42b)

Table 1. Atomic coordinates (x 10^5) and equivalent isotropic displacement parameters ($Å^2$ x 10^4). U(eq) is defined as one third of the trace of the orthogonalized Uij tensor. E.s.ds are in parentheses.

	x	y	z	U(eq)	S.o.f.#
C(1)	33561(15)	42650(16)	66568(15)	269(4)	
C(2)	30645(16)	31330(17)	71752(16)	300(4)	
C(3)	20344(16)	28765(16)	78343(16)	311(4)	
C(4)	12966(16)	37589(16)	78984(15)	291(4)	
C(5)	15519(15)	49591(16)	73394(15)	259(4)	
C(6)	7666(14)	58759(16)	73728(15)	256(4)	
C(7)	10358(14)	70417(16)	67708(14)	253(4)	
C(8)	2455(15)	79912(16)	67196(15)	276(4)	
C(9)	5600(15)	91182(16)	62222(15)	285(4)	
C(10)	16366(15)	93851(16)	56601(15)	271(4)	
C(11)	24010(14)	85083(15)	55757(15)	252(4)	
C(12)	21441(15)	73127(16)	62069(15)	253(4)	
C(13)	29892(14)	64104(15)	62995(14)	241(4)	
C(14)	26507(15)	52265(16)	67595(15)	250(4)	
C(15)	41768(15)	67554(15)	59526(15)	251(4)	
C(16)	51201(15)	60433(16)	63433(15)	266(4)	
C(17)	62532(15)	63638(16)	59578(16)	285(4)	
C(18)	64510(15)	74084(16)	51561(15)	261(4)	
C(19)	55171(14)	82199(15)	47410(15)	250(4)	
C(20)	57095(15)	92983(15)	39400(15)	259(4)	
C(21)	48022(15)	100774(15)	35410(15)	258(4)	
C(22)	50088(15)	111694(16)	26755(16)	288(4)	
C(23)	41331(16)	119489(17)	22783(16)	327(4)	
C(24)	30004(16)	116382(17)	26859(17)	329(4)	
C(25)	27609(15)	106239(16)	35032(16)	300(4)	
C(26)	36565(15)	98194(15)	40016(15)	258(4)	
C(27)	34763(15)	87597(15)	48978(15)	251(4)	
C(28)	43787(15)	79126(15)	51912(15)	248(4)	
O(31)	75021(10)	77934(11)	46949(11)	289(3)	
C(32)	84640(15)	69739(16)	49236(16)	289(4)	
C(33)	94806(15)	76125(16)	42314(16)	292(4)	
C(34)	105292(15)	68121(16)	42177(16)	297(4)	
C(35)	115010(16)	74946(17)	34611(17)	325(4)	
C(36)	126150(16)	67815(18)	34865(18)	348(5)	
C(37)	135528(17)	74580(20)	26900(20)	430(5)	
O(41)	61265(11)	113147(11)	22990(11)	330(3)	
C(42)	64192(17)	124263(17)	15077(17)	343(5)	
C(43)	76775(17)	123566(17)	11890(17)	345(5)	
C(44)	79676(19)	116640(20)	4755(19)	435(5)	
C(45)	92552(19)	115990(20)	1687(19)	433(5)	
C(46)	99430(20)	108100(20)	10600(20)	491(6)	
C(47)	112350(20)	108000(20)	7800(20)	538(6)	
C(51)	-3415(15)	56283(15)	80467(15)	263(4)	
C(52)	-12078(15)	50366(16)	78359(16)	295(4)	
C(53)	-22545(16)	48788(17)	84277(16)	302(4)	
C(54)	-24611(15)	53068(15)	92397(15)	272(4)	
C(55)	-16062(16)	58646(16)	94954(15)	287(4)	
C(56)	-5551(15)	60163(15)	88890(15)	275(4)	
O(57)	-35387(11)	51455(12)	97525(11)	329(3)	
C(58)	-37995(17)	56098(19)	105738(17)	376(5)	
C(91)	48390(80)	870(60)	6070(60)	860(20)	0.5
Cl(92)	42900(20)	11630(20)	-4240(20)	615(5)	0.5

Cl(94)	46260(70)	11090(90)	-1620(90)	550(20)*	0.123
Cl(95)	43040(80)	8050(80)	900(80)	700(20)*	0.135
Cl(96)	42540(80)	8850(80)	-7080(80)	800(30)*	0.135

- site occupancy, if different from 1.
* - U(iso) ($Å^2$ x 10^4)

Table 2. Molecular dimensions. Bond lengths are in Ångstroms, angles in degrees. E.s.ds are in parentheses.

C(1)-C(2)	1.361(3)	C(21)-C(22)	1.442(3)
C(1)-C(14)	1.436(3)	C(22)-O(41)	1.361(2)
C(2)-C(3)	1.415(3)	C(22)-C(23)	1.362(3)
C(3)-C(4)	1.363(3)	C(23)-C(24)	1.413(3)
C(4)-C(5)	1.429(3)	C(24)-C(25)	1.357(3)
C(5)-C(6)	1.416(3)	C(25)-C(26)	1.429(3)
C(5)-C(14)	1.438(2)	C(26)-C(27)	1.432(2)
C(6)-C(7)	1.407(2)	C(27)-C(28)	1.410(3)
C(6)-C(51)	1.499(2)	O(31)-C(32)	1.437(2)
C(7)-C(8)	1.425(3)	C(32)-C(33)	1.517(2)
C(7)-C(12)	1.440(2)	C(33)-C(34)	1.525(3)
C(8)-C(9)	1.361(3)	C(34)-C(35)	1.530(3)
C(9)-C(10)	1.406(3)	C(35)-C(36)	1.519(3)
C(10)-C(11)	1.384(3)	C(36)-C(37)	1.522(3)
C(11)-C(12)	1.441(2)	O(41)-C(42)	1.435(2)
C(11)-C(27)	1.470(2)	C(42)-C(43)	1.505(3)
C(12)-C(13)	1.414(3)	C(43)-C(44)	1.507(3)
C(13)-C(14)	1.426(2)	C(44)-C(45)	1.534(3)
C(13)-C(15)	1.469(2)	C(45)-C(46)	1.507(4)
C(15)-C(16)	1.382(3)	C(46)-C(47)	1.528(3)
C(15)-C(28)	1.440(2)	C(51)-C(56)	1.385(3)
C(16)-C(17)	1.410(2)	C(51)-C(52)	1.397(3)
C(17)-C(18)	1.363(3)	C(52)-C(53)	1.387(3)
C(18)-O(31)	1.362(2)	C(53)-C(54)	1.378(3)
C(18)-C(19)	1.438(3)	C(54)-O(57)	1.375(2)
C(19)-C(20)	1.390(3)	C(54)-C(55)	1.389(3)
C(19)-C(28)	1.431(2)	C(55)-C(56)	1.400(3)
C(20)-C(21)	1.391(3)	O(57)-C(58)	1.425(3)
C(21)-C(26)	1.434(2)		
C(91)-Cl(95)	1.105(11)	C(91)-Cl(94)#1	1.834(11)
C(91)-Cl(94)	1.333(14)	C(91)-Cl(96)	1.863(12)
C(91)-Cl(96)#1	1.520(12)	C(91)-Cl(92)#1	1.865(8)
C(91)-Cl(92)	1.679(7)	C(91)-Cl(95)#1	1.879(10)
C(91)-C(91)#1	1.739(14)		
C(2)-C(1)-C(14)	122.05(17)	C(12)-C(13)-C(14)	118.51(15)
C(1)-C(2)-C(3)	119.92(18)	C(12)-C(13)-C(15)	117.48(15)
C(4)-C(3)-C(2)	120.24(17)	C(14)-C(13)-C(15)	123.96(16)
C(3)-C(4)-C(5)	121.55(17)	C(13)-C(14)-C(1)	122.84(16)
C(6)-C(5)-C(4)	121.59(16)	C(13)-C(14)-C(5)	119.90(16)
C(6)-C(5)-C(14)	119.99(16)	C(1)-C(14)-C(5)	117.25(16)
C(4)-C(5)-C(14)	118.39(17)	C(16)-C(15)-C(28)	117.71(16)
C(7)-C(6)-C(5)	119.45(16)	C(16)-C(15)-C(13)	123.63(16)
C(7)-C(6)-C(51)	119.32(16)	C(28)-C(15)-C(13)	118.62(16)
C(5)-C(6)-C(51)	121.23(15)	C(15)-C(16)-C(17)	122.80(17)
C(6)-C(7)-C(8)	121.73(16)	C(18)-C(17)-C(16)	119.89(18)
C(6)-C(7)-C(12)	120.45(17)	O(31)-C(18)-C(17)	125.17(17)
C(8)-C(7)-C(12)	117.79(16)	O(31)-C(18)-C(19)	114.27(15)
C(9)-C(8)-C(7)	120.90(16)	C(17)-C(18)-C(19)	120.55(16)
C(8)-C(9)-C(10)	121.21(17)	C(20)-C(19)-C(28)	120.14(17)
C(11)-C(10)-C(9)	120.96(16)	C(20)-C(19)-C(18)	121.12(16)
C(10)-C(11)-C(12)	118.32(16)	C(28)-C(19)-C(18)	118.72(16)
C(10)-C(11)-C(27)	122.28(16)	C(19)-C(20)-C(21)	120.80(16)
C(12)-C(11)-C(27)	119.36(16)	C(20)-C(21)-C(26)	120.52(16)
C(13)-C(12)-C(7)	119.95(16)	C(20)-C(21)-C(22)	120.22(16)
C(13)-C(12)-C(11)	120.12(16)	C(26)-C(21)-C(22)	119.24(17)
C(7)-C(12)-C(11)	119.90(17)	O(41)-C(22)-C(23)	124.83(17)

O(41)-C(22)-C(21)	114.00(16)	C(35)-C(36)-C(37)	113.15(18)
C(23)-C(22)-C(21)	121.16(16)	C(22)-O(41)-C(42)	117.32(15)
C(22)-C(23)-C(24)	118.71(17)	O(41)-C(42)-C(43)	107.40(16)
C(25)-C(24)-C(23)	122.29(18)	C(42)-C(43)-C(44)	113.92(17)
C(24)-C(25)-C(26)	120.99(17)	C(43)-C(44)-C(45)	112.89(17)
C(25)-C(26)-C(27)	124.29(16)	C(46)-C(45)-C(44)	114.06(19)
C(25)-C(26)-C(21)	117.23(16)	C(45)-C(46)-C(47)	114.3(2)
C(27)-C(26)-C(21)	118.44(17)	C(56)-C(51)-C(52)	117.48(16)
C(28)-C(27)-C(26)	119.60(16)	C(56)-C(51)-C(6)	120.56(15)
C(28)-C(27)-C(11)	116.70(16)	C(52)-C(51)-C(6)	121.93(17)
C(26)-C(27)-C(11)	123.66(16)	C(53)-C(52)-C(51)	121.11(18)
C(27)-C(28)-C(19)	119.27(16)	C(54)-C(53)-C(52)	120.36(16)
C(27)-C(28)-C(15)	121.09(16)	O(57)-C(54)-C(53)	115.99(15)
C(19)-C(28)-C(15)	119.62(17)	O(57)-C(54)-C(55)	123.91(17)
C(18)-O(31)-C(32)	118.24(13)	C(53)-C(54)-C(55)	120.10(16)
O(31)-C(32)-C(33)	106.33(14)	C(54)-C(55)-C(56)	118.69(18)
C(32)-C(33)-C(34)	113.45(15)	C(51)-C(56)-C(55)	122.19(16)
C(33)-C(34)-C(35)	110.93(16)	C(54)-O(57)-C(58)	117.75(14)
C(36)-C(35)-C(34)	113.96(17)		

Cl(95)-C(91)-Cl(96)*1	148.5(9)	Cl(95)-C(91)-Cl(92)*1	134.2(7)
Cl(94)-C(91)-Cl(96)*1	133.2(8)	Cl(94)-C(91)-Cl(92)*1	125.2(6)
Cl(96)#1-C(91)-Cl(92)	134.2(6)	Cl(92)-C(91)-Cl(92)*1	121.5(4)
Cl(95)-C(91)-Cl(94)*1	119.3(8)	Cl(96)-C(91)-Cl(92)*1	104.5(4)
Cl(94)-C(91)-Cl(94)*1	115.7(6)	Cl(95)-C(91)-Cl(95)*1	114.6(6)
Cl(92)-C(91)-Cl(94)*1	108.4(5)	Cl(94)-C(91)-Cl(95)*1	104.5(7)
Cl(96)#1-C(91)-Cl(96)	119.1(6)	Cl(92)-C(91)-Cl(95)*1	101.1(5)
Cl(94)#1-C(91)-Cl(96)	90.2(5)		

Symmetry transformation used to generate equivalent atoms:
#1 : 1-x, -y, -z

Table 3. Anisotropic displacement parameters (Å^2 x 10^4) for the expression:

$$\exp\{-2\pi^2(h^2a^{*2}U_{11} + \ldots + 2hka^*b^*U_{12})\}$$

E.s.ds are in parentheses.

	U_{11}	U_{22}	U_{33}	U_{23}	U_{13}	U_{12}
C(1)	231(8)	280(9)	286(10)	-87(8)	-8(7)	-45(7)
C(2)	279(9)	289(9)	323(11)	-94(8)	-20(8)	-40(7)
C(3)	307(9)	251(9)	329(11)	-43(8)	-24(8)	-63(7)
C(4)	255(9)	289(9)	287(10)	-49(8)	2(7)	-78(7)
C(5)	243(9)	268(9)	251(10)	-67(8)	-10(7)	-65(7)
C(6)	211(8)	287(9)	249(9)	-66(7)	-4(7)	-59(7)
C(7)	208(8)	289(9)	242(10)	-67(8)	-6(7)	-59(7)
C(8)	200(8)	300(9)	285(10)	-61(8)	27(7)	-46(7)
C(9)	232(9)	286(9)	297(10)	-64(8)	9(7)	-16(7)
C(10)	243(9)	261(9)	275(10)	-52(8)	-1(7)	-55(7)
C(11)	191(8)	271(9)	267(10)	-60(7)	-3(7)	-61(7)
C(12)	218(8)	286(9)	237(9)	-65(8)	-2(7)	-65(7)
C(13)	218(8)	271(9)	222(9)	-73(7)	3(7)	-42(7)
C(14)	230(8)	274(9)	231(9)	-67(7)	-18(7)	-44(7)
C(15)	238(9)	256(9)	250(9)	-81(7)	18(7)	-51(7)
C(16)	239(9)	258(9)	275(10)	-63(7)	2(7)	-40(7)
C(17)	236(9)	281(9)	305(10)	-65(8)	-11(8)	-34(7)
C(18)	202(8)	281(9)	304(10)	-114(8)	24(7)	-56(7)
C(19)	213(8)	260(9)	281(10)	-105(8)	13(7)	-50(7)
C(20)	208(8)	261(9)	292(10)	-84(8)	40(7)	-72(7)
C(21)	233(9)	260(9)	266(10)	-78(8)	13(7)	-56(7)
C(22)	225(9)	296(9)	314(11)	-78(8)	36(8)	-62(7)
C(23)	288(10)	290(9)	313(11)	-5(8)	17(8)	-43(8)
C(24)	238(9)	317(10)	351(11)	-28(8)	-6(8)	-6(7)
C(25)	207(8)	305(9)	332(11)	-52(8)	13(8)	-42(7)
C(26)	235(8)	257(9)	266(10)	-76(8)	19(7)	-63(7)
C(27)	212(8)	262(9)	270(10)	-79(8)	-2(7)	-63(7)
C(28)	238(9)	261(9)	237(9)	-78(7)	10(7)	-59(7)
O(31)	191(6)	254(6)	363(8)	-50(6)	29(5)	-35(5)
C(32)	197(8)	271(9)	354(11)	-63(8)	-11(7)	-4(7)
C(33)	218(9)	272(9)	358(11)	-82(8)	9(8)	-42(7)
C(34)	224(9)	321(10)	349(11)	-125(8)	-7(8)	-36(7)
C(35)	255(9)	340(10)	377(11)	-125(9)	6(8)	-48(8)
C(36)	253(9)	401(11)	420(12)	-186(9)	-11(8)	-26(8)
C(37)	260(10)	567(14)	513(14)	-259(12)	38(9)	-65(9)
O(41)	226(6)	284(7)	372(8)	-4(6)	67(6)	-58(5)
C(42)	304(10)	295(10)	333(11)	1(8)	35(8)	-96(8)
C(43)	302(10)	323(10)	332(11)	-21(8)	17(8)	-100(8)
C(44)	408(12)	509(13)	383(12)	-149(10)	37(10)	-132(10)
C(45)	414(12)	470(12)	426(13)	-184(10)	101(10)	-140(10)
C(46)	503(13)	511(13)	460(14)	-199(11)	78(11)	-47(11)
C(47)	455(13)	497(14)	698(18)	-261(13)	-15(12)	-39(11)
C(51)	216(8)	241(9)	267(10)	-13(7)	3(7)	-44(7)
C(52)	253(9)	314(10)	302(10)	-90(8)	12(8)	-65(7)
C(53)	251(9)	321(10)	300(10)	-59(8)	-10(8)	-96(7)
C(54)	203(8)	261(9)	266(10)	4(7)	16(7)	-45(7)
C(55)	285(9)	281(9)	255(10)	-52(8)	10(8)	-39(7)
C(56)	212(8)	266(9)	307(10)	-49(8)	-6(7)	-61(7)
O(57)	240(7)	405(8)	316(8)	-103(6)	43(5)	-82(5)
C(58)	309(10)	466(12)	327(11)	-121(9)	60(9)	-75(9)
C(91)	1350(70)	600(40)	560(40)	-150(30)	-180(40)	230(40)
Cl(92)	597(12)	660(12)	529(14)	-166(12)	-25(10)	69(8)

Table 4. Hydrogen coordinates (x 10^4) and isotropic displacement parameters ($Å^2$ x 10^3). All hydrogen atoms were included in idealised positions with U(iso)'s set at 1.2*U(eq) or, for the methyl group hydrogen atoms, 1.5*U(eq) of the parent carbon atoms.

	x	y	z	U(iso)
H(1)	4048	4424	6213	32
H(2)	3552	2516	7095	36
H(3)	1857	2086	8234	37
H(4)	596	3572	8325	35
H(8)	-511	7835	7037	33
H(9)	43	9736	6255	34
H(10)	1842	10179	5334	33
H(16)	5000	5307	6895	32
H(17)	6878	5853	6256	34
H(20)	6470	9506	3662	31
H(23)	4281	12687	1738	39
H(24)	2385	12158	2377	40
H(25)	1986	10446	3748	36
H(32A)	8317	6279	4755	35
H(32B)	8610	6714	5685	35
H(33A)	9688	8223	4492	35
H(33B)	9255	8009	3495	35
H(34A)	10321	6177	3989	36
H(34B)	10791	6451	4944	36
H(35A)	11254	7791	2727	39
H(35B)	11642	8180	3646	39
H(36A)	12469	6076	3335	42
H(36B)	12886	6519	4210	42
H(37A)	14248	6955	2742	65
H(37B)	13299	7704	1969	65
H(37C)	13716	8148	2844	65
H(42A)	6254	13055	1801	41
H(42B)	5967	12599	883	41
H(43A)	8096	11996	1839	41
H(43B)	7949	13160	819	41
H(44A)	7558	12027	-179	52
H(44B)	7695	10861	842	52
H(45A)	9370	11319	-433	52
H(45B)	9552	12397	-79	52
H(46A)	9678	10002	1276	59
H(46B)	9788	11060	1678	59
H(47A)	11620	10269	1396	81
H(47B)	11401	10532	180	81
H(47C)	11511	11592	583	81
H(52)	-1078	4737	7278	35
H(53)	-2832	4473	8272	36
H(55)	-1732	6138	10070	34
H(56)	31	6398	9061	33
H(58A)	-4589	5435	10871	56
H(58B)	-3273	5254	11135	56
H(58C)	-3716	6459	10280	56

Table 5. Torsion angles, in degrees. E.s.ds are in parentheses.

C(14)-C(1)-C(2)-C(3)	0.4(3)	C(26)-C(21)-C(22)-O(41)	-179.62(16)
C(1)-C(2)-C(3)-C(4)	4.3(3)	C(20)-C(21)-C(22)-C(23)	-179.49(19)
C(2)-C(3)-C(4)-C(5)	-2.2(3)	C(26)-C(21)-C(22)-C(23)	-1.1(3)
C(3)-C(4)-C(5)-C(6)	177.54(18)	O(41)-C(22)-C(23)-C(24)	174.47(18)
C(3)-C(4)-C(5)-C(14)	-4.4(3)	C(21)-C(22)-C(23)-C(24)	-3.9(3)
C(4)-C(5)-C(6)-C(7)	-177.17(17)	C(22)-C(23)-C(24)-C(25)	4.2(3)
C(14)-C(5)-C(6)-C(7)	4.8(3)	C(23)-C(24)-C(25)-C(26)	0.6(3)
C(4)-C(5)-C(6)-C(51)	3.5(3)	C(24)-C(25)-C(26)-C(27)	176.97(19)
C(14)-C(5)-C(6)-C(51)	-174.59(16)	C(24)-C(25)-C(26)-C(21)	-5.6(3)
C(5)-C(6)-C(7)-C(8)	175.75(17)	C(20)-C(21)-C(26)-C(25)	-175.87(17)
C(51)-C(6)-C(7)-C(8)	-4.9(3)	C(22)-C(21)-C(26)-C(25)	5.7(3)
C(5)-C(6)-C(7)-C(12)	-6.0(3)	C(20)-C(21)-C(26)-C(27)	1.8(3)
C(51)-C(6)-C(7)-C(12)	173.34(16)	C(22)-C(21)-C(26)-C(27)	-176.66(16)
C(6)-C(7)-C(8)-C(9)	173.35(18)	C(25)-C(26)-C(27)-C(28)	166.83(17)
C(12)-C(7)-C(8)-C(9)	-4.9(3)	C(21)-C(26)-C(27)-C(28)	-10.6(3)
C(7)-C(8)-C(9)-C(10)	5.9(3)	C(25)-C(26)-C(27)-C(11)	-15.7(3)
C(8)-C(9)-C(10)-C(11)	1.4(3)	C(21)-C(26)-C(27)-C(11)	166.83(16)
C(9)-C(10)-C(11)-C(12)	-9.2(3)	C(10)-C(11)-C(27)-C(28)	153.92(18)
C(9)-C(10)-C(11)-C(27)	173.05(17)	C(12)-C(11)-C(27)-C(28)	-23.8(2)
C(6)-C(7)-C(12)-C(13)	-3.2(3)	C(10)-C(11)-C(27)-C(26)	-23.6(3)
C(8)-C(7)-C(12)-C(13)	175.11(17)	C(12)-C(11)-C(27)-C(26)	158.68(17)
C(6)-C(7)-C(12)-C(11)	178.75(16)	C(26)-C(27)-C(28)-C(19)	13.2(3)
C(8)-C(7)-C(12)-C(11)	-3.0(3)	C(11)-C(27)-C(28)-C(19)	-164.45(16)
C(10)-C(11)-C(12)-C(13)	-168.20(17)	C(26)-C(27)-C(28)-C(15)	-168.27(16)
C(27)-C(11)-C(12)-C(13)	9.6(3)	C(11)-C(27)-C(28)-C(15)	14.1(2)
C(10)-C(11)-C(12)-C(7)	9.9(3)	C(20)-C(19)-C(28)-C(27)	-6.9(3)
C(27)-C(11)-C(12)-C(7)	-172.30(15)	C(18)-C(19)-C(28)-C(27)	171.25(16)
C(7)-C(12)-C(13)-C(14)	13.4(3)	C(20)-C(19)-C(28)-C(15)	174.52(16)
C(11)-C(12)-C(13)-C(14)	-168.49(16)	C(18)-C(19)-C(28)-C(15)	-7.3(3)
C(7)-C(12)-C(13)-C(15)	-164.11(16)	C(16)-C(15)-C(28)-C(27)	-168.64(18)
C(11)-C(12)-C(13)-C(15)	14.0(3)	C(13)-C(15)-C(28)-C(27)	9.2(3)
C(12)-C(13)-C(14)-C(1)	164.16(17)	C(16)-C(15)-C(28)-C(19)	9.9(3)
C(15)-C(13)-C(14)-C(1)	-18.5(3)	C(13)-C(15)-C(28)-C(19)	-172.21(16)
C(12)-C(13)-C(14)-C(5)	-14.7(3)	C(17)-C(18)-O(31)-C(32)	11.7(3)
C(15)-C(13)-C(14)-C(5)	162.70(17)	C(19)-C(18)-O(31)-C(32)	-169.54(16)
C(2)-C(1)-C(14)-C(13)	174.29(18)	C(18)-O(31)-C(32)-C(33)	174.99(15)
C(2)-C(1)-C(14)-C(5)	-6.9(3)	O(31)-C(32)-C(33)-C(34)	-169.42(16)
C(6)-C(5)-C(14)-C(13)	5.6(3)	C(32)-C(33)-C(34)-C(35)	176.94(16)
C(4)-C(5)-C(14)-C(13)	-172.48(17)	C(33)-C(34)-C(35)-C(36)	174.27(17)
C(6)-C(5)-C(14)-C(1)	-173.25(17)	C(34)-C(35)-C(36)-C(37)	177.14(17)
C(4)-C(5)-C(14)-C(1)	8.6(3)	C(23)-C(22)-O(41)-C(42)	7.4(3)
C(12)-C(13)-C(15)-C(16)	154.15(18)	C(21)-C(22)-O(41)-C(42)	-174.07(16)
C(14)-C(13)-C(15)-C(16)	-23.2(3)	C(22)-O(41)-C(42)-C(43)	-177.74(16)
C(12)-C(13)-C(15)-C(28)	-23.6(2)	O(41)-C(42)-C(43)-C(44)	75.5(2)
C(14)-C(13)-C(15)-C(28)	159.02(17)	C(42)-C(43)-C(44)-C(45)	-179.60(18)
C(28)-C(15)-C(16)-C(17)	-5.9(3)	C(43)-C(44)-C(45)-C(46)	72.8(3)
C(13)-C(15)-C(16)-C(17)	176.34(17)	C(44)-C(45)-C(46)-C(47)	-176.40(19)
C(15)-C(16)-C(17)-C(18)	-0.9(3)	C(7)-C(6)-C(51)-C(56)	-63.6(2)
C(16)-C(17)-C(18)-O(31)	-177.59(16)	C(5)-C(6)-C(51)-C(56)	115.8(2)
C(16)-C(17)-C(18)-C(19)	3.7(3)	C(7)-C(6)-C(51)-C(52)	114.4(2)
O(31)-C(18)-C(19)-C(20)	-0.2(3)	C(5)-C(6)-C(51)-C(52)	-66.3(2)
C(17)-C(18)-C(19)-C(20)	178.57(18)	C(56)-C(51)-C(52)-C(53)	2.0(3)
O(31)-C(18)-C(19)-C(28)	-178.37(15)	C(6)-C(51)-C(52)-C(53)	-175.97(18)
C(17)-C(18)-C(19)-C(28)	0.4(3)	C(51)-C(52)-C(53)-C(54)	0.1(3)
C(28)-C(19)-C(20)-C(21)	-2.0(3)	C(52)-C(53)-C(54)-O(57)	177.59(17)
C(18)-C(19)-C(20)-C(21)	179.86(17)	C(52)-C(53)-C(54)-C(55)	-2.2(3)
C(19)-C(20)-C(21)-C(26)	4.6(3)	O(57)-C(54)-C(55)-C(56)	-177.59(16)
C(19)-C(20)-C(21)-C(22)	-177.03(17)	C(53)-C(54)-C(55)-C(56)	2.2(3)
C(20)-C(21)-C(22)-O(41)	2.0(3)	C(52)-C(51)-C(56)-C(55)	-2.0(3)

C(6)-C(51)-C(56)-C(55)	176.00(17)	C(53)-C(54)-O(57)-C(58)	-177.96(17)
C(54)-C(55)-C(56)-C(51)	-0.1(3)	C(55)-C(54)-O(57)-C(58)	1.9(3)